



ISSN 2310-9599

FOODS AND RAW MATERIALS

Vol.2 (№1) 2014

The Ministry of Education and
Science of the Russian
Federation

**Kemerovo Institute of Food
Science and Technology**

**FOODS AND
RAW MATERIALS**

Vol. 2, No. 1, 2014

ISSN 2308-4057 (Print)
ISSN 2310-9599 (Online)

Published twice a year.

Founder:
Kemerovo Institute of Food
Science and Technology
(KemIFST),
bul'v. Stroitelei 47, Kemerovo,
650056 Russia

**Editorial Office,
Publishing Office:**
office 1212, bul'v. Stroitelei 47,
Kemerovo, 650056 Russia,
tel.: +7(3842)39-68-45

<http://frm-kemtipp.ru>

e-mail: fjournal@mail.ru

Printing Office:
office 2006, ul. Institutskaya 7,
Kemerovo, 650002 Russia,
tel.: +7(3842)39-09-81

The Edition is registered by
Federal Service for Supervision in
the Sphere of Telecom,
Information Technologies and
Mass Communications
(Media Registration Certificate
PI no. FS77-52352
dated December 28, 2012)

ISSN 2308-4057 (Print)
ISSN 2310-9599 (Online)

Editor-in-Chief

Aleksandr Yu. Prosekov, Dr. Sci. (Eng.), Kemerovo Institute of Food
Science and Technology, Kemerovo, Russia

Deputy Editor-in-Chief

Olga V. Koroleva, Dr. Sci. (Biol.), Bach Institute of Biochemistry,
Moscow, Russia;

Zheng Xi-Qun, Dr., Prof., Vice President, Qiqihar University
Heilongjiang Province, Qiqihar, P. R. China.

Editorial Board

Gosta Winberg, M.D., Ph.D. Assoc. Prof., Karolinska Institutet,
Stockholm, Sweden;

Aleksandr N. Avstrieviskikh, Dr. Sci. (Eng.), OOO ArtLaif , Tomsk,
Russia;

Berdan A. Rskeldiev, Dr. Sci. (Eng.), Shakarim State University,
Semei (Semipalatinsk), Kazakhstan;

Aram G. Galstyan, Dr. Sci. (Eng.), All-Russian Research Institute of
Dairy Industry, Moscow, Russia;

Tamara A. Krasnova, Dr. Sci. (Eng.), Kemerovo Institute of Food
Science and Technology, Kemerovo, Russia;

Olga A. Neverova, Dr. Sci. (Biol.), Institute of Human Ecology,
Siberian Branch, Russian Academy of Sciences, Kemerovo, Russia;

Aleksei M. Osintsev, Dr. Sci. (Eng.), Prof., Kemerovo Institute of
Food Science and Technology, Kemerovo, Russia;

Viktor A. Panfilov, Dr. Sci. (Eng.), Prof., Moscow State University
of Food Production, Moscow, Russia;

Sergei L. Tikhonov, Dr. Sci. (Eng.), Ural State Academy of
Veterinary Medicine, Troitsk, Russia;

Irina S. Khamagaeva, Dr. Sci. (Eng.), East-Siberian State University
of Technology and Management, Ulan-Ude, Russia;

Lidiya V. Shul'gina, Dr. Sci. (Biol.), Pacific Research Fishery
Center, Vladivostok, Russia.

Secretary of Editorial Office

Ekaterina V. Dmitrieva, Cand. Sci. (Eng.), Kemerovo Institute of
Food Science and Technology, Kemerovo, Russia.

<p>Opinions of the authors of published materials do not always coincide with the editorial staff's viewpoint. Authors are responsible for the scientific content of their papers.</p>	<p>CONTENTS</p> <p>FOOD PRODUCTION TECHNOLOGY</p> <p>N. I. Davydenko and L. A. Mayurnikova <i>On the Possibility to Grow High-Selenium Wheat in the Kuznetsk Basin</i>..... 3</p> <p>V. A. Ermolaev <i>Effect of Vacuum Drying on Microstructure of Semi-Solid Cheese</i>..... 11</p> <p>S. A. Ivanova, V. A. Pavsky, M. A. Poplavskaya, and M. V. Novoselova <i>Studying the Biokinetics of Pigmented Yeast by Stochastic Methods</i>..... 17</p> <p>A. G. Khramtsov, I. A. Evdokimov, A. D. Lodygin, and R. O. Budkevich <i>Technology Development for the Food Industry: A Conceptual Model</i>..... 22</p> <p>M. G. Kurbanova and S. M. Maslennikova <i>Acid Hydrolysis of Casein</i>..... 27</p> <p>V. A. Mar'in and A. L. Vereshchagin <i>Effects of Humidity and the Content of Sprouted and Spoiled Buckwheat Grains on the Changes of Acid Number of Fat and Grain Acidity</i>..... 31</p> <p>Yu. T. Orlyuk and M. I. Stepanishchev <i>Assessment of Proteolysis and Lipolysis Intensity in Pechersky Cheese Ripening in the Presence of Penicillium Camemberti and Penicillium Roqueforti Molds</i>..... 36</p> <p>A. V. Pozdnyakova, A. N. Arkhipov, O. V. Kozlova, and L. A. Ostroumov <i>Composition and Microstructure Investigation for the Modeling and Classification of Dietary Fiber Derived From Plants</i>..... 40</p> <p>T. N. Safronova and O. M. Evtuhova <i>Development of Technological Parameters for the Hydrothermal Processing of Sprouted Wheat Grain Powder</i>..... 47</p> <p>L. A. Timasheva and E. V. Gorbunova <i>A Promising Trend in the P of fennel (Foeniculum Vulgare Mill.) whole Plants</i>..... 51</p> <p>A. D. Toshev, A. S. Salomatov, and A. S. Salomatova <i>A Method to Increase the Nutritional Value of Aerated Confectionery</i>..... 58</p> <p>BIOTECHNOLOGY</p> <p>A. I. Piskaeva, Yu. Yu. Sidorin, L. S. Dyshlyuk, Yu. V. Zhumaev, and A. Yu. Prosekov <i>Research on the Influence of Silver Clusters on Decomposer Microorganisms and E. Coli Bacteria</i>..... 62</p> <p>PROCESSES, EQUIPMENT, AND APPARATUSES FOR THE FOOD INDUSTRY</p> <p>D. M. Borodulin, D. V. Sukhorukov <i>Mixtures for Vertebroplasty: the Flowability of Their Components and a New Production Technology Using a Centrifugal Mixer</i>..... 67</p> <p>A. N. Pirogov <i>Rheometric Monitoring of the Formation of Milk-Protein Blob</i> 72</p> <p>FOOD HYGIENE</p> <p>P. E. Vloshchinskiy, I. P. Berezovikova, A. R. Kolpakov, and N.G. Klebleeva <i>Effect of Multicomponent Cereal Mixtures on Glucose Level in Blood of Experimental Animals</i>..... 82</p> <p>CHEMISTRY AND ECOLOGY</p> <p>Z. N. Esina, A. M. Miroshnikov, M. R. Korchuganova <i>Enthalpy of Phase Transition and Prediction of Phase Equilibria in Systems of Glycols and Glycol Ethers</i>..... 86</p> <p>ECONOMY OF THE AGROINDUSTRIAL COMPLEX</p> <p>V. P. Zotov, E. A. Zhidkova, and A. M. Dvorovento <i>The Main Labor-Forming Factors and the Assessment of Labor Efficiency in Agriculture (By the Example of Kemerovo Oblast)</i>..... 91</p> <p>INFORMATION</p> <p>Information for Authors..... 98</p>
<p>The Edition «Foods and Raw Materials» is included in the Russian index of scientific citation (RISC) and registered in the Scientific electronic library eLIBRARY.RU</p>	
<p>The information about edition is published in international reference system of periodical and proceeding editions of "Ulrich's Periodicals Directory".</p>	
<p>Subscription index for the unified «Russian Press» catalogue – 41672</p>	
<p>Signet for publishing June 11, 2014 Date of publishing June 11, 2014 Circulation 300 ex. Open price.</p>	
<p>Kemerovo Institute of Food Science and Technology (KemIFST), bul'v. Stroitelei 47, Kemerovo, 650056 Russia</p>	
<p>© 2014, KemIFST. All rights reserved.</p>	

ON THE POSSIBILITY TO GROW HIGH-SELENIUM WHEAT IN THE KUZNETSK BASIN

N. I. Davydenko* and L. A. Mayurnikova

Kemerovo Institute of Food Science and Technology,
bul'v. Stroitelei 47, Kemerovo, 650056 Russia,
*e-mail: nat1861@yandex.ru

(Received March 17, 2014; Accepted in revised form March 24, 2014)

Abstract: Selenium is an indispensable biologically active trace element; being part of the most important enzymes and hormones, it participates in most metabolic processes and has antioxidant properties. The Kuznetsk Basin (Kemerovo oblast) is a region where selenium deficiency is associated with adverse environmental conditions in addition to natural factors; as a result, the population experiences a severe shortage of this trace element. Fortified foods of mass consumption can be a major source of selenium, especially for socially disadvantaged strata. This paper shows the possibility of obtaining wheat with high selenium content in grain in the regional context. It is proved that the most significant factors that ensure wheat with good technological properties are the method, the phase, the amount and multiplicity of selenium application, and the simultaneous introduction of enriching supplements and complex mineral additives. The threshold quantities of selenium supplements are established.

Keywords: selenium, enrichment, wheat, climatic conditions, soils, Kemerovo oblast, technology, grain quality

UDC 664:631

DOI 10.12737/4089

INTRODUCTION

The Kuznetsk Basin is a region with well-developed chemical, metallurgical, and coal industries. Despite the environmental improvements observed in the past years, the situation remains unfavorable. As is known, an unfavorable environment increases the need for various micro- and macroelements to support body functions in aggressive conditions, including the need for selenium, an indispensable biologically active microelement, which is part of major enzymes and hormones; it participates in the majority of metabolic processes and has antioxidant properties [1, 2, 3, 4, 5, 6, 7]. Another important role of selenium is antagonism to heavy metals: mercury, arsenic, and cadmium and, to a lesser extent, to lead and thallium. [8, 9]. Thus, the population of Kemerovo oblast needs adequate selenium consumption; in addition, enriched staple foods can become a major source of selenium, especially for disadvantaged strata.

The adequate consumption of selenium by the human organism, according to various sources, is considered 50–200 mcg/day [9, 10]. Selenium deficiency develops if the human body receives 5 mcg/day of selenium or fewer, the toxicity threshold being 5 mg/day. Russia, according to the methodological recommendations 2.3.1.2432-08 "Norms of Physiological Requirements in Energy and Food Substances for Various Groups of the Population of the Russian Federation," has established requirement levels of 30–75 mcg/day. The physiological requirements are 55 mcg/day for adult women, 70 mcg/day for adult men, and 10–50 mcg/day for children. The upper permissible requirement level is 300 mcg/day.

At present, the main ways of selenium metabolism in the human organism have been decoded: in natural

conditions, selenium enters the human organism mainly as selenium-containing amino acids, selenomethionine (Se–Met) and selenocysteine (Se–Cys); the artificial introduction of selenium into a selenium-deficient organism is possible in the form of sodium selenite or sodium selenate [11].

The main cause of selenium deficiency is its shortfall in humans who live in a biogeochemical province with a low level of this element in foods, soils, and drinking water [9]. The Kuznetsk Basin is among such territories.

The selenium content in phytogenic foods depends on the plant type, the development stage, the geochemical characteristics of a vegetation period, the amount of the element available in soil, microorganism activity, and precipitation. The selenium content in zoogenic foods depends on the amount of the bioaccessible element in feeds [12].

Among foods most rich in selenium are cereal grains and products of their processing (brown bread, wheat, oats), mushrooms, nuts, garlic, horse radish, spinach, onions, pumpkins, strawberries, black currants, and cranberries; as well as meat and fish products [8, 12, 13, 14].

There are the following ways of solving the problem of selenium deficiency in humans.

The use of products with initially (naturally) high selenium contents, including foods imported from selenium-rich regions and countries.

The United States with its both selenium-rich and selenium-poor territories solves this problem by food haulage. There is an efficient practice of importing wheat from selenium-rich regions of Australia, Canada, and the United States, which leads to its increased level in the

blood of New Zealanders, Lithuanians, and Finns, whose soils are poor in this trace element [9, 15, 16].

It is possible to increase the selenium level in plants by enriching fertilizers with various selenium compounds. There is a practice of using fertilizers with various selenium forms [11, 17, 18, 19, 20]. However, this method may lead to intoxication during soil liming; therefore, the level of selenium in soils should be strictly controlled [11, 12, 21].

Finland's experience is illustrative. The optimization of the population's selenium status was accomplished at the national level in various ways: by introducing long-term fertilizer programs, by using biologically active and selenium-containing additives (primarily, baker's yeast enriched with selenium), and by purchasing grain from selenium-endemic countries (the United States, Canada, and Australia) [16, 22]. Slovenia enriches plant products with selenium by spraying plants with sodium selenate solutions; however, the share of selenium adsorbed by plants is low, only about 2–3% of the amount applied. There is a positive practice of enriching grain varieties in Australia [23]. The advisability of enriching corn with selenium was shown in the Republic of Malawi (East Africa) [24].

Taking into account the low selenium status of the region and relying on the available best practices of solving this problem, we set the goal of this work as to probe into the possibility of obtaining high-selenium wheat grain in the natural and climatic conditions of the Kuznetsk Basin.

OBJECTS AND METHODS OF RESEARCH

During the development of a high-selenium wheat technology, we chose as the object of enrichment the In Memory of Aphrodite wheat variety, which was bred by the Kemerovo Research Institute of Agriculture and which is now undergoing variety testing.

Sodium selenite and sodium selenate were tested as enriching additives (EAs).

Grain quality was assessed by the following indicators: color and smell, vitreousness, gluten quantity and quality, acidity, moisture contents, the general and fractional contents of trash and grain impurities, the content of small grains and grain sizes, the content of wheat grains damaged by chinch bugs, the content of foreign metal matters, infestation with pests, and ash contents.

The grain was analyzed by safety indicators at the test laboratory of the Kemerovo Interregional Veterinary Laboratory.

The quantitative content of selenium was determined by the inversion voltammetry method at the STAI analytical voltammetric complex (OOO YuMKh, Tomsk, Russia) using a mercury–graphite electrode, formed in situ (relative to a chlorine–silver electrode). The experiments were conducted with a 5-tuple replication, and the results were processed statistically.

RESULTS AND DISCUSSION

The field experiment was carried out at the Kemerovo Research Institute of Agriculture in 2009–2012 jointly with A.V. Myakashkina [25]. A diagram of the experiment to obtain high-selenium wheat is given in Fig. 1.

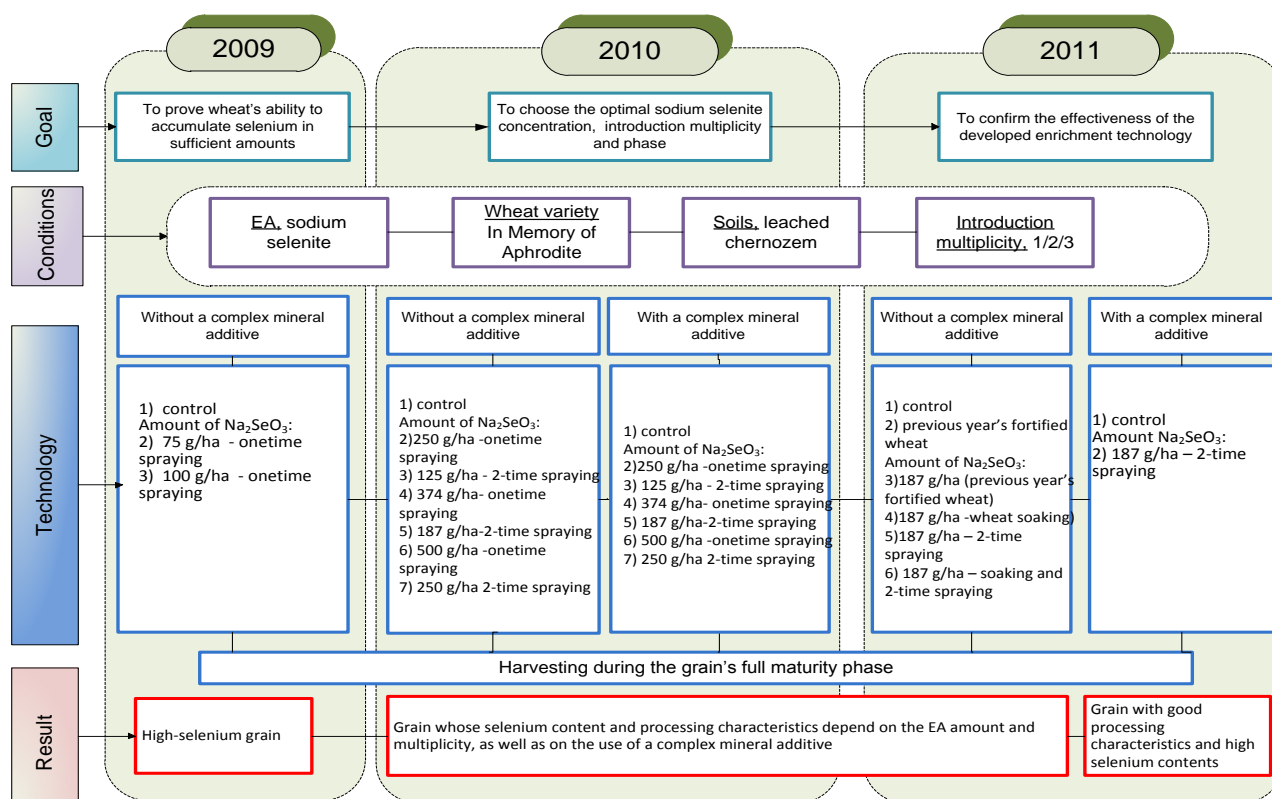


Fig. 1. Diagram of the experiment to grow high-selenium wheat.

The choice of wheat as the object of selenium enrichment was affected by the fact that this is a valuable grain crop capable of accumulating selenium and transforming it into an organic form, selenomethionine; there is a positive foreign experience in this sphere.

The following factors affecting selenium accumulation in plants were identified:

Raw material

1. The choice of wheat variety. As is known, the amount of selenium accumulated in grain depends on the quality and quantity of gluten protein. We chose the In Memory of Aphrodite wheat variety as the object of enrichment, which was bred at the Kemerovo Research Institute of Agriculture and which is characterized by high gluten qualities, as well as by a good resistance to diseases and pests in the conditions of the Kuznetsk Basin.

Variety characteristics: *Lutescens*; the mass of 1000 grains is 34–39 g; the number of kernels in an ear is 24.7–26.7. It is a middle-early variety. Against the infection background, it is poorly infected by dust-brand, powdery mildew, and middle leaf rust, having a high standability. The wet gluten content is 28%. Productivity is 3.26–4.02 t/ha.

2. The choice of the enriching selenium-containing additive. Sodium selenite was chosen as the selenium additive due to the following advantages:

- good water solubility;
- the ability to embed into organic compounds;
- favorable influence on biochemical processes in plants: all methods of treatment with sodium selenite (preplanting, extraroot, and binary) stimulate the extension of the leaf surface and footstalk; as a result, selenium increases the content of chlorophyll, the main photosynthetic pigment, and accelerates plant development, increasing plant biomass; and
- cost effectiveness (currently the cheapest selenium form).

3. The choice of the complex mineral additive was predetermined by the fact that selenium embeds into gluten protein; consequently, the higher the gluten content in grain, the more selenium the wheat can accumulate (up to 50% on average). We assumed that the application of a fertilizer that increased gluten would increase the cumulative properties of wheat in relation to selenium. In this context, we investigated the influence of a complex mineral additive, Master Osobyi (a fully soluble microcrystalline fertilizer (Na-18:P-18:K-18+micro), which contains microelements in the EDTA chelate form (Zn, Cu, Mn, Fe) and which is stable in a wide pH range. It can be used in the most sophisticated irrigation systems and for foliar application; it does not contain sodium, chlorine, and carbonates and has a very high degree of chemical purity, which is a decisive factor of efficient nutrition and foliar dressings, increasing NPK fixation by plants from soil and fertilizer).

Technology

It represents a totality of enrichment parameters: the method, the phase, and the multiplicity of application of the selenium-enriching additive. Several ways of enriching plants with selenium are known:

- applying selenium salts to soil (root irrigation),

- applying selenium-containing fertilizers,
- surface sprinkling with selenium salts, and
- applying selenium salts during seed sprouting.

Analysis of the existing methods of EA application allowed us to identify the following advantages of surface sprinkling:

- enriching plants with selenium through leaves at certain stages of development produces a larger effect than the use of fertilizer, because a plant during vegetation accumulates the largest dose of microelements, which allows us to obtain very high selenium contents in the ready product;
- the soil is not contaminated with selenium salts;
- surface sprinkling is the most economically advantageous way;
- the possibility to use this method does not depend on the properties of the soil where a plant grows; and
- extraroot enrichment makes it possible to deliver the necessary amount of a microelement directly into the plant, where it joins the metabolism several hours after the treatment.

The selenium additive was applied at two phases: the booting stage and the milk-ripe stage on the basis of biochemical processes during plant growth.

Soil and climatic conditions

Soil type influence on selenium contents in plants

The selenium content, as well as that of many other microelements in plants, depends on soil type. For normal selenium accumulation, plants need a fertile soil, the environment's neutral reaction, and the absence (small amounts) of heavy metals.

In the Kuznetsk Basin, three soil-evaluation zones were identified: low-, medium-, and high-bonitet soils (soil bonitation (from Latin *Bonitas*, goodness) is a relative evaluation of soils by their productivity).

By the degree of soil erosiveness, the Kuznetsk Basin falls into zones IV, V, VI, and VII, which are characterized by medium-to-small deflation, weak-to-strong washout, and, starting from zone VI, the soils are susceptible to the development of erosion processes. Table 1 shows data about the possibility of enriching plants with selenium depending on soil type, erosion zone, and soil bonitet, all other conditions being equal.

The analysis of soil characteristics has shown that the following six districts of the oblast are the most favorable for growing high-selenium wheat: Leninsk-Kuznetskii, Promyshlennovskii, Topki, Yurga, and Kemerovo. Chernozem and gray forest soils with their good fertility, high extent (7) of agricultural development, large plow land area, and bonitet prevail in these districts. The other districts are suitable for growing fortified stock, but, taking into account soil erosion and washout, there is the probability of a reduced efficiency of fortification.

Influence of climatic conditions on selenium accumulation

Since the gluten content in grain is 30% dependent on favorable climatic conditions, the growing of high-quality grain needs a sufficient amount of moisture, a relatively high air temperature, and intensive insolation. In addition, each plant-development phase requires its own temperature regime and rainfall. Table 2 gives aggregate data about climatic conditions in the Kuznetsk Basin in the 2009–2011 summer periods.

Table 1. Characteristics of the Kuznetsk Basin' soils by district

Soil type	Soil erosion zones	Soil bonitet zones	District	suitable/unsuitable for enrichment
Chernozem and gray forest soils	IV zone	High	Belovo	++
Chernozem and gray forest soils	IV zone	High	Leninsk-Kuznetskii	++
Chernozem and gray forest soils	IV zone	High	Promyshlennovskii	++
Chernozem and gray forest soils	VI zone	High	Prokopyevsk	+
Chernozem and gray forest soils	IV zone	High	Topki	++
Chernozem and gray forest soils	IV zone	High	Yurga	++
Podzolized chernozem	IV zone	Medium	Kemerovo	++
Sod-podzol and podzolized gray forest soils	V zone	Medium	Yaya	+
Sod-podzol and podzolized gray forest soils	V zone	Medium	Mariinsk	+
Sod-podzol and podzolized gray forest soils	V zone	Medium	Tyazhinskii	+
Sod-podzol and podzolized gray forest soils	VII zone	Medium	Tisul'	+
Sod-podzol and podzolized gray forest soils	VII zone	Medium	Novokuznetsk	+
Podzolized gray forest soils	IV zone	High	Krapivinskii	+
Podzolized gray forest soils	V zone	Medium	Izhmorskii	+
Sod-podzol and podzolized gray forest soils	VII zone	Medium	Chebula	+
Sod-podzol, light-gray and gray soils.	V zone	Low	Yashkino	+

++ well-suited for enrichment, + poorly suited for enrichment

Table 2. Meteorological conditions in the Kuznetsk Basin, 2009–2011

Indicators	May				June				July				August			
	Ten-day periods			Per month												
	1	2	3		1	2	3		1	2	3		1	2	3	
Average annual air temperature, °C	7.1	9.3	12.7	9.7	15.0	16.1	17.8	16.3	18.9	18.9	18.7	18.8	17.5	15.7	13.1	15.4
Average annual precipitation, mm	13	15	17	43	16	22	25	63	16	24	24	64	21	17	21	59
Air temperature, °C																
2009	9.3	14.3	11.4	11.7	16.2	12.2	13.4	13.9	18.6	20.8	18.2	19.1	17.4	14.7	16.1	16.1
2010	6.2	6.4	12.7	8.6	15.9	18.5	15.6	16.7	16.9	18.9	15.3	17.0	15.3	13.8	16.9	15.4
2011	6.2	6.4	12.7	8.6	15.9	18.5	15.6	16.7	16.9	18.9	15.3	17.0	15.3	13.8	16.9	15.4
Precipitation, mm																
2009	22	9	24	55	54	12	36	102	24	12	36	72	38	7	17	62
2010	7	9	13	29	5	1	17	23	53	39	44	136	48	20	5	73
2011	7	9	13	29	5	1	17	23	53	39	44	136	48	20	5	73
Hydrothermal index 2009			1	1.3				2.4				1.3				1.3
Hydrothermal index 2010				1.00				0.46				2.60				1.53
Hydrothermal index 2011				1.00				0.46				2.60				1.53

The 2009 vegetation period was characterized by good moisture provision until the heading phase of the grain crops. Precipitation in June and May was 55 and 102 mm, respectively, which was above the norm by 28–63%. The temperature was slightly below the norm but sufficient for forming good quantitative indicators of wheat quality. The second half of vegetation was more arid compared to the first half: 72 mm of rainfall

in July (the norm being 64 mm) and 62 mm of rainfall in August (the norm being 59 mm). The average daily temperatures in July exceeded the norm, creating, in combination with reduced humidity, an "uncomfortable" atmosphere for plant development and increasing the probability of obtaining dry feeble grain. The ripening of spring wheat by calendar days went until September 15. The hydrothermal index (HTC), the ratio of

precipitation to evaporated moisture, during the period of grain formation and filling was 1.3.

The 2010 vegetation period was characterized by insufficient moisture provision until the heading phase of grain crops. The rainfall in June and May was 23 and 29 mm, respectively, which was 63–67% of the norm, in consequence of which the quantitative characteristics of the grain suffered. In the second half of vegetation, an abundant rainfall was observed: 136 mm in July (the norm being 64 mm) and 124 mm in August (the norm being 59 mm). The low average daily temperatures in July, limited sunshine, and excessive moisture increased the length of the vegetation period of grain crops. The ripening of spring wheat by calendar days went until September 15 and longer. Ripening unevenness was observed; 50% and more of stalks were behind in development phases the main haulm stand. The HTC during grain formation and filling was 1.53–2.60.

The 2011 vegetation period was characterized by insufficient moisture provision during the planting–tillering period of grain crops, which largely affected the formation of the reproductive organs. During the tillering period of spring wheat, HTC = 0.2–0.6, which affected negatively the formation of wheat productivity. Moisture shortages in May and June were accompanied

by high temperatures, by 2–3°C higher than the norm.

The flowering period (the beginning of milk ripeness) was characterized by high average daily temperatures, 19.5°C, and nonproductive rainfall, 2.0 mm; HTC = 1.1. This did not provide the kernels with the necessary amount of moisture, which, in turn, affected gluten quality. During the grain filling period, a sufficient moisture provision was observed; HTC = 1.3; and the number of sunshine hours was 20 below the norm. The harvest time was accompanied by periodic rains.

Thus, the most favorable period for growth, grain development, and gluten accumulation was the summer of 2009.

Analysis of sensitivity of grain quality to fortification methods

Test results of 2009

The goal of the experiments in 2009 was to prove the hypothesis of the possibility of wheat fortification by the example of the In Memory of Aphrodite variety in the conditions of Kemerovo oblast. Moreover, of special interest was to establish the effect of EAs on productivity.

The results of field tests (Table 3) confirmed this hypothesis: the findings showed that the In Memory of Aphrodite wheat variety was suitable for enrichment with selenium by the surface sprinkling method in the conditions of Kemerovo oblast.

Table 3. Enriching additive's effect on wheat yields and selenium contents in grain, 2009

Indicator	Sample no.		
	No. 1 (Control)	No. 2	No. 3
Introduction method	=	Surface spraying	Surface spraying
Concentration of Na ₂ SeO ₃ solution, %	0	0.025	0.05
Amount of sodium selenite applied, g/ha	0	75	125
Total amount of sodium selenite introduced per 1 ha	0	60 g/250 L	125 g/250 L
Planting date	May 20, 2009		
Harvesting date	15.09.2009 г.		
Yield, t/ha	2.72 ± 0.024	2.75 ± 0.024	2.80 ± 0.024
Amount of selenium in grain, mg/kg	0.010 ± 0.002	0.015 ± 0.0037	0.027 ± 0.0037

In their quality, the samples are competitive with the control group and correspond to the requirements for commercial grain. It was established that wheat samples treated with sodium selenite exceeded the control group by their linear dimensions: by up to 25% in length and by up to 50% in width. The difference compared to the control group of an indicator such as the mass of 1000 grains was about 3%; the acidity decreased with the increased concentration of the salt applied.

The application of sodium selenite affected the productivity insignificantly; the samples treated with sodium selenite showed a positive tendency to increase productivity.

The mathematical treatment of the data obtained by the correlation analysis method (after Pearson) show the reciprocal influence of various qualitative characteristics on one another: indicators such as gluten and selenium contents in grain are interdependent and directly proportional; i.e., the more the gluten in grain, the larger the selenium content is.

Test results of 2010

At this stage, we studied the effect of irrigation

multiplicity and the presence of fertilizer, as well as determined the optimal amount of sodium selenite to apply. To this end, we simulated 14 wheat samples that differed in all the above characters.

The evaluation of the grain quality of these wheat samples showed that, by organoleptic indicators, all the experimental samples were as good as the control group. The data about the quantity and quality of gluten in the samples are given in Table 4.

In the table results, we can trace a dependence of gluten quantity on the multiplicity of sodium selenite application and on the use of the Master Osobyi complex mineral additive. All other conditions being equal, the application of this additive contributes to an increase in the gluten amount by 10–17% on average.

In the table results, we can trace a dependence of gluten quantity on the multiplicity of sodium selenite application and on the use of the Master Osobyi complex mineral additive. All other conditions being equal, the application of this additive contributes to an increase in the gluten amount by 10–17% on average.

Table 4. Grain yields and selenium contents, 2010

Sample no.	Amount of Na ₂ SeO ₃ , applied, g/ha	Irrigation multiplicity, times	Amount of fertilizer applied, kg/ha	Amount of selenium in grain, mg/kg	Yields, t/ha
Sample no. 1	0	1	0	0.01 ± 0.015	2.69 ± 0.74
Sample no. 2	0	1	4	0.01 ± 0.015	2.74 ± 0.248
Sample no. 3	224	1	0	0.017 ± 0.021	2.76 ± 0.248
Sample no. 4	224	1	4	0.023 ± 0.009	2.83 ± 0.496
Sample no. 5	112	2	0	0.020 ± 0.004	2.76 ± 0.248
Sample no. 6	112	2	4	0.023 ± 0.009	2.90 ± 0.248
Sample no. 7	374	1	0	0.033 ± 0.009	2.6 ± 0.496
Sample no. 8	374	1	4	0.040 ± 0.007	2.7 ± 0.496
Sample no. 9	187	2	0	0.030 ± 0.002	3.0 ± 2.484
Sample no. 10	187	2	4	0.049 ± 0.004	3.32 ± 2.484
Sample no. 11	500	1	0	0.047 ± 0.002	1.5 ± 0.248
Sample no. 12	500	1	4	0.050 ± 0.007	1.5 ± 0.248
Sample no. 13	250	2	0	0.042 ± 0.012	2.78 ± 2.484
Sample no. 14	250	2	4	0.051 ± 0.004	2.85 ± 2.484

In the table results, we can trace a dependence of gluten quantity on the multiplicity of sodium selenite application and on the use of the Master Osobyi complex mineral additive. All other conditions being equal, the application of this additive contributes to an increase in the gluten amount by 10–17% on average.

After a onetime application of sodium selenite at a high concentration (500 g/ha), a grain class reduction was observed, probably, due to the negative influence of high concentrations of sodium selenite on plant development; after a two-time application of sodium selenite, the concentration of selenium in the solution was significantly lower, which positively affected plant growth and development, and samples treated with sodium selenite at stage 2 contained by 5–11% more gluten, the difference with the control group reaching 17%.

In 2010 the use of sodium selenite also affected the linear dimensions of wheat grains: as the salt concentration increased to 374 g/ha, the grain dimensions increased (the length, up to 7%, the width, up to 30%); in addition, three factors influenced this indicator: the amount of sodium selenite applied, the multiplicity of its application, and the use of fertilizer. After a onetime application of sodium selenite at a concentration of 500 g/ha, the biometric characteristics of grain deteriorated, and the grain became hollow. After the application of the same amount of salt at stage 2, the indicators did not decrease but rather increased compared to the control group by 16–25%. The application of the complex mineral additive also affects this indicator: the linear dimensions of the grain exceeded those of the

samples not treated by fertilizer.

The largest amount of selenium accumulated by wheat, 0.051 mg/kg (sample 14), was obtained during surface sprinkling of plants with sodium selenite in the amount of 250 g/ha. The second largest in selenium content was sample 12; however, a onetime EA application led to the inhibition of plant growth and reduced productivity. Sample 10 also showed good results although the amount of selenite used was much lower, which was economically more profitable. Moreover, this sample had the highest productivity.

Since the selenium content in the grain of samples 14, 12, and 10 was approximately the same (within the experimental error), we may assume that the two-time application of sodium selenite in the amount of 187 g/ha together with the use of the complex mineral additive is optimal (sample 10).

Test results of 2011

The main goal of research in 2011 was to confirm the data obtained in 2010. In addition, it was interesting to study plant growth and development from wheat grains with the high selenium content of the 2010 harvest, as well as to evaluate the effect of seed soaking in a sodium selenite solution before planting.

All the samples showed sufficiently good qualitative results, but the samples treated only with surface sprinkling had better indicators than the samples with seeds soaked before planting. The results of determining selenium contents in the wheat of 2011 and wheat productivity are given in Table 5.

Table 5. Grain yields and selenium contents, 2011

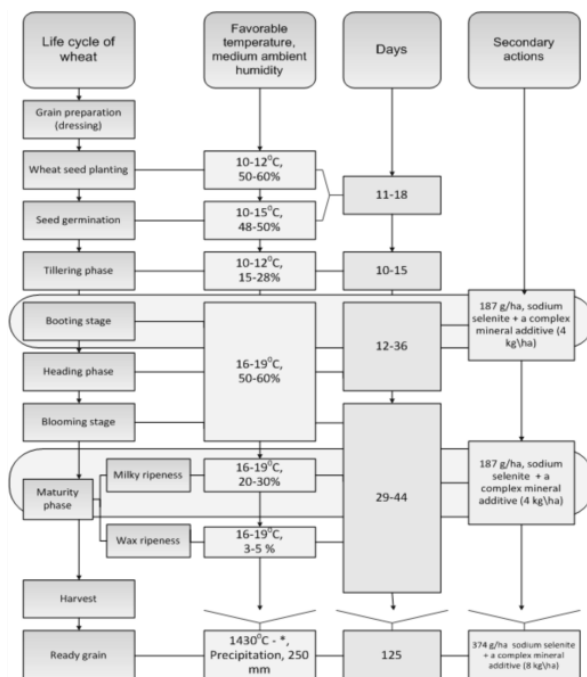
Sample no.	Amount of Na ₂ SeO ₃ , applied, g/ha	Application multiplicity, times	Amount of fertilizer applied, kg/ha	Amount of selenium in grain, mg/kg	Yields, t/ha
Sample no. 1	0	0	0	0.01 ± 0.015	2.69 ± 0.74
Sample no. 2*	0	0	0	0.015 ± 0.015	2.74 ± 0.248
Sample no. 3**	187	1	0	0.020 ± 0.024	2.76 ± 0.248
Sample no. 4*	187	1	0	0.037 ± 0.024	2.83 ± 0.496
Sample no. 5**	187	2	0	0.052 ± 0.049	2.76 ± 0.248
Sample no. 6	187	2	4	0.087 ± 0.024	2.90 ± 0.248
Sample no. 7	187	3	0	0.085 ± 0.024	2.6 ± 0.83

* seed from the 2010 crop grain, ** seed soaked in a sodium selenite solution before planting

It follows from the table data that the 2011 results on the whole confirm the data obtained in 2009–2010: the two-time treatment of wheat with sodium selenite in the amount of 187 g/ha leads to an increase in productivity by 7–30%; moreover, the application of the Master Osobyi mineral additive helps increase the ability to accumulate selenium by more than 60%. Sample 7 decreased its productivity by 13%; we may assume that EA application in amounts of more than 500 g/ha even in series leads to the inhibition of plant development and the reduction of productivity.

The 2011 results also showed the inadvisability of using high-selenium seed for planting: the selenium content in grain grown from it was higher than in the control group but fairly low, 0.015 mg/kg (before planting, 0.030 mg/kg); we may assume that selenium was used during plant growth and development. Seed soaking in a sodium selenite solution before planting led to an insignificant increase of selenium in the finished grain.

Our research has shown that it is possible to grow high-selenium wheat in the conditions of the Kuznetsk Basin. The result of the 2009–2011 research was a technology of fortifying wheat with selenium, which is given in Fig. 2 and the main elements of which are the life cycle of plant growth and development, the most favorable meteorological conditions, and the phases of EA and fertilizer application. The novelty of the proposed high-selenium wheat method was confirmed by a Russian patent.



Note: * 1430°C is the sum of positive temperatures (above 5°C) during the vegetation period (75–110 days)

Fig. 2. Technology of enriching wheat with selenium.

REFERENCES

- Zubarevich, L.A., *Soedineniya selena i zdorov'e* (Selenium Compounds and Health) (KoloS, Moscow, 2004).
- Selen v zhizni cheloveka i zivotnykh* (Selenium in Human and Animal Life), ed. by Nikitina, L.P. and Ivanova, V.N. (VINITI, Moscow, 1995).
- Shchelkunov, L.F., Dudkin, M.S., Golubkina, N.A., et al., Selen i ego rol' v pitanii (Selenium and its role in nutrition), *Gigiena Sanitariya* (Hygiene Sanitation), 2000. № 5. P. 32.
- Brown, K.M. and Arthur, J.R., Selenium, selenoproteins, and human health: A review, *Public Health Nutrition*, 2001. № 4. P. 593.
- Tutel'yan, B.A., Knyazhev, N.E., Khotimchenko, S.A., et al., *Selen v organizme cheloveka: metabolizm, antioksidantnye svoistva, rol' v kantserogeneze* (Selenium in the Human Organism: Its Metabolism, Antioxidant properties, and Role in Carcinogenesis) (Izd. Ross. Akad. Med. Nauk, Moscow, 2002).
- Cénac, A., Simonoff, M., Moretto, P., and Djibo, A., A low plasma selenium is a risk factor for peripartum cardiomyopathy: A comparative study in Sahelian Africa, *Int. Journ. Cardiol.*, 1992. № 36. P. 57.
- Contempre, B., Dumont, J.E., Deneff, J.F., et al., Effects of selenium deficiency on thyroid necrosis, fibrosis, and proliferation: A possible role in myxoedematous cretinism, *Eur. Journ. Endocrinol.*, 1995. № 133. P. 99.
- Skal'nyi, A.V. and Kudrin, A.V., *Radiatsiya, mikroelementy, antioksidanty, i immunitet (mikroelementy i antioksidanty v vosstanovlenii zdorov'ya likvidatorov avarii na ChAES)* (Radiation, Microelements, Antioxidants in the Recovery of the Health of Liquidators of the Chernobyl Nuclear Accident) (Lir Market, Moscow, 2000).
- Tutel'yan, B.A., Knyazhev, N.E., Khotimchenko, S.A., et al., *Selen v organizme cheloveka: metabolizm, antioksidantnye svoistva, rol' v kantserogeneze* (Selenium in the Human Organism: Its Metabolism, Antioxidant properties, and Role in Carcinogenesis) (Izd. Ross. Akad. Med. Nauk, Moscow, 2002).
- Aro, A., in *Expert Group Papers of the Workshop on Addition of Nutrients to Food: Nutritional and Safety Consideration*, (ILSI Press, Lisbon, 1997). P. 1.
- Golubkina, N.A., Skal'nyi, A.V., Sokolov, Ya.A., et al., *Selen v meditsine i ekologii* (Selenium in Medicine and Ecology) (KMK, Moscow, 2002).
- Problemy biogeokhimii i geokhimicheskoi ekologii* (Problems of Biogeochemistry and Geochemical Ecology), ed. by Ermakov, V.V. (Nauka, Moscow, 1999).
- Volkotrub, L.P. and Andronova, T.V., Rol' selena v razviti i preduprezhdenii zabolovani (The role of selenium in the development and prevention of diseases), *Gigiena sanitariya* (Hygiene Sanitation), 2001. № 3. P. 57.
- Golubkina N.A., Vliyanie geokhimicheskogo faktora na nakoplenie selena zernovymi kul'turami i sel'skokhozyaistvennymi zivotnymi v usloviyakh Rossii, stran SNG i Baltii (The effect of the geochemical factor on the selenium accumulation by cereal grains and farm animals in Russia), *Problemy regional'noi ekologii* (Probl. Reg. Ecol.), 1998. № 4. P. 94.

15. *Selen v zhizni cheloveka i zivotnykh* (Selenium in Human and Animal Life), ed. by Nikitina, L.P. and Ivanova, V.N. (VINITI, Moscow, 1995).
16. Aspila, P., History of selenium supplemented fertilization in Finland, in *Proceedings: Twenty Years of Selenium Fertilization*, ed. by Eurola, M. (Helsinki, 2005). P. 8.
17. Gorelikova, G.A., Mayurnikova, L.A., and Poznyakovskii, V.M., Nutritsevtik selen: nedostatochnost' v pitanii, mery ptofilaktiki (Nutraceutical selenium: Insufficiency in nutrition, prevention measures), *Vopr. pitaniya* (Probl. Nutrition), 1997. № 5. P. 8.
18. Zhang, J.-S., Biological effects of nano red elemental selenium, *BioFactors*, 2001. V. 15. P. 27.
19. Mayurnikova, L.A., Shigina, E.V., and Gorelikova, G.A., Deficit selena i puti ego korrleksii v organizme cheloveka (Selenium deficiency and ways of its correction in the human organism), *Pivo napitki* (Beer Beverages), 2005. № 1. P. 34.
20. Broadley, M. R., Alcock, J., Alford, J., Cartwright, P., Fairweather-Tait, S.J., Foot, I., Hart, D.J., Hurst, R., Knott, P., McGrath, S.P., Meacham, M.C., Norman, K., Mowat, H., Scott, P., Stroud, J.L., Tovey, M., Tucker, M., White, P.J., Young, S.D., and Zhao, F.J., Selenium biofortification of high-yielding winter wheat (*Triticum aestivum* L.) by liquid or granular Se fertilization, *Plant Soil*, 2010. V. 332, P. 5.
21. Gromova, O.A. and Gogoleva, I.V., Selen - vpechatlyayushchie itogi i perspektivy primeneniya (Selenium: Impressive results and prospects of application), *Trudnyi patsient* (Hard Patient), 2007. № 14. P. 25.
22. Eurola, M., Ekholm, P., Ylinen, M., Koivistonon, P., and Varo, P., Effects of selenium fertilization on the selenium content of cereal grains, flour, and bread produced in Finland, *Cereal Chem.*, 1990. V. 67. № 4. P. 334.
23. Sager, M. and Hoesch, J., Selenium uptake in cereals grown in lower Austria, *Journ. Central Eur. Agric.*, 2006. V. 7. № 1. P. 71.
24. Chilimba, A.D.C., Potential for safe and efficient biofortification of maize crops with selenium in Malawi, *PhD. Dissertation*, Univ. of Nottingham, 2011.
25. Myakashkina, A.V., Identification and analysis of factors that form the quality of wheat with high selenium contents, *Cand. Sci. (Eng.) Dissertation*, Kemerovo, 2012. 156 p.



EFFECT OF VACUUM DRYING ON MICROSTRUCTURE OF SEMI-SOLID CHEESE

V. A. Ermolaev

Kemerovo Institute of Food Science and Technology,
bul'v. Stroitelei 47, Kemerovo, 650056 Russia,
phone: +7 (904) 965-85-39, e-mail: ermolaevvla@rambler.ru

(Received January 29, 2014; Accepted in revised form February 28, 2014)

Abstract: Both theoretical and applied studies on microstructure of cheese immediately after a technological cycle and dry cheese obtained by vacuum drying are described. The aim of the microstructure studies is a more comprehensive evaluation of the product quality. Images of cheese upon high- and low-temperature secondary heating at different magnification were studied. The effect of drying on cheese microstructure was investigated. Analysis and identification of various components in the cheese mass using microstructure studies were performed. Calcium phosphate depositions were detected with electron microscopy. Calcium lactate was detected in mature cheese.

Keywords: microstructure, vacuum drying, cheese, microvoids, macrograins, residual pressure, temperature, shrinkage, pores

UDC: 637.35.04
DOI 10.12737/4113

INTRODUCTION

Vacuum drying, performed at residual pressure above the water triple point, is one of the most advanced methods of food products dehydration. In Russia, it has been widely used in chemical, pharmaceutical, medical, food, and other industries, that is, in the areas where materials are especially sensitive to the effects of high temperatures [1–4].

Vacuum dryers allow for a product of high purity and quality. In function of the material properties and requirements to the final product, time of drying and temperature modes vary. Vacuum drying proceeds in two stages. During the first stage, drying rate is constant and the material temperature is close to the temperature of water saturation at given pressure. During the second stage, the rate of drying decreases and the material temperature increases approaching the temperature of the heat transfer medium. Intensity of heat transfer in the second stage decreases sharply. Increase in the rate of water evaporation in vacuum dryer may be achieved by increase in the temperature of the heat transfer medium or decrease of pressure [2, 5].

Considering cheese as a subject of vacuum drying, it should be noted that changes in cheese properties in the process of drying depend on both physicochemical properties, structure, and forms of moisture deposition in the material on one hand and thermophysical characteristics accounting for mass and energy transfer features on the other. Major structural elements of cheese are macrograins, layers between them, microvoids, and micrograins [6, 7]. Protein network forms the basis of each macrograin, while micrograins are embedded into its cells as lipid or lipoid drops or depositions of crystals [8, 9].

All structural components of cheese undergo deep changes in the course of maturation, producing texture and pattern typical of the cheese variety [5, 10–12].

Knowledge on changes in capillary structure of cheese mass in the course of ageing and further storage is required for correct design of the drying process.

In connection with the entry of large volumes and assortment of domestic and imported dairy products, including the concentrated ones, in the market, thorough and comprehensive control of the source composition and how it meets the requirements of the current standards is needed. Today, the main document regulating the dairy products, including cheese, is the Technical regulations of milk and dairy products, according to which evaluation of quality and identification of milk processing products proceed basing on the major physicochemical, organoleptic, and microbiological parameters. For the most thorough control of the dairy products source materials, different methods are used.

Internationally, histology methods of composition identification are used to control quality and exclude the possibility of adulteration of dairy products [13–16].

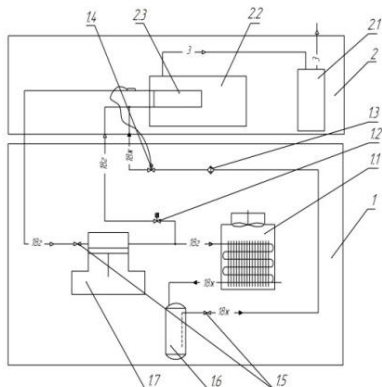
Today, one of the modern methods is scanning electron microscopy, allowing for investigation of structure of aged cheese prior to realization and dry cheese, upon vacuum drying [17, 18].

MATERIALS AND METHODS

The semi-solid rennet cheese varieties Sovetskii, Gollandskii, and Ozernyi were the subjects of the study. Vacuum drying of cheese was performed on an INEI-6M freeze-dryer (Laboratory of methods and instruments for biochemical analysis, Institute for Biological Instrumentation, Russian Academy of Sciences) (Fig. 1).

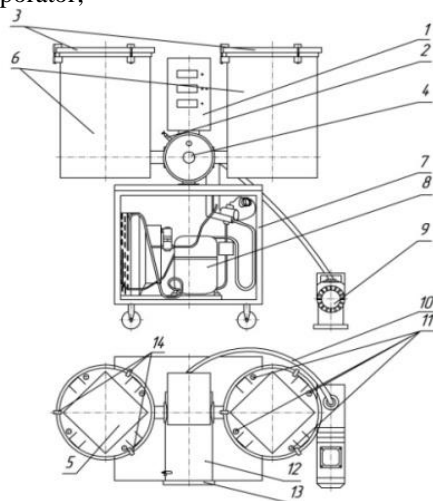


(a), outside appearance;



(b), principal scheme of the freeze-dryer:

1, freezer; 1.1, condenser; 1.2, solenoid valve; 1.3, drying filter; 1.4, thermostatic expansion valve; 1.5, cut-off valve; 1.6, receiver; 1.7, compressor; 2, vacuum unit; 2.1, vacuum pump; 2.2, desublimator; 2.3, evaporator;



(c), sublimation unit design:

1, control panel; 2, pressure release valve; 3, drying chamber lid; 4, evaporator; 5, product shelf; 6, drying chamber; 7, refrigerator unit bucket; 8, refrigerator unit; 9, vacuum pump; 10, vacuum pump flexible tubing; 11, incandescent lamp; 12, desublimator; 13, desublimator lid; 14, fixator of the drying chamber lid.

Fig. 1. «INEI-6M» freeze-dryer.

The refrigerator unit of the sublimation dryer is designed to remove moisture evaporating from the product in the process of drying through condensation on the surface of evaporator, since the temperature of the latter one is much lower than the dew point temperature (-35 – 45) $^{\circ}\text{C}$). Because of this, partial pressure over the surface of evaporator is lower than the partial pressure of water vapor in the drying chamber under conditions of residual pressure of 10–100 Pa in the system.

The process of drying consists of the following stages. The product is placed on the shelves 5, which are put into the drying chambers 6. The chambers are closed with the lids 3. The refrigerator unit 8 is turned on using the control panel 1; then, the instrument takes approximately 10–15 min to reach the freezing out mode. The freezing out mode is detected by the evaporator temperature 4 (the temperature should not be higher than -35 $^{\circ}\text{C}$), then the vacuum pump 9 is turned on, and the drying mode starts. Due to the low pressure in the chambers, the product is frozen and sublimation starts. Then, incandescent lamp 11 is turned on and the product is heated to remove residual water [19, 20].

Microstructure studies and elaboration of the electron microscopy technique application to cheese samples were performed on a JEOL JSM-6390 LA (JEOL, Japan) scanning electron microscope.

RESULTS AND DISCUSSION

Quality of the material being dried depends on the preparation of the material, rate, and evenness of drying. For maximum retaining of all the initial properties of the product, the material should be of high quality, since high-quality products are more appropriate by their physicochemical composition, and their structure is undamaged; therefore they would be more fully-featured when dried. In this connection, only the high-quality cheese was used for drying. Figure 2 presents cross section of freeze-dried cheese.

Upon vacuum drying, cheese dimensions practically did not change and it became porous. Prior to drying, linear dimensions of Sovetskii and Gollandskii cheese samples were 117 and 120 mm, and after drying, 114 and 115 mm, respectively. Diameter of the Ozernyi cheese prior to drying was 130 mm, and after drying, 124 mm. Linear shrinkage of cheese in the process of vacuum drying occurs only by 3–5%. Mass fraction of water in cheese samples did not exceed 5%. Vacuum drying was performed at 2–3 kPa.

Figures 3–8 present images of microstructure of Sovetskii, Gollandskii, and Ozernyi cheese samples before and after the vacuum drying. For convenience of microstructure analysis and comparison of capillary structure of the cheese mass, the same magnification, that is, 50, 200, and 2000-fold magnification, was used for all samples.



(a)



(b)



(c)



(d)

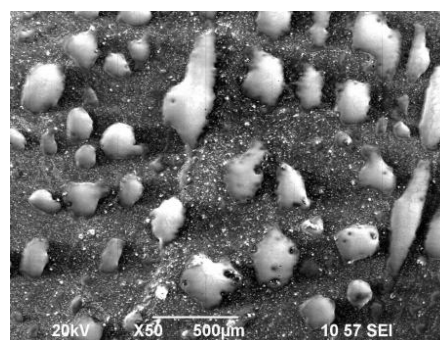


(e)

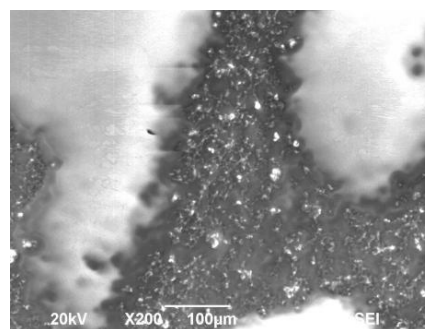


(f)

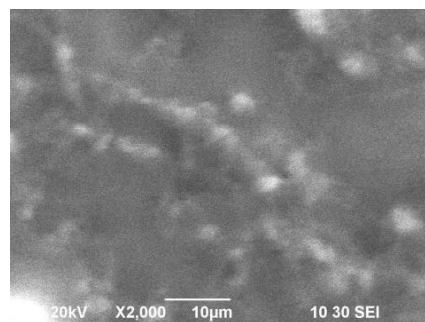
Fig. 2. *End.* Cross sections of cheese of different varieties before (a, c, and e) and after (b, d, and f) freeze-drying: (a, b) cheese variety Sovetskii; (c,d) Gollandskii; and (e, f) Ozernyi.



(a)



(b)



(c)

Fig. 3. Microstructure of the Sovetskii cheese sample prior to drying: (a) magnification of 50×; (b) 200×; and (c) 2000×.

Structure, texture, and pattern of cheese characterize the correctness of the development of biochemical and physicochemical processes upon cheese production. The structure of the dense product is the size and spatial arrangement of individual particles or components.

Each type of cheese has its own microstructure, but in general, the structure of all rennet cheese varieties contains the same structural elements. Its macrograins contain various inclusions, or micrograins.

Fat globules from 50 to 300 μm in size are evenly spread over the cheese surface. At magnification of 1000× and 2000×, cell-like structure of the cheese mass is observed. The cell-like structure is formed by protein matrix with capillaries of 10–12 μm retaining moisture. After vacuum drying, structure of cheese unfolds. In dry cheese, due to low water content of 4–7 %, structure and capillaries, which were not detected in the microimages of cheese before drying, are better seen.

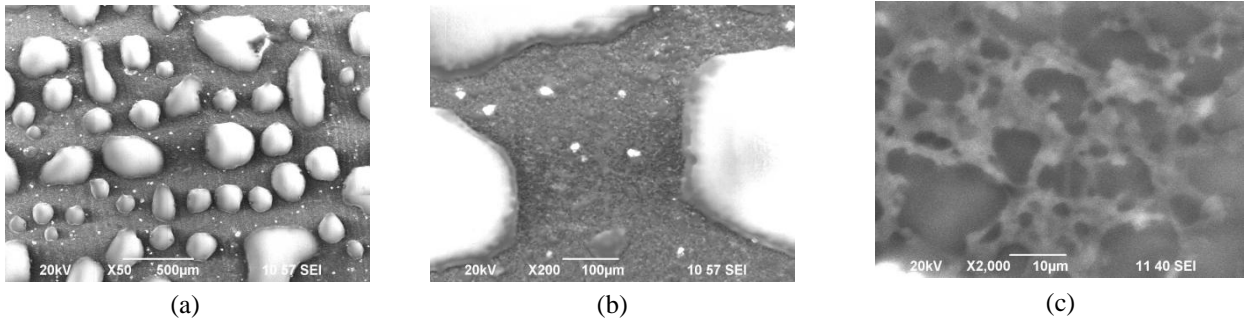


Fig. 4. Microstructure of the Gollandskii cheese sample prior to drying: (a) magnification of 50×; (b) 200×; and (c) 2000×.

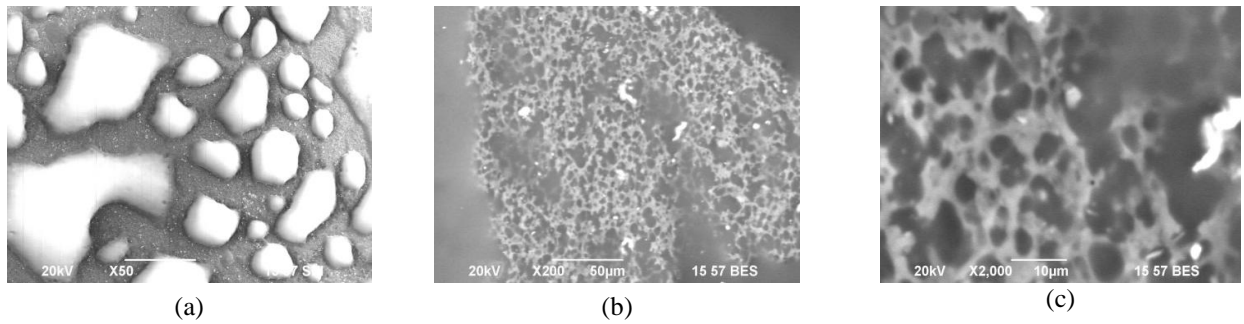


Fig. 5. Microstructure of the Ozernyi cheese sample prior to drying: (a) magnification of 50×; (b) 200×; and (c) 2000×.

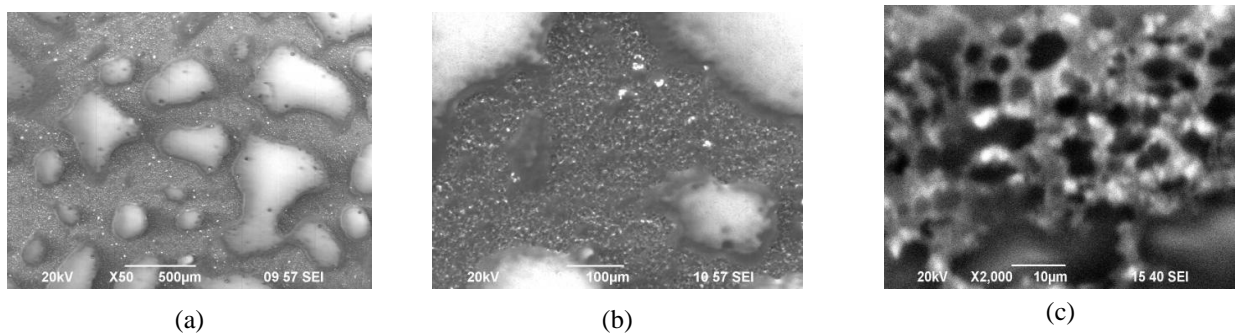


Fig. 6. Microstructure of the dried Sovetskii cheese sample: (a) magnification of 50×; (b) 200×; and (c) 2000×.

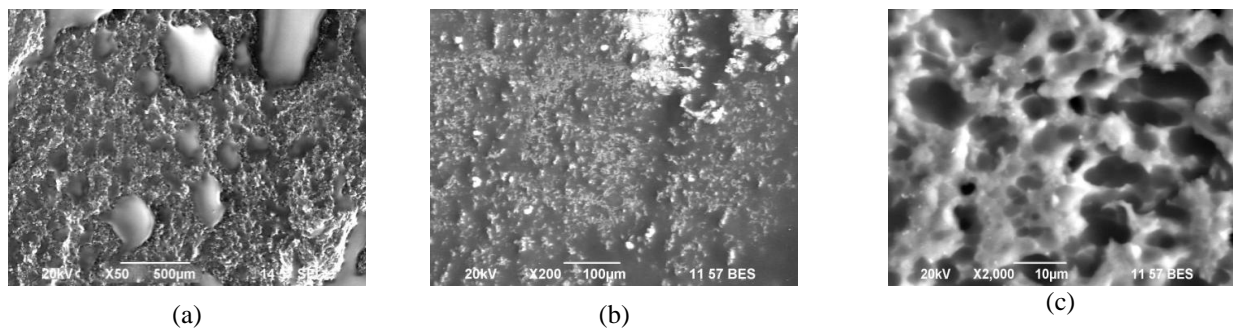


Fig. 7. Microstructure of the dried Gollandskii cheese sample: (a) magnification of 50×; (b) 200×; and (c) 2000×.

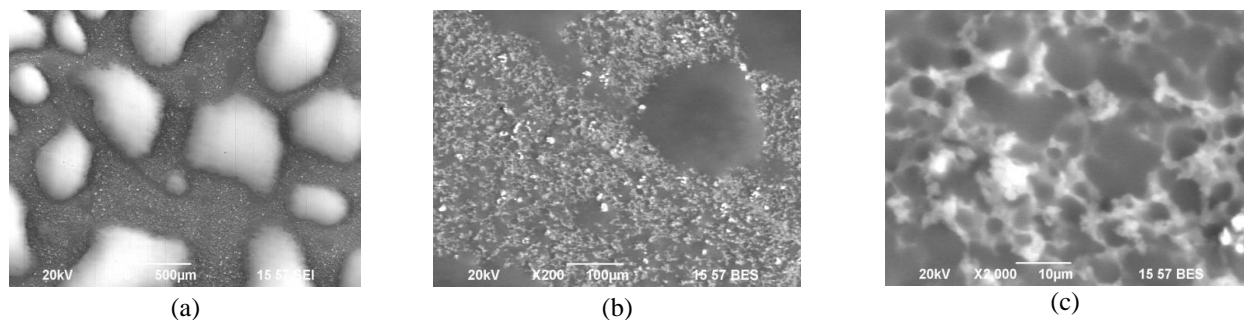


Fig. 8. Microstructure of the dried Ozernyi cheese sample: (a) magnification of 50×; (b) 200×; and (c) 2000×.

After the dryer has reached the residual pressure mode, heating is turned on, water boils rather soon at the low pressure, and leaves the protein mass of the cheese. Intensive vapor formation and moisture diffusion from the cheese surface occur. Size of capillaries containing the moisture do not change after drying and even become larger, reaching 5–15 μm .

After drying, fat globules merge into larger shapes with size reaching from 100 to 700 μm , that is, fat globule size in the dry cheese is almost twice as large as in cheese before drying. Studies on microstructure of different solid cheese varieties proved that no shrinkage of cheese occurs upon vacuum drying.

Electron microscopy revealed calcium phosphate depositions in cheese. In the course of microstructure studies of cheese sample before and after drying, individual particles contained in cheese ionized in the electron beam and produced g by low on the microimages (Fig. 9).

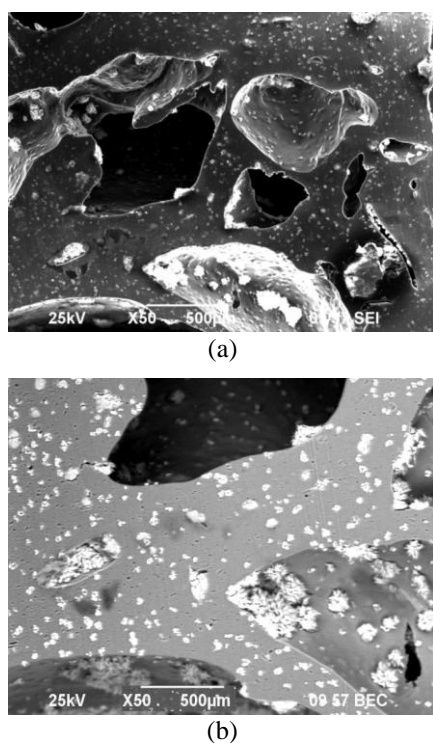


Fig. 9. Depositions of calcium salts in Kostromskoi cheese sample: (a) before and (b) after drying.

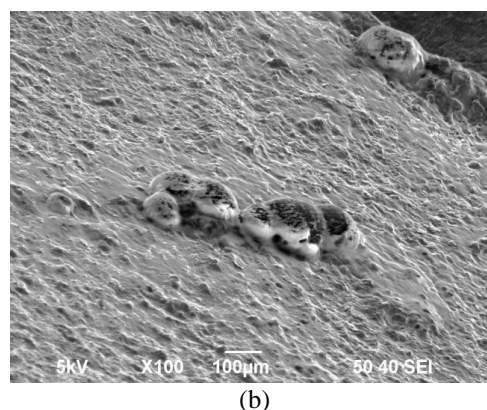
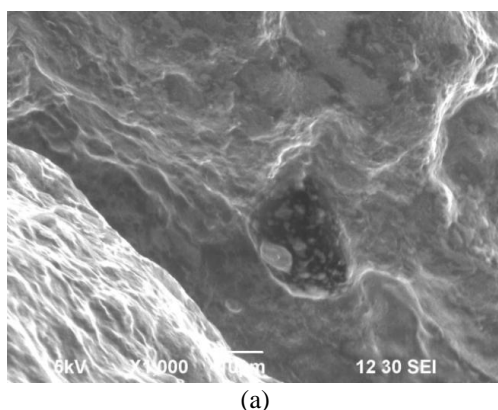


Fig. 11. Calcium lactate in mature cheese samples: (a) Kostromskoi and (b) Rossiiskii.

To identify the particles, analysis of element distribution over the cheese mass was performed. Maps of element distribution in cheese before and after drying were obtained. In the maps of element distribution, sites of phosphate and calcium localization are distinctly seen. Locations of phosphate and calcium overlap. Also, these sites overlap with the glowing particles in the images.

Calcium phosphate shows weak conductivity. Under the effect of electron beam it is ionized and produces glowing in the images. In dry cheese, calcium phosphate concentrates and the particles increase in size. Particles of calcium phosphate in Kostromskoi cheese sample before drying were of 10–12 μm and evenly spread. After drying, calcium phosphate particles increased in size to 20–30 μm . In dry cheese, calcium phosphate is concentrated and the particles are aggregated. It concentrates the most in pores and microvoids of the cheese.

Calcium phosphate is present in cheese in the form of accumulations of crystal micrograins. Crystal micrograins are round-shaped formations (Fig. 10), comprising wedge-like crystals, 20–30 μm in diameter.

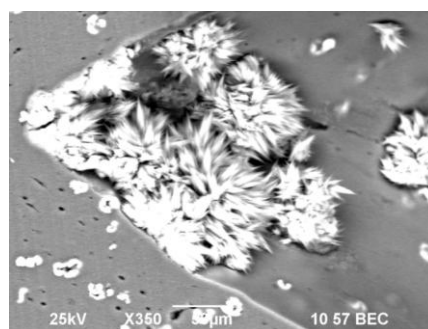


Fig. 10. Calcium phosphate in a sample of dry Kostromskoi cheese.

In mature cheese of the Kostromskoi or Rossiiskii variety, calcium lactate was detected (Fig. 11). Formation of calcium lactate should be associated with the process of cheese ripening, since it only occurs in mature cheese. Size of calcium lactate particles in Kostromskoi and Rossiiskii cheese samples was 200 \times 150 μm . Figure 12 presents images of calcium lactate in Rossiiskii cheese sample.

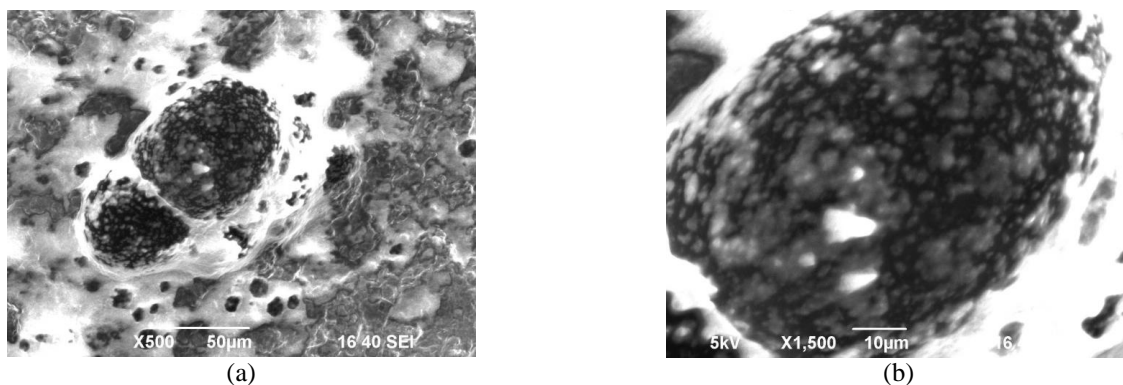


Fig. 12. Calcium lactate in Rossiiskii cheese sample at magnification of a, 500×, and b, 1500×.

Therefore, images of cheese microstructure obtained with a scanning electron microscope allowed investigation of cheese structure before and after drying and their comparison. Structure of cheese is a protein matrix pierced with capillaries containing moisture; fat globules are contained in the protein matrix and on surface of cheese. Capillaries are of round and oval shape. The number and size of the capillaries influence the cheese pattern, which is characterized by shape and

arrangement of holes and voids. Calcium phosphate depositions were detected using the electron microscopy. Calcium phosphate particles in cheese before drying are 10–12 µm big. After drying, they increase to 20–30 µm. Calcium phosphate particles in the dry cheese concentrate and agglomerate into larger particles. The highest concentration of calcium phosphate is reached in pores and microvoids of the dry cheese. In mature cheese samples, calcium lactate was detected.

REFERENCES

1. Ermolaev, V. A., and Prosekov, V. A., *Vakuumnnye tekhnologii molochno-belkovykh kontsentratorov* (Vacuum Technologies of Concentrated Dairy Products), Kemerovo: Kuzbassvuzizdat, 2010.
2. Kharaev, G. I., Kotova, T. I., Komissarov, Yu. A., and Khanturgaeva, G. I., Optimal drying mode based on mathematical modeling of the process, *Khranenie i pererabotka sel'khozsyrya* (Storage and Processing of Raw Materials for Agriculture), 2007, no. 9, pp. 28–29.
3. Chernyshev, A. N., Experimental determination of wood deformity and strength under vacuum, *Derevoobrabatyvayushchaya promyshlennost'* (Wood Processing Industry), 2006, no. 2, pp. 9–11.
4. Ratnikova, L. B., Vloshchinskii, P. I., Shirochenko, G. I., and Romanov, V. P. Vacuum infrared drying: A technology of gentle processing of plant and animal raw materials, *Vestnik sibirskogo universiteta potrebitel'skoi kooperatsii* (Bulletin of the Siberian University of Consumer Cooperation), 2012, no. 1 (2), pp. 96–100.
5. Devahastin, S., Suvarnakuta P., Soponronnarit S., and Mujumdar A.S., A comparative study of low-pressure superheated steam and vacuum drying of a heat-sensitive material, *Drying Technol.*, 2004, vol. 22, pp. 1845–1867.
6. Sadovaya, T. N., Study of blue mold cheese microstructure, *Tekhnika i tekhnologiya pishchevykh proizvodstv* (Methods and Technology of Food Production), 2010, no. 4, pp. 45–50.
7. Dikhanbaeva, F. T., Microstructure of pickled cheese made from camel milk, *Syrodelie i maslovelie* (Cheese and Butter Manufacture), 2010, no. 2, pp. 38–39.
8. Tul'nikov, A. V., Development of resource-saving technology of solid rennet cheese production “Otechestvennyi” with increased food and biology value, *Cand. Sci. Dissertation*, Voronezh, 2004.
9. Ong, L., Dagastine, R. R., Kentish, S. E., and Gras, S. L., Microstructure and composition of full fat cheddar cheese made with ultrafiltered milk retentate, *Foods*, 2013, no. 2, pp. 310–331.
10. Drying Technologies in Food Processing, Chen, X. D., and Mujumdar, A. S., Eds., United Kingdom: Blackwell Publishing, 2008.
11. Yosuke, T., and Takehiro, G., Rokko Butter CO LTD, Dry cheese and method for producing the same. Patent application 004290087 JP, IPC A23C19/086; A23C19/00; A23C19/086; published 21.10.2004.
12. Uphus, A., Huellmann, M. D., Westfalia Separator AG, Method and device for producing a concentrate of fresh cheese with a high content of dry solids. Patent application 1642494 EP, IPC A01J25/11; A23C19/05; A01J25/00; published 05.04.2006.
13. Serrano, J., Velazquez, G., Lopetcharat, K., Ramirez, J. A., and Torres, J. A., Effect of moderate pressure treatments on microstructure, texture, and sensory properties of stirred-curd cheddar shreds, *J. Dairy Sci.*, 2004, vol. 87, no. 2, pp. 3172–3182.
14. Ermolaev, V. A., Chesnokov, N. S., Maslennikova, G. A., and Duisembaeva, S. K., Study of the effect of specific surface area on concentrating in the process of vacuum concentrating of liquid dairy products, *Tekhnika i tekhnologiya pishchevykh proizvodstv* (Methods and Technology of Food Production), 2010, no. 4, pp. 68–72.
15. Golubeva, L. V., Avakimyan, A. B., Grebenshchikov, A. V., and Kitaev, Ss. Yu., Microstructure of cheese before and after smoking, *Molochnaya promyshlennost'* (Dairy Products Industry), 2009, no. 8, pp. 67–68.
16. Ginzburg, A. S., Gromov, M. A., and Krasovskaya, G. I., *Teplotfizicheskie kharakteristiki pishchevykh produktov: Spravochnik* (Thermal Physical Characteristics of Food Products: Reference Book), Moscow: Pishchevaya promyshlennost', 1980.
17. Zakharova, L. M., Ermolaev, V. A., and Arkhipova, V. A., Kinetics and mass exchange upon vacuum drying of low-fat curdled cheese, *Molochnaya promyshlennost'* (Dairy Products Industry), 2008, no. 10, pp. 86–87.

STUDYING THE BIOKINETICS OF PIGMENTED YEAST BY STOCHASTIC METHODS

S. A. Ivanova*, V. A. Pavsky, M. A. Poplavskaya, and M. V. Novoselova

Kemerovo Institute of Food Science and Technology,
bul'v. Stroitelei 47, Kemerovo, 650056 Russia,
*e-mail: pavvm2000@mail.ru

(Received February 17, 2014; Accepted in revised form March 3, 2014)

Abstract: A country that owns high-performance computing facilities and mathematical modeling algorithms is able to provide its competitiveness in all the sectors of economy. The application of mathematical modeling is environmentally safe and cost effective and increases the technical and general culture of production. First of all, this concerns the development of new technologies. That is why the creation of new products in both the pharmaceutical and food industries is already impossible without the use of mathematical modeling. Today this is a necessity, the fulfilment of which has already been specified in relevant technical regulations. The simultaneous use of both mathematical methods and experiment provides not only the reduction of time, energy, and financial expenditures, but also the acquisition of additional information and the establishment of a direction of studies. This considerably reduces the time between the generation of an idea and its implementation in the form of a product. The technologies of the use of L-phenylalanine ammonia-lyase for the achievement of certain objectives in medicine, biotechnology, agriculture, and food industry have been developed by now. The insufficient application of algorithmic and mathematical approaches by researchers for development and analysis can be considered as a factor limiting the active use of biotechnological methods in the production of this enzyme. The description of microbial biosynthesis mechanisms by classical mathematical methods encounter some difficulties due to the combined effect of numerous chemical, physical, biological, engineering, and other factors. Another important thing is the more profound study of the kinetics of microbiological synthesis susceptible to both internal and external effects. The batch cultivation of pigmented yeast has been studied by probabilistic methods. A stochastic model providing the system study of the biosynthesis of L-phenylalanine ammonia-lyase by pigmented yeast has been formulated. The cultivation of microorganisms is described by the birth-and-death process. The mathematical expectation and dispersion of the number of population members are proposed as efficiency characteristics. The dependence between the amount of synthesized enzyme and the birth and death rates of a cultivated population is derived through the concentration of cultivated microorganism biomass and the birth and death rates of its members.

Key words: cultivation of microorganisms, biosynthesis of enzyme, probability, stochastic model, mathematical expectation, dispersion, differential equations

UDC: 663.12:519.245
DOI 10.12737/4117

INTRODUCTION

Microbiological synthesis products (enzymes) find wide application in various branches of petrochemical, food, and processing industries, medicine, pharmacology, etc. The principal stages of fermentation are the selection of a producing strain and the determination of conditions for its cultivation, during which the microbiosynthesis of a certain enzyme proceeds. Fermentation is most often implemented as a continuous process (maintaining the cultivation conditions throughout the entire period of its duration), but many metabolites can be obtained only via batch synthesis with the withdrawal of a product at the end of the process. The regularities governing the formation of an enzyme complex strongly depend on many process parameters (physicochemical, engineering, biological, and other factors [1–7]), the adjustment of which provides the efficient organization of this process. The technology of such a process usually ensures the simultaneous attainment of a maximum of both productivity and

quality at minimum expenditures.

Since the synthesized enzyme is extracted from a cultivated biomass or a cultural liquid, it is necessary to perform a series of studies on the effect of the birth and death rates of cultivated population members on the amount of formed biomass. The consumption of time in this project will be reduced by constructing a mathematical model, which adequately describes the process of fermentation.

The objective of this work is to construct mathematical models providing the system description of the microbial cultivation and biosynthesis of the target enzyme and to study the kinetic regularities governing the duration of batch cultivation.

OBJECTS AND METHODS OF STUDY

Biokinetic regularities were studied using the cultivation of the *Escherichia coli* strain, a recombinant *Rhodesporidium foruloides* L-phenylalanine ammonia-lyase producer, grown at the Research Institute of Bioengineering of the Kemerovo Institute

of Food Science and Technology [8–10]. The submerged batch cultivation of yeast in a fermenter was performed following the existing producer recommendations (in a culture medium containing (g/l): glucose, 20.0; peptone, 10.0; yeast extract, 5.0), at a temperature of 26°C for 24 h in the regime of non-controlled pH. Control measurements were performed every half hour beginning from the moment of pitching. The biomass and protein concentrations were determined from the absorbance in compliance with the manufacturer’s manuals for an UV-1800 spectrophotometer (Shimadzu, Japan) [9].

Mathematical models were constructed using the tools of probability and stochastic process and queueing theories, in particular, the birth-and-death process [11–20] together with the differential equation generation method designed immediately for the derivation of the mathematical expectations and dispersions of random values [21–24].

The process of biokinetics is considered as a dynamic system of flows. This allows it to be described as a queueing system represented by a labeled graph of states (Fig. 1). The source of arrivals (birth of population members) is assumed to be inexhaustible and characterized by the parameter μ . The death of population members is considered to be the service of arrivals and characterized by the parameter λ . The state C_n is understood to mean a system state, in which the population size is equal to n . The transition from the state C_n to the state C_{n+1} means that the population size has increased by unity, and the transition from C_n to C_{n-1} means the death of one population member. It has been assumed that the fraction of cells dying per time unit is *averagingly* the same independently of the start moment of time counting [2, 25, 26]. The kinetics of the growth and death of a microorganism population is described with an exponential distribution [18, 19, 21].

Model. Let μ be the intensity of a flow of arrivals to a queueing system. The number k of arrivals to a system is a random value ξ obeying the Poisson law

$$P\{\xi = k\} = \frac{(\mu t)^k}{k!} e^{-\mu t},$$

where the intensity μ is determined as the average number of population members born per unit time, $t \in [0, \infty)$, $k = 0, 1, 2, \dots$.

An arrival that has just entered the system is immediately served. The service time is a random value η distributed in compliance with the exponential law

$$P(\eta < t) = 1 - e^{-\lambda t},$$

where $\lambda = 1/t_{av}$ is the intensity of service, and t_{av} is the average arrival service time determined as the average life of a population member.

It is required to find the mathematical expectation $M_i(t)$ (average value) of the random parameter characterizing the number of cultivated population members at a time moment t under the condition that

their number is $M_i(0) = i$ at an initial time moment and the dispersion is $D(t)$, $D(0) = 0$, $t \in [0, \infty)$, $i = 0, 1, 2, \dots$.

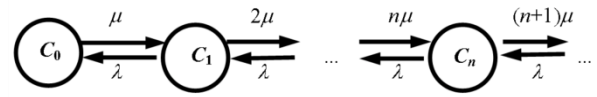


Fig. 1. Labeled graph of states C_n , $n = 0, 1, 2, \dots$, for a system S , where μ and λ are the parameters characterizing the process.

The formulated model is described by the birth-and-death process formalized with the cognominal set of equations, which correspond to the labeled graph of states in Fig. 1 [11, 22]. Let us introduce the generating

function $F(z, i, t) = \sum_{k=0}^i z^k P_k(t)$, where $P_k(t)$ is the

probability that the system is in the state C_n , $n = 0, 1, 2, \dots$, at a time moment $t \in [0, \infty)$, and apply it to the set of birth-and-death equations. Performing necessary rearrangements, we obtain the partial differential equation [11, 21, 22, 24]

$$\frac{\partial}{\partial t} F(z, t, i) + (z-1)n\lambda \frac{\partial}{\partial z} F(z, t, i) = \mu(z-1)F(z, t, i), \quad (1)$$

with the initial condition

$$F(0, t, i) = z^i$$

(z is the complex variable, and $|z| < 1$), from which we obtain the set

$$\begin{cases} \frac{dM_i(t)}{dt} + \lambda M_i(t) = \mu, \\ \frac{dD(t)}{dt} + 2\lambda D(t) = \frac{d}{dt} (M_i^2(t) - M_i(t)) - \\ - 2\lambda (M_i^2(t) - M_i(t)) + 2\mu M_i(t). \end{cases} \quad (2)$$

in compliance with the definition and method [21–24] for the generation of equations just for momenta.

The solution of set (2) with consideration for the initial conditions

$$M_i(0) = i, \quad D(0) = 0$$

has the form [21, 23, 24]:

$$M_i(t) = \frac{\mu}{\lambda} + \left(i - \frac{\mu}{\lambda} \right) \cdot e^{-\lambda t}, \quad (3)$$

$$D(t) = (1 - e^{-\lambda t}) \cdot \left(\frac{\mu}{\lambda} + i \cdot e^{-\lambda t} \right). \quad (4)$$

The amount of the target microorganism cultivation product is determined from the dependence [25, 26]

$$\frac{dP(t)}{dt} = \alpha \frac{dX(t)}{dt} + \beta X(t), \quad (5)$$

where $X(t)$ is the biomass concentration, $P(t)$ is the product concentration, and α and β are the size constants of growing and non-growing associates in g/g and g/(g h), respectively.

RESULTS AND DISCUSSION

The batch cultivation of pigmented yeast has been

modelled. A microorganism population member is understood to mean 1 gram of biomass in a unit cultural solution volume at each time moment t , $t \in [0, \infty)$. Since μ and λ are the average population growth and death rates per unit time, respectively, they can be determined by considering the studied process as pure birth [11, 12]. From Eq. (1) at $\lambda=0$ we similarly obtain

$$\frac{\partial}{\partial t} F(z, t, i) = \mu(z-1)F(z, t, i) \quad (6)$$

From Eq. (6) we obtain the differential equation

$$\frac{dM_i(t)}{dt} = \mu,$$

the solution of which at the initial condition

$$M_i(t_0) = M_0$$

has the form

$$M_0(t) = \mu \cdot t + M_0, \quad (7)$$

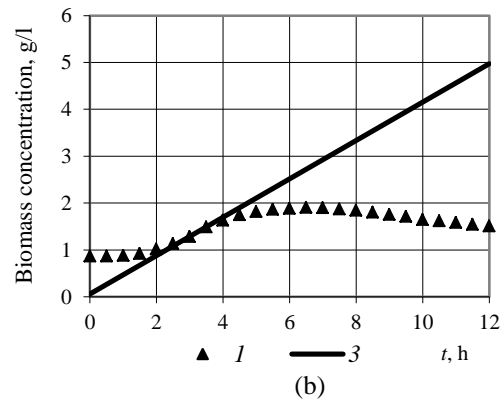
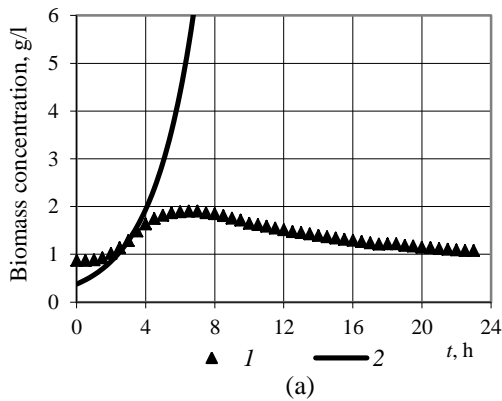


Fig. 2. Biomass concentration versus cultivation duration: (1) experimental data, (2) exponential growth curve $M_0 \exp(\mu(t-t_0))$, (3) $M_0(t)$.

The comparison of experimental and theoretical values of $M_0(t)$ enable us to estimate the average deviation between them on the interval from t_1 to t_2 h, where t_2 is the time moment, at which the death of population members begin to prevail over their birth, and to calculate $\lambda = 0.112$ g/(l h) from it as the average number of dead population members per unit time.

Let $M(t)$ be the average concentration of the biomass of cultivated microorganisms at a time moment t , $t \in [t_0, \infty)$; then, using the solution of set (2) with the initial conditions

$$M(t_0) = M_0, \quad D(t_0) = 0,$$

we obtain [21, 23, 24]

$$M(t) = \frac{\mu}{\lambda} + \left(M_0 - \frac{\mu}{\lambda} \right) \cdot e^{\lambda(t-t_0)}, \quad (8)$$

$$D(t) = 1 - e^{-\lambda(t-t_0)} \cdot \left(\frac{\mu}{\lambda} + M_0 \cdot e^{-\lambda(t-t_0)} \right), \quad (9)$$

The found parameters μ , λ , and t_0 were substituted into Eqs. (8) and (9). The obtained results of modeling with consideration for the mean square deviation

The growth of a population during the batch cultivation of microorganisms has a complicated character: the growth of the amount of biomass is intensively accelerated within a short time period (exponential growth phase) after initial relative constancy [1–6]. For this reason, the death of population members during this process period was neglected. Denoting the initial and finite time moments characterizing the exponential growth phase (with a maximum population growth rate) as t_0 and t_1 , respectively, we determined this interval for our sampling as (3, 3.5). The further increase in the duration of cultivation is accompanied by the death of population members, thus decelerating the growth of the biomass concentration (Fig. 2a). The average growth rate of population members $\mu = 0.4094$ g/(l h) was determined using Eq. (7) $M_0(t) = 0.4094 \cdot t + 1.2876$ and the equation of a line passing through two points (Fig. 2b).

$\sqrt{D(t)}$ are plotted in Fig. 3.

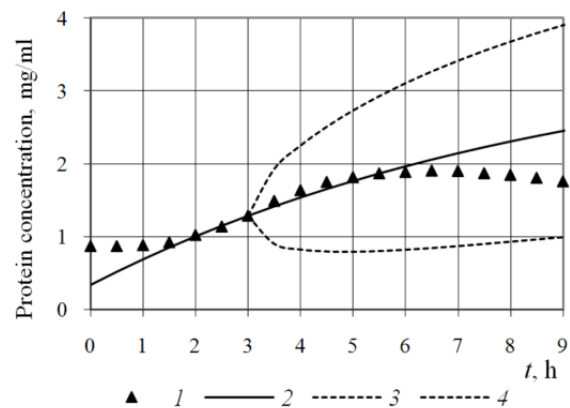


Fig. 3. Protein concentration versus cultivation duration: (1) experimental data, (2) $M(t)$, (3, 4) $M(t) \pm \sqrt{D(t)}$.

In the considered variant, cultivation for more than 8 h is unreasonable and leads to additional time and energy expenditures. This is explained by a high death rate of population members, as the deviation between theoretical and experimental values in this case is more

than half the theoretical “ideal” biomass concentration. Moreover, it is desirable to restrict the process of cultivation by 6.0 ± 0.5 h for our strain characterized by the synthesis of a higher target product fraction with respect to the cultivated biomass [8–10]. A more precise value of t_2 can be obtained after analyzing the quality and amount of the target fermentation product. The proposed model gives a rather adequate description up to 12 h of cultivation (calculation error does not exceed 10%). The use of the standard deviation alone enables the estimation of the interval, into which experimental biomass concentrations almost reliably (with a probability > 0.95) fall in the case of cultivating the considered microorganism strain under the earlier defined conditions.

The biosynthesis of the target product (enzyme) was analyzed from the viewpoint of the dependence between the concentrations of the yeast biomass and the product of its activity (produced enzyme). Let us use Eq. (5) and modify it taking into account Eq. (3) as

$$\frac{dP(t)}{dt} = \gamma_p \frac{dM(t)}{dt} + \delta_p, P(t_0) = P_0, \quad (10)$$

where γ_p is the product yield with respect to the formed biomass, mg/g, and δ_p is the correction coefficient, mg/(ml h).

The solution of Eq. (10) has the form

$$P(t) = \gamma_p (M(t) - X_0) + \delta_p (t - t_0) + P_0, \quad (11)$$

The average fraction of synthesized protein per unit weight of the formed biomass of the pigmented yeast strain under the earlier selected cultivation conditions is $\gamma_p = 0.27$ mg/g (corresponding to a nearly 33.5% expression for cultivation without induction [8, 10]). Our studies show that the averaged parameter $\delta_p = 0.11$ mg/(ml h) for different pigmented yeast strains, including the strain considered in this work. Note that the calculation error is up to 9.0% for the considered strain (from 5 to 12% for other strains), if the parameter δ_p is considered to be nonsignificant. The use of the averaged value of this parameter has allowed the calculation error to be decreased, in some cases, by three times. We defined this parameter as the fraction of the target product (protein), which passes into solution from the biomass of dead species (microorganisms both accumulate the enzyme inside and secrete it into a cultivation solution during their life activity). It appears that this parameter directly depends on both the intensity of the death of population members (λ) and the amount of enzyme accumulated inside a microorganism. The experimental and theoretical dependences $P(t) = 0.27(M(t) - M_0) + 0.11(t - t_0) + P_0$ of the concentration of formed enzyme (L-phenylalanine ammonia-lyase) in the cultivation of pigmented yeast on the interval $[t_0, t_2]$ are plotted in Fig. 4. An increase in the cultivation duration above 6.0 h reduces the amount of both biomass and enzyme. The target product loss is more than 5% of the maximum amount for 8 h of cultivation and nearly 15% for 10 h of

cultivation in addition to energetic and material expenditures. It is obvious that the duration must not exceed 5.5–6.0 h for our strain. Further refinement is possible during the activity studies of the produced enzyme. The parameter t_2 , at which not only the maximum amount of the target microorganism cultivation product, but also its highest quality is attained, is uniquely determined in this case.

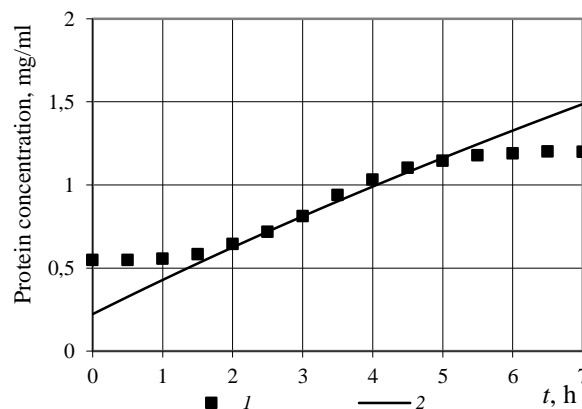


Fig. 4. Target biosynthesis product concentration versus cultivation duration: (1) experimental data, (2) $P(t)$.

The constructed stochastic model has allowed us to find the mathematical expectation and dispersion of the number of microorganism population members at an arbitrary moment of cultivation, to determine the recommended duration of fermentation, and to describe the amount of the synthesized enzyme. A method of estimating the parameters of this model has also been developed.

The batch cultivation of pigmented yeast was modeled using the well-known Markovian “birth-and-death” process. However, the Markovian process proved to be insufficient for the system study of the process of cultivation, as its characteristic property, such as the absence of aftereffects, was violated [24]. The use of heuristic equation (5) transformed into Eq. (10) after modernization has allowed us to solve the formulated problem. Naturally, the proposed model has some shortcomings, e.g., very high dispersion, and is sewed of two processes, but the application of numerical method in this case gives only a quantitative results and does not reflect the depth of study.

Hence, the system study of the cultivation of pigmented yeast has been performed. The relationship between the synthesized enzyme amount and the birth and death rates of a cultivated population has been derived through the concentration of the biomass of cultivated microorganisms and the birth and death rates of its members. The proposed model has provided the quantitative description of the biosynthesis of L-phenylalanine ammonia-lyase and the selection of a recommended duration for the cultivation of a producing strain for the efficient organization of biosynthesis.

REFERENCES

1. Varfolomeev, S. D. and Kalyuzhnyi, S.V., *Biotehnologiya: Kineticheskie osnovy mikrobiologicheskikh protsessov* (Biotechnology: Kinetic Principles of Microbiological Processes), Moscow: Vysshaya shkola, 1990.
2. Rubin, A.B., Pyr'eva, N.F., and Riznichenko, G.Yu., *Kinetika biologicheskikh protsessov* (Kinetics of Biological Processes), Moscow: Izd. MGU, 1987.
3. Pirt, S.J., *Principles of Microbial and Cell Cultivation*, Oxford: Blackwell, 1975.
4. Tsiperovich, A.S., *Fermenty. Osnovy khimii i tekhnologii* (Enzymes. Principles of Chemistry and Technology), Kiev: Tekhnika, 1971.
5. Nikitin, G.A., *Biokhimicheskie osnovy mikrobiologicheskikh proizvodstv* (Biochemical Principles of Microbiological Production), Kiev: Vysshaya shkola, 1992.
6. Bisswanger, H., *Enzyme Kinetics. Principles and Methods*, Weinheim: Wiley-VCH, 2008.
7. Glick, B.R. and Pasternak, J.J., *Molecular Biotechnology. Principles and Application of Recombinant DNA*, Washington, DC: ASM Press, 2000.
8. Babich, O.O., Soldatova, L.S., and Razumnikova, I.S., Klonirovanie i ekspressiya gena L-fenilalanin-ammonii-liazy v *Escherichia Coli* i vydelenie rekombinantnogo belka (Cloning and expression of the L-phenylalanine-ammonium-lyase gene in *Escherichia Coli* and extraction of recombinant protein), *Tekhnika i tekhnologiya pishchevykh proizvodstv* (Technics and Technology of Food Industry), 2011, no. 1, pp. 8–13.
9. Babich, O.O., *Biotehnologiya L-fenilalanin-ammonii-liazy* (Biotechnology of L-Phenylalanine-ammonium-lyase), Novosibirsk: Nauka, 2013.
10. Babich, O.O., Dyshlyuk, L.S., and Milent'eva, I.S., Expression of recombinant L-phenylalanine ammonia-lyase in *Escherichia Coli*, *Food and Raw Materials*, 2013, vol. 1, no. 1, pp. 48–53.
11. Feller, W. *An Introduction to Probability Theory and Its Applications*, New York: Wiley, 1968, vol. 1.
12. Venttsel', E.S. and Ovcharov, L.A., *Teoriya sluchainykh protsessov i ee inzhenernye prilozheniya* (Theory of Stochastic Processes and Its Engineering Applications), Moscow: Vysshaya shkola, 2000.
13. Kleinrock, L. *Queueing Systems. Theory*, New York: Wiley, 1975, vol. 1.
14. Saaty, T.L., *Elements of Queueing Theory with Application*, New York: McGraw Hill, 1961.
15. Haefner, J.W. *Modeling Biological Systems: Principles and Applications*, New York: Springer, 2005.
16. Zhu, G.-Y., Zamamiri, A.M., Henson, M.A., and Hjortso, M.A., Model predictive control of continuous yeast bioreactors using cell population models, *Chemical Engineering Science*, 2000, vol. 55, no. 24, pp. 6155–6167.
17. Zhang, Y., Henson, M.A., and Kevrekidis, Y.G., Nonlinear model reduction for dynamic analysis of cell population models, *Chemical Engineering Science*, 2003, vol. 58, no. 2, pp. 429–445.
18. Xiong, R., Xie, G., Edmondson, A.E., and Sheard, M.A., A mathematical model for bacterial inactivation, *International Journal of Food Microbiology*, 1999, vol. 46, no. 1, pp. 45–55.
19. Gordeeva, Yu.L., Ivashkin, Yu.A., and Gordeev, L.S., Modeling the continuous biotechnological process of lactic acid production, *Theoretical Foundations of Chemical Engineering*, 2012, vol. 46, no. 3, pp. 279–283.
20. Skichko, A.S. and Kol'tsova, E.M., Mathematical model for describing oscillations of bacterial biomass, *Theoretical Foundations of Chemical Engineering*, 2006, vol. 40, no. 5, pp. 503–513.
21. Khoroshevsky, V.G. and Pavsky, V.A., Calculating the efficiency indices of distributed computer system functioning, *Optoelectronics, Instrumentation and Data Processing*, 2008, vol. 44, no. 2, pp. 95–104.
22. Yustratov, V.P., Pavskii, V.A., Krasnova, T.A., and Ivanova, S.A., Mathematical modeling of electro dialysis demineralization using a stochastic model, *Theoretical Foundations of Chemical Engineering*, 2005, vol. 39, no. 3, pp. 259–262.
23. Ivanova, S.A. *Stokhasticheskie modeli tekhnologicheskikh protsessov pererebotki dispersnykh sistem obezhirennogo moloka* (Stochastic Models of the Processing of Dispersed Skim Milk Systems), Kemerovo, KemTIPP, 2010.
24. Pavsky, V.A., Pavsky, K.V., and Khoroshevsky, V.G., Vychisleniye pokazatelei zhivuchesti raspredelennykh vychislitel'nykh sistem i osushchestvivosti resheniya zadachi (Calculating the characteristics of the robustness of distributed computational systems and the feasibility of problem solutions), *Iskusstvennyi intellekt* (Artificial Intelligence), 2006, no. 4, pp. 28–34.
25. Riznichenko, G.Yu., *Matematicheskie modeli v biofizike i ekologii* (Mathematical Models in Biophysics and Ecology), Moscow–Izhevsk: Institut komp'yuternykh issledovaniy, 2003.
26. Bozhkov, A.I., *Biotehnologiya. Fundamental'nye i promyshlennye aspekty* (Biotechnology. Fundamental and Industrial Aspects), Kharkiv: Fedorko, 2008.



TECHNOLOGY DEVELOPMENT FOR THE FOOD INDUSTRY: A CONCEPTUAL MODEL

A. G. Khrantsov, I. A. Evdokimov, A. D. Lodygin, and R. O. Budkevich*

North Caucasus Federal University,
pr. Kulakova 2, Stavropol, 355029 Russia,
*e-mail: budkev@mail.ru

(Received February 19, 2014; Accepted in revised form February 24, 2014)

Abstract: The information available on high technology in food industry is systematized. Different approaches to the development and integration of scientific knowledge are discussed. According to the European Institute for Food Processing (EU-IFP), there are three possible areas where a breakthrough in food science can occur: biotechnology (BIOTECH), nanotechnology (NANO), and information and communication technology (ICT). A transition is expected of high technology in food industry to convergent technologies in a combination with cognitive science (COGNITIVE). The four components of high technology are analyzed using food industry examples. We believe that the transfer of scientific knowledge into food industry can facilitate the technological development of the Russian agroindustrial complex.

Keywords: high technology, convergent technologies, food industry, biotechnology, nanotechnology, information technology, cognitive technologies

UDC 664

DOI 10.12737/4121

INTRODUCTION

The modern pace of scientific progress and the generation of new ideas breaks ahead of their practical application. Scientific findings in various areas of knowledge, including in food industry, do not get a chance to be transformed into a new technology. Thus, the development of a conceptual approach to the implementation of new discoveries in industry is required. The term *high technology* (*high tech/hi-tec*) dates back to the 1950s, when it was used initially in atomic energy research [1]. Later it found use in research papers on economics and finance [2]. In 1971, Robert Metz abbreviated it to *high-tech* [3, 4]. The term was used to denote the leading technologies of its time. The branches of industry that are most dependent on science are usually labeled high technology. According to the presentation (<http://www.highte-cheurope.com>) of the first European Institute for Food Processing (EU-IFP), there are three subdivisions of high-tech: biotechnology (BIOTECH), nanotechnology (NANO), and information and communication technology (ICT).

The project leading to the establishment of the EU-IFP was named HighTech Europe (HTE). It was a joint initiative of European research institutions and industrial associations. This project can be seen as a new era in the history of food industry; it will promote research and development needed to establish a lasting integration of scientific findings with experimental engineering and/or technological developments and the subsequent transfer of knowledge from scientists to industrialists. What are the strategic areas of development in food industry?

The core of the development of HighTech in food processing is the presence of an *lighthouse watcher*, or the principles of evaluation and description of food industry to create a comprehensive database. The

objective is to combine the potential sources of innovation with the needs of the industry, keeping in mind the ethical and social dimension. The lighthouse watcher comprises the following building blocks: scientific knowledge, the needs of the industry, personnel policy, and a sustainable development plan.

Scientific knowledge is a key factor in the development of HighTech in food industry. The three main blocks within the project (BIOTECH, NANO, and ICT) will determine the development strategy for food processing. These areas have the greatest innovation "strength" and are a promising source of the future high-tech food production. The strategic goal is to link together a chain for the transfer of HighTech knowledge, which can lead the way into the future of food industry. The structure combines scientific knowledge (universities) with intermediate centers and/or high-tech pilot institutions that can transfer technology to private entrepreneurs through regional organizations and industrial associations.

We think that this list is clearly lacking the *membrane technology* (MT), which has literally "broke into" food industry, e.g., dairy production, in recent years. It should find a proper place among high technologies, at least along with bio- and nanotechnology, or as an indispensable part of the latter (biomembrane and nanomembrane technologies). Being naturally connected with them, the MT can also be interpreted and viewed (used) as a nanobiomembrane technology. This is the exact direction taken by the members of our leading federal research school 7510.2010.04 Living Systems. By the way, the same route is followed by many teams at research institutes of the Russian Academy of Sciences and higher education institutions. A good example is Kemerovo Technological Institute of Food Industry (KTIFI), which

has successfully systematized virtually all the branches of food industry for Siberia and Central Asia.

Anticipating the development of high-tech, the US National Science Foundation and the Department of Commerce named the new technologies *convergent technologies* [5, 6, 7]. Cognitive research (COGNITIVE) compliments to the three research areas listed above. The convergence of technologies is reflected in the increasing interdependence of the four fields and their combined influence on society. Cognitive studies play a systemic role in the convergence of technologies; i.e., they are a means to check the consistency of products and services to the psychophysiological and ergonomic characteristics of man [8]. Figure 1 shows the architecture of convergent technologies according to the Albright Strategy Group [6].

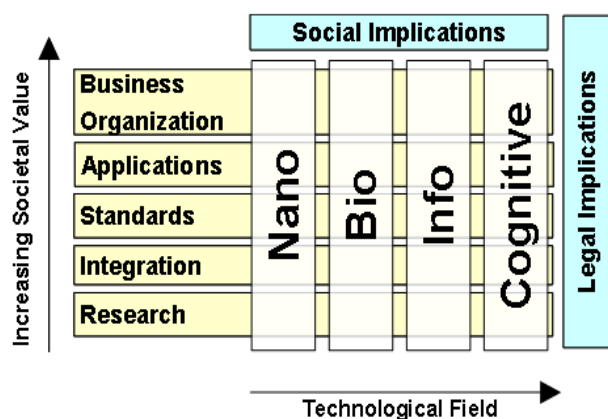


Fig. 1. Architecture of convergent technologies [6].

Biotechnology. The term *biotechnology* refers to any technology involving biological systems, living organisms, or derivatives thereof that is used to make or modify products and processes for a specific purpose [9]. This field is widely applied in food technology and, given the modern level of science, merges with the other two fields (NANO and ICT).

It should be noted that, by the decision of the Federal Government of the Russian Federation of April 2012, Russia adopted a Comprehensive Program on Biotechnology for the period until 2020. The program was developed in accordance with the decision of the Government Commission on High Technology and Innovation [10]. The program emphasizes that the key areas in the innovative development of a modern economy are information technology, nanotechnology, and biotechnology. The program is designed, *inter alia*, to stimulate production and consumption in the existing domestic markets, especially in the agricultural and food sector. It should be noted that the program highlights, among other priorities, agricultural and food biotechnology. The agricultural section of the program is closely related to the food section; its priorities include biological protection of plants, creation of plant varieties using biotechnology methods, molecular breeding of animals and birds, creation of transgenic and cloned animals, soil biotechnology and biofertilizers, biological products for animal husbandry and stock raising, animal feeding protein, processing of agricultural waste, and biological ingredients in premixes and feeds.

The priority area on food biotechnology covers the production of dietary protein; enzyme preparations for food production; engineering of pre-, pro-, and synbiotics; functional foods including therapeutic, preventive, and pediatric foods; and development of food ingredients, including vitamins and functional mixtures. It mentions, as a separate item, deep processing of raw materials, which is believed to drastically reduce the amount of waste in food industry. These issues call for a separate discussion within individual branches of food industry. They can be found in every issue of this journal and in the specialized journal *Food Industry Technology and Equipment* published by the KTIFI.

Nanotechnology in food industry has been formalized only in the past few years. The concept was phenomenologically introduced by Richard Feynman at a conference at the California Institute of Technology in 1979. At that conference he presented a paper "There's plenty of room at the bottom," which dealt with possibilities of manipulating individual atoms and molecules and controlling the creation of materials on a nanometer scale with the prospect of technical, industrial, and biological applications [11]. Afterwards, nanotechnology delivered a breakthrough not only in physics, chemistry, materials and engineering sciences, environmental monitoring, manufacturing sector, and quantum computing but also began to be widely used in clinical research and biotechnology. The studies were focused on new phenomena, properties, synthesis methods, and structures on a scale of 1 to 100 nm [12].

Most of the materials do change their properties on a nanoscale. The properties depend on the projected position of each atom or molecule [13]. Nanotechnology has close connections to other sciences and technologies, including biotechnology, chemistry, physics, and engineering. Nanotechnology can be used in health care, biology, biochemistry, agriculture, and food industry [14]. The US Department of Agriculture (USDA) was the first to promote the application of nanotechnology in agriculture and food industry by publishing a corresponding plan in 2003.

Nanotechnology has a great potential to revolutionize agriculture and food industry. Products manufactured on a nanoscale may influence the safety, bioavailability, and nutritional properties of food and enable molecular synthesis of new products and ingredients [15, 16]. The main prospects of nanotechnology in food manufacturing and agriculture are to improve safety in food and processing industries, increase the ability of plants to absorb nutrients, improve the taste and nutritional value of foods, optimize the methods of food delivery, pathogen detection, and functional food creation, and contribute to the protection of the environment and improvement of the economic efficiency of storage and transportation. When used in food production, nanotechnology can help deal with the issues related to the development of new functional materials, processing of raw materials on a micro- and nanoscale, and development of new approaches, as well as machines and equipment, for food processing [17]. Possible applications of nanotechnology in food processing are shown in Table 1.

Table 1. Application matrix of nanoscience and nanotechnology in the main areas of food science and technology [17]

Application area	Purpose and fact	Approaches
Design of nanomaterials	Nanoparticles, nanoemulsions, nanocomposites, nanobiocomposites (nanobipolymeric starch), and nanolaminates	Novel materials with self-assembling, self-healing, and manipulating properties
Nanosensors and nanobiosensors	Quality control and food safety	Detection of very small amounts of chemical contaminants Monitoring and tagging of food items Electronic nose and tongue for sensor evaluation Food born pathogen identification by measurement of nucleic acid, protein or any other indicator metabolite of microorganism
Processing	Nanofiltration	Selective passage of materials on the basis of shape and size
	Nanoscale enzymatic reactor	Improved understanding of process
	Heat and mass transfer; nanofabrication	Enhanced heat resistance of packages
	Nanocapsules for modification of absorption	Nanoceramic pan to reduce time of roasting and amount of consumed oil, reduction of trans fatty acids due to usage of plant oil instead of hydrogenated oil and finally resulted in safe nano food development of nanocapsules that can be incorporated into food to deliver nutrients to enable increased absorption of nutrients
New products	Packaging	Nanocomposites application as barriers, coating, release device, and novel packaging modifying the permeation behavior of foils, increasing barrier properties (mechanical, thermal, chemical, and microbial), improving mechanical and heat-resistance properties, developing active antimicrobial surfaces, sensing as well as signaling microbiological and biochemical changes, developing dirt repellent coatings for packages
	Delivery	Nanomyccells for targeted delivery of nutrients (nutrition nanotherapy). Nanocapsulation for controlled release of nutrients, proteins, antioxidants, and flavors
	Formulation	Production of nanoscale enzymatic reactor for development of new products. Nutritional value enhancement by omega 3 fatty acid, haemo-, lycopene, beta-carotene, phytosterols, DHA/EPA
	Evaluation	Enzyme and protein evaluation as nanobiological system for development of new products
	DNA recombinant technology	Recombinant enzyme production in nanoporous media with special numerous applications

Since nanotechnology is promoted using a variety of strategies and new approaches based on the formation, interpretation, and prediction of structural and physicochemical properties of nanoparticles and nanomaterials, one needs the third building block-ICT-of the HighTech food industry concept.

Information and communication (computer) technologies have been little known in food industry so far. Studies in the field of computer technology, computer science, and molecular modeling have been the key to the development of procedures in nanobiotechnology and nanoinformatics. These techniques can be used to create high-quality concepts and project design assumptions. Now bioinformatics is used as a computer tool for DNA and protein sequence

data analysis, and nanoinformatics is used to describe particles and materials in nanobiotechnology applications through their modeling in different states at the atomic level by means of computational chemistry strategies. A major challenge is, of course, to safely insert foreign objects into the intricate system of the human body. Computer methods are a natural opportunity to accelerate the development of innovation in life sciences. The computational approach is important in the early stages of project development on a nanoscale. It can be used to predict the structures of nanotransport systems for specific drugs or molecular devices [18, 19]. Large molecular systems are currently used as vehicles or platforms because they can be divided into different chemical groups depending on

their properties (solubility, affinity, and selectivity) and used for different types of cells [18, 19, 20].

In recent years, computational molecular design has become an extremely important area in the studies of new materials [21]. This outcome has become possible due to the increase in processing power and the integration of methods of computational chemistry [22].

Computational chemistry is a powerful tool for the design, modeling, simulation, and visualization of nanomaterials [22] and nanoparticles such as dendrimers [23, 24, 25, 26, 27], metal nanoparticles [28, 29, 30], nanocapsules [31], nanospheres [32], and quantum dots [20]. These nanoparticles are used in nanomedicine as carriers, sensors, and early disease detection systems [20, 23, 24]. Owing to the recent discoveries in computational chemistry, it has been possible to build computerized nanomolecule models. The latter can be used by experimental researchers as a method to design new nanostructures [33]. The main advantage of computer-aided nanodesign is that it allows one to explore, relatively quickly and at low cost, a large number of engineered structures in order to, *inter alia*, test their stability and predict their properties [34].

Cognitive Technologies. This area has its roots in computer technology. Currently, the term *cognitive* is undergoing a transformation: its meaning is being broadened to embrace the connotations of *knowledge* and *behaving like an intelligent being*. The concept of cognitive studies that is developed by B.M. Velichkovskii [8] considers this area as an interdisciplinary field in its

origin, methods, and prospects of practical use. In the coming convergence of technologies, cognitive studies play a systemic role since they enable the testing of products by means of the psychophysiological characteristics of humans. The central objective is to create cognitive technologies, i.e., high-tech tools, materials, and procedures that improve case analysis carried out by a human and increase the effectiveness of human activity. As applied to food industry, a notable example is the development of functional foods that influence human cognition and psychophysiology in general [35]. These developments [36] can be already discussed in the context of cognitive studies. The prospects of these technologies are intertwined with those of bionics and devices such as the electronic nose and electronic tongue [37] that are used to test products and improve their safety [37].

Thus, being based on the four pillars of the modern progress—biotechnology, nanotechnology, information technology, and cognitive technologies, including membrane technologies, the food technology is becoming a growth point of high-tech both in Russia and worldwide.

The world biotech industry is developing at a rapid pace; in one or two decades, there will be solutions and products suitable for mass use. We hope that by that time Russia will have an environment for the development of biotechnology and will be among the stakeholders and beneficiaries of high technology in general and food high-tech in particular.

REFERENCES

1. Atomic power for Europe, *The New York Times*, Feb. 4, 1957, p. 17.
2. Metz, R., Market place: keeping an eye on big trends, *The New York Times*, Nov. 4, 1969, p.64.
3. Berdyugin, D.V., Evaluation of the science and technology potential of high-tech industries in China, *Izvest. IGEA*, 2008, no. 5 (61).
4. Metz, R., Market place: so what made E.D.S. plunge? *The New York Times*, Nov. 11, 1971, p. 72.
5. *Converging Technologies for Improving Human Performance Nanotechnology, Biotechnology, Information Technology and Cognitive Science. NSF/DOC-Sponsored Report*, Roco, M.C. and Bainbridge, W.S., Eds., Arlington: National Science Foundation, 2002, p. 482.
6. *Managing Nano-Bio-Info-Cogno Innovations: Converging Technologies in Society*, Bainbridge, W.S. and Roco, M.C., Eds., New York: Springer, 2005.
7. Canton, J., NBIC convergent technologies and the innovation economy: challenges and opportunities for the 21st century, in *Managing Nano-Bio-Info-Cogno Innovations: Converging Technologies in Society*, New York: Springer, 2006.
8. Velichkovskii, B.M., Vartanov, A.V., and Shevchik, S.A., Systemic role of cognitive studies in the development of converging technologies, *Vestn. Tomsk. Gos. Univ.*, 2010, no. 334, pp. 186–191.
9. *The Convention on Biological Diversity*, United Nations, 1992.<http://www.cbd.int/convention/articles/default.stm?a=cdb-02>.
10. *Comprehensive Program for Biotechnology Development in the Russian Federation for the Period until 2020 (VP-P8-2322)*, Apr. 24, 2012, no. 1853p-P8, Moscow: RF Gov., 2012.
11. Drexler, K.E., Nanotechnology: the past and the future, *Science*, 1992, vol. 255, no. 5042, pp. 268–269.
12. Tomalia, D.A., The dendritic state, *Materials Today*, 2005, vol. 8, no. 3, pp. 34–46. doi: 10.1016/S1369-7021(05)00746-7.
13. Roco, M.C., Mirkin, C.A., and Hersam, M.C., Nanotechnology research directions for societal needs in 2020: summary of international study, *J. Nanoparticle Res.*, 2011, vol. 13, no. 3, pp. 897–919. doi: 10.1007/s11051-011-0275.
14. Doyle, M., Nanotechnology: a brief literature review, in *Food Research Institute: Briefings*, Univ. Wisconsin-Madison, 2006, pp. 1–10. http://fri.wisc.edu/docs/pdf/FRIBrief_Nanotech_Lit_Rev.pdf.
15. Aguilera, J.M., Why food microstructure? *J. Food Eng.*, 2005, vol. 67, nos. 1–2, pp. 3–11.
16. Blundell, J.E. and Thurlby, P.L., Experimental manipulations of eating advances in animal models for studying anorectic agents, *Pharm. Therapeut.*, 1987, vol. 34, no. 3, pp. 349–401.

17. Rashidi, L. and Khosravi-Darani, K., The applications of nanotechnology in food industry, *Crit. Rev. Food. Sci. Nutr.*, 2011, vol. 51, no. 8, pp. 723–730. doi: 10.1080/10408391003785417
18. Tentony, L., A model-based approach to the assessment of physicochemical properties of drug delivery materials, *Comput. Chem. Eng.*, 2003, vol. 27, no. 6, pp. 803–812. doi: 10.1016/S0098-1354(02)00266-1
19. Thierry, B., Drug nanocarriers and functional nanoparticles: applications in cancer therapy, *Curr. Drug Deliv.*, 2009, vol. 6, no. 4, pp. 391–403. doi: org/10.2174/156720109789000474
20. Kang, W., Chae, J., Cho, Y., Lee, J., and Kim, S., Multiplex imaging of single tumor cells using quantum-dot-conjugated aptamers, *Small*, 2009, vol. 5, no. 22, pp. 2519–2522. doi: 10.1002/smll.200900848
21. Rickman, J. M. and LeSar, R., Computational materials research, *Ann. Rev. Mater. Res.*, 2002, vol. 32, no. 1. doi: 10.1146/annurev.mr.32.010101.100002
22. Gao, H., Modelling strategies for nano- and biomaterials, in *European White Book on Fundamental Research in Materials Science*, Germany: Max Planck Inst., 2001, pp. 144–148.
23. Belting, M. and Wittrup, A., Macromolecular drug delivery: basic principles and therapeutic applications, *Mol. Biotech.*, 2009, vol. 43, no. 1, pp. 89–94. doi: 10.1007/s12033-009-9185-5
24. Belting, M., Wittrup, A., Developments in macromolecular drug delivery, *Methods Mol. Biol.*, 2009, vol. 480, pp. 1–10. doi: 10.1007/978-1-59745-429-2_1.
25. Diekmann, S. and Lindhorst, T., Dendrimers, *Rev. Mol. Biotech.*, 2002, vol. 90, pp. 157–158. doi: 10.1016/S1389-0352(01)00074-5
26. Newkome, G. and Shreiner, C., Poly(amidoamine), polypropylenimine, and related dendrimers and dendrons possessing different 1-2 branching motifs: an overview of the divergent procedures, *Polymer*, 2008, vol. 49, no. 1, pp. 1–173. doi: 10.1016/j.polymer.2007.10.021
27. Jang, W. D., Kamruzzaman Selim, K. M., and Lee, C., Bioinspired application of dendrimers: from biomimicry to biomedical applications, *Prog. Polymer Sci.*, 2009, vol. 34, no. 1, pp. 1–23. doi: 10.1016/j.progpolymsci.2008.08.003
28. Lee, W., Piao, L., Park, C., Lim, Y., Do, Y., Yoon, S., and Kim, S., Facile synthesis and size control of spherical aggregates composed of Cu₂O nanoparticles, *J. Colloid Interface Sci.*, 2010, vol. 342, no. 1, pp. 198–201. doi: 10.1016/j.jcis.2009.10.027
29. Murali Mohan, Y., Vimala, K., Thomas, V., Varaprasad, K., Sreedhar, B., Bajpai, S., and Mohana Raju, K., Controlling of silver nanoparticles structure by hydrogel networks, *J. Colloid Interface Sci.*, 2010, vol. 342, no. 1, pp. 73–82. doi: 10.1016/j.jcis.2009.10.008.
30. Prasad, K. and Jha, A., Biosynthesis of CdS nanoparticles: an improved green and rapid procedure, *J. Colloid Interface Sci.*, 2010, vol. 342, no.1, pp. 68–72. doi: 10.1016/j.jcis.2009.10.003
31. Fan, D. and Hao, J., Magnetic aligned vesicles, *J. Colloid Interface Sci.*, 2010, vol. 342, no. 1, pp. 43–48. doi: 10.1016/j.jcis.2009.10.013.
32. Lee, H., Yang, H., and Holloway, P., Functionalized CdS nanospheres and nanorods, *Z. Phys. B: Condens. Matter*, 2009, vol. 404, no. 22, pp. 4364–4369, doi: 10.1016/j.physb.2009.09.020.
33. Bewick, S., Yang, R. and Zhang, M., Complex mathematical models of biology at the nanoscale. *Wiley Interdiscip. Rev. Nanomed. Nanobiotech.*, 2009, vol. 1, no. 6, pp. 650–659. doi: 10.1002/wnan.61.
34. Shapiro, B., Bindewald, E., Kasprzak, W., and Yingling, Y., Protocols for the *in silico* design of RNA nanostructures, *Methods Mol. Biol.*, 2008, vol. 474, pp. 93–115. doi: 10.1007/978-1-59745-480-3_7.
35. Tkachenko, E.I. and Uspenskii, Yu.P., *Pitanie, mikrobiotsenoz i intellekt cheloveka* (Nutrition, Microbiocenosis, and Human Intellect), St. Petersburg: Spets. Literatura, 2006.
36. Zhilenkova, O.G., Shenderov, B.A., Klodt, P.M., Kudrin, V.S., and Oleskin, A.V., Dairy products as a potential source of compounds modifying consumer behavior, *Moloch. Prom-st.*, 2013, no. 10, c. 45–49.
37. Baldwin, E.A., Bai, J., Plotto, A., and Dea, S., Electronic noses and tongues: applications for the food and pharmaceutical industries, *Sensors*, 2011, vol. 11, no. 5, pp. 4744–4766. doi: 10.3390/s110504744.



ACID HYDROLYSIS OF CASEIN

M. G. Kurbanova* and S. M. Maslennikova

Kemerovo State Institute of Agriculture,
ul. Markovtseva 5, Kemerovo, 650056 Russia,
*e-mail: kurbanova-mg@mail.ru

(Received February 14, 2014; Accepted in revised form February 26, 2014)

Abstract: Protein hydrolysates have a high biological and nutritional value and are widely used in various sectors of the food, medical, and pharmaceutical industries. This article deals with the chemical hydrolysis of the milk protein casein in the presence of hydrochloric or sulfuric acid and reports the hydrolysis parameters minimizing the loss of amino acids. In casein hydrolysis, peptide bonds of protein molecules break to form di- and tripeptides and free amino acids, enhancing protein absorption by the body. Inadequate intake of digestible forms of protein leads to disruption of growth processes and impairs the immune resilience of the human body. To avoid the decomposition of labile amino acids, hydrolysis was performed with triply distilled 6 M hydrochloric or sulfuric acid in a vacuum in sealed ampoules for 4, 8, or 24 (± 0.05) h at a temperature of $110 \pm 5^\circ\text{C}$ and a substrate-to-acid ratio of 1 : 15, 1 : 20, or 1 : 25. The compositions of the casein hydrolysates obtained at various hydrolysis times are presented. For a more detailed evaluation of the properties of the casein hydrolysates, the hydrolysis time effect on the molecular weight distribution of proteins and peptides has been investigated. The problem of obtaining protein hydrolysates with the desired composition and properties remains topical.

Keywords: acid hydrolysis, casein, protein, degree of hydrolysis, peptides, amino acids, hydrolysates

UDC 637.136.045:664.162.036.2
DOI 10.12737/4124

INTRODUCTION

Protein hydrolysates are the products of the hydrolytic decomposition of proteins. They consist mainly of separate amino acids, their sodium salts, and polypeptide residues. During hydrolysis, the peptide bonds in protein molecules break to yield di- and tripeptides and free amino acids, thus increasing protein assimilation in the living organism. Mixtures of various peptides are more rapidly and more completely absorbed in the digestive tract than proteins themselves. In addition, protein hydrolysates may contain various physiologically active peptides necessary for regulation of a number of essential functions of the living organism. Note that peptides contained in hydrolysates can possibly exert a favorable effect on the absorption of some essential micronutrients. Protein hydrolysis is used to produce preparations for the following applications: blood substitution and parenteral nutrition in medicine; protein deficiency compensation, resistance enhancement, and improvement of youngsters' development in veterinary; sources of amino acids and peptides for bacterial and culture growth media in biotechnology. Casein hydrolysates contain peptides that are capable to form stable coordination compounds (chelates) with calcium ions and to considerably raise the absorbability of the latter [2–4]. Again there are data indicating that phosphopeptides of β -casein, like κ -casein glycomacropeptide and peptides of whey proteins, markedly increase the bioavailability of iron and can be considered as favorable factors in anemia prophylaxis.

In view of this, milk protein hydrolysates are widely used in the food, medical, pharmaceutical, and fragrance industries as rich sources of

nonmacromolecular nitrogen compounds, amino acids, and proteins.

The chemical methods employed in the hydrolysis of milk proteins are facile and do not require use of uncommon or expensive enzymes, but they need severe processing conditions. The production of protein hydrolysates by acid hydrolysis is carried out above 100°C at pH 1–2 using inorganic (hydrochloric, sulfuric, orthophosphoric) acids. The rate of release and destruction of individual amino acids depends mainly on the nature of the protein.

The peptide bonds ($\text{H}-\text{N}-\text{C}=\text{O}$) forming the polymer chain of a protein molecule undergo hydrolysis in the presence of an acid or alkali. This causes polymer chain scission and can finally lead to the constituent amino acids. The peptide bonds occurring in α -helices or β -structures are more resistant to hydrolysis and various chemical treatments than the same bonds in single chains [1]. Investigating the chemical hydrolysis of casein, we revealed considerable structural changes in protein subunits. In addition, spectroscopic data indicate that oxyacids, dicarboxylic acids, and other compounds undergo decomposition and racemization as well, though to a lesser extent. Some authors reported that terminal structural deformations take place in nonmacromolecular peptides, which are biologically active compounds, to make them unrecognizable by cell receptors [4, 5, 7]. However, the following advantages of acid hydrolysis are noted in some reports: protein breakdown proceeds to a sufficient extent, and any bacterial contamination of the hydrolysate (including by metabolism products) is ruled out.

Here, we report a promising method of the acid hydrolysis of casein and characterize the resulting hydrolysates.

OBJECTS AND METHODS OF STUDY

The substrate was edible casein containing 85 wt % protein. In order to avoid the decomposition of the resulting labile amino acids, acid hydrolysis was performed using triply distilled 6 M hydrochloric or sulfuric acid in a vacuum in sealed ampoules at $110 \pm 5^\circ\text{C}$ for $(4-24) \pm 0.05$ h. After the experiment time was over and the hydrolysis process was complete, the ampoules with the resulting casein hydrolysates were cooled and unsealed and their contents were transferred into a small conical or round-bottom flask. Hydrochloric or sulfuric acid was evaporated to dryness using a rotary evaporator at $40-65^\circ\text{C}$. For more complete removal of hydrochloric (sulfuric) acid from the hydrolysates, 1.5 mL of water was introduced into the flask and evaporation was repeated. This operation was done two times.

Total nitrogen was quantified on a RAPID N ELEMENTAR protein analyzer according to European standards. The total protein content was calculated by multiplying the total nitrogen content by a conversion factor of 6.38.

Amino nitrogen was determined spectrophotometrically using 2,4,6-trinitrobenzenesulfonic acid (TNBS). This method is based on spectrophotometric determination of the chromophores resulting from primary amine--TNBS reactions. The degree of hydrolysis was determined as the ratio of amino nitrogen to total nitrogen. The molecular weight distribution of proteins and peptides in the hydrolysates was estimated by Laemmli's protein electrophoresis method.

RESULTS AND DISCUSSION

Some experiments were intended to find rational casein hydrolysis conditions that would maximize amino acid survival in the hydrolysate. As distinct from some globular proteins, caseins are readily decomposable by chemicals because, even in their native state, they are in a low-ordered conformation that is like a disordered structure of denaturated globular proteins [3]. This is explained by the very low proportion of α -helices and by the low structural organization of the main casein components. This fact is due to the high proline content of these proteins (8.5 to 16%), which apparently deforms the helix into a disordered ball [1, 6].

The compositions of the casein hydrolysates obtained by treating casein with 6 M hydrochloric acid are presented in Table 1.

The data listed in Table 1 demonstrate that, at a substrate-to-acid ratio of 1 : 25 and a temperature of $110 \pm 5^\circ\text{C}$, the hydrolysis process is directed in the right way and proceeds to a sufficient extent. The degree of hydrolysis is $32.75 \pm 2.29\%$ in 4.00 ± 0.05 h and $65.50 \pm 4.59\%$ in 8.00 ± 0.05 h and reaches its maximum value of $96.20 \pm 6.73\%$ in 24.00 ± 0.05 h. As the

substrate-to-acid ratio is decreased to 1 : 15 and 1 : 20, the degree of hydrolysis in 24.00 ± 0.05 h falls to 82.69 ± 5.79 and $92.99 \pm 6.50\%$, respectively. This is possibly due to the polypeptide chain being insufficiently strongly attacked by the hydrochloric acid solution. It was also discovered that ammonia accumulates as the hydrolysis time is extended. For example, as the hydrolysis time is lengthened from 4.00 to 24.00 h at substrate-to-acid ratios of 1 : 15, 1 : 20, and 1 : 25, the ammonia weight fraction increases from 0.015 to 0.095%, from 0.034 to 0.156%, and from 0.085 to 0.200%, respectively.

The same trend is observed for the weight fraction of amino nitrogen. This is obviously due to the increase in the number of cleaved amide bonds in separate amino acids. For the sake of comparison, we carried out casein hydrolysis with 6 M sulfuric acid under the same conditions. The results of these experiments are presented in Table 2.

The data listed in Table 2 suggest that, as the hydrolysis time is extended, amino nitrogen and ammonia accumulate and the degree of hydrolysis increases. The intensity of the process increases with an increasing volume of the acid. For example, the degree of hydrolysis at a substrate-to-acid ratio of 1 : 15 and a hydrolysis time of 24.00 ± 0.05 h is $74.42 \pm 5.20\%$, while the degree of hydrolysis at substrate : acid = 1 : 25 and a hydrolysis time of 24.00 ± 0.05 h is $88.52 \pm 6.19\%$.

In the sample with substrate : acid = 1 : 15, the weight fraction of ammonia increases by a factor of 1.78; as the substrate-to-acid ratio is increased to 1 : 20 and 1 : 25, the ammonia weight fraction grows by a factor of 2.81 and 3.49, respectively. This finding is not in conflict with data obtained by other researchers [3-5, 7]. Thus, we have ascertained that casein hydrolysis proceeds more rapidly and more efficiently under the action of 6 M hydrochloric acid.

In order to evaluate the properties of the resulting acid hydrolysates in greater detail, we studied the hydrolysis time effect on the molecular weight distribution of proteins and peptides in the hydrolysates. The results of these experiments are presented in Table 3.

Some experiments demonstrated that the amount of proteins and peptides accumulated is proportional to the hydrolysis time. For example, at a hydrolysis time of 4.00 ± 0.05 , 8.00 ± 0.05 , and 24.00 ± 0.05 h, the reaction mixture consists mainly of peptides with a molecular weight of >20 , $5-20$, and <5 kDa, respectively, at any substrate-to-acid ratio.

The same trend is observed in casein hydrolysis with 6 M sulfuric acid (Table 4). For example, at a substrate-to-acid ratio of 1 : 15 and a hydrolysis time of 4.00 ± 0.05 h, the proportion of peptides with a molecular weight of over 20 kDa is 14.24%.

Table 1. Compositions of the casein hydrolysates obtained by treating casein with 6 M hydrochloric acid

Hydrolysis time, h	Weight fraction, %			Degree of hydrolysis, %
	total nitrogen	ammonia	amino nitrogen	
Initial casein sample	13.32 ± 0.93	0	0	0
Substrate : acid = 1 : 15				
4.00 ± 0.05	13.32 ± 0.93	0.015 ± 0.001	0.076 ± 0.005	19.48 ± 1.36
8.00 ± 0.05		0.062 ± 0.004	0.310 ± 0.022	39.30 ± 2.75
24.00 ± 0.05		0.095 ± 0.007	1.976 ± 0.138	82.69 ± 5.79
Substrate : acid = 1 : 20				
4.00 ± 0.05	13.32 ± 0.93	0.034 ± 0.002	0.136 ± 0.010	26.15 ± 1.83
8.00 ± 0.05		0.138 ± 0.010	0.550 ± 0.039	52.38 ± 3.67
24.00 ± 0.05		0.156 ± 0.011	3.126 ± 0.219	92.99 ± 6.50
Substrate : acid = 1 : 25				
4.00 ± 0.05	13.32 ± 0.93	0.085 ± 0.006	0.284 ± 0.020	32.75 ± 2.29
8.00 ± 0.05		0.144 ± 0.024	1.148 ± 0.0080	65.50 ± 4.59
24.00 ± 0.05		0.200 ± 0.070	3.880 ± 0.272	96.20 ± 6.73

Table 2. Compositions of the casein hydrolysates obtained by treating casein with 6 M sulfuric acid

Hydrolysis time, h	Weight fraction, %			Degree of hydrolysis, %
	total nitrogen	ammonia	amino nitrogen	
Initial casein sample	13.32 ± 0.93	0	0	0
Substrate : acid = 1 : 15				
4.00 ± 0.05	13.32 ± 0.93	0.014 ± 0.001	0.068 ± 0.004	17.54 ± 1.23
8.00 ± 0.05		0.056 ± 0.004	0.279 ± 0.02	35.37 ± 2.47
24.00 ± 0.05		0.356 ± 0.025	1.778 ± 0.12	74.42 ± 5.20
Substrate : acid = 1 : 20				
4.00 ± 0.05	13.32 ± 0.93	0.031 ± 0.002	0.122 ± 0.008	23.54 ± 1.64
8.00 ± 0.05		0.124 ± 0.008	0.495 ± 0.034	47.14 ± 3.30
24.00 ± 0.05		0.140 ± 0.01	2.813 ± 0.19	88.19 ± 6.17
Substrate : acid = 1 : 25				
4.00 ± 0.05	13.32 ± 0.93	0.077 ± 0.005	0.256 ± 0.01	29.48 ± 2.06
8.00 ± 0.05		0.099 ± 0.02	1.033 ± 0.07	58.95 ± 4.12
24.00 ± 0.05		0.190 ± 0.006	3.492 ± 0.24	88.52 ± 6.19

Table 3. Molecular weight distribution of the proteins and peptides resulting from casein hydrolysis in 6 M hydrochloric acid

Hydrolysis time, h	Relative content, %, at a given molecular weight, kDa			
	>20	10–20	5–10	<5
Substrate : acid = 1 : 15				
4.00 ± 0.05	14.02 ± 0.98	38.50 ± 2.69	26.00 ± 1.82	21.48 ± 1.50
8.00 ± 0.05	6.02 ± 0.42	14.12 ± 0.98	37.06 ± 2.59	42.80 ± 2.99
24.00 ± 0.05	0 ± 0.07	7.02 ± 0.49	8.42 ± 0.59	84.56 ± 5.92
Substrate : acid = 1 : 20				
4.00 ± 0.05	12.72 ± 0.89	26.25 ± 1.84	30.40 ± 2.13	30.63 ± 2.14
8.00 ± 0.05	4.02 ± 0.28	10.12 ± 0.71	33.06 ± 2.31	52.80 ± 3.69
24.00 ± 0.05	0 ± 0.06	2.10 ± 0.15	3.52 ± 0.25	94.38 ± 6.61
Substrate : acid = 1 : 25				
4.00 ± 0.05	10.27 ± 0.72	20.42 ± 1.43	40.80 ± 1.94	28.51 ± 1.36
8.00 ± 0.05	3.73 ± 0.26	7.53 ± 0.53	21.62 ± 1.51	67.12 ± 4.69
24.00 ± 0.05	0 ± 0.06	0.52 ± 0.03	1.87 ± 0.13	97.61 ± 6.83

Table 4. Molecular weight distribution of the proteins and peptides resulting from casein hydrolysis in 6 M sulfuric acid

Hydrolysis time, h	Relative content, %, at a given molecular weight, kDa			
	>20	10–20	5–10	<5
Substrate : acid = 1 : 15				
4.00 ± 0.05	14.24 ± 0.99	39.19 ± 2.74	27.95 ± 1.96	18.62 ± 1.30
8.00 ± 0.05	8.17 ± 0.57	15.06 ± 1.05	38.58 ± 2.70	38.19 ± 2.67
24.00 ± 0.05	0 ± 0.08	7.12 ± 0.50	15.92 ± 1.11	76.96 ± 5.39
Substrate : acid = 1 : 20				
4.00 ± 0.05	12.24 ± 0.86	29.19 ± 2.04	32.95 ± 2.30	25.62 ± 1.79
8.00 ± 0.05	7.17 ± 0.50	12.06 ± 0.84	30.58 ± 2.14	50.19 ± 3.51
24.00 ± 0.05	0 ± 0.08	1.92 ± 0.13	7.12 ± 0.50	90.96 ± 5.39
Substrate : acid = 1 : 25				
4.00 ± 0.05	10.45 ± 0.73	17.20 ± 1.20	41.84 ± 2.93	30.51 ± 2.14
8.00 ± 0.05	3.41 ± 0.23	8.56 ± 0.59	25.91 ± 1.81	62.12 ± 4.35
24.00 ± 0.05	0 ± 0.06	3.92 ± 0.27	5.47 ± 0.38	90.61 ± 6.34

As the hydrolysis time is increased, the amount of peptides with a molecular weight of over 20 kDa decreases to $8.17 \pm 0.57\%$, and disappears entirely in 24.00 ± 0.05 h owing to the attack of the chemical agent on the polypeptide chain and the buildup of nitrogen-containing compounds with a lower molecular weight. As a consequence, the proportion of peptides with a molecular weight of <5 kDa increases to become $18.62 \pm 1.30\%$ at a hydrolysis time of 4.00 ± 0.05 h and, as the hydrolysis time is extended to 24.00 ± 0.05 h, their amount increases further by a factor of 4.1 to become $76.96 \pm 5.39\%$. It was observed that, as the concentration of the chemical agent is raised, the degree of hydrolysis increases and this leads to an increase in the proportion of peptides with a molecular weight of <5 kDa. For example, at a hydrolysis time of 24.00 ± 0.05 h, the proportion of peptides with a molecular weight of < 5 kDa increases by a factor of

1.3, specifically from 76.96 ± 5.39 to $90.61 \pm 6.3\%$.

Note also that, as the hydrolysis time is extended, free amino acids build up intensively, and sulfuric acid, a dibasic one, ensures severer hydrolysis conditions than hydrochloric acid. The largest amount of amino acids accumulates in 24 h at a substrate-to-acid ratio of 1 : 25.

CONCLUSIONS

Our experiments demonstrated that the 24-h-long hydrolysis of casein at the optimal substrate-to-acid ratio, which is 1 : 25, affords casein hydrolysates with a high degree of hydrolysis and the maximum amount of amino acids accumulated. It should be taken into account that the proportion of peptides with a molecular weight of <5 kDa is $90.61 \pm 6.34\%$ in the hydrolysis with sulfuric acid and $97.61 \pm 6.83\%$ in the hydrolysis with hydrochloric acid.

REFERENCES

- Gorbatova, K.K., *Fiziko-khimicheskie i biokhimicheskie osnovy proizvodstva molochnykh produktov* (Physicochemical and Biochemical Foundations of the Manufacturing of Dairy Products), Moscow: GIORD, 2003.
- Kruglik, V.I., *Produkty pitaniya i ratsional'noe ispol'zovanie syr'evykh resursov: Sbornik nauchnykh rabot* (Foods and Rational Use of Raw Material Resources: Collected Works), Kemerovo: Kemerov. Tekhnol. Inst. Pishchevoi Prom-sti., 2007, issue 14, pp. 128–129.
- Kruglik, V.I., *Nauchnye i prakticheskie aspekty sozdaniya produktov dlya detskogo pitaniya* (Scientific and Practical Aspects of Designing Baby Foods), Kemerovo: Kuzbassvuzizdat, 2005.
- Kruglik, V.I., *Poluchenie, svoistva i primeneniye molochno-belkovykh kontsentratov: Sbornik nauchnykh trudov* (Preparation, Properties, and Application of Milk Protein Concentrates: Collected Works), Sokolova, E.N., Ed., Moscow: Agropromizdat, 1991, pp. 106–110.
- Kurbanova, M.G., *Nauchnoe obosnovaniye i tekhnologicheskie aspekty gidroliza kazeina* (Casein Hydrolysis: Scientific Foundations and Technological Aspects), Kemerovo, 2012.
- Mikhalkina, G.S., Tat'yanchikov, A.V., Vasil'eva, L.I., Petrova, S.P., and Kharitonov, V.D., RF Patent 2199233, 2003.
- Vigovsky, B., Konop, N., Malov, P., and Malov, A.N., *Journal of Allergy and Clinical Immunology*, 2003, vol. 111, pp. 533–540.



EFFECTS OF HUMIDITY AND THE CONTENT OF SPROUTED AND SPOILED BUCKWHEAT GRAINS ON THE CHANGES OF ACID NUMBER OF FAT AND GRAIN ACIDITY

V. A. Mar'in* and A. L. Vereshchagin

Biysk Institute of Technology (branch of I.I. Polzunov Altai State Technical University),
ul. Trofimova 27, Biysk, 659305 Russia,
*phone: 8-905-980-22-78, e-mail: tehbiysk@mail.ru

(Received January 14, 2014; Accepted in revised form March 3, 2014)

Abstract: The connection between buckwheat grain quality and the changes of the acid number of fat (AN) and grain acidity after eight months of storage has been investigated. Parameters of buckwheat with different content of moisture, germinated grains, and spoiled grains were determined. The studies performed have shown that oxidative damage to buckwheat grain increases concomitantly to the increase of humidity and content of germinated and spoiled seeds. All three defects of grain (increased humidity and increased content of germinated and spoiled seeds) accelerate the hydrolysis of grain lipids, and this leads to an increase of the acid number of fat. AN can be considered an indicator of grain freshness and should be introduced as an indicator of buckwheat quality for inward inspection of grain.

Keywords: Acidity, acid number of fat, spoiled grain, sprouted grains, humidity, buckwheat

UDC 633.12

DOI 10.12737/4126

INTRODUCTION

Buckwheat is the second most popular grain (after rice) on the Russian market. It accounts for over 20% of total consumption. All buckwheat on the Russian market is produced domestically.

Buckwheat (*Fagopyrum esculentum Moench.*) is the most common cereal crop in the Altai region: in 2012, buckwheat cultivation area occupied more than 420 thousand hectares in this region, this amounting to almost half of the total cultivation area of buckwheat in Russia. Altai region ranks first in the production of buckwheat in Russia. Grain from this region is supplied to all regions of Russia, and the volume of production amounted to 119 thousand tons in 2012 [1].

However, deterioration of the quality of incoming grain was observed during the recent years. Operational experience at OAO "Biiskii elevator" showed that the harvested buckwheat grain often remained in floor storage for several months prior to the post-harvest treatment and contained large amounts of moisture, spoiled, and sprouted grains upon submission for processing [2].

This is due to the deterioration of farming conditions and standards and the lack of post-harvest processing resulting in spoilage of grain and changes in its technological properties [3, 4].

Quality of the raw grain has a considerable effect on the storage ability of buckwheat. Deterioration of grain quality due to adverse environmental influences resulting in germination, spoilage, or frost damage, decreases the storage ability of the grain and makes the cereals produced from this grain more prone to spoilage upon storage.

In contrast to grain, which is alive and therefore

capable of active resistance to various adverse influences, cereal is more vulnerable to microorganisms, moisture and heat, and therefore it becomes spoiled much easier and faster than grain. Biochemical processes occurring during storage of cereals are primarily manifested as lipid changes.

The content of lipids in buckwheat reportedly varies from 1.5 to 4.0 % [5], being maximal in the embryo (7–14 %) and minimal in the shell (0.4–0.9 %) [6]. Analysis of the neutral lipid fraction revealed the predomination of palmitic (16:0), oleic (18:1), and linolenic acid (18:2) residues in the triglycerides (16, 42, and 32%, respectively) [7]. The rate of oxidation for linolenic acid is twice higher than that for oleic acid, and 20 times higher than that for palmitic acid [8]. Lipid oxidation impairs the organoleptic characteristics of grain.

Rancidification is caused by the hydrolysis of lipids; the extent of this process depends on such parameters as grain humidity and the content of sprouted and spoiled grains, in which the process of hydrolysis had already started. Organoleptic detection of the beginning of cereal spoilage is impossible, since distinctive and easily identifiable changes in appearance and odor do not occur during the initial stage. Measurements of the acid number of fat (AN) reported by L.G. Priezzheva included the investigation of rice groats, millet, peeled rye flour, and top grade wheat flour; changes in the AN during the guaranteed shelf life of Hercules oat flakes were reported in [9].

The aim of the present work was to investigate the effect of humidity and the proportion of sprouted and spoiled buckwheat grains on the changes of acid number (AN) of the fat and grain acidity.

OBJECTS AND METHODS OF STUDY

Buckwheat batches (moisture content up to 20% by mass, sprouted grain content up to 4.0%, spoiled grain content up to 1.6%) stored at the manufacturer's facilities without post-harvest handling were the objects of the present study.

Batches of buckwheat grain of Dialog variety harvested in the foothill area of Altai region were selected for the study. Samples were collected from batches of buckwheat harvested in 2012 and stored at the manufacturer's facilities for eight months. Samples from batches of grain harvested in 2013, stored for one month or less, and lacking spoiled and sprouted grains were used for comparison. Samples were collected at the grain handling center, and a representative sample was formed and used for the study. The analysis of acidity and AN in grain samples differing with regard to humidity and the content of spoiled and sprouted grains was of especial interest for the present study. The quality parameters were assessed using conventional methods.

The method of acidity assessment was based on the ability of grain components to neutralize alkali and involved titration of an aqueous slurry of ground grain.

Fifty grams of grain were selected from the composite sample and ground until the fragments passed through a sieve with openings of 0.8 mm in diameter. Ground grain was transferred onto a glass plate; a smooth layer was formed and pressed down by another glass plate to obtain a 3–4 mm thick layer. A 5-g sample of ground grain was transferred into a flask, mixed with 100 cm³ of distilled water, and stirred until all clumps disappeared. Phenolphthalein (5 drops of a 3% solution) was added to the suspension; the mixture was stirred and titrated with 0.1 M sodium hydroxide.

Acidity (X) was expressed in degrees of acidity as the volume of 1 mole/dm³ sodium hydroxide solution required to neutralize the acid in 100 g of the product and calculated according to formula 1 of the conventional procedure.

$$X = V \times 100 / m \times 10, \quad (1)$$

where V is the volume of exactly 0.1 M alkali solution required for titration, cm³; m is the mass of the ground grain sample, g; 1/10 is the factor used to convert the volume of 0.1 M sodium hydroxide solution to moles/dm³.

The acid number of fat was determined according to a procedure involving the extraction of fat from ground grain by hexane, solvent removal, drying of the fat, and titration of the fatty acids extracted by a 0.1 M KOH solution.

For this, 2 g of phenolphthalein were dissolved in 40 cm³ of ethanol in a 100 cm³ volumetric flask.

Potassium hydroxide (5.6 g) was dissolved in 500 cm³ of distilled water in a 1000 cm³ volumetric flask, and the solution was cooled to room temperature.

The solution containing alcohol and ether was prepared by mixing the required amount of ethyl alcohol and diethyl ether at a ratio of 1:1, adding five drops of phenolphthalein, and titrating with 0.1 M KOH until a weak pink coloration appeared.

Fifty grams of grain were taken from the composite sample and ground in a laboratory mill until the fragments passed through a sieve with openings of 0.8 mm in diameter. Ten grams of the ground product were mixed with 50 cm³ of hexane and stirred with a magnetic stirrer for 10 minutes. The mixture was allowed to stand for 10 minutes to separate the precipitate and the solvent.

The top (hexane) layer of the supernatant was decanted through a paper filter into a flask containing calcium chloride. Hexane was completely removed from the flask using a rotary evaporator at 70 °C, and afterwards the flask was placed into an oven, dried at 70 °C for one hour, cooled to room temperature for 30 minutes in a desiccator over calcium chloride, and weighed on a laboratory balance. The weight of the fat was calculated as the difference in the weight of the flask kept in a desiccator and the weight of the flask containing the extracted fat. All the extracted fat was dissolved in 10 cm³ of ethanol-ether mixture, five drops of phenolphthalein solution (concentration 2 g/cm³) were added, and the mixture was titrated with potassium hydroxide until a weak pink coloration appeared and persisted for 30 s.

Acid number of the fat in the sample under investigation, mg KOH/g fat, was calculated according to formula 2 of the conventional procedure.

$$AN = 5.611 AK/m, \quad (2)$$

where 5.611 is a constant calculated as the weight of KOH contained in 1 cm³ of 0.1 mole/dm³ solution; A is the volume of 0.1 M KOH used for titration, cm³; K is the correction coefficient for the titer of 0.1 M KOH; m is the mass of the extracted fat after drying, g.

Since the hydrolysis of fat occurring during the decay of reserve substances in grain begins earlier than that of proteins and carbohydrates, the AN assay is a more sensitive indicator of acceptable grain quality [10]. Analyses performed in the laboratory showed that the organoleptic parameters of the grain batches investigated complied to the existing requirements.

Batches of buckwheat grain received from the growers were divided into three groups:

- 1 - with moisture content ranging from 11.0 to 20.0%;
- 2 - with the content of germinated seeds ranging from 0 to 4.0 %;
- 3 - with the content of damaged grains ranging from 0 to 1.6 %.

All other parameters of the samples conformed to the existing requirements. Germinated seeds were not detected and the content of spoiled grains did not exceed 0.2% in samples of the first group; moisture content in the samples of the second and third groups did not exceed 14.5 %.

RESULTS AND DISCUSSION

The level of unground buckwheat consumption is fairly stable, and the demand for it is expected to grow in the near future. Increasing production volumes in Russia provide for the domestic market demand for buckwheat; domestic production of buckwheat is sufficient to satisfy the demand completely.

The quality of cereal products is an important factor for competition on the market. Wholesale consumers of unground buckwheat have recently come up with a number of critical remarks concerning the significant deterioration of cereal quality within the guaranteed period of shelf life. Organoleptic parameters of the cereal deteriorate, uncharacteristic odors appear, taste changes occur, and the cereal eventually becomes moldy and unfit for consumption. Moisture content in the grain is one of the main factors affecting the storage ability of the grain. High humidity is the main cause of poor conservation of wet and humid grain, as well as the products of processing of such grain.

Grain humidity is an important indicator of its quality. Grain can easily absorb and release moisture, since it has a capillary porous structure. Moist grain breathes intensively, and the concomitant enzymatic processes lead to adverse changes of the quality of the original grain. Such grain can easily germinate and is vulnerable to microorganisms.

The quality of cereals is directly dependent on the quality of grain from which the cereals were produced. However, the existing requirements are not sufficient for the assessment of grain freshness, especially in the initial period of grain deterioration when the changes of the organoleptic characteristics are slight. Buckwheat freshness is characterized by the maximal value of buckwheat AN, at which the product still retains its characteristic organoleptic parameters. At higher AN values, the product acquires an unusual odor, taste and color. Therefore, the AN value, which characterizes the degree of lipid hydrolysis resulting in the formation of free fatty acids, can be used to characterize the freshness of grain and predict changes in the quality parameters during grain storage. Accumulation of free fatty acids in grains reduces the quality of cereals.

Research conducted at Biisk Institute of Technology during the last few years showed that the AN of buckwheat grain supplied for the production of unground buckwheat ranges from 4.2 to 16.5 mg KOH/g; such grain meets the existing requirements and is accepted for processing and buckwheat grain production. Results of the measurements of fat AN and grain acidity for buckwheat grain of varying quality are reported in the present article.

All the measurements were conducted in 10 replicates and processed statistically. The effect of the content of moisture, germinated grains, and spoiled grains on the acidity and AN was investigated for buckwheat grain. The average values are reported in the present article.

The effect of moisture content (by mass) on indicators of oxidative damage in grain stored for one month is illustrated by Fig. 1. This grain was analyzed as it was received by the processing facility; no sprouted or spoiled grains were detected in the batches.

Grain acidity decreases with increasing moisture content, and increases as the content of spoiled and sprouted grains increases; this can be attributed to different mechanisms of the biochemical processes. Increasing humidity results in the dilution of acids,

while spoilage processes result in an increase of acid concentration.

The results show that an increase in humidity in the fresh grain leads to a 1.3-fold increase in AN and a 1.5-fold decrease in acidity. The currently existing requirements allow unground buckwheat production from grain with a moisture content below 16 % (at groats mills equipped with dryers), and this corresponds to a threshold AN of 9 mg KOH/g.

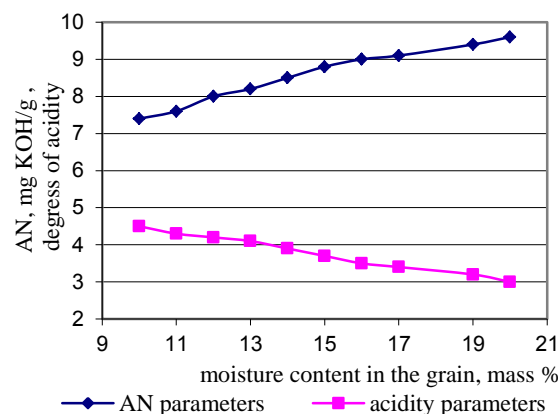


Fig. 1. Effect of moisture content on acidity and AN.

The effect of moisture content on AN parameters after 8 months of storage is illustrated by Fig. 2.

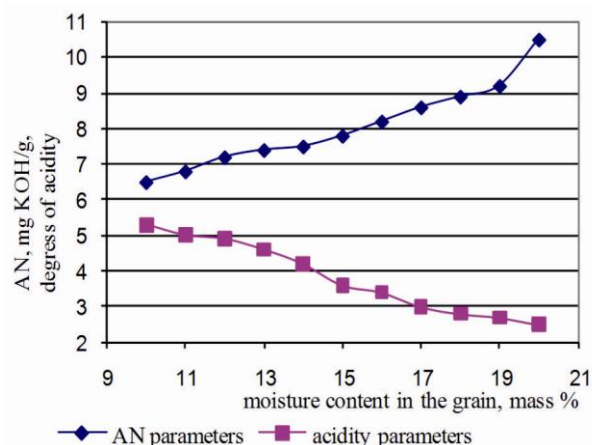


Fig. 2. Effect of moisture content on acidity and AN.

The data show that a 2.1-fold increase in humidity of the stored grain leads to a 1.6-fold increase in AN and a 2.1-fold decrease in acidity. The currently existing requirements allow unground buckwheat production from grain with a moisture content below 16 % (at groats mills equipped with dryers), and this corresponds to a threshold AN of 8.2 mg KOH/g.

Comparison of the results illustrated by Figures 1 and 2 reveals the identical character of processes in samples stored for 1 and 8 months, with an increase of AN and a decrease of acidity that can be attributed to protein hydrolysis processes resulting in the formation of amino acids.

The effect of the content of sprouted grains on oxidative spoilage of buckwheat grain is illustrated by Fig. 3.

The data shows that a 4.0-fold increase in the content of sprouted grains results in a 1.3-fold increase of AN and a 1.1-fold increase in acidity. The currently existing requirements allow cereal production from grain with a content of germinated seeds below 3% (by mass), and this corresponds to a threshold AN of 8 mg KOH/g.

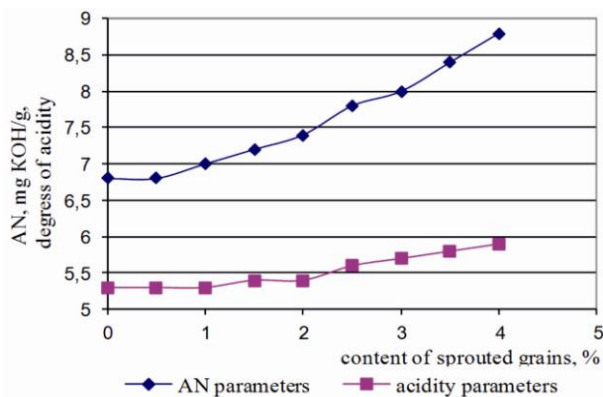


Fig. 3. Effect of the content of sprouted grains on oxidative deterioration of buckwheat.

The effect of the content of spoiled grains on oxidative deterioration of buckwheat grain is illustrated by Fig. 4.

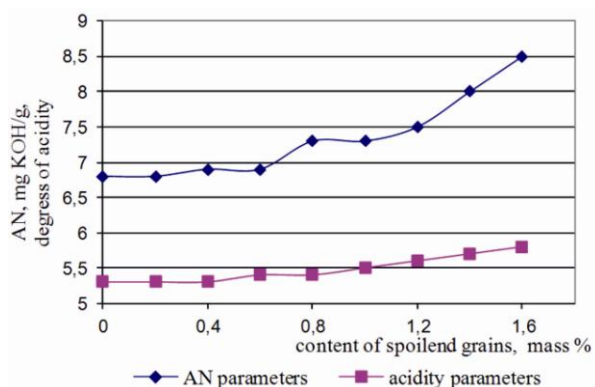


Fig. 4. Effect of the content of damaged grains on oxidative deterioration of buckwheat.

The data presented shows that a 1.6-fold increase in the content of damaged grains results in a 1.3-fold increase of the AN and a 1.1-fold increase in acidity. The currently existing requirements allow the production of third-grade unground buckwheat from grain containing 1.2 mass. % of damaged seeds at the highest, this being equivalent to a threshold AN value of 7.5 mg KOH/g.

The direction of changes related to the content of sprouted and spoiled grains is the same for acidity and AN, in contrast to the previous case. This change in the shape of the curves can be explained by the replacement of chemical hydrolysis processes by biochemical processes occurring during germination and spoilage of buckwheat and resulting in increases of grain acidity and AN.

Notably, the acidity of the grain cannot objectively characterize buckwheat quality due to opposite changes concomitant to quality deterioration. Grain acidity reportedly increases after drying of moist and wet grain.

All three factors (increased humidity or a high content of germinated or damaged grains) accelerate lipid hydrolysis in the grains, and this leads to an increase of the acid number of fat. AN can be regarded as an indicator of grain freshness, and it must be included into the range of buckwheat quality parameters assessed during input control. The data obtained suggest that AN is related to the history of grain storage and general quality of the grain.

Use of AN as an indicator will eliminate the need to control such parameters as humidity, the content of sprouted grains, and the content of damaged grains, and will allow for the use of one parameter in the monitoring of the proper storage conditions that ultimately determine organoleptic characteristics of buckwheat grain processing products; at the same time, the amount of work required for input control will be reduced.

The experiments performed yielded four threshold values of AN for the assessment of buckwheat quality, namely, 9.0, 8.2, 8.0, and 7.5. The minimal value, i.e. 7.5 mg KOH/g, should serve as a unified threshold value.

Thus, buckwheat grain with an AN higher than 7.5 mg KOH/g should not be accepted for processing for the production of unground buckwheat cereal.

REFERENCES

1. Bulavin, R.E., Itogi raboty zernopererabatyvayushchikh predpriyatii v 2012 g. (Results of grain processing enterprises in 2012), *Khleboprodukty (Bakery Products)*, 2013, no. 4, pp. 12–13.
2. Mar'in, V.A., Fedotov, E.A., and Vereshchagin, A.L., Pererabotka zerna grechikhi s vlazhnost'yu vyshe 17% (Processing of buckwheat grain with a moisture content above 17%), *Khleboprodukty (Bakery Products)*, 2008, no. 4, pp. 50–52.
3. Zlachevskii, A.L., Bulavin, V.E., Korbut, A.V., Gan, E.A., and Kobuta, I.V., Grain policy of the EEA (Zernovaya politika EEP), St. Petersburg: Tsentr integratsionnykh issledovaniy (Integration Research Center), 2012, p. 120.
4. Mazza, G., Storage, processing, and quality aspects of buckwheat seed, In: J. Janick and J.E. Simon (eds.), *New crops*, New York: Wiley, 1993, pp. 251–254.
5. Steadman, K.J., Burgoon, M.S., Lewis, B.A., and Edwardson, S.E., Buckwheat seed milling fraction: description, macronutrient composition and dietary fibre, *Journal of Cereal Science*, 2001, vol. 33, pp. 271–278.
6. Bonafaccia, G., Marocchini, M., and Kreft, I., Composition and technological properties of the flour and bran from common and tartary buckwheat, *Food Chemistry*, 2003, vol.80, pp.9–15.
7. Christa, K. and Soral-Šmietana, M., Buckwheat grains and buckwheat products – nutritional and prophylactic value of their components – a review, *Czech Journal of Food Science*, 2008, vol. 26, pp. 153–162.

8. Przybylski, R., Eskin N.A.M, Malcolmson, L.M., Ryland, D., and Mazza, G. Formation of off-flavour components during storage of buckwheat, *Proceedings of the 7th International Symposium on Buckwheat*, 12–14 August 1998, Winnipeg, Canada, pp. 3–7.
9. Mar'in, V.A., Vereshchagin, A.L., and Fomin, I.G., *Izmeneniye kislotochnogo chisla zhira v period garantirovannogo sroka khraneniya v khlop'yakh ovsyanykh "Gerkules"* (Changes of the acid number of fat during the guaranteed shelf life of Hercules oat flakes), *Tekhnika i tekhnologiya pishchevykh proizvodstv (Engineering and technology of food production)*, 2013, no. 3, pp. 126–129.
10. Priezzheva, L.G., *Metodika opredeleniya norm svezhesti i godnosti khleboproduktov po kislotnomu chislu zhira* (Methods for determining the standards of freshness and shelf life of baked foods using the acid number of fat), *Khleboprodukty (Bakery Products)*, 2012, no. 1, pp. 50–53.



ASSESSMENT OF PROTEOLYSIS AND LIPOLYSIS INTENSITY IN PECHERSKY CHEESE RIPENING IN THE PRESENCE OF *PENICILLIUM CAMEMBERTI* AND *PENICILLIUM ROQUEFORTI* MOLDS

Yu. T. Orlyuk and M. I. Stepanishchev*

Institute of Food Resources, National Academy of Sciences,
ul. M. Raskovoi 4A, Kiev, 02660 Ukraine,
*phone/fax: (38044) 517-08-92, e-mail: stepanishchev@i.ua

(Received January 22, 2014; Accepted in revised form March 4, 2014)

Abstract: High intensity of proteolysis and lipolysis in the curd due to the activity of mold enzymes is characteristic of mold-ripened cheeses. The intensity of proteolysis and lipolysis in cheese curd during the ripening process of Pechersky cheese containing two types of mold has been investigated in order to delineate the optimal production parameters. The results showed that the intensity of enzymatic processes in Pechersky cheese was higher than in Roquefort and Camembert cheeses. This is due to the bidirectional ripening of Pechersky cheese, with mold *Penicillium roqueforti* mediating the ripening starting from the center of the block and the mold *Penicillium camemberti* mediating the ripening starting from the surface of the block. The data obtained allow for a reduction of the ripening time of Pechersky cheese to 21 days.

Keywords: *P. camemberti*, *P. roqueforti*, Pechersky cheese, proteolysis, lipolysis

UDC 637.3

DOI 10.12737/4128

INTRODUCTION

The consumption of mold-ripened cheeses in the CIS has shown a tendency to increase during the last ten years. Unfortunately, domestic companies produce a limited range of such cheeses and the demand for these cheese varieties is met only partially. Production of mold-ripened cheese is more profitable than that of hard cheeses due to the lower cost of raw materials per unit of final product. Soft cheeses, including mold-ripened cheese, account for up to 40% of cheese production volume in Western Europe [1]. The share of such cheeses in the total production volume in the world is increasing every year due to their high biological value and unique organoleptic characteristics. According to the experts' estimates, cheeses with white surface mold account for about (7–8)% of the total cheese production volume in Europe and for about (2–3)% of world production volume. French companies alone produce more than 300 000 tons of cheese with white surface mold per year.

Unstable quality parameters remain the main disadvantage of domestic mold-ripened cheeses. The use of foreign technologies for the production of mold-ripened cheese cannot provide for stable quality parameters, and therefore modifications taking the features of the domestic production facilities into account must be introduced into the technologies. Thus, improvement of the existing domestic technologies for the production of mold-ripened cheese and the development of new technologies are tasks of high priority.

The presence of mold microflora possessing high proteolytic and lipolytic activity is characteristic of mold-ripened cheese [2]. Biochemical processes that occur in cheese during ripening are associated with the

development of microorganisms and their enzymatic activity that depends on many factors, such as active acidity, redox potential and water activity of the cheese mass, and ripening conditions (temperature, relative humidity, and intensity of air exchange in the maturation chamber) [3, 4, 5]. Proteolysis and lipolysis processes that determine the organoleptic characteristics of cheese can be controlled by selecting the technological parameters of cheese production and the regimen of cheese ripening [6, 7, 8]. Proteolysis is a critical process in the production of all kinds of cheeses, since it is responsible for the structural changes and has a significant effect on the formation of cheese taste and flavor. Intensity of proteolysis is much higher in mold-ripened cheeses than in other types of cheese; for example, the content of soluble nitrogen in blue cheese amounts to (50–65) mass % [9]. The level of proteolysis in cheese with white surface mold is rather high, although lower than that in blue cheese [4, 10]. The content of soluble nitrogen in the outer part of the block of mature Camembert cheese is 35% of the total nitrogen content, and that in the middle of the block is 25% [4, 10].

Free fatty acids are formed in the cheese mass during lipolysis, and the volatile fatty acids among them account for the flavor and taste of the cheese.

OBJECTS AND METHODS OF RESEARCH

Proteolysis in ripening cheese was evaluated by monitoring the content of nitrogen compounds (total nitrogen, total soluble nitrogen) according to the modified Kjeldahl method developed at VNIIMS (All-Union Research Institute of Butter and Cheese Production). Qualitative and quantitative composition of amino acids in cheese was determined by ion exchange

chromatography using the amino acid analyzer Biotronik LC 2000 (Germany). Samples for chromatography were prepared by hydrolyzing cheese samples with 6 n. hydrochloric acid at a temperature of $(108 \pm 2)^\circ\text{C}$ for 24 hours and further evaporation in vacuo at a temperature of 45°C . Caseins and cleavage products thereof were detected by electrophoresis in polyacrylamide gels. Sample preparation included removal of fat by hexane extraction, drying, and dissolving the proteins obtained in a buffer (pH 8.3) with sodium dodecyl sulfate and β -mercaptoethanol. Spectrophotometry was used to quantitate the protein fractions. The densitograms obtained were processed using computer software Image Pro Gel Analyzer, Version 2.0, and Total Lab 1D.

Lipolysis intensity was assessed by measuring the amount of free fatty acids (FFA) and volatile fatty acids (VFA). VFAs were quantitated using distillation; namely, 30 ml sulfuric acid were added to a cheese sample (5 g), the mixture was distilled and titrated with 0.1 n. sodium hydroxide solution, and FFAs were analyzed by chromatography using a Kupol 55 device (Russia).

RESULTS AND DISCUSSION

Samples of cheese (Pechersky, Roquefort and Camembert) for the experiment were produced from normalized milk with a fat content (f.c.) of 3.2 %. The milk was pasteurized at $(72 \pm 2)^\circ\text{C}$ for (15–20) s. The milk was cooled to fermentation temperature of $(32 \pm 1)^\circ\text{C}$, and calcium chloride together with milk-clotting enzyme was added to it. The curd was cut and kneaded for 30 min in the case of Camembert, 40 min in the case of Pechersky, and 60 min in the case of Roquefort, to obtain a granular curd. The duration of curd treatment varied due to the different requirements to water content (w.c.) in the cheese samples, namely, 60% by weight in Camembert, 50% in Pechersky, and 45% in Roquefort. The processed curd was placed into self-pressing forms. After self-pressing and the increase of active acidity in the cheese mass to (4.6 ± 0.1) pH units, cheese blocks were salted in brine during 80 min in the case of Camembert, 120 min in the case of Pechersky, and 180 min in the case of Roquefort, to obtain cheese curd with a salt content (s.c.) of 1, 2 and 3 mass. %, respectively. The salted cheese blocks were dried for (60–120) min. Holes of 3 mm in diameter were pierced in Roquefort and Pechersky cheeses to provide conditions for the development of *Penicillium roqueforti* mold. Cheese blocks were placed into maturation chambers with relative air humidity of (94–96)% and air temperature of $(8 \pm 0.5)^\circ\text{C}$ for Roquefort, $(10 \pm 0.5)^\circ\text{C}$ for Pechersky cheese, and $(12 \pm 0.5)^\circ\text{C}$ for Camembert. *Penicillium roqueforti* mold (produced by the company Danisco) was added into the cheese mass during the molding of cheese blocks. *Penicillium camemberti* mold (produced by Danisco) was applied to the surface of the cheese block by spraying. Changes in proteolysis and lipolysis parameters of Pechersky cheese samples during ripening were assessed by comparing the parameters with those of

Camembert and Roquefort cheeses produced under similar conditions.

Proteolysis during ripening of the test cheese samples was assessed by measuring the ratio of soluble nitrogen content to the total nitrogen content (Fig. 1).

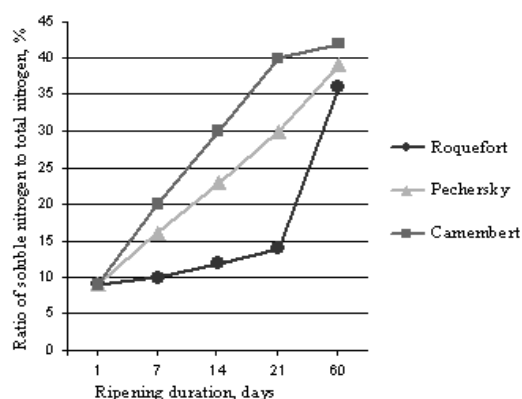


Fig. 1. Changes in the soluble nitrogen: total nitrogen ratio in test samples of cheese during ripening.

Graphic processing of the results showed that the above named ratio equaled 39% for Camembert cheese samples and 30% for Pechersky cheese samples on day 21 of ripening, this being more than twice higher than the respective parameter for Roquefort cheese (14%). Proteolysis intensity in test samples of cheese was also evaluated using information on the content and composition of free amino acids in these samples. The content of free amino acids in test samples of cheese on day 21 of ripening is illustrated by Fig. 2. Analysis of the results showed that total content of free amino acids in the samples of Pechersky cheese was 23% lower than in samples of Camembert cheese, with the most pronounced differences noted for aspartic acid, serine, glutamic acid, proline, alanine, phenylalanine, and lysine, and 19% higher than in Roquefort cheese, with the most pronounced differences noted for aspartic acid, valine, methionine, isoleucine, and leucine.

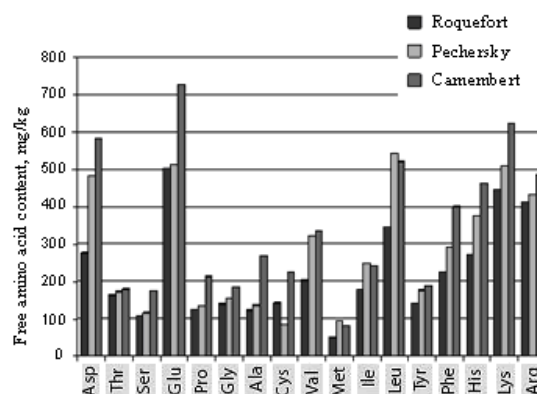


Fig. 2. Amino acid composition of experimental samples of cheese on day 21 of ripening.

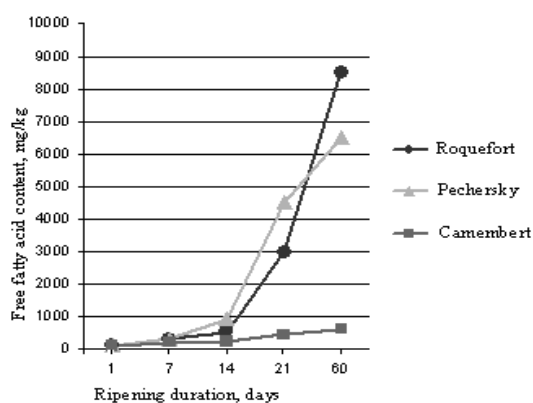
Results of the analysis of fractional composition of proteins in cheese samples during ripening are shown in Table 1.

Table 1. Content of protein fractions in cheese during ripening

CHEESE SAMPLE	FRACTIONAL COMPOSITION OF PROTEINS, %					
	Peptides 120-70 kDa	α -casein	β -casein	Peptides 28-26 kDa	Peptides 20-18 kDa	Peptides 16-12 kDa
Roquefort						
After self-pressing	3.26	41.48	37.52	5.39	5.28	1.07
Day 21 of ripening	6.86	34.01	29.84	9.62	10.31	3.78
Camembert						
After self-pressing	3.41	40.85	36.21	5.64	6.37	1.74
Day 21 of ripening	12.24	19.20	27.19	16.85	15.57	4.35
Pechersky						
After self-pressing	3.88	41.02	36.73	5.24	5.93	1.52
Day 21 of ripening	12.21	25.02	28.57	12.72	12.37	3.56

Analysis of the results revealed a tendency to a decrease of the number of casein fractions in test samples during the ripening of cheese. The content of α -casein decreased by 18% in Roquefort cheese, by 53% in Camembert cheese, and by 39% in Pechersky cheese on day 21 of maturation. The content of β -casein decreased from 37.52 % to 29.84 % in Roquefort cheese, from 36.21 % to 27.19 % in Camembert cheese, and from 36.73 % to 28.57 % in Pechersky cheese.

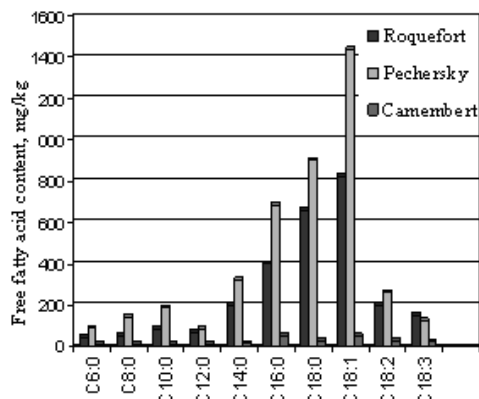
The content of FFAs (mg per kg cheese) was measured to assess lipolysis during the ripening of test cheese samples. Graphic processing of the results showed that the content of FFAs in cheese on day 21 of ripening equaled 400 mg/kg for Camembert, 4500 mg/kg for Pechersky cheese, and 3000 mg/kg for Roquefort cheese (Fig. 3). Low FFA content in Camembert cheese is due to lower lipolytic activity of enzymes from the mold *P. camemberti*, as compared with those of the mold *P. roqueforti*.

**Fig. 3.** Changes in the level of lipolysis in Roquefort, Pechersky, and Camembert cheese during ripening.

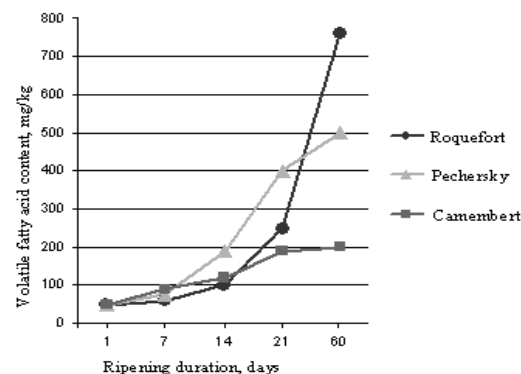
The fatty acid composition was determined on day 21 of ripening, in order to perform a more detailed assessment of lipolysis in test samples of cheese (Fig. 4).

The results revealed a high content of palmitic, stearic, oleic, linoleic, and linolenic acids in Roquefort

and Pechersky cheeses. The latter three acids are essential, and their content in Roquefort and Pechersky cheeses amounts to 30% of the total FFA content.

**Fig. 4.** Fatty acid composition of Roquefort, Camembert and Pechersky cheeses on day 21 of ripening.

The content of VFAs in test samples of cheese at different stages of ripening was assayed as well (Fig. 5).

**Fig. 5.** Changes of the content of volatile fatty acids during ripening of the cheeses under investigation.

The results showed that VFAs accumulate in all test samples during ripening. A significant increase of

VFA content in Roquefort cheese (from 243 to 765 mg/kg) was observed between the 21-st and 60-th days of maturation, while in Camembert cheese it occurred between days 1 and 21 of maturation (from 44 to 178 mg/kg), and the increase of VFA content in Pechersky cheese was intense throughout the ripening period (from 44 mg/kg on day 1 to about 500 mg/kg on day 60). VFA content in Roquefort, Camembert and Pechersky cheese increased 6.1-, 4.2- and 8.6-fold, respectively, during the first 21 days of ripening, this being indicative of a higher enzyme activity of a combination of two types of mold (*P. camemberti* and *P. roqueforti*).

Pechersky cheese occupies an intermediate position between the blue cheeses of Roquefort type and white-mold cheeses of Camembert type. The studies performed allowed for the conclusion that the proteolysis level in Pechersky cheese ripened for 21 day reaches that of mature Camembert cheese (which usually ripens within 14 days), and the lipolysis level of Pechersky cheese ripened for 21 day is close to that of mature Roquefort cheese (ripened for 60 days). Simultaneous development of two types of mold during the ripening of Pechersky cheese allows for faster ripening and the production of cheese with unique organoleptic characteristics.

REFERENCES

1. Shergina, I.A., Klassifikatsiya i osobennosti proizvodstva myagkikh syrov (Classification of soft cheeses and specific features of their production), *Syrodeliye i maslodeliye (Cheesemaking and butter-making)*, 2008, no. 4, pp. 8–9.
2. Singer, S., *The History and Processing of Cheese*, Charleston: Bazaar Press, 2011.
3. Tamime, A.Y., *Processed Cheese and Analogues*, New York: John Wiley and Sons, 2011.
4. Law, B.A. and Tamime, A.Y., *Technology of Cheesemaking*, New York: John Wiley and Sons, 2011.
5. Carroll, R. and Hobson, P., *Making Cheese, Butter and Yogurt*, North Adams: Storey publishing, 2012.
6. Pitt, J.I. and Hocking, A.D., *Fungi and Food Spoilage*, Berlin: Springer, 2009.
7. Heather, P., *The Life of Cheese: Crafting Food and Value in America*, University of California Press, 2012.
8. Langley Sammis, J., *Cheese Making*, Memphis: General books, 2012.
9. Lison, K., *The Whole Fromage: Adventures in the Delectable World of French Cheese*, New York: Crown Publishing group, 2013.
10. Chen, L.-S., Ding, Q.-B., Ma, Y., Chen, L.-G., and Maubois J.-L., The effect of yeast species from raw milk in China on proteolysis in Camembert-type cheese, *Food and Bioprocess Technology*, 2012, vol. 5, pp. 2548–2556.



COMPOSITION AND MICROSTRUCTURE INVESTIGATION FOR THE MODELING AND CLASSIFICATION OF DIETARY FIBER DERIVED FROM PLANTS

A. V. Pozdnyakova^{a,*}, A. N. Arkhipov^b, O. V. Kozlova^a, and L. A. Ostroumov^a

^aKemerovo Institute of Food Science and Technology,
bul'v. Stroitelei 47, Kemerovo, 650056 Russia,

*phone/fax: +7 (3842) 39-68-74, e-mail: anjap12@mail.ru

^bLtd. "KPF Milorada",

ul. Godovikova 9, Moscow, 129085 Russia,

phone: (495) 956-98-01, e-mail: trade@milorada.ru

(Received January 20, 2014; Accepted in revised form January 30, 2014)

Abstract: Investigation of the composition and microstructure of dietary fiber derived from plants showed that the stabilizers investigated differ with regard to size and shape of the particles and the density of particle distribution. The composition and microstructure of dietary fiber derived from plants have been studied using electron microscopy. Spectrometric profiles of chemical composition have been obtained, and the content of the predominant chemical elements in food microstructure stabilizers has been determined. Some similarity concerning the content of certain chemical elements and the ratio of the contents of different elements has been detected upon the analysis of food structure stabilizers of the same type (carboxymethylcellulose, gum, and sodium pyrophosphate). Mathematical processing of photomicrographs of structure stabilizer samples has been performed, and masks for the assessment of the content of microcavities in the particles of the structure stabilizers investigated have been created.

Key words: dietary fiber, stabilizer, microstructure, electron microscopy, histogram, carboxymethylcellulose, sodium alginate, sodium pyrophosphate, xanthan gum

UDC 637.131:677.044.12

DOI 10.12737/4129

INTRODUCTION

Dairy products are among the most important components of human food. They account for 20% of protein supply and 30% of fat supply in the human diet. Creation of products with predefined properties and rational use of raw materials are the priority directions for the development of dairy products manufacturing technologies [1, 5, 6].

Adherence to scientifically based formulations and compliance of the final product composition with regulatory requirements concerning the composition of raw materials are among the most important issues to be controlled during the assessment of quality of dairy products. Hundreds of dairy products available on the market are in constant demand and often actively marketed; therefore sellers and manufacturers of dairy products alike are always tempted to adulterate these products. Therefore, reliable methods for the identification of raw materials found in dairy products are necessary to prevent faulty and adulterated foods from being sold [2, 7, 8, 9].

The question of reliable determination of the type of components found in dairy products is currently especially acute due to the widespread adulteration of foods with texture stabilizers. The use of these components implies adding them to foods to induce gelling of liquid systems. Structure stabilizers currently in use comprise anionic polysaccharides, both natural (pectin, agar, agaroid, and pyrophosphate) and artificial (oxidized starch). Alginates, cellulose derivatives, and

carboxymethyl cellulose (CMC), as well as various gums, are widely used abroad [3, 10, 11, 12]. Classification of stabilizers can be based on one of the following criteria: description of all compounds as polysaccharide materials, assignment of names referring to botanical species, origin (plant, animal, or artificial), or chemical properties. Classification taking the origin of the stabilizers into account is currently preferred; according to this classification, all stabilizers are assigned to groups of modified natural or semi-synthetic stabilizers, chemically modified natural stabilizers or compounds similar to them, or synthetic gums obtained by chemical synthesis.

Agar is one of the classic structure stabilizers widely used in confectionery industry. However, the increasing shortage of agar sources necessitates the replacement of agar with other structure stabilizers. Various types of pectins are an example of promising structure stabilizers. They are currently used in food and pharmaceutical industry. Pectins are capable of forming gel systems characterized by a specific set of physical and chemical properties. Furthermore, pectin was shown to exert beneficial effects on the human organism, and the resources for pectin production are virtually unlimited [4, 13, 14, 15].

The aim of the present work was to compare the microstructure and composition of various structure stabilizers of plant origin for the subsequent development of procedures for the detection of adulterated products.

OBJECTS AND METHODS OF THE STUDY

Texture stabilizers of five different types, namely, carboxymethylcellulose CMC Akutsel 3265, CMC 4500-6000, sodium alginate NO4-600, sodium pyrophosphate SAPP 40, and xanthan gum, were the objects of the present study.

Scanning electron microscopy (SEM) analysis of stabilizer microstructure was conducted using a scanning electron microscope JSM-7500 FA. Photographs at magnification ranging from 100 to 500× were produced for each sample.

Analysis Station JEOL JED-2300 was used to investigate the composition of the structure stabilizers. X-ray microanalysis performed with this device yielded spectrometric profiles from which the chemical composition of the structure stabilizers was inferred.

Computational processing of photomicrographs revealing the stabilizer structure involved assessment of the content of microcavities using Corel Photo Paint X3 software; masks were created by extracting elements according to color, transformation of the photograph into a binary image and determination of the content of the elements of interest using a histogram.

RESULTS AND DISCUSSION

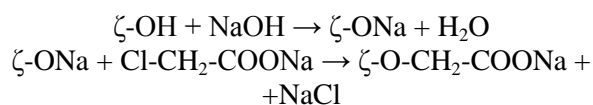
Investigation of the microstructure was performed for five types of structure stabilizers with different bulk densities (Table 1).

Table 1. Bulk density of the structure stabilizers investigated

Structure stabilizer	Bulk density, g/dm ³
CMC Akutsel 3265	450
CMC 4500-6000	490
Sodium alginate NO4-600	600
Sodium pyrophosphate SAPP 40	710
Xanthan gum	830

Microphotographs of CMC Akutsel 3265 at magnifications of 100, 200, and 500× are shown in Fig. 1. These photomicrographs show that the structure of CMC Akutsel 3265 comprises particulate elements shaped as elongated fibers with a rough surface; particle diameter ranges from 20 to 30 μm. The bulk density of CMC Akutsel 3265 equaled 450 g/dm³ and was the lowest among those of all the structure stabilizers studied.

CMC (carboxymethyl cellulose) is a salt of a weak carboxylic acid produced in a reaction of sodium monochloroacetate with alkaline cellulose according to the following scheme:



Each anhydropyranose unit of the carboxymethylcellulose molecule contains three -OH groups capable of reacting with sodium monochloroacetate. The substitution of all three OH groups is theoretically possible; however, the degree of

substitution in real CMC samples ranges from 0.4 to 1.2. The pK values of the carboxyl groups are 4.0 and 4.4 at degrees of substitution equal to 0.5 and 0.8, respectively. Approximately 90% and 10% of the carboxyl groups are ionized at pH 7.0 and 5.0, respectively. Carboxymethyl cellulose is an ionogenic cellulose ester, and therefore its stabilizing effect depends on salt concentration and other properties of the medium.

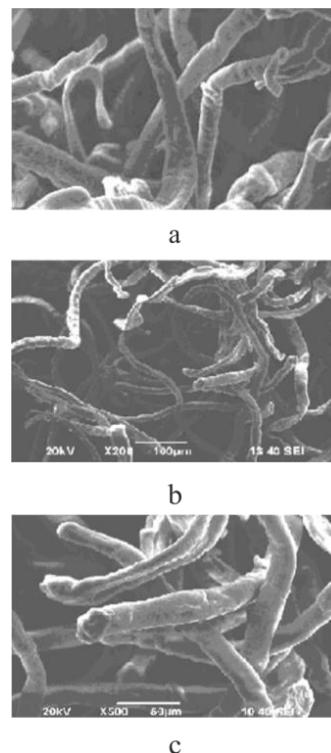


Fig. 1. Microstructure of CMC Akutsel 3265 at magnifications of 100 (a), 200 (b), and 500× (c).

The composition of CMC Akutsel 3265 is shown in Table 2.

The results demonstrate the predomination of oxygen (42.78 %) in CMC Akutsel 3265. Chlorine content is the lowest (0.07 %).

Table 2. Component composition of CMC Akutsel 3265

Element	Relative content, mass. %
Carbon	31.15±0.93
Nitrogen	21.90±0.65
Oxygen	42.78±1.28
Sodium	4.01±0.12
Chlorine	0.07±0.002

The microphotograph shown in Fig. 1-a was used to determine the content of microcavities in CMC Akutsel 3265. Filtering of background elements was necessary in this case. It was accomplished by increasing the contrast and correcting the mask manually. The results of microcavity detection in CMC Akutsel 3265 are shown in Fig. 2.

The content of microcavities in CMC Akutsel 3265 was 51.24±2.2% according to the histogram.

Thus, a low bulk density of 450 g/dm^3 is characteristic of CMC Akutsel 3265; the structure elements of this material have the form of elongated fibers with a diameter of $20\text{--}30 \text{ }\mu\text{m}$. Chemical elements present in CMC Akutsel 3265 include carbon, nitrogen, oxygen, sodium, and chlorine. The content of microcavities in this structure stabilizer amounted to $51.24\pm 2.2\%$.

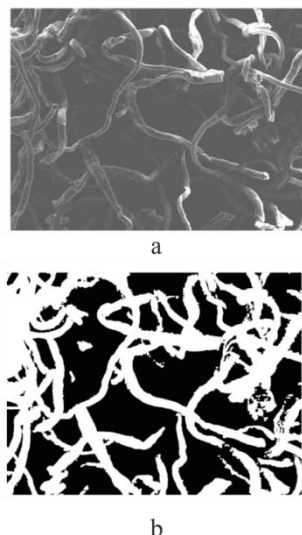


Fig. 2. The results of assessment of the content of microcavities in CMC Akutsel 3265: a – photomicrograph at a magnification of $100\times$; b – mask of the photomicrograph shown in Fig. 2-a.

Photomicrographs of the structure of CMC 4500-6000 at a magnification of 100, 200, and $500\times$ are shown in Fig. 3.

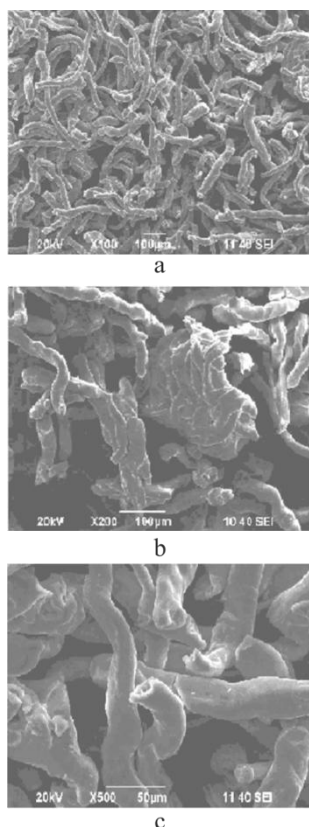


Fig. 3. Microstructure of CMC 4500-6000 at magnifications of 100 (a), 200 (b) and $500\times$ (c).

These photomicrographs reveal the similarity of the microstructure of the structure stabilizer CMC 4500-6000 to that of CMC Akutsel 3265, with a denser arrangement of the elements in the former due to a higher bulk density (490 g/dm^3). As evident from Fig. 3-b and 3-c, some fibers in CMC 4500-6000 interweave, forming large clusters of particulate elements of more than $200 \text{ }\mu\text{m}$ in size. The diameter of the fibers is $20\text{--}35 \text{ }\mu\text{m}$.

Results of the analysis of the chemical composition of CMC 4500-6000 are shown in Table 3. The content of oxygen, sodium, and chlorine in this stabilizer is higher than in CMC Akutsel 3265, while the content of carbon and nitrogen is lower.

Table 3. Component composition of CMC 4500–6000

Element	Content, mass %
Carbon	28.84 ± 0.86
Nitrogen	17.29 ± 0.52
Oxygen	48.01 ± 1.44
Sodium	5.63 ± 0.17
Chlorine	0.24 ± 0.01

The results of microcavity detection in CMC 4500-6000 are illustrated by Fig. 4. The photomicrograph shown in Fig. 3a was used for the analysis.

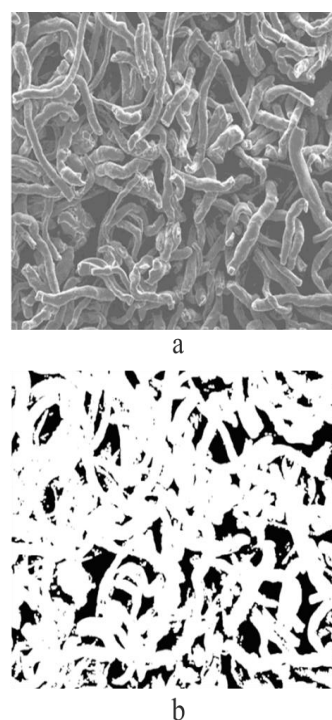


Fig. 4. The results of evaluation of the content of microcavities in CMC 4500-6000: a – photomicrograph at a magnification of $100\times$; b – mask of the photomicrograph shown in Fig. 4-a.

Since the elements of CMC 4500-6000 could not be reliably separated from the background using the color parameter, the selection borders were reduced by two pixels using contour selection after color selection.

The content of microcavities in CMC 4500-6000 was $20.28\pm 1.2\%$ according to the histogram.

The results show that the microstructure of CMC 4500-6000 is constituted by irregularly shaped fibers of 20–35 μm in diameter, the chemical components of this stabilizer include carbon, nitrogen, oxygen, sodium, and chlorine, and the content of microcavities equals $20.28 \pm 1.2\%$.

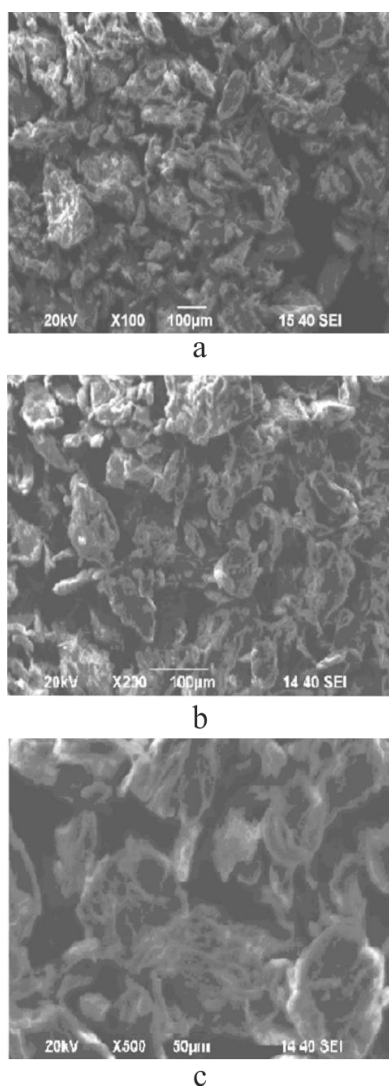


Fig. 5. Microstructure of sodium alginate NO4-600 at magnifications of 100 (a), 200 (b) and 500 \times (c).

Photomicrographs of sodium alginate NO4-600 at a magnification of 100, 200, and 500 \times are shown in Fig. 5. As evident from Fig. 5, structural elements of sodium alginate NO4-600 are particles of irregular shape ranging from 20 to 250 μm in size. Crystalline formations are present on the surface of the particles. Both rounded and elongated particles were detected. The bulk density of sodium alginate NO4-600 is 600 g/dm^3 .

The composition of sodium alginate NO4-600 is illustrated by Table 4; as evident from the data obtained, the presence of calcium and the absence of nitrogen distinguish sodium alginate NO4-600 from the structure stabilizers described above. Oxygen is the predominant component of sodium alginate NO4-600 (52.91 %), and the content of chlorine (0.19 %) is the lowest.

Table 4. Component composition of sodium alginate NO4-600

Element	Content, mass. %
Carbon	37.37 ± 1.12
Oxygen	52.91 ± 1.58
Sodium	9.26 ± 0.28
Chlorine	0.19 ± 0.006
Calcium	0.27 ± 0.01

Photographs of the microcavities in the structure of sodium alginate NO4-600 are shown in Fig. 6; these images were obtained by processing the photomicrograph in Fig. 5-a.

The content of microcavities inferred from the mask obtained (Fig. 6-b) was $33.79 \pm 1.1\%$.

Thus, the basic structural elements of sodium alginate NO4-600 are dispersed particles of irregular shape with the size of 20–250 μm and crystalline formations on the surface. Carbon, oxygen, sodium, chlorine and calcium are among the components of sodium alginate NO4-600. Computational processing of the photomicrographs yielded a value of $33.79 \pm 1.1\%$ for the content of microcavities in this structure stabilizer.

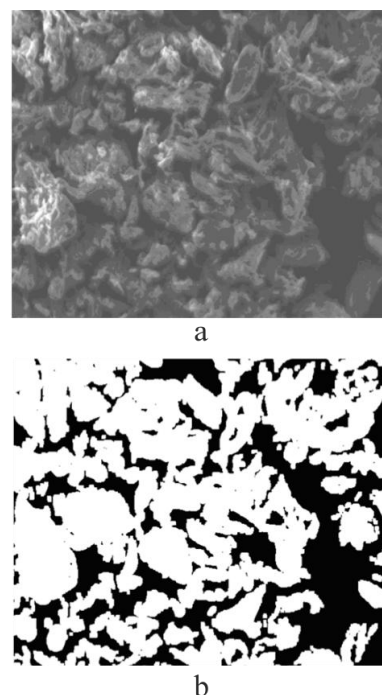


Fig. 6. Microcavities in sodium alginate NO4-600: a – photomicrograph at a magnification of 100 \times ; b – mask of the photomicrograph shown in Fig. 6-a.

Photomicrographs of sodium pyrophosphate SAPP 40 at a magnification of 100, 200, and 500 \times are shown in Fig. 7.

Dense arrangement and high coverage are characteristic of the microstructure of sodium pyrophosphate SAPP 40. The particle size ranges from 5 to 90 μm . This structure stabilizer has a high bulk density of 710 g/dm^3 .

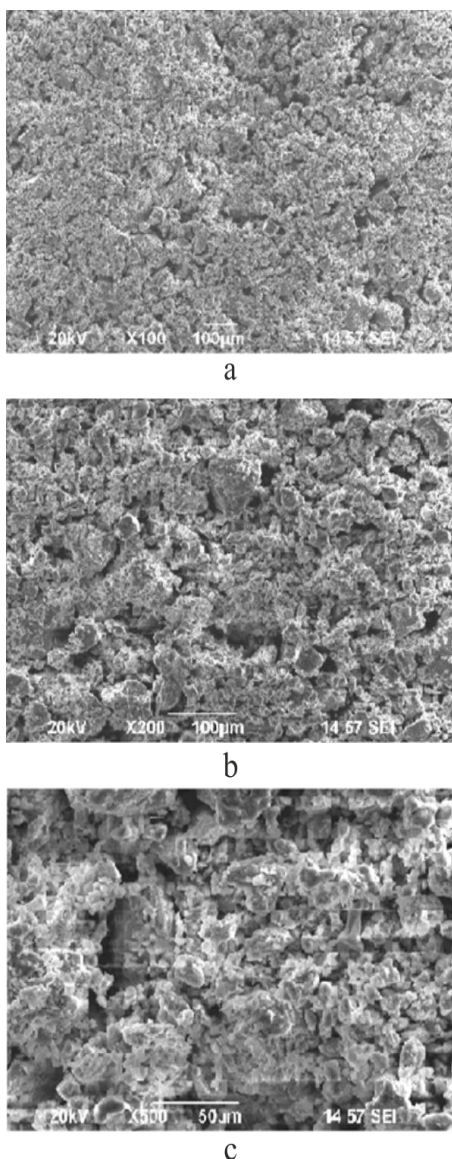


Fig. 7. Microstructure of sodium pyrophosphate SAPP 40 at magnifications of: a – 100; b – 200; c – 500 \times .

Results of the analysis of the composition of sodium pyrophosphate SAPP40 are shown in Table 5.

Table 5. Component composition of sodium pyrophosphate SAPP 40

Element	Content, mass. %
Carbon	8.21 \pm 0.25
Oxygen	51.94 \pm 1.55
Sodium	18.22 \pm 0.54
Phosphorus	21.63 \pm 0.65

The results of the quantitation of microcavities in sodium pyrophosphate SAPP 40 are shown in Fig. 8.

Analysis of the results presented in Fig. 8 showed that the content of microcavities in this stabilizer was 3.26 \pm 0.1%.

Thus, the structure of sodium pyrophosphate SAPP 40 is formed by closely spaced fine particles of irregular

shape and a size of 5–90 μ m. The content of microcavities is 3.26 \pm 0.1%.

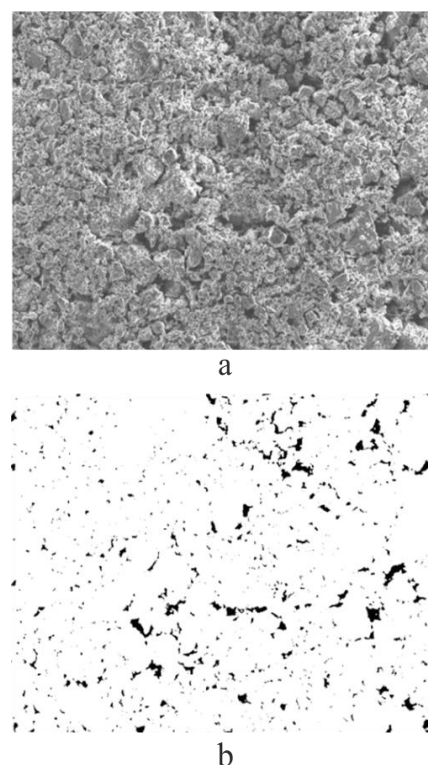


Fig. 8. Assessment of the content of microcavities in sodium pyrophosphate SAPP 40: a – photomicrograph at a magnification of 100 \times ; b – mask of the photomicrograph shown in Fig. 8-a.

Photomicrographs of xanthan gum at a magnification of 100, 200, and 500 \times are shown in Fig. 9.

Xanthan gum is characterized by the highest bulk density among all structure stabilizers studied (830 g/dm³) and has a dense fine structure. Most granules are elongated and range from 5 to 40 μ m in size (Fig. 9-c). Such particle size allows for rapid formation of highly viscous solutions in both hot and cold food systems and results in the production of high-quality foods. Some of the structural elements of xanthan gum form conglomerates. Microcavities of irregular shape are also present in the structure (Fig. 9-a).

The composition of xanthan gum is shown in Table 6.

Xanthan gum contains carbon, nitrogen, oxygen, and potassium.

Quantitation of the content of microcavities in xanthan gum was performed using a microphotograph taken at a magnification of 500 \times , in order to make the quantitation error as low as possible. The results are presented in Fig. 10. The content of microcavities in the structure of xanthan gum was 6.51 \pm 0.3%.

Thus, the microstructure of xanthan gum is formed by closely spaced elongated granules of 5–40 μ m in size. Carbon, nitrogen, oxygen, and potassium are found in this stabilizer. According to the results of computational processing, the content of microcavities in xanthan gum equals 6.51 \pm 0.3%.

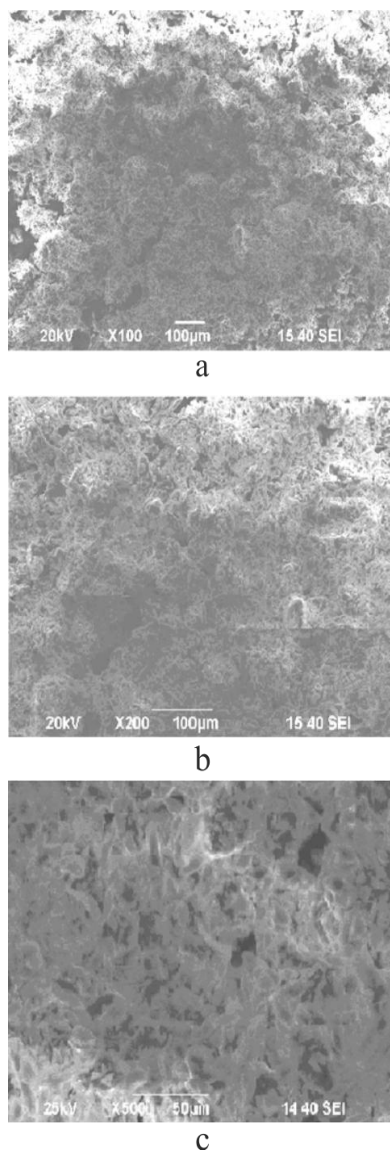


Fig. 9. Microstructure of xanthan gum at a magnification of 100 (a), 200 (b), and 500× (c).

Table 6. Composition of xanthan gum

Element	Content, mass %
Carbon	30.08±0.90
Nitrogen	23.42±0.70
Oxygen	46.38±1.39
Potassium	0.12±0.004

Analysis of the data shows that xanthan gum has the lowest specific surface area ($9.07 \cdot 10^{-6} \text{ cm}^2$) of all of the structure stabilizers investigated, and therefore its bulk

density (830 g/dm^3) is the highest. Nitrogen was not detected in sodium alginate NO4-600. Sodium was not detected in xanthan gum. Chlorine was not detected in sodium pyrophosphate SAPP 40. In general, such elements as carbon, nitrogen, oxygen, sodium, and chlorine were detected in all structure stabilizers investigated, although the content of these elements varied.

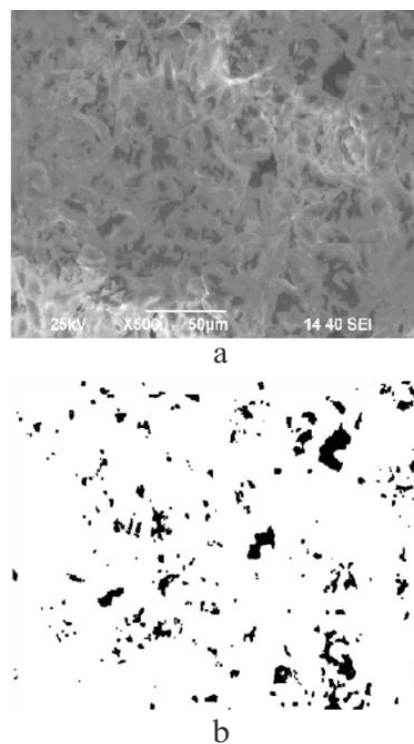


Fig. 10. Evaluation of the content of microcavities in xanthan gum:
a – photomicrograph at a magnification of 500×,
b – mask of the photomicrograph shown in Fig. 10-a.

Elongated fibers ranging from 15 to 60 μm in size were found among the structural elements of all types of carboxymethylcellulose investigated, with interweaving fibers forming large objects (above 200 μm in size) detected in CMC 4500-6000. The size of the elements of sodium alginate NO4-600 ranged from 20 to 250 μm . Sodium pyrophosphate SAPP 40 contained closely spaced fine particles of 5–90 μm in size. Structure elements of xanthan gum had a distinct elongated shape, their size was smaller (5–40 μm) than that of the other stabilizer particles, and the particles of this stabilizer were spaced more closely than in the others due to the high bulk density of the stabilizer (830 g/dm^3).

REFERENCES

- Anisenko, O.V., Stepavenko, O.V., and Shcherbatenko, A.V. Sposoby immobilizatsii ureazy na neorganicheskikh nositelyakh (Methods of urease immobilization on inorganic carriers), *Biologiya – nauka XXI veka: trudy VIII Mezhdunarodnoy Pushchinskoy shkoly-konferentsii molodykh uchenykh (Pushchino, 17-21 maya 2001 g.) (Biology in the XXI century: Proceedings of the VIII International Pushchino School and Conference for Young Researchers (Pushchino, May 17-21, 2001))*, Pushchino, 2004, p. 249.
- Beregova, I.V., Pektiny i karraginany v molochnykh produktakh novogo pokoleniya (Pectins and carrageenans in dairy products of the new generation), *Molochnaya promyshlennost' (Dairy industry)*, 2006, no. 6, pp. 44–46.

3. Dankvert, S.A. and Dukin, I.M., Sovremennoe sostoyanie i perspektivy razvitiya molochnogo kompleksa Rossii (Current state and perspectives of development of the dairy industry in Russia), *Molochnaya promyshlennost' (Dairy industry)*, 2006, no. 1, pp. 10–11.
4. Kitova, A. E., Kuvichkina, T.N., Arinbasarova, A. Yu., et al., Degradatsiya 2,4-dinitrofenola svobodnymi i immobilizovannymi kletkami *Rhodococcus erythropolis* HL PM-1 (Degradation of 2,4-dinitrophenol by free and immobilized cells of *Rhodococcus erythropolis* HL PM-1), *Prikladnaya biokhimiya i mikrobiologiya (Applied Biochemistry and Microbiology)*, 2004, vol. 40, no. 3, pp. 307–311.
5. Makeeva, I.A., Nauchnyye podkhody k formirovaniyu ponyatii potrebitel'skikh svoystv i kharakteristik molochnykh produktov v period intensivnogo razvitiya ikh assortimenta (Scientific approaches to the formation of concepts of consumer properties and characteristics of dairy products during intensive expansion of the range thereof), *Khraneniye i pererabotka sel'khozsyrya (Storage and processing of agricultural raw materials)*, 2006, no. 3, pp. 48–53.
6. Ashin, V.V., RF Patent 2 007 144 734, 2009.
7. Samuilova, O.K. and Vladimova, L.Ya., Funktsii stabilizatorov i emul'gatorov v molochnykh produktakh (Functions of stabilizers and emulsifiers in dairy products), *Pererabotka moloka (Milk processing)*, 2004, no. 2, p. 22.
8. Cheng, J., Teply, B.A., Sherifi, I., et al., Formulation of functionalized PLGA–PEG nanoparticles for *in vivo* targeted drug delivery, *Biomaterials*, 2007, vol. 28, pp. 869–876.
9. Sharma, A., Qiang, Y. Antony, J. et al., Dramatic increase in stability and longevity of enzymes attached to monodisperse iron nanoparticles, *IEEE Trans. Magn.*, 2007, vol. 43, pp. 2418–2420.
10. Gu, H., Xu, K., and Xu, C., Biofunctional magnetic nanoparticles for protein separation and pathogen detection, *J. of the American Chemical Society Chem. Commun.*, 2006, pp. 941–949.
11. Jeng, J., Lin, M.F., and Cheng, F.Y., Using high-concentration trypsin-immobilized magnetic nanoparticles for rapid *in situ* protein digestion at elevated temperature, *Rapid Commun. Mass Spectrom.*, 2007, vol. 21, pp. 3060–3068.
12. Kaushik, A., Khan, R., Solanki, P.R., et al., Iron oxide nanoparticles–chitosan composite based glucose biosensor, *Biosens. Bioelectron.*, 2008, no. 24, pp. 676–683.
13. Lee, J., Lee, Y., Youn, J.K. et al, Simple synthesis of functionalized superparamagnetic magnetite/silica core/shell nanoparticles and their application as magnetically separable high-performance biocatalysts, *Small*, 2008, no. 4, pp. 143–152.
14. Kim, M.J., An, G.H., and Choa, Y.H., Functionalization of magnetite nanoparticles for protein immobilization, *Diffus. Defect Data, Pt. B*, 2007, pp. 895–898.
15. Qiu, J., Peng, H., and Liang, R., Ferrocene modified Fe₃O₄-SiO₂ magnetic nanoparticles as building blocks for construction of reagentless enzyme-based biosensors, *Electrochem. Comm.*, 2007, no. 9, pp. 2734–2738.



DEVELOPMENT OF TECHNOLOGICAL PARAMETERS FOR THE HYDROTHERMAL PROCESSING OF SPROUTED WHEAT GRAIN POWDER

T. N. Safronova^{a,*} and O. M. Evtuhova^b

^aInstitute of Trade and Economics,
ul. L. Prushinskoi 2, Krasnoyarsk, 660075 Russia,
*phone: +7(391)2219294, e-mail:safronova63@mail.ru
^bSiberian Federal University,
pr. Svobodnyi 79, Krasnoyarsk, 660041 Russia

(Received December 26, 2013; Accepted in revised form February 3, 2014)

Abstract: The present work is devoted to the development of technological parameters for the hydrothermal processing of powdered sprouted wheat and justification of use of the powder produced as a food additive. Introduction of sprouts into the diet stimulates metabolism and hematopoiesis, boosts immunity, compensates for vitamin and mineral deficiency, normalizes the acid-alkaline balance, promotes the elimination of toxins from the body, stimulates digestion, and slows the aging process. The use of sprouted wheat grains in public catering is very limited due to the short shelf-life of this product. Storage of dried grains provides a solution for this problem; however, it necessitates the development of a technology for the use of dried sprouted wheat grain. The present study was a part of research on the powder produced from sprouted wheat and centered on the process of hydrothermal treatment of dry sprouted wheat powder. Conventional methods were used in the present work for the analysis of physical and chemical parameters. A range of factors, including the protein content of the powder, the degree of mechanical damage of the starch granules, and the pH value of the solution, affects the water absorption capacity of the powder produced from sprouted wheat. Treatment time, temperature, and mash ratio at pH 4.5 and pH 7.0 were varied in experiments performed to determine the optimum operating parameters of the hydrothermal processing. As a result of the study, an energy-efficient technology has been developed for the hydrothermal processing of powdered sprouted wheat grains. The following process parameters were selected: an optimum swelling temperature of 45°C, hydrothermal treatment duration of 60 min at pH 4.5, and an optimum mash ratio of 1:1.25.

Keywords: technological parameters of hydrothermal processing, powdered germinated wheat grains, the degree of powder swelling

UDC 641.1/3

DOI 10.12737/4132

INTRODUCTION

Dormant plant seeds are used as the raw material to prepare a large variety of foods. Sprouted wheat grains are known as a natural organic food, containing a broad range of nutrients in balanced natural amounts and combinations. Introduction of sprouts into the diet stimulates metabolism and hematopoiesis, boosts immunity, compensates for vitamin and mineral deficiency, normalizes the acid-alkaline balance, promotes the elimination of toxins from the body, stimulates digestion, and slows the aging process. Grains with sprouts shorter than 5 mm contain a sufficient amount of antioxidants, which decelerate or prevent oxidative processes when used in low concentrations. Furthermore, enzyme systems of the grain are activated during germination, and complex nutrients are cleaved into smaller molecules easily digestible by the human organism. The use of sprouted wheat grains in public catering is very limited due to the short shelf-life of this product. Storage of dried grains provides a solution for this problem; however, it necessitates the development of a technology for the use of dried germinated wheat. The aim of the present work was to develop technological parameters for the

hydrothermal processing of powder produced from sprouted wheat grains.

OBJECTS AND METHODS OF RESEARCH

The powder produced by grinding dried sprouted wheat grains (Technical Specification (TU) 9290-002-50765127-03, OOO SibTar, Novosibirsk) in a Robot Coupe R4 cutter (ROBOT COUPE) was the object of investigation in the present work. The powder had a beige color and a typical smell of wheat flour; particles of 250–300 µm in size constituted 80 ± 0.05% of the powder, and the size of the rest of the particles ranged from 300 to 450 µm; the solids content of the powder was 96.5 ± 0.05%.

Conventional methods were used for the analysis of the physical and chemical characteristics, namely, the content of dry matter was assayed according to GOST (State Standard) R 50189-92 using a moisture analyzer ELVIZ-2C, and active acidity was assayed using a multichannel ion meter Ekspert-001 (3.0.4). The degree and rate of swelling of the sprouted wheat powder were determined according to the procedure developed at the Belarusian branch of VNIMI (All-Union Research Institute of Dairy Industry): namely, 1 g of dry powder obtained from sprouted wheat was placed into a centrifuge tube, and

water was added to a ratio of 1:1–1:2. The mixture was incubated in a steamer (Stlf Cooking Center 61) for 60 min at a temperature of 25 ± 1 , 45 ± 1 , 65 ± 1 , or 85 ± 1 °C. The samples were then centrifuged for 5 min at 1000 rpm, the supernatant was decanted, and the moisture content of the residue was measured.

The degree of swelling of the samples was determined according to the formula (1):

$$A = (m - m_0)100/m_0, \quad (1)$$

where A is the degree of swelling, %; m is powder weight after hydration, g; m_0 is the weight of dry powder, g.

The mass of the powder after swelling was determined according to the formula (2):

$$m = m_0(100 - B)/(100 - B_1), \quad (2)$$

where m is mass of the powder after swelling, g; B is the moisture content of dry powder, mass. %; B_1 is the moisture content of hydrated powder, mass. %.

The optimal amount of water required for the swelling of sprouted wheat powder (mash ratio) was determined.

Statistical analysis of the results was performed using nonparametric tests implemented in the software package Statistica 6.0. The difference between values was considered to be significant at a confidence level of 95% ($p < 0.05$), both for the comparison of mean values between two samples and for multiple comparison of means.

RESULTS AND DISCUSSION

The capacity of powdered sprouted wheat to absorb water is an important factor for further industrial use as an additive in foodstuffs, for example, in minced meat and fish. High water absorbing capacity of the powder is a positive feature, since it allows for an increase of the final product yield. A range of factors, the content of protein being the most important of them, affect the water absorption capacity of the powder obtained from

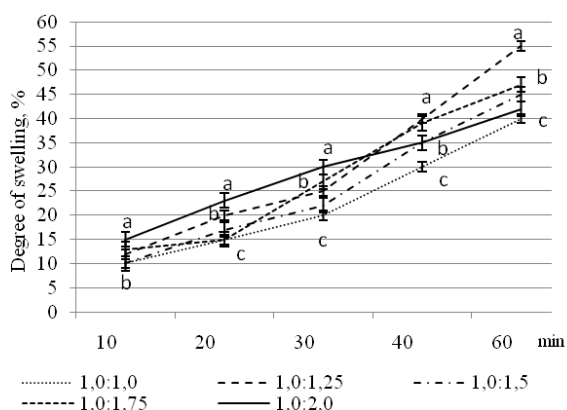


Fig. 1. Changes in the degree of powder swelling during 60 minutes at 25°C, pH 7.0 (different letters denote intra-group difference for multiple comparison of the means, LSD test, $p < 0.05$).

sprouted wheat grains. The contact of powder particles with water leads to osmotic binding of the latter; free interstitial protein is the first to bind water, followed by protein surrounding individual starch granules and protein present on large powder particles, that is, intact cells or cell groups of the endosperm [1–3].

The swelling of starch granules depends on the temperature and the degree of mechanical damage to the granules. Binding of water by intact starch grains mainly occurs through adsorption, and therefore the volume of the grains increases only slightly (up to 44% of water can be bound through adsorption). Grinding of the seeds into powder causes disruption of 15–20% of starch grains. The amount of water absorbed by such grains can be as high as 200% of their dry weight [4–6].

Swelling of colloids occurs in two stages. First, water molecules are adsorbed on the surface of the powder particles due to the presence of active and hydrophilic groups in colloids. The hydration process is accompanied by heat release. Thermal motion of the flexible side chains of the proteins enabled by loose packing of protein and starch macromolecules results in the formation of small gaps into which the water molecules penetrate, giving rise to the second stage of swelling, namely, osmotic water binding. The amount of water bound by proteins is approximately twice higher than the weight of the proteins themselves [7–10].

According to earlier reports, maximal hydration of gluten rinsed by phosphate buffer with a pH value ranging from 3.7 to 8.5 is observed at acidic and alkaline pH values, and minimal hydration is observed at a pH of about 6.0–6.5 [10–11].

The changes of the degree of swelling of sprouted wheat grain powder during 60 min of incubation at pH 4.5 or 7.0 and the effect of varying temperature and mash ratio on these changes are illustrated by Figures 1–8.

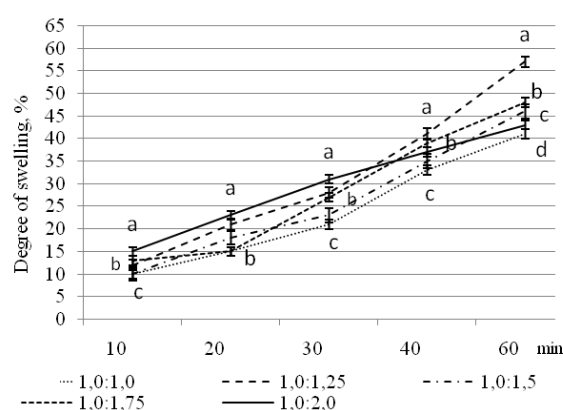


Fig. 2. Changes in the degree of powder swelling during 60 minutes at 25°C, pH 4.5 (different letters denote intra-group difference for multiple comparison of the means, LSD-test, $p < 0.05$).

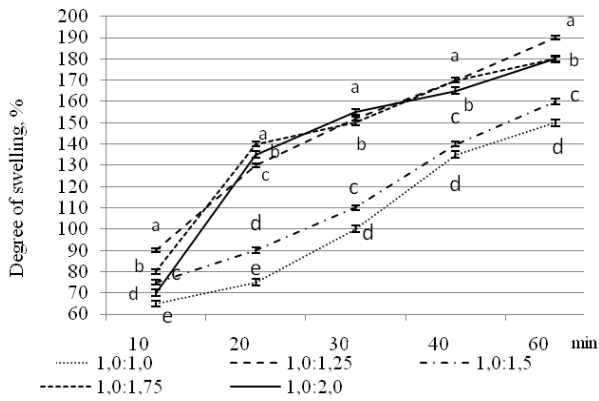


Fig. 3. Changes in the degree of powder swelling during 60 minutes at 45°C, pH 7.0 (different letters denote intra-group difference for multiple comparison of the means, LSD test, $p < 0.05$).

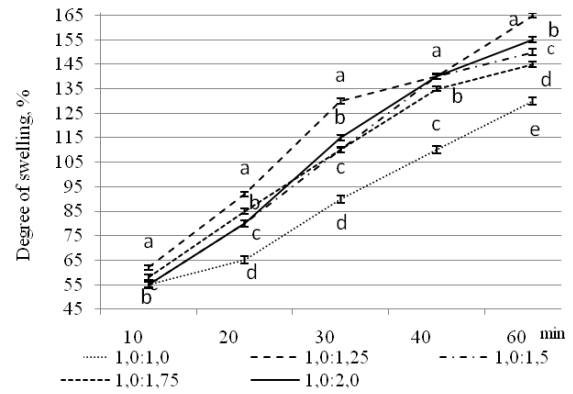


Fig. 6. Changes in the degree of powder swelling during 60 minutes at 65°C, pH 4.5 (different letters denote intra-group difference for multiple comparison of the means, LSD test, $p < 0.05$).

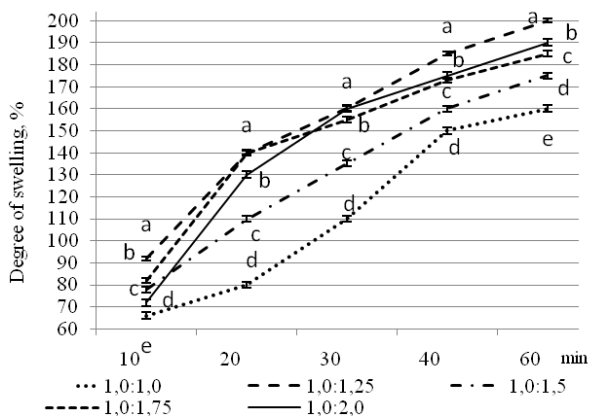


Fig. 4. Changes in the degree of powder swelling during 60 minutes at 45°C, pH 4.5 (different letters denote intra-group differences for multiple comparison of the means, LSD test, $p < 0.05$).

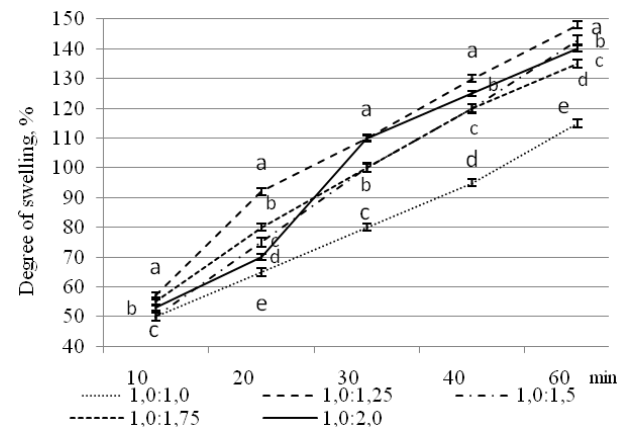


Fig. 7. Changes in the degree of powder swelling during 60 minutes at 85°C, pH 7.0 (different letters denote intra-group difference for multiple comparison of the means, LSD test, $p < 0.05$).

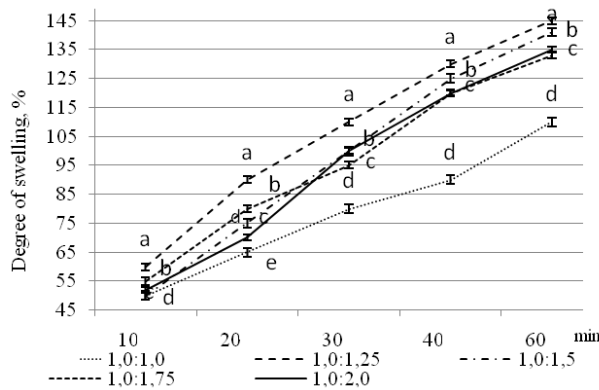


Fig. 5. Changes in the degree of powder swelling during 60 minutes at 65°C, pH 7.0 (different letters denote intra-group difference for multiple comparison of the means, LSD test, $p < 0.05$).

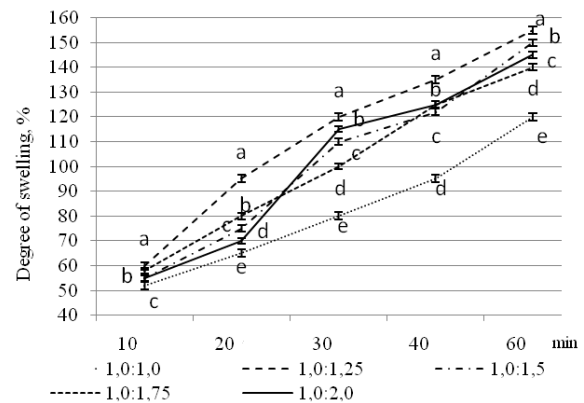


Fig. 8. Changes in the degree of powder swelling during 60 minutes at 85°C, pH 4.5 (different letters denote intra-group difference for multiple comparison of the means, LSD test, $p < 0.05$).

Changes in the amount of moisture retained by the powder at the beginning of the hydrothermal processing were slight at all the temperatures tested. Further penetration of moisture retained by surface tension resulted in intense absorption of water. The effect of

temperature was more pronounced at this stage, with the rate of water absorption being higher at 45–65°C than at 25°C. Maximal swelling of gluten proteins is known to occur at 30°C, while maximal swelling of starch grains occurs at 50°C. This difference in the optimal swelling

temperatures for proteins and starch in the powder is due to differences in the molecular weight and structure of these substances. Analysis of the data concerning the swelling of powder produced from sprouted wheat grains showed that the maximal degree of powder swelling (201%) was observed at the following parameters of hydration: mash ratio of 1:1.25, temperature of 45 °C, and treatment duration of 60 min at pH 4.5. These parameters were considered optimal. The development of an energy-efficient technology for the hydrothermal processing of sprouted grain powder was addressed in an experiment which involved a change in the mode of steam convector operation: namely, the convector was switched on and off for 10–15 min (T cycl), and the results were compared to those obtained at constant heating (T const). The degree of swelling of the powder was measured (Fig. 9).

The experiment did not reveal a statistically significant difference between the values of the degree of swelling of dried sprouted wheat powder attained at T const and T cycl. Thus, we have developed an energy-saving technology for the hydrothermal processing of powdered sprouted wheat intended for use as a food

additive. The parameters of the process were the following: temperature of 45°C, mash ratio of 1:1.25, and hydrothermal treatment duration of 60 min at pH 4.5.

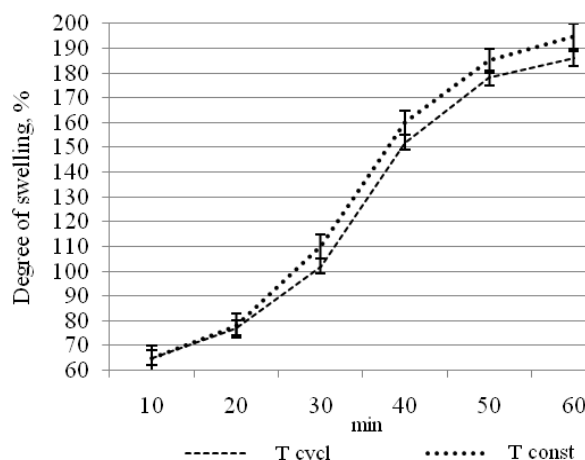


Fig. 9. Changes in the degree of powder swelling at different steamer operation modes.

REFERENCES

1. Reinhart's, P., Whole grain breads: new techniques, extraordinary flavor, Random House LLC, 2011.
2. Galchus, R., Homegrown sprouts: a fresh, healthy, and delicious step-by-step guide to sprouting year round, Quarry Books, 2013.
3. Haag, M., Food sense: a guide to eating sensibly, Xlibris Corporation, 2011.
4. Haas, E. and Levin, B., Staying healthy with nutrition, rev: the complete guide to diet and nutritional medicine, Random House LLC, 2012.
5. Watson, R., Preedy, V., and Patel, V., Nuts and seeds in health and disease prevention, Academic Press, 2011.
6. Preedy, V., Watson, R., and Patel, V. Flour and breads and their fortification in health and disease prevention, Academic Press, 2011.
7. Arendt, E. and Zannini, E., Cereal grains for the food and beverage industries, Elsevier, 2013.
8. Issues in food production, processing, and preparation: 2013 Edition, Scholarly Editions, 2013.
9. Zhao, Y., Specialty foods: processing technology, quality, and safety, CRC Press, 2012.
10. Dunford, N.T., Food and industrial bioproducts and bioprocessing, John Wiley & Sons, 2012.
11. Bewley, D.J., Bradford, K., and Hilhorst, H., Seeds: physiology of development, germination and dormancy, Springer, 2012.



A PROMISING TREND IN THE PROCESSING OF FENNEL (*FOENICULUM VULGARE MILL.*) WHOLE PLANTS

L. A. Timasheva* and E. V. Gorbunova

Crimean Agrotechnological University, South Branch,
National University of Life and Environmental Science of Ukraine,
Agrarnoe, Simferopol, Crimea, 95492 Ukraine,
*phone/fax: +3(0652)22-39-66, e-mail: admin@csau.crimea-ua.com

(Received January 22, 2014; Accepted in revised form March 4, 2014)

Abstract: Aromatic plants are a valuable source of biologically active substances. The use of aromatic plant processing products in the pharmaceutical, perfume and cosmetic, and food industries is of great interest. The search for new plant sources of biologically active substances and the study of their composition and properties are still topical. Fennel (*Foeniculum vulgare Mill.*) is a promising aromatic raw material containing a number of biologically active substances. Until now, essential oils were obtained only from fennel fruits and, less frequently, from whole plants. However, fennel raw materials contain microelements and macroelements, organic acids, proteins, carbohydrates, vitamins, tannins, polysaccharides, amino acids, coumarins, and flavonoids, which make the processing of whole plants reasonable. A rich spectrum of valuable fennel components requires the search for methods of their exhaustive recovery from plant raw materials, and this can be provided only with a complex processing technology. For this reason, the objective of our work was to develop a technology for the processing of fennel, a promising plant, on the basis of the steam distillation of raw materials and the aqueous alcoholic extraction of waste solid residues remaining after the recovery of essential oil with the purpose of obtaining aqueous alcoholic extracts, to study the other types of wastes formed in the course of processing, and to determine the field of their application. A promising trend in the processing of fennel was scientifically substantiated. Some regularities in the change of the yield of fennel essential oil components and their distribution between the plant organs depending on plant vegetation stages and weather in the submountain Crimea were established. The technical maturity of plants for industrial processing was defined. Waste residues after the extraction of essential oil were studied, and some new natural biologically active products were obtained.

Key words: fennel, raw materials, processing, essential oil, aqueous alcoholic extract of fennel waste residues

UDC 635.757:665.52

DOI 10.12737/4134

INTRODUCTION

At present, the demand for natural fragrances, food additives, and flavors considerably grows. Fennel (*Foeniculum vulgare Mill.*) is a raw material for the production of a number of fragrances forming the basis of contemporary perfumery and cosmetics and widely applied in medicine and food industry.

Fennel is a perennial (biennial, if cultivated) herbal plant of the Apiaceae family with a height of up to 2 m. Leaves are multi-pinnatisect. Flowers are small golden-yellow and form a complex double multiradiate umbrel. Fennel fruits are fragrant, greenish-brown or grey-green, naked, costate, large, elongated and represent nearly cylindrical cremocarps, which can easily split into two mericarps after maturation [1, 2].

Fennel fruits are used in industrial processing, but their uneven maturation and fall lead to considerable harvest losses, so some studies on the processing of whole plants were performed in 1970, although the essential oil from whole plants differed from the essential oil from mature fruits in quality: the content of anethol, a principal component, was less than 60% and did not satisfied the fennel essential oil quality standard [3].

It should be noted that all the technology for the processing of fennel in the form of whole plants basically have a character of research rather than recommendation,

as indicated by the fact that the attention in each communication is paid only to the yield of essential oil. The proposed technology for the processing of whole fennel plants allows the more exhaustive utilization of initial raw materials and their diversification depending on the demand for the target product.

It is commonly known that the processing of plant raw materials for the production of products of different quality and destination is accompanied by the generation of bulky waste residues at each stage. In this connection, the problem of the complex processing of essential oil and medicinal plant raw materials with the use of resource-saving technologies is topical [4, 5].

Such an approach to the processing of plant raw materials necessitates the complex studies of initial essential oil raw materials and waste residues of their processing, and also the improvement of methods for the production of essential oil, extracts, and other biologically active components. Special attention is currently paid to the development of environmentally-safe and low-waste technologies for the complex processing of plant raw materials [6].

The lack of works on the complex utilization of fennel plants has necessitated the more detailed study of the biochemical composition of raw materials and the development of complex fennel processing technologies,

which must provide the most exhaustive extraction of biologically active substances with different spectra of activity.

Objective of our studies was to substantiate the possibility of the complex processing of fennel (*Foeniculum vulgare* Mill.) plants from theoretical and experimental viewpoints.

According to the stated objective, we solved the following problems:

- (1) To study the dynamics of the accumulation and distribution of essential oil in fennel plants during the vegetation period in Southern Ukraine;
- (2) To study the qualitative composition of raw materials at different vegetation stages of a plant and to determine the optimal time period for the harvesting of raw materials;
- (3) To study the qualitative change of raw materials during the storage of fennel and to determine the period of its storage; and
- (4) To study the qualitative composition of fennel waste residues after steam distillation and to propose efficient methods of their processing.

OBJECTS AND METHODS OF STUDY

The studies were performed for the period of 2011–2013 at the Department of Technology and Equipment of Fat and Essential Oil Production of the Crimean Agrotechnological University (South Branch, National University of Life and Environmental Science of Ukraine) in the Research Laboratory of Quality of Raw Materials and Processing Products of the Institute of Essential Oil and Medicinal Plants of the National Academy of Sciences of Ukraine (now, the Crimea Institute of Agricultural Industry).

The object of study was fennel (*Foeniculum vulgare* Mill.) whole plants, which were cut at a level of 50 cm from the ground surface and grown in Southern Ukraine, and also its distillate, essential oil, distillation water, aqueous and aqueous alcoholic extracts, and essential oil extraction waste residues.

The mass content of essential oil in raw materials was determined via steam distillation on a Clevenger apparatus [7]. Samples of fennel essential oil, distillation water, and obtained extracts were taken for analysis in compliance with GOST 30145-94. The qualitative composition of essential oil, distillation water, and aqueous alcoholic extracts and the quantitative content of components in them were established by gas-liquid chromatography on a Kristall 2000 M chromatograph with a PEG 20 M quartz capillary column. The identification of components was performed in the temperature-programmed regime. The yield of extracted substances in the extract of fennel waste residues was determined via exhaustive extraction, which consisted in their preliminary and complete evaporation on a water bath and subsequent holding in a thermocabinet and the terminal weighting of a residue. The result was calculated in percents with respect to the initial material mass [9].

The mass content of flavonoids in the extract of fennel waste residues on a rutin basis was determined by the adopted method for plant raw materials [1], the qualitative analysis of tannins was performed by means of qualitative reactions, their quantitative estimation was performed via redox titration [10], and ascorbic acid was determined

titrimetrically. The products obtained from fennel—essential oil and aqueous and aqueous alcoholic extracts—were analyzed by the standard methods [10]. In addition to the quantitative estimation of yield and dynamics, the obtained products were analyzed by organoleptic, physicochemical, and biochemical methods. In the analysis of extracts and essential oils, the color, odor, density, refraction index, and component composition of target products were determined [1, 10].

RESULTS AND DISCUSSION

The performed studies were aimed at determining the technical maturity of fennel raw materials and studying the dynamics of the accumulation of essential oil and biologically active substances in the different organs of a plant at various vegetation stages.

The development stages of fennel plants and the content of essential oil and biologically active substances were determined beginning from the stage of shooting to the complete maturation of central umbrel fruits.

The vegetation stages of fennel plants are usually the following:

- (1) Shooting (formation of stems);
- (2) Budding (formation of flowers on umbrels);
- (3) Early blossom of central umbrels (10% of plants have open flowers on their umbrels);
- (4) Full blossom of central umbrels (75% of plants have open flowers on their umbrels);
- (5) Milky maturity of fruits on the central umbrel (fruits begins to mature on the umbrels of 10% of plants, and the crushing of their endosperm gives a dense milky-white liquid);
- (6) Milky-wax maturity of fruits on the central umbrel (the fennel fruit maturation stage, at which endosperm is uncrushable, but easily cuttable for 10% of plants);
- (7) Wax maturity of fruits on the central umbrel (the fennel fruit maturation stage, at which endosperm is uncrushable, but easily cuttable for 75% of plants); and
- (8) Complete maturation of fruits on the central umbrel (the terminal maturation stage, at which fruits are colored as ripe).

It has been established that the amount of essential oil is minimal at the budding stage and maximal at the stage of the milky-wax maturity of fruits on the central umbrel (Fig. 1). Hence, the stage of the milky-wax maturity of fruits on the central umbrel is the stage of the technical maturity of fennel plants, i.e., the period of the maximum accumulation of essential oil. Relying on the obtained data incorporated into the project of the National Standard of Ukraine on industrial fennel raw materials, it is possible to recommend the epigeal fennel part cut at the stage of milky-wax maturity of fruits on the central umbrel for the industrial processing in the form of whole plants.

Essential oil from whole fennel plants represents a colorless or slightly yellow sweetish liquid with bitter taint and specific fennel odor. The relative density was from 0.950 to 0.963 g/cm³, and the refractory index was 1.5300 to 1.5350 at a temperature of 20°C. A typical chromatographic pattern of fennel essential oil from whole plants at the milky-wax maturity stage is shown in Fig. 2.

As is shown by the performed studies, the component composition of essential oil also changes in different vegetation periods of plants [3, 11]. The amount of anethol,

a principal essential oil component, was observed to be minimal at the stages of the budding and early blossom of fennel plants and maximal at the stage of the milky-wax maturity of fruits on the central umbrel.

The results of studying the component composition of freshly cut fennel plants show that the mass content of essential oil in the different organs of plants is

various and changes in the process of vegetation from 0.44 to 1.5% in stems, from 0.6 to 1.3% in leaves, and from 3.5 to 5.3% in umbrels with fruits on absolute dry matter basis (Fig. 3).

The complex technology of the processing of fennel raw materials is proposed to be implemented as follows (Fig. 4).

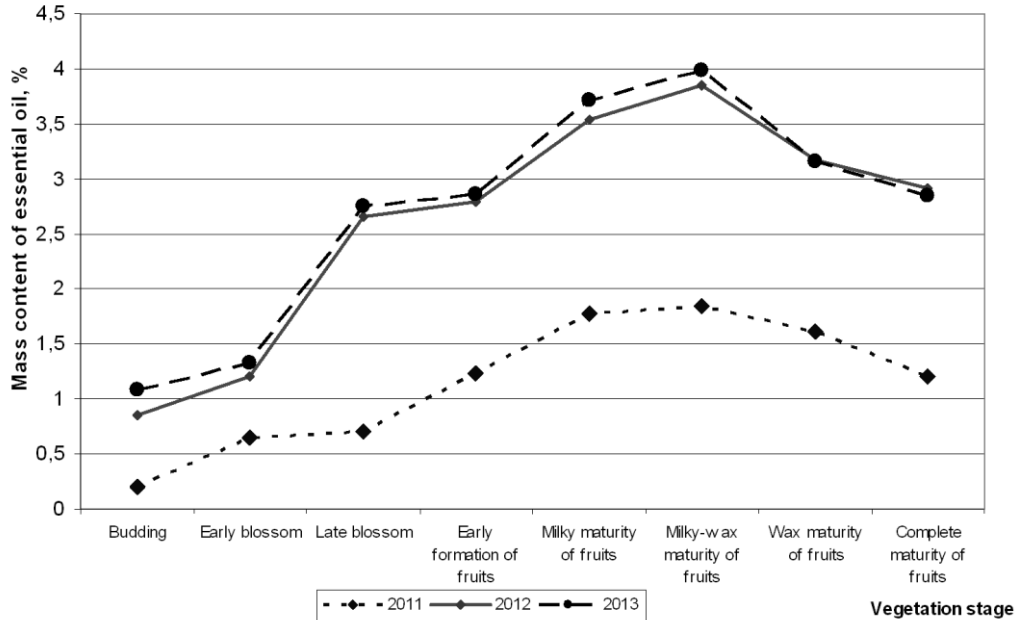


Fig. 1. Content of essential oil in fennel plants at different vegetation stages.

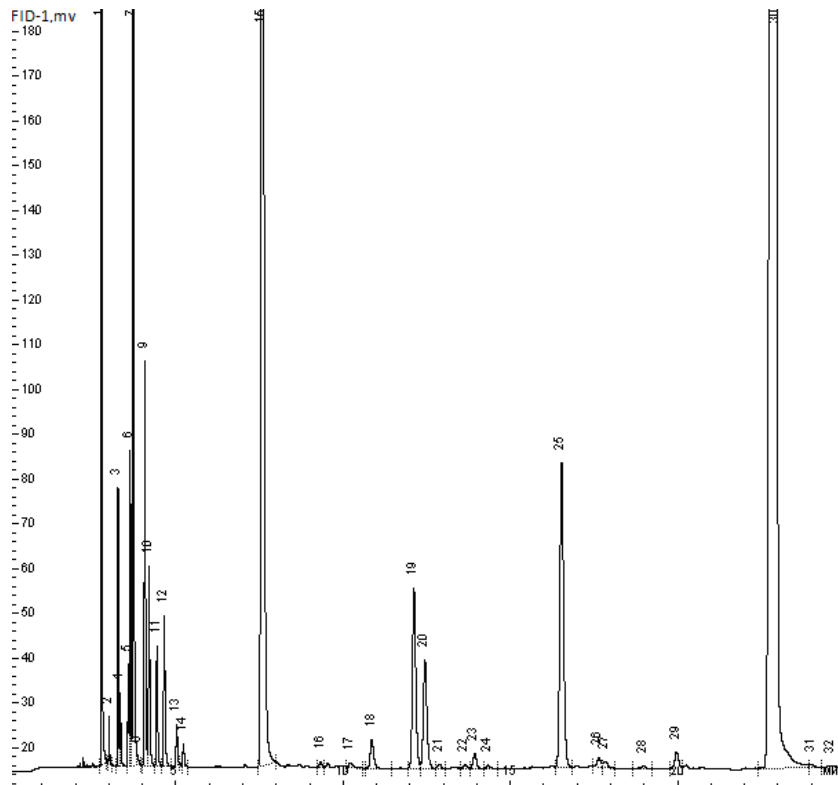


Fig. 2. Typical chromatographic pattern of fennel essential oil.

Table 1. Component composition of fennel essential oil at different vegetation stages (average over the period of 2011–2013)

Component	Mass content of components in essential oil, %				
	Budding	Blossom of central umbrels	Milky maturity of fruits on the central umbrel	Milky-wax maturity of fruits on the central umbrel	Complete maturity of fruits on the central umbrel
α -Pinene	3.17	9.24	8.20	7.41	6.44
Camphene	0.04	0.02	0.04	0.05	0.10
β -Pinene	0.11	0.92	0.94	0.72	0.17
β - Phellandrene	7.17	1.30	2.42	4.27	0.96
1,8-Cineole	1.23	1.33	1.06	0.91	1.37
Fenchone	4.84	2.84	2.99	4.94	10.09
Linalool	0.05	0.05	0.09	0.11	1.43
Methylchavicol	2.49	2.36	2.41	2.83	2.73
Anethol	68.12	67.32	68.52	69.60	63.91

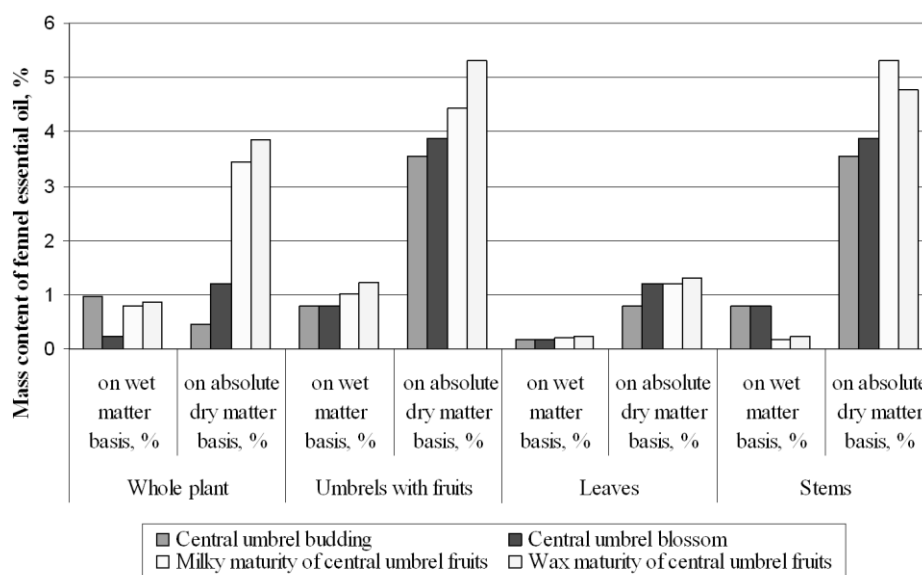


Fig. 3. Content of fennel essential oil in the plant organs at different vegetation stages.

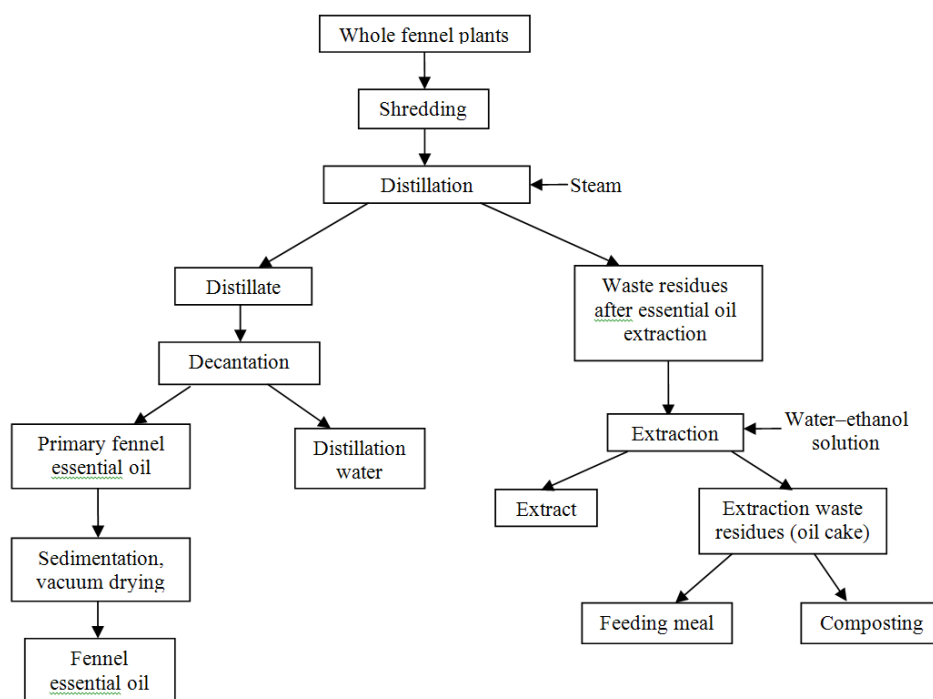


Fig.4. Scheme of the complex technology for the processing of fennel plants.

Industrial fennel raw materials are shredded to a size of 3–5 cm on a shredder, thereupon essential oil is obtained via steam distillation. The process is recommended to be performed for 120 min at a distillation rate of 0.5 kg/(kg h) and a steam pressure of 0.5 MPa. The curve of the extraction of essential oil depending on the time of the process is plotted in Fig. 5. From the curve it can be seen that 64.8% of the essential oil obtained from the raw materials throughout the entire period of experiment is distilled for first 30 min of the process, 84.1% for 60 min, 90.9% for 90 min, and 95.5% for 120 min, thereupon its amount increases almost uniformly until the end of experiment. Within a range of 150–300 min, the curve demonstrates an almost imperceptible ascent corresponding to 0.2% of the distilled product, so it is possible to say about the complete extraction of essential oil from the raw materials for 120 min under the conditions of the performed experiment.

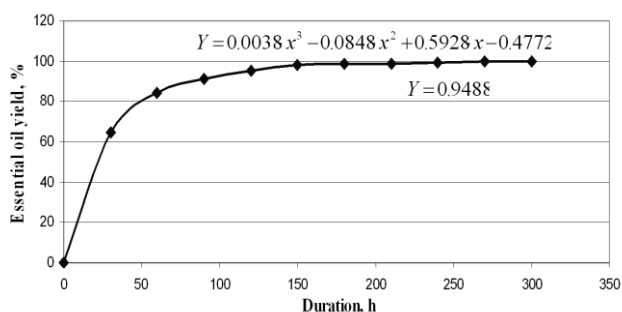


Fig. 5. Dynamics of the exhaustive extraction of fennel essential oil.

The liquid and solid waste residues formed in the process of distillation are not utilized, but subjected to recycling. Liquid wastes are distillation water (distillation fraction water) obtained in the steam distillation of volatile organic components from fennel plants. In the essential oil production, distillation water is a distillation process waste and amounts more than 70% of the weight of processed raw materials; it is not recycled in the technological process, but disposed into sewers [6]. However, distillation water contains a variety of biologically active components, which are so necessary in the pharmaceutical, perfume and cosmetic, and food industries. It is known that some fennel components are water-soluble. For this reason, it is possible to say that distillation water is a saturated aqueous extract.

The obtained distillation water is a colorless slightly opaque finely fennel-scented liquid, on the surface of which the formation of small essential oil drops is observed after sedimentation. The component composition of fennel water is given in Table 2 and in the chromatographic pattern (Fig. 6a).

Anethol is the dominant component of distillation water, and its concentration is 87.68%. The value of distillation water consists not only in the possibility of obtaining some additional amount of components, but also in its biological activity. It is historically known that fennel tinctures and decoctions are used in folk

medicine and included into pharmaceutical drugs as an invigorant, expectorant, anti-inflammatory, bactericidal, disinfectant, diuretic, mild laxative, and tonic remedy [12].

Table 2. Component composition of essential oil in the distillation water of fennel*

Principal components	Retention time, min	Mass content, %
Fenchone	7.310	7.00
Camphor	10.694	0.47
Linaool	12.026	0.49
Methylchavicol	16.294	1.47
Anethol	22.708	87.68

*Mass content of essential oil in the distillation water was 0.05%.

Hence, distillation water is a commercial product and can be used in the perfume and cosmetic industry as an aqueous fennel extract and as a flavor in the alcoholic beverage industry or for the separation of anethol.

Solid residues are subjected to extraction with aqueous alcoholic solutions to obtain the target products. Extraction waste residues are washed with water and used to obtain feeding meal for farm animals or composting.

Fennel essential oil usually composes a small portion of all the biologically active components accumulated inside a plant, so fennel waste residues obtained after essential oil extraction contain valuable organic components (extractive substances) of interest. Extractive substances are represented by a great number of components of different classes [13]. The study of the extraction of extractive substances from fennel waste residues shows that the application of the obtained product is advantageous.

The content of extractive substances is one of the important quality characteristics of an extract obtained from fennel waste residues. It is known that the process of their extraction depends on a number of factors, such as the size of particles and the concentration of a solvent [6, 13]. In view of this, there occurs the necessity for studying the effect of technological factors on the yield of extractive substances from raw materials to select the most suitable regime of extraction.

Ethanol, which is widely applied for the extraction of biologically active components from plant raw materials, was used as an extragent. Ethanol as an extragent has a number of advantages [6]: it does not form hazardous components with extracted raw materials and does not provoke the corrosion of equipment, has a relatively low boiling temperature (78°C), is environmentally friendly, and represents a very good preservative. This enables the use of obtained extracts in the perfume and cosmetic, food, and pharmaceutical industries. For this reason, the secondary raw materials remaining after the extraction of essential oil are extracted with aqueous alcoholic solutions of different concentration.

In our studies it has been established that the total yield of extractive substances depends on the concentration of a solvent [13]. The content of extractive substances extracted with aqueous alcoholic extragents with a concentration varied from 20 to 90% is less than 7%. Their yield grows with increasing ethanol concentration, attains a maximum (9.17%) for a 60% aqueous alcoholic solvent, and then decreases to 6.94% for a 90% aqueous alcoholic solvent (Fig. 6).

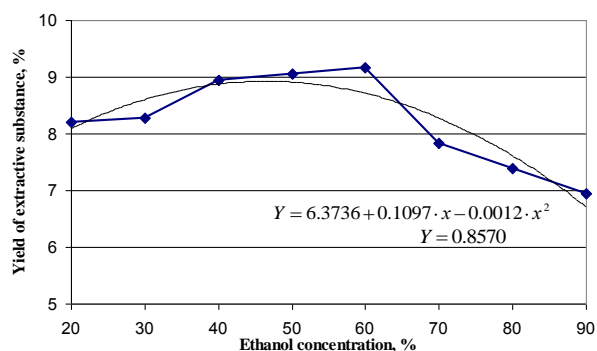


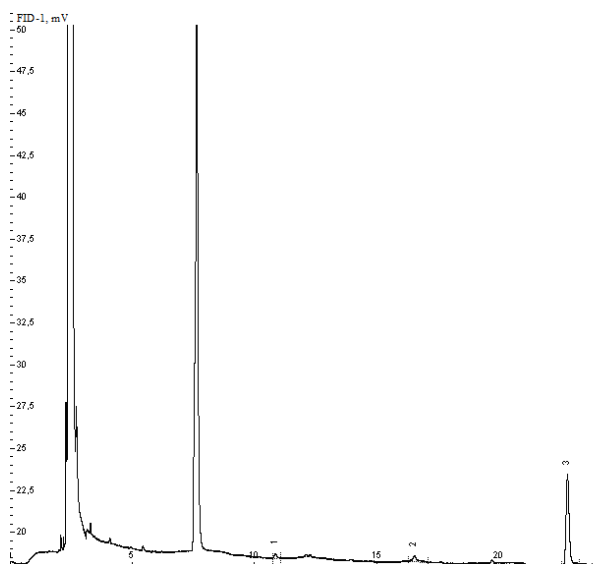
Fig. 6. Yield of extractive substances versus ethanol concentration.

The obtained aqueous alcoholic extract of fennel waste residues (ethanol concentration, 60%) is a transparent light-yellow finely fennel-scented liquid. The refractory index of the aqueous alcoholic extract is 1.5010, and its density is 0.9651 g/cm³.

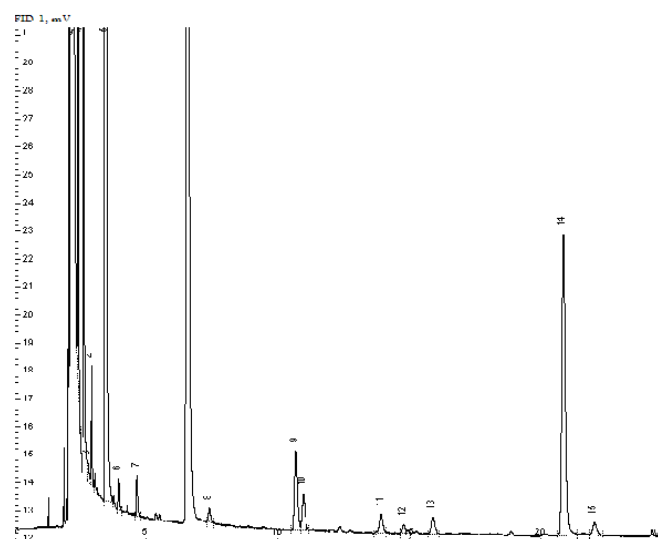
The component composition of the aqueous alcoholic extract obtained at an ethanol concentration of 60% and a temperature of 20°C is presented in the chromatographic pattern (Fig. 7b) and Table 3.

Table 3. Component composition of the aqueous alcoholic extract of fennel waste residues

Principal components	Retention time, min	Mass content, %
α -Pinene	2.352	9.8
Camphene	2.594	40.2
Limonene	3.420	39.5
Camphor	10.663	1.1
Anethol	20.852	6.4



(a)



(b)

Fig. 7. Chromatographic pattern of (a) distillation water and (b) aqueous alcoholic extract of fennel waste residues.

Among the fennel extract components, camphene and limonene are of special interest [13]. Camphene is used in the production of fragrances and insecticides and represents an intermediate in the synthesis of camphor, which is a valuable product for many chemical industries. Limonene is included into many perfumery products, shampoos, washing and cleaning products, and household and industrial solvents and used to degrease metals before industrial painting and in household chemicals, e.g., for the cleaning of wooden coverings and the removal of grease from hands. It is a perfect environmentally-friendly alternative to toxic and hazardous solvents and petrochemicals [14].

In our studies, it has been established that the aqueous alcoholic extract of fennel waste residues contains 8.1% of flavonoids, 1.2% tannins, 0.1% of coumarins, and 0.1% of ascorbic acid on absolute dry matter basis.

CONCLUSIONS

Hence, the performed studies have shown that fennel (*Foeniculum vulgare Mill.*) is a promising crop, the complex processing of which enables the production of new natural biologically active products.

Some regularities of the change in the quantitative and qualitative composition of fennel essential oil and

its distribution between the plant organs depending on a vegetation stage and weather have been shown for the first time. The optimal time period for the harvesting of raw materials has been determined. The epigeal fennel part cut at a level of 50 cm from the ground surface at the stage of milky-wax maturity of fruits on the central umbrel is recommended for industrial processing. A project of the National Standard of Ukraine on industrial fennel raw materials has been developed.

The developed technology for the extraction of new natural biologically active products from primary and secondary raw materials (essential oil, natural perfume water, aqueous alcoholic extract) results in the rational use of the valuable plant material, and its products contain a wide variety of biologically active components typical for the given plant. The proposed technology for the processing of fennel raw materials has been put into industrial practice at TRIA Ltd. (Simferopol) in September–October 2013.

REFERENCES

1. Gorbunova, E.V., Obosnovanie ispol'zovaniya *Foeniculum vulgare* Mill. dlya polucheniya tselevykh productov (Substantiating the use of *Foeniculum vulgare* Mill. for the production of target products), *Naukovi pratsi Krims'kogo agrotekhnologichnogo universiteta (tekhnichni nauki)* (Proceedings of the Crimean Agrotechnological University: Engineering Sciences), 2011, no. 138, pp. 128–134.
2. Anubhuti, P., Rahul, S., and Kant, K.C., Standardization of fennel (*Foeniculum vulgare*), its oleoresin and marketed ayurvedic dosage forms, *Journal of Pharmaceutical Sciences and Drug Research*, 2011, vol. 3, no. 3, pp. 265–269.
3. Gorbunova, E.V. and Timasheva, L.A., Izuchenie dinamiki nakopleniya efirnogo masla v protsesse vegetatsii rastenii fenkhelya (Studying the dynamics of the accumulation of essential oil during the vegetation of fennel plants), *Naukovi pratsi Krims'kogo agrotekhnologichnogo universiteta (tekhnichni nauki)* (Proceedings of the Crimean Agrotechnological University: Engineering Sciences), 2012, no. 146, pp. 164–170.
4. Gorbunova, E.V., Ekstragirovanie otkhodov fenkhelya posle izvlecheniya efirnogo masla (Extraction of fennel waste residues after the recovery of essential oil), *Naukovi pratsi Krims'kogo agrotekhnologichnogo universiteta (tekhnichni nauki)* (Proceedings of the Crimean Agrotechnological University: Engineering Sciences), 2013, no. 153, pp. 153–158.
5. Kapás, Á., András, C.D., Dobre, T.G., Vass, E., Székely, G., Stroescu, M., Lányi, S., and Ábrahám, B., The kinetic of essential oil separation from fennel by microwave assisted hydrodistillation (MWHHD), *University Politehnica of Bucharest Scientific Bulletin, Series B: Chemistry and Materials Science*, 2011, vol. 73, no. 4, pp. 113–120.
6. Gorbunova, E.V., Tekhnologicheskie osobennosti kompleksnoi pererabotki tselykh rastenii fenkhelya obyknovennogo (Engineering peculiarities of the complex processing of whole fennel plants), *Tekhnika i tekhnologiya pishchevykh proizvodstv* (Technics and Technology of Food Industry), 2013, no. 3, pp. 9–15.
7. *Quality Control Methods for Medicinal Plant Materials*, Geneva: World Health Organization, 1998.
8. *European Pharmacopoea*, Strasbourg: Maisonneuve, 1998.
9. Karnick, C.R., *Pharmacopoeial Standards of Herbal Plants*, Delhi: Sri Satguru Publications, 1994, vol. 1, pp. 139–141; vol. 2, p. 71.
10. Goryachev, M.I. and Pliva, I., *Metody issledovaniya efirnykh masel* (Methods of Studying Essential Oils), Alma-Ata: Izdatelistvo akademii nauk Kazakhskoi SSP, 1962.
11. Chaouche, T., Haddouchi, F., Lazouni, H.A., and Bekkara, F.A., Phytochemical study of the plant *Foeniculum vulgare* Mill., *Der Pharmacia Lettre*, 2011, vol. 3, no. 2, pp. 329–333.
12. Radulović, N.S. and Blagojević, P.D., A note on the volatile secondary metabolites of *Foeniculum vulgare* Mill. (Apiaceae), *Facta Universitatis Series: Physics, Chemistry and Technology*, 2010, vol. 8, no. 1, pp. 25–37.
13. Patel, J.B., Patel, B., Patel, R.K., and Patel, B.H., Comparative evaluation of extraction methods for extraction of essential oil from *Foeniculum vulgare*, *Journal of Pharmaceutical Science and Bioscientific Research*, 2012, vol. 2, no. 4, pp. 176–178.
14. Coşge, B., Kiralan, M., and Gürbüz, B., Characteristics of fatty acids and essential oil from sweet fennel (*Foeniculum vulgare* Mill. var. *dulce*) and bitter fennel fruits (*F. vulgare* Mill. var. *vulgare*) growing in Turkey, *Natural Product Research*, 2008, vol. 22, no. 12, pp. 1011–1016.



A METHOD TO INCREASE THE NUTRITIONAL VALUE OF AERATED CONFECTIONERY

A. D. Toshev^{a,*}, A. S. Salomatov^{a,**}, and A. S. Salomatova^b

^aSouth Ural State University (National Research University),
pr. Lenina 76, Chelyabinsk, 454080 Russia,

*phone: +7 (351) 267-99-53, e-mail: a.d.toshev@mail.ru

**phone: +7 (351) 267-97-33, e-mail: SalomatovAS@mail.ru

^bChelyabinsk State Academy of Agricultural Engineering,
pr. Lenina 75, Chelyabinsk, 454080 Russia,
phone: +7 (351) 267-96-28, e-mail: SalomatovaAS@yandex.ru

(Received February 07, 2014; Accepted in revised form February 17, 2014)

Abstract: A technology and a formulation for the production of meringue of increased nutritional value have been developed. Stepwise introduction of components of a complex additive including puffed barley (6%) and eggshell powder (2%) has been implemented in the new technology. The effect of the above named additive on heat treatment of meringues has been investigated; for this, test samples of pastry were baked at a temperature of 100°C until the content of solids reached 96%. Changes of temperature in the surface layer, central part, and bottom of the sample were monitored during baking. The process of baking of the samples can be arbitrarily divided into three stages, namely, warming, baking, and drying. Dynamics of changes in the surface temperature of the test sample was comparable to that registered for the control sample; the surface was thoroughly heated and moisture evaporated almost completely during 12–15 minutes after the beginning of treatment. The duration of warming for the center of the test samples decreased by 15.4%, and the duration of baking decreased by 6.8%. The additive also had a marked effect on the dynamics of temperature distribution in the bottom of the samples during baking; however, the duration of warming for the test sample was comparable to that for the control sample due to additional heating of the system upon contact with the metallic baking sheet. Introduction of the additive resulted in a decrease of baking time due to the increase of heat conductance of the foam mass containing the additive. Introduction of a complex additive combining components of plant and animal origin to the technology of meringue production contributes to increased production intensity and decreased energy consumption.

Key words: meringue, complex additives, puffed cereals, eggshell, heat treatment

UDC 664.1:664.7

DOI 10.12737/4135

INTRODUCTION

The problem of preservation and promotion of health and increasing life expectancy has received considerable attention worldwide since the mid-20th century. Therefore, the significance of dietary fiber that can have a beneficial effect on health as a component of functional food has increased. Cell walls of barley endosperm contain large quantities of β -glucan, a dietary fiber that has received special attention due to its ability to reduce the level of cholesterol in the blood and thereby diminish the risk of cardiovascular diseases. Moreover, recent reports show that this fiber prevents a sharp increase in blood glucose levels after food consumption [1, 2, 3]. There is scientific evidence showing that diets characterized by low glycemic index may reduce insulin resistance and prevent the development of diabetes. Research involving long-term observations of 90000 women and 45000 men showed that insulin-independent diabetes mellitus was 30% less likely to develop in people who regularly consumed cereal-based foods. The high capacity for reducing the glycemic index of foods characteristic of β -glucan is related to its ability to form viscous solutions decelerating starch hydrolysis and cholesterol absorption. The daily dose of β -glucan recommended by

the U.S. Department of Food and Drug Administration is 3 g or at least 0.75 g per serving [1, 2, 4, 5].

A trend of using barley flour containing β -glucan as an alternative to wheat flour in the production of pasta, bread, and ethnic foods, has been growing during the recent years. The use of barley flour is justified from the standpoint of health benefits, but its negative effect on the structure and consumer characteristics of the products hinders its widespread use in the food industry. Therefore, current research on β -glucan-enriched foods is focused on finding ways of introducing it into the formulation so that the consumer characteristics of the final product remain similar to those of the conventional analog [2, 6, 7].

The wide prevalence of diseases caused by excess body weight, which is, in its turn, usually caused by consumption of food containing large amounts of easily digestible carbohydrates, requires changing the existing technologies in order to reduce the glycemic index of foods. The use of complex additives obtained by combining materials of plant and animal origin, for instance, puffed barley combined with eggshell powder, is one of the approaches to increasing the nutritional value of food while reducing the glycemic index. Components of the complex additive were selected

using the concepts of food combinatorics which takes the mutual effects of the ingredients into account. For example, puffed barley contains the polysaccharide β -glucan capable of lowering the glycemic index of foods [2, 8, 9], and eggshell contains large amounts of calcium (more than 3 %), which requires the presence of B-vitamins [10, 11] for absorption; the content of the above named vitamins in barley may amount to 7.0 mg %. Thus, the components of the complex additive complement each other. The use of the additive described above contributes to complex enrichment of foods and the reduction of their glycemic index.

Meringue with a sugar content of at least $95 \pm 1\%$ was chosen as the object of investigation. Part of the sugar required by the formula (8%) was replaced by a complex additive, namely, 6% of sugar was replaced by puffed barley (PB) and 2%—by eggshell powder (ESP). The ratio of components in the complex additive and the parameters of its introduction were determined using experimental assessment of the rheological, structural, and mechanical properties of the foam mass; these experiments are beyond the scope of the present article.

The aim of the present study was to characterize the effect of the complex additive on the duration of meringue baking.

OBJECTS AND METHODS OF RESEARCH

The effect of the complex additive on heat treatment of meringue was investigated. Samples of aerated mass in which 8% of sugar was replaced with the additive described above were prepared. The samples were baked at 100°C until the content of solids reached 96%. Temperature distribution in the surface layer, central part, and bottom of the samples under investigation was monitored during baking using a probe inserted into the samples at various depths. The temperature displayed by the device was recorded every 5 minutes. The samples weighed 50 ± 2 g.

RESULTS AND DISCUSSION

The effect of a complex additive on the process of meringue baking was investigated. The temperature at which the meringues were baked was not higher than 100°C , because otherwise surface cracking and sugar caramelization resulting in a dark discoloration of the pastries would occur. Preliminary experiments showed that baking at a temperature above 100°C resulted in drying of the product crust, while a considerable amount of moisture was still retained in the center of the pastries. Evaporation and release of moisture from the center of the pastries resulted in cracking of the meringue surface, which is an unacceptable defect of the product. Notably, the duration of meringue baking largely depended on the thickness of the layer of the aerated mass deposited onto the baking sheets. The aerated mass has a low thermal conductivity due to a foamy structure, and therefore the baking process takes a considerable amount of time. The additive introduced into the aerated mass affected the thermal conductivity of the system, and hence the duration of baking changed.

Baking is one of the principal production stages determining the quality and consumer appeal of the meringue. Moisture contained in the aerated egg mass evaporates during meringue baking, this resulting in the formation of a brittle airy structure.

The heat treatment process was investigated in order to determine the duration of baking of the meringue containing a complex additive. Cake-shaped samples weighing 50 ± 2 g were deposited on parchment-lined baking sheets using a pastry bag. A probe was inserted into the test samples in order to follow the temperature changes during baking. The probe was inserted to different depths in order to monitor the temperature changes in the surface layer, center, and bottom of the product. The temperature displayed by the device was recorded every 5 min. The meringues were baked in a steam convection oven at 100°C . The effect of the complex additive on the temperature distribution in the bulk of the meringue is illustrated by Figs. 1, 2, and 3.

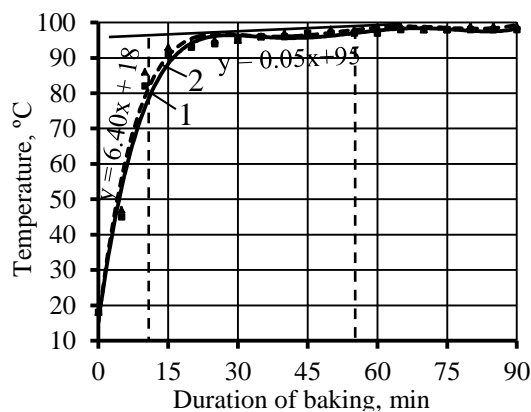


Fig. 1. Temperature change in the surface layer of the meringue during baking:

- 1 – control;
- 2 – meringue containing a complex additive.

As shown in Fig. 1, the process of baking of the control semi-finished product (curve 1) can be divided into three phases, namely, warming, baking and drying. The process of meringue crust warming takes 11–12 min and is characterized by a rapid temperature increase to 80°C . Formation of the meringue structure and redistribution of moisture occur at the baking step, during which the temperature in the surface layer increases by 15°C at most. The formation of the structure of the surface layer of the meringue is completed after 55 ± 1 min of baking. The drying step resulting in the setting of structure follows the process of baking and is accompanied by a slight temperature change ($1\text{--}2^\circ\text{C}$). The temperature curve characterizing the process of baking of a meringue containing the complex additive follows a similar pattern (curve 2).

The meringue surface was heated evenly, the additive having no significant effect on temperature distribution in the surface layer. Therefore, the effects of additives on temperature distribution in the deeper layers were investigated (Figs. 2, 3).

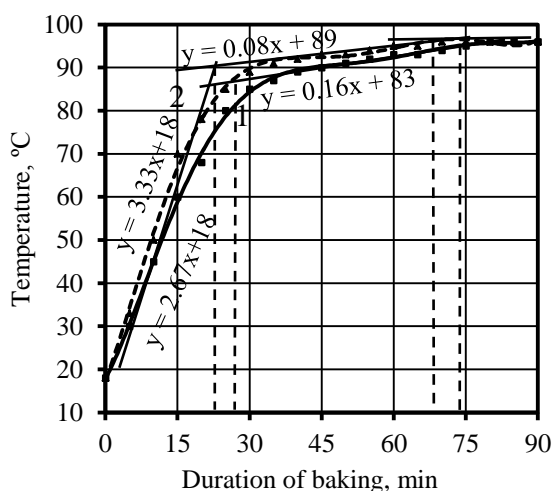


Fig. 2. Temperature changes in the center of the meringue during baking:

- 1 – control;
2 – meringue containing a complex additive.

As shown in Fig. 2, warming of the central part of the control meringue sample (curve 1) is characterized by a temperature increase to 80°C and takes 25 ± 1 min, twice as long as the process of crust warming (Fig. 1). Baking of the semi-finished product is characterized by formation of a porous structure and a gradual increase in temperature of the mass. The baking process is completed at 74 ± 1 min when a temperature of 95 ± 1 °C is reached. Baking is followed by setting of the structure of the meringue, during which the temperature increases by 1–2 °C at most. Drying takes 5 ± 1 min and is accompanied by setting of the porous structure and formation of a brittle meringue. Changes occurring in the deep layers of meringue containing a complex additive differ from those occurring in the control sample with regard to the duration of several processes. Notably, the warming process for curve 2 is shorter, taking only 22 ± 1 min, and the baking process is completed at 68 ± 1 min. Drying time is also reduced to 3 ± 1 min. Reduction of the baking time due to the effect of the additive was especially pronounced for deep layers of the meringue. Temperature changes in the meringue bottom were investigated to obtain a complete characteristic of the effect of the additive on the baking process (Fig. 3).

As shown in Fig. 3, warming of the bottom of a control meringue takes 22 ± 1 min and results in a temperature increase to 60°C (curve 1). The process of bottom warming is more intensive than the warming of the center of the meringue (Fig. 2). This is probably due to additional heating of the aerated mass caused by contact with the metal baking tray. The baking process, during which the temperature increases to 95°C, starts after the warming and is completed at 71 ± 1 min. The drying step is characterized by a slight increase in temperature resulting in setting of the structure. The course of temperature change in the bottom of a meringue containing a complex additive (curve 2) is similar to that recorded for the control sample, with the additive having no effect on the duration of the process of warming. However, the

stage of actual baking for curve 2 is completed at 67 ± 1 min. Therefore, the additive has a higher thermal conductivity than the bulk of the foam mass and provides for a faster increase of temperature and a decrease of the baking time from 80 to 70 minutes, that is, by 12.5 %.

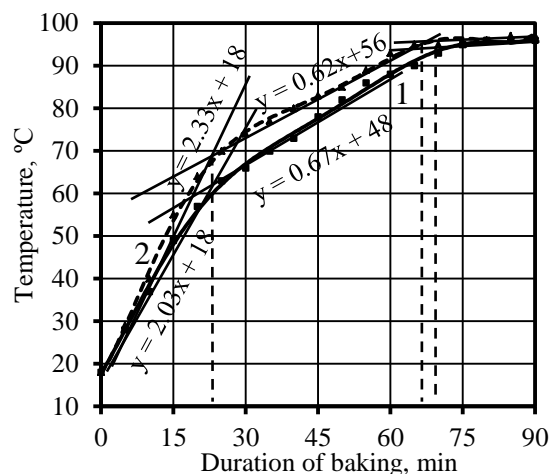


Fig. 3. Temperature change in the meringue bottom during baking:

- 1 – control;
2 – meringue containing a complex additive.

Microscopic analysis of meringue samples containing the complex additive was conducted using scanning electron microscopy (microscope JEOL JSM-6460LV). The method is based on irradiation of the sample site under investigation by a finely focused electron beam and registration of the signals of the secondary backscattered electrons forming upon the interaction of the electron beam with the sample surface. Secondary electron emission occurred in an area close to the beam incidence site and this allowed for the formation of an image characterized by a relatively high resolution. The resulting signal was amplified and processed, and the images obtained were displayed on a computer screen. A procedure for the microscopic study of the structure was devised and a magnification of 5000 x was shown to be optimal. Results of the experiment are shown in Fig. 4.

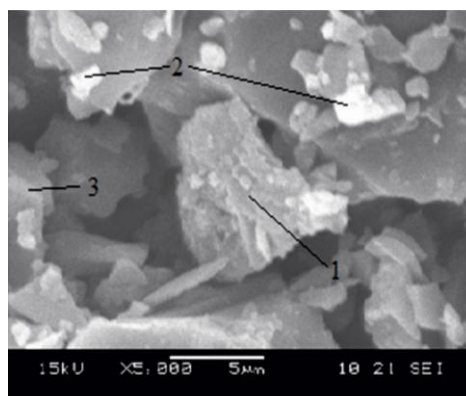


Fig. 4. Structure of meringue containing the complex additive: 1 – PB, 2 – ESP, 3 – meringue.

A microscopic study of sample structure (Fig. 4) revealed a uniform distribution of the additive in the bulk of meringue. Puffed barley particles characterized by a layered structure (1) could be seen in the photographs. Smaller eggshell particles were visible as well (2). Images of meringue layers constituted most of the photograph (3).

Investigation of the cooling process of meringue containing the complex additive showed that the semi-

finished baked product requires gentle cooling by convection for 35÷40 minutes at a temperature of 20÷25 °C and air flow rate of 1.5÷2.0 m/s.

The work performed allowed for a 12.5% reduction of meringue baking time due to the replacement of 8% sugar by a complex additive including puffed barley (particle size $1.5\text{--}2.0 \cdot 10^{-3}$ m) and ground eggshell (particle size $40 \cdot 10^{-6}$ m) in a 3:1 ratio.

REFERENCES

1. Lee, S., Inglett, G.E., Palmquist, D., and Warner K., Flavor and texture attributes of foods containing β -glucan-rich hydrocolloids from oats, *Food Science and Technology*, 2009, vol. 42, no. 1, pp. 350-357.
2. Cavallero, A., Empilli, S., Brighenti, F., and Stanca, A.M., High (1→3,1→4)- β -Glucan Barley Fractions in Bread Making and their Effects on Human Glycemic Response, *Journal of Cereal Science*, 2002, vol. 36, no. 1, pp. 59–66.
3. Volikakis, P., Biliaderis, C.G., Vamvakas, C., and Zerfiridis, G.K., Effects of a commercial oat- β -glucan concentrate on the chemical, physico-chemical and sensory attributes of a low-fat white-brined cheese product, *Food Research International*, 2004, vol. 37, no. 1, pp. 83–94.
4. Lyly, M., Salmenkallio-Marttila, M., Suortti, T., Autio, K., Poutanen, K., and Lahteenmaki, L., The sensory characteristics and rheological properties of soups containing oat and barley β -glucan before and after freezing, *Food Science and Technology*, 2004, vol. 37, no. 7, pp. 749–761.
5. Xu, J., Chang, T., Inglett, G.E., Kim, S., Tseng, I., and Wirtz, D., Micro-heterogeneity and micro-rheological properties of high-viscosity oat β -glucan solutions, *Food Chemistry*, 2007, vol. 103, no. 4, pp. 1192–1198.
6. Oliveira, R.J., Matuo, R., da Silva, A.F., Matiazi, H.J., Mantovani, M.S., and Ribeiro, L.R., Protective effect of β -glucan extracted from *Saccharomyces cerevisiae* against DNA damage and cytotoxicity in wild-type (k1) and repair-deficient (xrs5) CHO cells, *Toxicology in Vitro*, 2007, vol. 21, no. 1, pp. 41–52.
7. Lazaridou, A. and Biliaderis, C.G., Molecular aspects of cereal β -glucan functionality: Physical properties, technological applications and physiological effects, *Journal of Cereal Science*, 2007, vol. 46, no. 2, pp. 101–118.
8. Xu, J., Inglett, G.E., Chen, D., and Liu, S.X., Viscoelastic properties of oat β -glucan-rich aqueous dispersions, *Food Chemistry*, 2013, vol. 138, no. 1, pp. 186–191.
9. Comin, L.M., Temelli, F., and Saldaña, M.D.A., Barley β -glucan aerogels as a carrier for flax oil via supercritical CO₂, *Journal of Food Engineering*, 2012, vol. 111, no. 4, pp. 625–631.
10. Fink, D., Rojas-Chapana, J., Petrov, A., Tributsch, H., Friedrich, D., Kuppers, U., Wilhelm, M., Apel, P.Yu., and Zrineh, A., The "artificial ostrich eggshell" project: Sterilizing polymer foils for food industry and medicine, *Solar Energy Materials and Solar Cells*, 2006, vol. 90, no. 10, pp. 1458–1470.
11. Titchenal, C.A. and Dobbs, J., A system to assess the quality of food sources of calcium, *Journal of Food Composition and Analysis*, 2007, vol. 20, no. 8, pp. 717–724.



RESEARCH ON THE INFLUENCE OF SILVER CLUSTERS ON DECOMPOSER MICROORGANISMS AND *E. COLI* BACTERIA

A. I. Piskaeva*, Yu. Yu. Sidorin, L. S. Dyshlyuk, Yu. V. Zhumaev, and A. Yu. Prosekov

Kemerovo Institute of Food Science and Technology,
bul'v. Stroitelei 47, Kemerovo, 650056 Russia,
*phone/fax: +7 (923) 606-33-73, e-mail: a_piskaeva@mail.ru

(Received January 20, 2014; Accepted in revised form January 30, 2014)

Abstract: Modern methods of slime waste disposal utilized by wastewater treatment plants were analyzed. Domestic and foreign experience in the application of silver clusters in reducing pathogenic and conditionally pathogenic microorganisms inhabiting the waste sludge was studied. The main mechanisms of bactericidal and bacteriostatic effects silver clusters are capable of exerting on microorganisms were considered. Strains of microorganisms with the ability to recycle organic and inorganic substances present in the waste sludge into ecologically pure humus fertilizer in the course of their vital activity were selected. The effects of different concentrations of silver clusters on growth and development of the microorganisms decomposing organic compounds (*Microbacterium terregens* BSB-570, *Streptococcus termophilus* St5, *Lactobacillus* sp. 501 (2A4), *Rhodococcus erythropolis*, *Bacillus fastidiosus*, *Arthrobacter* sp. (*Arthrobacter paraffineus*) ATCC 15591, etc.), as well as on the *Escherichia coli* bacteria chosen as a model organism, were studied. For the first time, decomposers modified with silver clusters, i.e. resistant to high concentrations of silver clusters, able not only to grow, but also to reproduce normally and, consequently, to recycle the waste sludge, were obtained. Bacteriostatic and bactericidal concentrations of silver clusters with respect to decomposers and optimal concentration, at which the useful microorganisms are able to grow and reproduce actively and the pathogenic *Escherichia coli* die, were determined.

Keywords: silver clusters, nano-silver, destruction, pathogen, ion, nanoparticles, sludge, waste

UDC: 60:661.857
DOI 10.12737/4136

INTRODUCTION

Today, problems of environment protection and rational nature management, as well as improvement of ecological safety, are considered to be of paramount importance worldwide. Wastes formed in the process of industrial wastewater treatment belong to the most abundant contaminants of practically all components of the environment (surface and ground waters, soil, vegetative cover, and atmospheric air). These sediments, differing by chemical and physical properties, are called slimes. Very often, they are harmful for living organisms and the environment.

Most often, slimes formed in the course of wastewater treatment are buried at the industrial waste disposal sites upon slime treatment with bonding cement, bitumen, glass, or polymers. However, these waste disposal sites pose serious danger for the environment. Self-purification of the contaminated areas without human interference lasts for decades; besides, the inherent capacity of the environment for self-restoration decreases each year. Consequently, the problem of maximally efficient slime purification, which would take into account contaminant composition, economic, and ecological factors, becomes urgent [1].

In most cases, due to the lack in sufficient amount of specialized waste disposal sites meeting the requirements of construction norms and rules of the

Russian Federation 2.01.28-85, the factories are forced to store wastes on their territories, often without adhering to the burial rules, which leads to soil and surface water contamination due to dissolving of slimes under the effects of atmospheric factors.

The amount of accumulated wastes and new wastes produced each year is so high that the slimes hold the first place in the extent of negative effect they produce on the environment and man, leaving behind such factors as noise, radioactive wastes, chemical fertilizers, and oil spills.

In most slimes, in addition to various organic and inorganic compounds, considerable amount of pathogenic microorganisms is contained. This natural slime microflora—thermotolerant coliform bacteria, *Escherichia coli*, *Chlostridium perfringens*, *Salmonella enteritidis*, *Salmonella virchow*, etc.—poses a great danger, as it possesses the ability to excrete toxic compounds affecting human body.

The aim of the work was to study the effect of silver clusters on microorganisms capable of waste decomposing in the course of their vital activity and on *E. coli* to determine antipathogen activity of silver clusters. The study was conducted to develop new microbiological method of waste slime purification and processing under conditions of Siberian Federal District.

E. coli was chosen as a model organism since this rod-like bacterium is one of the best studied prokaryotic

microorganisms and one of the most important subjects in biotechnology and microbiology. *E. coli* is well adapted to growth and proliferation under laboratory conditions [2].

Silver clusters (silver nanoparticles) are a type of colloidal silver of highest quality more homogeneous and of smaller size than classic colloidal silver preparations [www.vector-vita.com].

The authors have elaborated an original, so-called AGL (ARGENTUM LYSOL), method of synthesis of stable silver nanoparticles with mean diameter in the range of 1–2 nm (particles of this size may be referred to clusters). The particular feature of the method is the use of a natural polymer gelatin as a ligand instead of the standard povidone. Also, synthesis according to the standard technique (chemical synthesis using silver nitrate), or AGM synthesis (ARGENTUM MEDICAL) allowing to produce silver nanoparticles 1–10 nm in diameter was performed. Silver clusters produced by NPTs “Vector-Vita” with particle size distribution in the range of 1–8 nm are an example of the technique utilization. Therefore, monodispersity of the closest analogue of silver clusters is almost three times lower. Figure 1 presents size distribution curves for particles synthesized according to AGM and AGL methods.

On the whole, silver clusters contain highly dispersed metallic silver particles in the nanometer size range. The terms “silver clusters”, “nano-silver”, and “silver nanoparticles” are essentially synonymous. However, silver clusters differ considerably by their physicochemical properties from other nano-sized forms of silver. Their small size provides for the high efficiency, stability, and safety [3].

Owing to their unique physical and chemical properties that are defined by the high surface area-to-volume ratio and other size effects, antibacterial and antiviral properties of silver clusters are enhanced considerably, if compared to other metals, while silver as such remains absolutely safe for human health upon appropriate application.

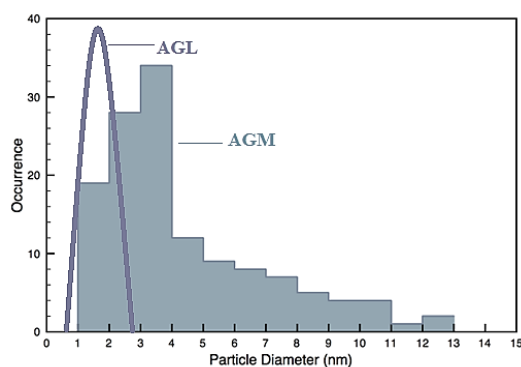


Fig. 1. Size distribution of silver nanoparticles produced by two methods of synthesis, AGL and AGM.

In view of a rather wide spectrum of antibacterial effect of silver-based preparations, there is a chance that the bactericidal effect is exerted not only against pathogens, but against normal microflora of human body as well. However, the theoretical assumption is not applicable to silver clusters. Solutions of metallic silver

in the form of clusters not only have been proven to be safe for the organism, but also are used in preventive and therapeutic doses in place of antibiotics. Silver preparations are administered to normalize microbiocenosis and suppress disease-causing microorganisms. Although, today there is no shared opinion on the reasons of such selectivity, the researchers agree that silver administration in the first place results in suppression of pathogenic flora, which promotes development of normal flora.

Biocidal effect of silver clusters is explained by three main mechanisms: interference in electron transport, binding to bacterial DNA, and interaction with cell membrane.

Complex formation with sulfhydryl groups may inactivate enzymes on cell surface and alter respiration processes in cell membrane. The DNA-bound silver ions block transcription, and binding with cell surface components interrupts bacteria respiration and adenosine triphosphate (ATP) synthesis [4]. In *Candida albicans* yeast (and not in *E. coli*) irreversible interaction of silver ions with cysteine residue of phosphomannose isomerase interrupts synthesis of cell wall, which, in turn, leads to loss of essential nutrients [5]. Silver clusters suppress phosphate consumption, repress DNA functions, and inhibit transmembrane transport of organic and inorganic substances [6, 7].

The effect of silver on a microbial cell occurs in two steps: 1) adsorption and 2) active transport of ions inside cell. Up to 90% of internalized silver ions are retained in the membrane; cell metabolism is disturbed as a result of inactivation of enzymes and transport proteins (permeases). Electron microscopy studies demonstrated that silver ions caused morphological changes in bacterial cells [8].

Silver ions inhibit consumption and exchange of phosphates in *E. coli* and cause loss of accumulated phosphate, as well as mannitol, succinate, glutamine, and proline. The effect of Ag^+ is blocked by thiols and, to a lesser extent, bromide. In the presence of *N*-ethylmaleimide, Ag^+ does not cause phosphate leakage but still inhibits exchange between intracellular and extracellular phosphates [9]. Another mechanism of silver ion effect, especially at low concentrations, was reported in the work [10]. The authors demonstrated that low concentrations of Ag^+ caused massive leakage of protons through membrane of *Vibrio cholera*, which ultimately resulted in complete deenergizing and, most probably, death of a cell.

Authors of the work [11] studied the ability of bacteria to consume Ag^+ ions from solutions by the examples of *Bacillus cereus*, *B. subtilis*, *E. coli*, and *Pseudomonas aeruginosa*. Consumption of Ag^+ from solution by the bacteria occurred rather efficiently: approximately 89% to the total Ag^+ was removed from a 1 mM solution.

In the work [12], oligodynamic effect of silver on *Bacillus subtilis* (1 strain), *Enterobacteriaceae* (26 strains), *Legionellaceae* (13 strains), *Micrococcaceae* (6 strains), and *Pseudomonas aeruginosa* (4 strains) was studied. *B. subtilis* and *Legionellaceae* demonstrated the highest susceptibility. The effect of small amounts of

silver on various bacteria groups differed considerably: non-pathogenic microorganisms were less susceptible than *Staphylococcus aureus*.

Silver clusters possess pronounced antibacterial effects if compared to other metals. Bactericidal effect of silver clusters was found to be 1750 times stronger than that of carbolic acid and 3.5 times stronger than that of mercuric chloride and lime chloride [13].

The studies demonstrated that susceptibility of various pathogenic and non-pathogenic organisms to silver was different. Pathogenic microflora is much more sensitive to silver ions than the non-pathogenic microflora.

MATERIALS AND METHODS

Strains of microorganisms decomposing organic compounds and possessing the ability to adsorb silver clusters on their surface, including *Microbacterium terregens* BSB-570, *Streptococcus thermophilus* St5, *Lactobacillus* sp. 501 (2L4), *Rhodococcus erythropolis*, *Bacillus fastidiosus*, and *Arthrobacter* sp. (*Arthrobacter paraffineus*) ATCC 15591, were subjects of the work.

Adaptation of the microorganisms and their modification with silver clusters was performed by cultivation of the strains at various concentrations of silver clusters (from 0 to 400 µg/mL) in liquid nutrient medium.

Solutions containing silver clusters 1–2 nm in diameter at concentration of 10000 µg/mL were prepared at the chair of Bionanotechnology of the Kemerovo Institute of Food Science and Technology. The solutions were introduced into nutrient medium containing cultures of decomposer microorganisms and in the medium for cultivation of *E. coli*.

Nutrient medium for cultivation of *M. terregens* BSB-570, *R. erythropolis*, *B. fastidiosus*, and *Arthrobacter* sp. (*A. paraffineus*) ATCC 15591 contained (g/L) yeast extract, 5.0; pepton, 15.0; sodium chloride, 5.0; and distilled water, 1.0 L. Temperature of cultivation was set to 30–34°C. Duration of cultivation was 3 days.

Nutrient medium for cultivation of *S. thermophilus* St5 and *Lactobacillus* sp. 501 (2L4) contained (g/L) papain digest of soybean flour, 5.0; peptic digest of animal tissue, 5.0; yeast extract, 2.5; beef extract, 5.0; lactose, 5.0; ascorbic acid, 0.5; magnesium sulfate, 0.25; and distilled water, 1.0 L. Temperature of cultivation was 40°C. Duration of cultivation was 2 days.

Nutrient medium for cultivation of *E. coli* contained (g/L) pancreatic hydrolysate of fish flour, 10.0; enzymatic peptone, 10.0; lactose, 10.0; yeast extract, 5.0; purified bile, 1.0; neutral red, 0.05; crystal violet, 0.001; and agar, 13.0. Temperature of cultivation was 37°C. Duration of cultivation was 3 days.

During the whole process of cultivation, samples were monitored with an AxioVert.A1 (Carl Zeiss AG) microscope at ×40 and ×100 magnification each 8 h during the first day and each 12 h, the following days. Final concentrations were selected taking into account decomposer survival and complete death of *E. coli* culture.

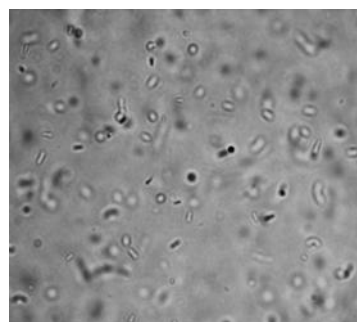
RESULTS AND DISCUSSION

Results of the study of the effect of various silver cluster concentrations on decomposer microorganisms are presented in Table 1.

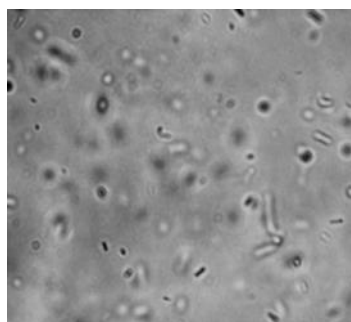
Figure 2 demonstrates the results of the *Microbacterium terregens* BSB-570 microscopy.

Table 1. Threshold concentrations of silver clusters for decomposer microorganisms

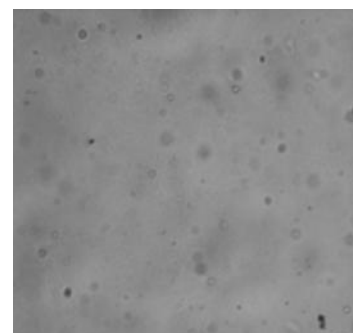
Strain	Concentration, µg/mL		
	bacteriostatic	bactericidal	optimal
<i>Microbacterium terregens</i>	100	400	50
<i>Streptococcus thermophilus</i> St5	200	500	100
<i>Lactobacillus</i> sp. 501	200	450	100
<i>Arthrobacter paraffineus</i>	50–100	250	50
<i>Bacillus fastidiosus</i>	50–100	300	50
<i>Rhodococcus erythropolis</i>	50–100	300	50



(a)



(b)



(c)

Fig. 2. *Microbacterium terregens* BSB-570 strain in the medium containing silver clusters at concentration of (a) 50 µg/mL, (b) 150 µg/mL, and (c) 300 µg/mL at ×100 magnification.

Analysis of the data presented in Table 1 showed that silver cluster concentration of 50 $\mu\text{g/mL}$ is optimal for most decomposer microorganisms. At this concentration, they are capable of normal growth and proliferation and thus processing of the compounds comprising waste slimes.

According to Fig. 2, cultivation of the *Microbacterium terregens* BSB-570 strain at concentration of silver clusters of 150 $\mu\text{g/mL}$ resulted in irreversible processes of culture death. However, they proceeded very slowly and only upon constant increase of silver concentration. The culture is capable of proliferation even at silver concentration of 250 $\mu\text{g/mL}$. Concentration of 50–100 $\mu\text{g/mL}$ was found to be optimal.

According to the data on the effect of silver clusters on *E. coli* growth on a dense nutrient medium (Table 2,

Fig. 3), concentration of 100 $\mu\text{g/mL}$ was found to be lethal for the culture. At 50 $\mu\text{g/mL}$, the number of colonies decreases more than twofold.

Table 2. The effect of various concentrations of silver clusters on growth of *Escherichia coli*

Silver cluster concentration in the medium, $\mu\text{g/mL}$	Number of <i>E. coli</i> colonies	
	after 24 h	after 36 h
100	0	0
50	79	104
Control (0)	196	254

Figure 3 presents *E. coli* strains obtained after 72 h of cultivation at 37°C on nutrient media with varying concentration of silver clusters.

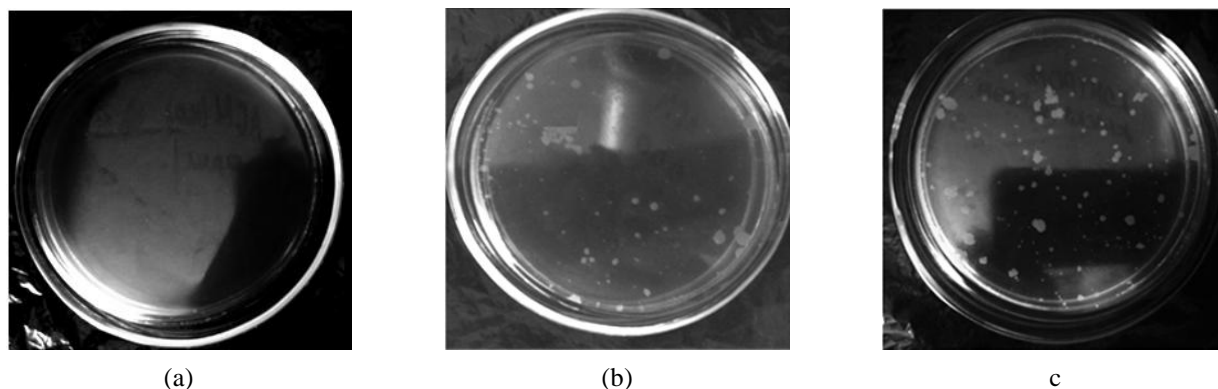


Fig. 3. Cultivation of *E. coli* on a dense nutrient medium at concentration of silver clusters of (a) 100 $\mu\text{g/mL}$ and (b) 50 $\mu\text{g/mL}$; (c) control samples grown in the absence of silver.

Figure 4 demonstrates the results of microscopy investigation of the *E. coli* culture.

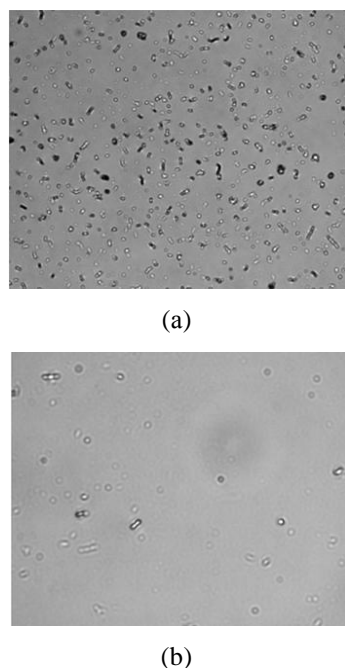


Fig. 4. Microscopy analysis of *E. coli* culture at $\times 100$ magnification, after 24 h cultivation: (a) control sample (no silver) and (b) silver clusters concentration of 100 $\mu\text{g/mL}$.

As follows from Fig. 4, after 24-h cultivation, the number of bacteria decreased considerably. The ability to proliferate was practically absent. Therefore, at silver cluster concentration of 100 $\mu\text{g/mL}$ in the nutrient medium no *E. coli* growth occurs. At the same time, this concentration does not cause bactericidal or bacteriostatic effect on the decomposer microorganisms. At this concentration, they are capable of normal growth and proliferation.

Basing on the results of the work, we can conclude the following:

1. The effect of various concentrations of silver clusters (from 0 to 450 $\mu\text{g/mL}$) in the liquid nutrient medium on growth and proliferation of decomposer microorganisms was studied.
2. Microorganisms decomposing various organic and inorganic compounds modified with silver were obtained.
3. Bacteriostatic and bactericidal concentrations of silver clusters were defined for all decomposer microorganisms under study.
4. The efficiency of the effect of the silver clusters against pathogenic bacteria was proven by the example of *Escherichia coli*.
5. Concentrations of silver clusters allowing for growth and active proliferation of decomposer microorganisms and death of *E. coli* bacteria were chosen. The optimal concentration of silver clusters was found to be 100 $\mu\text{g/mL}$.

REFERENCES

1. Arustamov, E.A., *Bezopasnost' zhiznedeyatel'nosti* (Safety of Living), Moscow: Dashkov and co., 2006.
2. Feng, P., Weagent, S.D., Grant, M.A., and Burkhardt, W., Enumeration of *Escherichia coli* and the Coliform Bacteria, in *Bacteriological Analytical Manual*, Gaithersburg, MD: AOAC Intl, 2002, 8th edition.
3. Kostyleva, R.N., and Burmistrov, V.A., Comparative analysis of bactericidal activity of colloidal silver preparations, in *Serebro i vismut v meditsyne* (Silver and Bismuth in Medicine), Novosibirsk, 2005, pp. 53–60.
4. Trevors, J.T., Silver Resistance and Accumulation in Bacteria, *Enzyme Microb. Technol.*, 1987, no. 9, pp. 331–333.
5. Wells, T.N., Scully, P., Paravicini, G., Proudfoot, A.E., and Payton, M.A., Mechanism of Irreversible Inactivation of Phosphomannose Isomerases by Silver Ions and Flamazine, *Biochemistry*, 1995, no. 34 (24), pp. 7896–7903.
6. Ivanov, V.N., Larionov, G.M., and Kulish, N.I., Some experimental and clinical data on application of silver ions in management of drug-resistant microorganisms, in *Serebro v meditsyne i tekhnike* (Silver in Medicine and Technology), Novosibirsk: Siberian Branch of the Russian Academy of Medical Sciences, 2005, pp. 53–62.
7. Savadyan, E.Sh., Mel'nikova, V.M., and Belikov, G.P., Modern trends in application of silver-based antiseptics, *Antibiotiki i khimioterpiya* (Antibiotics and Chemotherapy), 1999, vol. 34, no. 11, pp. 874–878.
8. Tolgskaya, M.S., and Chumakov, A.A., *Bol'shaya meditsynskaya entsyklopediya* (Great Medical Encyclopedia), Petrovskii, B.V., Ed., Moscow: Sovetskaya Enciklopediya, 1984, vol. 2, pp. 142–143.
9. Schreurs, W.J., and Rosenberg, H., Effect of Silver Ions on Transport and Retention of Phosphate by *Escherichia coli*, *J. Bacteriol.*, 2002, vol. 152, no. 1, pp. 7–13.
10. Dibrov, P., Dzioba, J., Gosink, K.K., and Häse, C.C., Chemiosmotic Mechanism of Antimicrobial Activity of Ag⁺ in *Vibrio cholera*, *Antimicrob. Agents Chemother.*, 2002, vol. 46, no. 8, pp. 2668–2670.
11. Mullen, M.D., Wolf, D.C., Ferris, F.G., Beveridge, T.J., Flemming, C.A., and Bailey, G.W., Bacterial Sorption of Heavy Metals, *Appl. Environ. Microbiol.*, 1989, vol. 55, no. 12, pp. 3143–3149.
12. Müller, H.E., Oligodynamic Action of 17 Different Metals on *Bacillus subtilis*, *Enterobacteriaceae*, *Legionellaceae*, *Micrococcaceae*, and *Pseudomonas aeruginosa*, *Zentralbl. Bakteriolog. Mikrobiol. Hyg. B*, 1985, vol. 182, no. 1, pp. 95–101.
13. Kul'skii, P.A., *Serebryanaya voda* (Silver Water), Kiev: Naukova Dumka, 1987.



MIXTURES FOR VERTEBROPLASTY: THE FLOWABILITY OF THEIR COMPONENTS AND A NEW PRODUCTION TECHNOLOGY USING A CENTRIFUGAL MIXER

D. M. Borodulin* and D. V. Sukhorukov

Kemerovo Institute of Food Science and Technology,
bul'v. Stroitelei 47, Kemerovo, 650056 Russia,
*phone: 8-950-272-59-94, e-mail: Pioner_dias@mail.ru

(Received March 7, 2014; accepted in revised form March 17, 2014)

Abstract: The article deals with the production of bone cement, which is used in various fields of medicine. A new technology for producing medical cement mixtures is presented. Particular attention is paid to use of bone cement in the treatment of vertebral compression fractures associated with osteoporosis. The incidence rate of osteoporosis and its clinical manifestations is expected to increase four times in the next half-century due to the growth of population and the increase in life expectancy. Problems of contemporary medicine that are associated with obtaining granular mixtures of preset quality and composition are discussed. Information about the flowability of the components of cement mixtures is presented. The concept of a criterion of flowability is introduced for the first time for rationally choosing a mixing method according to the flowability of the components for preparing quality cement mixtures. Flowability data for cement mixture components have been obtained to optimize the mixing process. A dimensionless equation is set up to calculate the power requirement for the mixing process. The quality of the resulting granular compositions depends primarily on the physicomachanical properties of the materials being mixed. A continuous, centrifugal, bone cement mixing unit is described, and the principle of its operation is considered. The performance of continuous mixers has been evaluated in terms of output capacity, specific energy consumption, and heterogeneity coefficient. The new, centrifugal mixer has been demonstrated to be more efficient in bone cement production than the pulsating mixer.

Keywords: vertebroplasty, centrifugal mixer, pulsating mixer, bone cement, polymethyl methacrylate, flowability, hydroxylapatite ceramic, tricalcium phosphate ceramic

UDC 621.929.2/9
DOI 10.12737/4137

INTRODUCTION

The problem of treating osteoporosis is a challenge for present-day health care, for this disease has become quite widespread among the elderly. Approximately 40% of the women and 13% of the men older than 50 years have had one bone fracture or more [8, 10].

It is predicted that the incidence rate of osteoporosis and its clinical manifestations, such as femoral neck fracture, will have increased four times within the next half-century because of the growth of population and the increasing life expectancy [5, 10].

Conventional methods of curing compression fractures of vertebral bodies involve use of analgesics and muscle relaxants, immobilization, bed rest, physiotherapy, and wearing a body jacket [2, 9].

These methods suffer from the following drawbacks: lengthy confinement to bed and the impossibility of early mobilization because of the marked pain syndrome lead to lack of appetite, to impaired glucose tolerance, and to development of hypostatic pneumonia, phlebotrombosis, and, as a consequence, pulmonary artery thromboembolism. In addition, the hypodynamia implied by the bed rest regime diminishes the density of bone tissue (by up to 2% per week), thus causing progress of osteoporosis [6, 7]. For this reason,

vertebroplasty is being increasingly used in the symptomatic treatment of pathological compression fractures associated with osteoporosis and osteopenia.

The results of clinical application of vertebroplasty, analyzed by many authors, demonstrated the high effectiveness of this technique in restoring the supporting ability of vertebral column segments affected by tumor-induced osteolysis. This method is primarily indicated for those oncological patients who cannot be subjected to radical surgery for some reason.

Application of vertebroplasty to patients with metastatic spinal injuries would shorten the bed rest period, extend the patient mobilization period, prevent the progress of the pain syndrome, and reduce the risk of neurological complications. Vertebroplasty, a minimally invasive procedure, would make it possible to shorten the hospital stay time. In combination with less frequent use of analgesics, it would reduce the cost of the hospital treatment of this category of patients.

Vertebroplasty is widely used abroad in the treatment of pain syndrome and pathological fractures that are due to metastatic injuries of the vertebral column and osteoporosis. The largest number of vertebroplastic manipulations in the world have been carried out in the United States and Western Europe;

among the countries of the Commonwealth of Independent States, the leaders in this field are the Russian Federation and Ukraine [1, 2, 4, 11].

Vertebroplastic bone cement has been employed in medicine over more than 50 years. It has found application not only in endoprosthetics for fixing components of an endoprosthesis to a bone, but also in other areas (plastic repair of vertebral bodies, stomatology, etc.). Bone cement fills the space between the endoprosthesis and the bone and forms an elastic zone intended both for functioning as a shock absorber and for uniformly distributing the load throughout the bone surrounding the endoprosthesis. The uniform redistribution of the load from the endoprosthesis to the bone is particularly important for the hip endoprosthesis stem, whose shape is generally imperfectly fitted to the shape of the femoral canal. This generates increased- and decreased-load zones (nonuniform distribution of forces).

Research areas in osteoporosis prosthetics (vertebroplasty) are the injective application and heterogeneity of bone cements. Bone cements are mainly produced manually or using a pulsating mixer. These technologies do not ensure the necessary product output rate; furthermore, they are insufficiently efficient from the economic standpoint. Russia's vertebroplasty is dominated by foreign brands of bone cement, which are well-promoted and avowed. The most demanded bone cements are acrylic ones, such as Vertebroplastic (De Puy Inc., Blackpool, England), DP-Pour (Den Plus Inc., Montreal, Canada), and Antibiotic Simplex (How Medical International Limited, London, England). Other popular options are calcium phosphate cements, namely, ChronOS Inject (Mathys Medical Ltd., Bettlach, Switzerland) and Biopex (Mitsubishi, Saitama, Japan).

The existing Russian brands of bone cement are in low demand, because they are less known and fall within the same price category, even though they are practically equal in their properties to their western analogues.

Preliminary studies demonstrated that the most promising apparatuses for preparing cement mixtures for vertebroplasty are continuous centrifugal mixers (CCMs). They ensure high-intensity mixing owing to the directed organization of the motion of thin, rarefied layers of the material (equal in size to the diameter of the particles being mixed). In addition, the centrifugal mixers reliably smooth the pulsations of the entering material flows. In continuous centrifugal apparatuses, it is possible to combine mixing and comminution processes. This feature provides means to obtain high-quality mixtures at large component-to-component ratios and is one of the basic advantages of the centrifugal technology.

The CCMs suggested here make it possible to produce bone cements that are equal in quality, if not superior, to the existing cements at lower expenses. This mixing method is technologically simpler than mixing in the pulsating apparatuses that are currently used in the preparation of cement mixtures.

Therefore, the problem of developing novel, high-performance CCMs for producing quality bone cements

is of high scientific and practical significance for public health care throughout the Russian Federation.

EXPERIMENTAL

In order to find a rational method of mixture preparation, we studied the flowability of cement components.

Granular materials are typically two-phase systems consisting of solid particles dispersed in air or in a gas medium.

The flowability of a material (Q) is a complex characteristic depending on many factors: density, particle-size distribution, particle shape, and particle surface conditions. The basic factors determining the flowability of powders are interparticle friction and cohesion (cohesive forces acting between particles), which counteract the motion of the particles relative to one another. Flowability is calculated via the formula:

$$Q = \frac{G_M}{S \cdot \tau}, \left[\frac{\text{kg}}{\text{m}^2 \cdot \text{s}} \right] \quad (1)$$

where m is the amount of material (kg), S is the outflow area (m^2), and τ is the material outflow time (s).

For estimating the effect of the flowability of cement components on the inertial forces in the flow of the materials being mixed, we will introduce the criterion of flowability Si :

$$Si = \frac{Q}{\rho \cdot d \cdot n}, \quad (2)$$

where ρ is the density of the material (kg/m^3), d is the average diameter of the cones (m), and n is the rotational frequency of the rotor (s^{-1}).

The flowability of cement components was measured using a setup that does not subject the granules to compression (Fig. 1). The setup has a hopper with a conical base. At the bottom of the hopper, there is a shutter plate, in a guiding slot, that can be moved to regulate the material outflow area S . The resulting mixture is collected in a receiving bin.

Experiments were performed in two modes. In the first mode, the material flew by gravity. In the second, the material was moved using a blade stirrer mounted inside the hopper. In both cases, the same amount of material (m) was placed in the hopper and the material outflow time τ at a fixed outflow area S was measured with a stop watch.

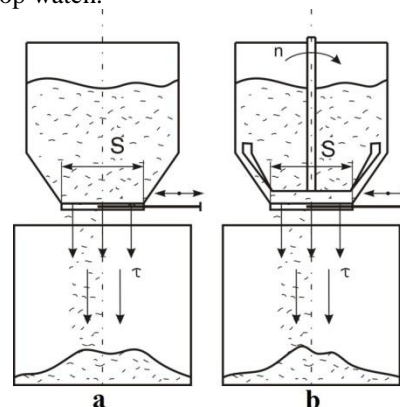


Fig. 1. Flowability determination setup (a) without a stirrer and (b) with a blade stirrer.

The experimental data of this study provide a basis for husing whether it is appropriate to use a CCM, whose advantage is that it yields a homogeneous mixture by crushing the conglomerates resulting from the introduction of a liquid phase into the granular material.

For obtaining bone cement, the Department of Food Production Engineering of the Kemerovo Institute of Food Science and Technology developed a mixing unit consisting of the new centrifugal mixer [3] and doser block.

The new CCM was used to prepare a pilot batch of bone cement consisting of polymethyl methacrylate (PMMC), a hydroxylapatite (HAP) bioactive calcium phosphate ceramic, and a tricalcium phosphate (TCP) ceramic, with PMMC : HAP : TCP = 90 : 5 : 5. The same experiments were performed using the base design of the mixer (Big Bill Orbital Bench Top Shaker, M49235, Barnstead International, Dubuque, Iowa).

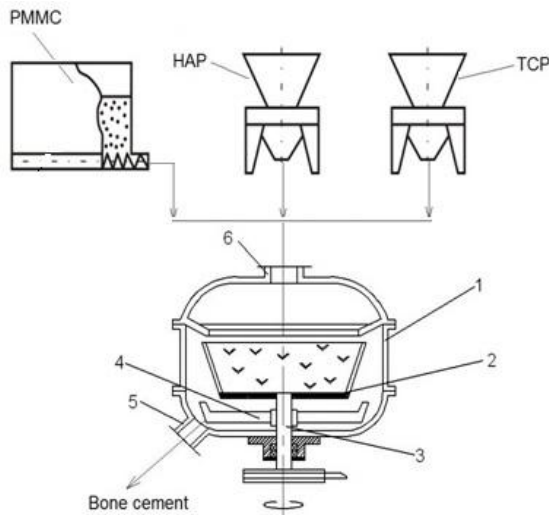


Fig. 2. Mixing unit: (1) mixer body, (2) disc, (3) shaft, (4) discharging blades, (5) outlet pipe, and (6) inlet pipe.

The centrifugal mixer (Fig. 2) operates in the following way. Granular materials, fed with volume dosers through inlet pipe 6, find themselves on the base of disc 2 of the rotating rotor and spread uniformly over the disc under the action of the centrifugal force. Next, the particles move upwards on the surface of a hollow, thin-walled, truncated cone, rounding elbow-shaped turbulizers and crossing past the latter. Thus, the particles being mixed are multiply separated and meet again and this improves the quality of the resulting mixture. The granular mass reaches the upper edge of the cone and is thrown out of the cone by the centrifugal force. The finished mixture falls onto the bottom of the apparatus and is brought out of the latter by discharging blades 4 through outlet pipe 5.

The organization of the straight and crossing material flows in this CCM makes the components flow pattern in the apparatus close to the perfect mixing model.

The particles of the components being mixed are under the action of both the centrifugal force and the drag force from air. As a consequence, they are

involved in swirling motion until they leave the apparatus. Mixing in the swirling flow is due to the deceleration of lower layers of the material upon their contact with the rotor surface and, subsequently, with the mixer walls. Since air has a certain viscosity, its layers that are adjacent to the inner surface of the rotating rotor are set in rotary motion by viscous friction forces. These layers experience the same forces as the mixture particles. The air drag sets the granular material in motion, forming turbulent dust–gas flows.

One of the most important characteristics of mixing efficiency is the heterogeneity coefficient of the key component of the mixture, V_c . It characterizes the uniformity of the distribution of the components in the mixture. We also determined the product output capacity of the apparatus and specific energy requirement, which are equally important process parameters. These data are presented in Table 3.

RESULTS AND DISCUSSION

The particle diameters and densities of the materials whose flowability was determined are listed in Table 1.

Table 1. Some properties of cement components

Cement component	Particle diameter, m	Particle density, kg/m ³
Polymethyl methacrylate	800×10^{-6}	1190
Hydroxylapatite bioactive calcium phosphate ceramic	300×10^{-8}	3156
Tricalcium phosphate ceramic	100×10^{-6}	3140

The flowability and criterion of flowability data calculated for the cement components via formulas (1) and (2) are listed in Tables 2 and 3.

Table 2. Flowability data for the cement components flowing by gravity

	Flowability Q , kg/(m ² s)		
	PMMC	HAP	TCP
	31.09512	40.67651	37.13355
Criterion of flowability S_i			
s-1	PMMC	HAP	TCP
9	0.014395889	0.01956542	0.01833756
11	0.011778455	0.01600807	0.01500345
13	0.009966385	0.01354529	0.01269523
15	0.008637533	0.01173925	0.01100253
17	0.007621353	0.01035816	0.00970812
20	0.00647815	0.00880444	0.0082519

The materials subjected to mechanical stirring show a higher flowability (Tables 2, 3). Note also that the physicomachanical properties of the materials are similar and have no significant effect on their flowability, which remains invariable throughout the outflow area range.

These experiments were followed by determination of the flowability of a pilot batch of bone cement consisting of polymethyl methacrylate, a hydroxylapatite bioactive calcium phosphate ceramic,

and a tricalcium phosphate ceramic. The mixture begins its motion at a 2/3 open outflow area ($S = 0.001024 \text{ m}^2$), and its flowability remains the same when the shutter is fully open. This is due to the fact that PMMC, which has strong adhesive properties, causes particle arching in the conical part of the hopper, thus hampering the mutual motion of the other particles of the mixture and slowing down their flow. Therefore, the materials considered here can be assigned to poorly flowing ones.

Table 3. Flowability data for the cement components moved by the blade stirrer

	Flowability Q , kg/(m ² s)		
	PMMC	HAP	TCP
	32.093	43.10864	38.10774
Criterion of flowability Si			
s ⁻¹	PMMC	HAP	TCP
9	0.01485787	0.02073528	0.01881864
11	0.012156439	0.01696523	0.01539707
13	0.010286218	0.01435519	0.01302829
15	0.008914722	0.01244117	0.01129118
17	0.007865931	0.0109775	0.00996281
20	0.006686042	0.00933087	0.00846839

Experiments demonstrated that the flowability of the materials depends markedly on their particle size distribution and density. Using the Statistica 6.0 program package, we estimated the functional relationship between the independent variables d and ρ and the response Q , by the multiple regression method.

Table 4 presents the goodness-of-fit parameters of this regression analysis. For example, the coefficient of determination for PMMC is $R^2 = 0.99$, indicating that the results of the regression analysis account for more than 99% of the scatter of the variables around the mean value. The regression model obtained by this analysis is highly significant, since the significance level p for the materials is close to zero.

Table 4. Regression analysis data

Regression parameters	PMMC	HAP	TCP
Multiple R	0.99	0.99	1
Multiple R^2	0.99	0.99	1
Corrected R^2	0.98	0.99	0.99
Fisher test F	86.93	529.5	1892
Significance level p	0.075	0.03	0.016
Standard error of estimation	7.937	5.12	2.045

In order to see which independent variable (d or ρ) is the most significant factor in the flowability of the materials, it is necessary to examine the standardized regression coefficients $Beta$ and unstandardized regression coefficients B listed in Table 5.

As is clear from Table 5, the most significant factor in the flowability of a material is its density: the weighting factors of density are large compared to those of particle diameter. Some of the $Beta$ values for d are

negative, indicating that the flowability of the granular material decreases with an increasing particle diameter.

Table 5. Multiple regression data

Polymethylmethacrylate					
	$Beta$	Standard error	B	Standard error	p -Level
Free term			-2320	4555	0.7
d	0.25	1.95	177.6	1374	0.92
ρ	1.24	1.95	1.78	2.78	0.63
Hydroxylapatite ceramic					
Free term			-2943	2654	0.46
d	-0.07	0.679	-390	3784	0.93
ρ	0.92	0.68	2.1	1.53	0.4
Tricalcium phosphate ceramic					
Free term			1167	1451	0.56
d	-1.15	0.53	-6486	3020	0.27
ρ	-0.15	0.53	-0.26	0.914	0.82

Processing the experimental data yielded the following empirical relationship for determining the flowability of the mixture as a function of particle density and diameter:

$$Q = 4910 + 2214d + 6\rho + 816d^2 - 2d\rho - 0.0017\rho^2; R^2=0.957 \quad (3)$$

Dimensionless equation (3) is valid only for the granular materials considered here, with particle diameters of 0.003 to 0.8 mm and densities of 1200 to 3160 kg/m³.

For elucidating the behavior of the bone cement components under the action of the inertial forces, we analyzed the motion of their particles on the rotor of the centrifugal mixer (Fig. 2) at a rotational frequency of $n = 9-20 \text{ s}^{-1}$. The results obtained are presented in Tables 2 and 3, from which it is clear that the criterion of flowability Si decreases with an increasing rotational frequency of the rotor. The largest Si values were obtained for the hydroxylapatite ceramic at the lowest rotational frequency of the rotor; however, because of the high density of this material, these values are close to the values observed for poorly flowing materials ($Si = 0.02$).

To set up a dimensionless equation describing the mixing of granular materials, it is necessary to calculate the criterion of power K_N using the formula

$$K_N = \frac{N}{\rho \cdot n^3 \cdot d_k^5}, \quad (4)$$

where N is the useful power spent on the mixing of the granular materials (W), ρ is the density of the particles of the material (kg/m³), d_k is the mean diameter of the conical rotor on which the particles move (m), and n is the rotational frequency of the rotor (s⁻¹).

The calculated criterion of power data demonstrate that K_N increases as the diameter and rotational frequency of the conical rotor are increased. This is due to the fact that the holdup capacity of the mixer grows with an increasing cone diameter. The K_N values for the mixture components fall in the range from 4 to 16, which is characteristic of poorly flowing materials (for

readily flowing ones, $K_N = 0.05\text{--}0.5$). This is explained by the fact that poorly flowing materials, possessing adhesive properties, hamper the motion of the particles relative to one another and on the cone surface. As a consequence, the flowability of the material decreases. This leads to a buildup of the material on the rotor and, accordingly, to an increase in the power required for mixing.

Figure 3, plots the criterion of power versus the criterion of flowability at $n = 9\text{--}20\text{ s}^{-1}$ and $d_k = 0.4\text{ m}$ for the main component of bone cements – polymethyl methacrylate.

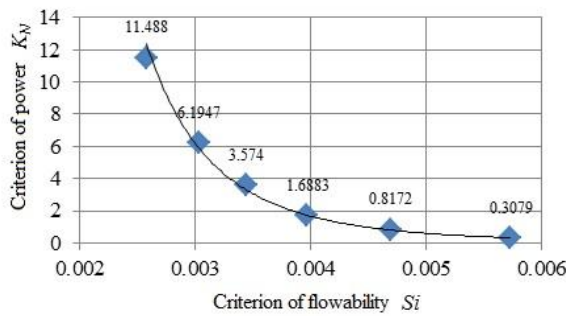


Fig. 3. Criterion of power K_N versus criterion of flowability S_i .

It is clear from Fig. 3 that the criterion of power and, accordingly, the power consumed decrease dramatically with an increasing criterion of flowability. Note here that K_N depends more strongly on the interparticle and particle–rotor surface friction than on the inertial forces. Between 0.004 and 0.006, K_N is practically independent of the criterion of flowability. In this K_N range, the energy requirement depends only on the inertial forces, which far exceed the interparticle and particle–inner rotor surface friction forces.

Experimental data processing using the EXCEL program yielded the following dimensionless equation for the mixing of granular materials:

$$K_N = 2 \cdot 10^{-11} \cdot S_i^{-4.5}, \quad (5)$$

Dimensionless equation (5) is valid only for granular materials with particle diameters of 0.003 to 0.8 mm. Equation (5) is convenient for approximate engineering and economic calculations; however, it is necessary to take into account that this equation leads to a large error of $\pm 30\%$. In more accurate calculations, it is necessary

to use dimensionless relationships established for each particular component of the mixture.

In view of the aforesaid, it can be hypothesized that the centrifugal mixer is the most appropriate means of preparing bone cements. Since the centrifugal forces exert an intense action on the material being mixed, the poorly flowing components undergo uniform mixing without forming agglomerates.

In order to verify this hypothesis, we determined the quality of the mixtures obtained with the new CCM and with the base mixer at a fixed product output rate. The rotational frequency of the rotor in these experiments was $n = 12.5\text{ s}^{-1}$. The performance of these mixers was characterized in terms of specific energy requirement. The results of the experimental tests of the two mixers are presented in Table 6.

Table 6. Testing data for the two mixers

Mixer	Product output rate	Specific energy requirement	V_c
	kg/h	kW h/m ³	%
New CCM	200	0.66	4.21
Base design	200	1.28	7.03

An analysis of these data demonstrates that, for obtaining quality bone cements, it is pertinent to employ the new CCM for the reason that, other conditions being equal, it affords better mixtures at a lower energy input than the base apparatus.

CONCLUSIONS

The criterion of flowability introduced in this study provides means to find the most rational mixing technology, to predict the behavior of the mixture during the process, and to more precisely tune the proportions of the components to be mixed.

A dimensionless equation accurate to 6% has been set up for determining the energy requirement for the mixing of the granular materials considered in the article.

As compared to the base apparatus, the new CCM as an element of the processing line in the manufacturing of bone cements would afford a higher product output rate at a low steel and energy intensity. This would make it possible to manufacture, at a lower cost, quality bone cements capable of meeting competition with their foreign analogues.

REFERENCES

1. Valiev, A.K., Dolgushin, B.I., Aliev, M.L., et al., *Materialy III s'ezda onkologov i radiologov SNG* (Proceedings of the III Congress of Oncologists and Radiologists of the Commonwealth of Independent States), Minsk, 2004, p. 255.
2. Dzindzhikhadze, R.S., Lazarev, V.A., et al., *Neirokhirurgiya (Neurosurgery)*, 2005, no. 1, pp. 36–40.
3. Borodulin, D.M., Andryushkov, A.A., and Voitikova, L.A., RF Patent 2496561, *Byulleten' izobretenii (Inventions bulletin)*, 2013, no. 19.
4. Pedachenko, E.G. and Kushchev, S.V., *Ukrainskii meditsinskii chasopis (Ukrainian medical journal)*, 2006, no.6, pp. 96–101.
5. Do, H.M., Kim, B.S., Marcellus, M.L., et al., *American Journal of Neuroradiology*, 2005, vol. 26, pp. 1623–1628.
6. Irani, F.G., Morales, J.P., Sabharwal, T., et al., *British Journal of Radiology*, 2005, vol. 78, pp. 261–264.
7. Jensen, M.E., McGraw, J.K., et al., *Journal of Vascular and Interventional Radiology*, 2007, vol. 18, pp. 325–330.
8. Lips, P., *American Journal of Medicine*, 1997, vol. 103, no. 2, pp. S3–S11.
9. McGraw, J.K., Gardella, J., Barr, J.D., et al., *Journal of Vascular and Interventional Radiology*, 2003, vol. 14, pp. 827–831.
10. Rigg, B.L. and Melton, L.J., *Bone*, 1995, vol. 17, no. 5, pp. 505–511.
11. Stallmeyer Bernadette, M.J., Zoarski, G.H., and Obuchowski, A.M., *Journal of Vascular and Interventional Radiology*, 2003, vol. 14, no. 6, pp. 683–696.

RHEOMETRIC MONITORING OF THE FORMATION OF MILK–PROTEIN BLOBS

A. N. Pirogov

Kemerovo Institute of Food Science and Technology,
bul'v. Stroitelei 47, Kemerovo, 650056 Russia,
e-mail: prmeh@kemtipp.ru

(Received March 7, 2014; Accepted in revised form March 17, 2014)

Abstract: This paper presents the results of the theoretical and experimental studies of newly designed devices, namely, the VRSh-1 ball rheometer and the Sgustok-1S dual-range rotary viscometer, for the continuous automatic monitoring of structure formation processes in milk–protein blobs. Each type of rheometers is studied to substantiate and select their geometric and kinematic parameters and the shape of measuring elements. It has been shown that the mechanical actions on the structure of milk–protein blobs during the rheometric monitoring of their formation must be minimal to obtain reliable data on their readiness. It has been proven that the monitoring of the formation of blobs by the method of the low-amplitude dynamic oscillations of a ball does not necessitate the measurement of the phase shift of its oscillations, and the total force of the resistance of a strengthening clot to the displacements of a ball inside it should be selected as a control parameter, which is in direct proportion to the amplitude of linear displacements of a ball in a viscoelastic medium (blob). Such a solution simplifies the design of a rheometer and makes it possible to obtain a similar rheogram, which precisely and reliably describes the coagulation of a milk mixture. The possibility of switching the rigidity ranges of force indicators without stopping the electrical drive, the design of which prevents a formed blob from dynamic impacts, thus providing the precision of monitoring and the preservation of the structure of a blob, has been designed for the method a cylinder rotating in a formed blob. The algorithm of the computer approximation of rheometric monitoring results for the formation of milk–protein blobs with the possibility of correcting its consistence at the terminal stage of coagulation is described.

Keywords: milk blobs, process rheometers, monitoring, quality, image identification, approximation

UDC 637.13:532.135
DOI 10.12737/4138

INTRODUCTION

Milk and dairy products hold a specific place among the most popular foods, which help a human organism to adapt to deteriorating environmental conditions [1]. The principal stage of the production of any cultured dairy product is the coagulation of proteins and the formation of a blob of desired consistency, the main characteristic of which is the strength and mechanostuctural properties [2]. The readiness of a milk–protein blob in the production of cheeses was estimated visually at most enterprises until now [3]. The reliability of the results of such a monitoring depends to a considerable degree on the experience of an operator and its sensory sensitivity. In parallel, the active acidity pH in the production of rennet blobs and the Turner titrable acidity (°T) in the production of cultured dairy product blobs are measured.

Instrumental monitoring is performed using different laboratory instruments (rheometers). For example, there is the known laboratory rheometer used to improve the recipe of dairy products and the technology of their production, namely, the Barkan geleometer [4], on which the “crushability” of a rennet blob at the moment of its readiness is measured via the cyclic indentation of a cone. Elastograms are obtained using a thromboelastograph, which does not give the precise kinetic picture of the formation of blobs due to the partial destruction of their structure.

A non-destructive method and a laboratory instrument for studying the coagulation of milk have been developed. The instrument consists of a temperature-controlled bath, inside which vessels filled with a milk mixture are placed on the axis connected with the electrical drive. The surface of the milk mixture in each vessel is radiated with a laser beam, which is fixed on the scales of a special screen after reflection with a photo camera fastened immovably on the instrument. The locations of reflected beams are changed proportionally to the change in the mechanostuctural (rheological) properties of formed blobs upon the cyclic inclination of the vessels by the electric driver. The obtained results are used to plot “conditional rheological parameter–process duration” rheograms [5, 6].

There exist the Scott–Blair rotary elastometers and the torquemeters that are applied in the bulk method of production to monitor the structural strength of formed blobs via the rotation of a cylinder submerged into a milk mixture. In this case, the process is stopped immediately after a desired blob strength and active acidity pH = 4.5–4.7 are attained.

The common shortcoming of all the above listed devices for the monitoring of the readiness of milk–protein blobs is the absence of a control signal, which would allow these instruments to be included into an automatic process control system for monitoring the

formation of milk blobs and their readiness for subsequent process operations.

The quality of cultured dairy product blobs in the process of their production is provided by meeting a number of conditions, such as the quality of initial raw materials and cultures and the adherence to technical regulations and process parameters. The readiness of blobs is determined at the end of their coagulation stage by measuring the Turner titrable acidity of samples (°T) [7]. In particular, it has been shown [8] that the relation between the active and titrable acidities is more or less clearly visible only for raw milk.

For these reasons, the development of scientifically substantiated methods and devices for the continuous automatic rheometric monitoring of the structure formation of milk-protein blobs in the production of dairy products by the bulk method and corresponding software for the implementation of this monitoring is a topical scientific problem of great research and practical interest for not only the food industry, but also for the other industries, in which structured liquid media are produced or used.

The objective of this work is to scientifically substantiate and develop a methodology, equipment, and software for the automatic rheometric monitoring of the formation of milk-protein blobs.

OBJECTS AND METHODS OF STUDY

Studied medium. To study the formation of rennet and acid clots, a standard milk mixture was prepared using dry skim milk of the same batch. This eliminated the effect of the heterogeneity of raw materials on experimental results. Reconstituted skim milk was obtained by dissolving dry milk (100 g) in distilled water (1 dm³). For proteins to swell, the milk was allowed to stand for 12 h at a temperature of 4 ± 2°C. The obtained milk was pasteurized at a temperature of 80 ± 2°C and cooled to a temperature of 32 ± 2 °C. In particular, dry skim milk is also used at enterprises in the production of cheese products in the inter-season period, when the production of raw milk is abruptly reduced [9].

The Maxiren®, KG-50, and Fromase 2200® milk-coagulating preparations were used for the coagulation of milk.

To intensify the acid-rennet coagulation of milk and improve the mechanostructural (rheological) properties of blobs, ripened milk (20–40%) was added to the reconstituted skim milk [10]. The ripening of milk was performed as follows: fresh milk was pasteurized at a temperature of 63°C and, after a culture (0.1 %) and calcium chloride (10·10⁻³ kg/100 kg) were added, held at a temperature of 12°C for 6–12 h until a required titrable acidity of 22–25°T was attained [11]. In compliance with the cheese production technology, the milk mixture in a cheese vat must be stirred after the addition of coagulating preparations and allowed to stand in a quiescent state until the formation of a blob with a required strength (density). This is why it is necessary to provide minimal mechanical actions on the structure of a blob, especially at the stage of its flocculation, to obtain a rheogram, which reliably describes the process of its formation.

The rheogram of a strengthened blob in the coordinates “compressing force F –absolute linear strain Δl ” is shown in Fig. 1. It has the three specific regions:

- (1) Region AB is nearly linear and is typical for the materials obeying the Hooke’s law. In this region, the change in the compressing force F produces proportional elastic strains Δl ;
- (2) Region BC is characterized by the violation of proportionality between the compressing force and the absolute linear strains due to the appearance of some plastic strains, which slightly grow until the maximal compression force F_{max} is attained at point C ; and
- (3) Region CD corresponds to the brittle destruction of a blob with a resulting decrease of its resistance to load.

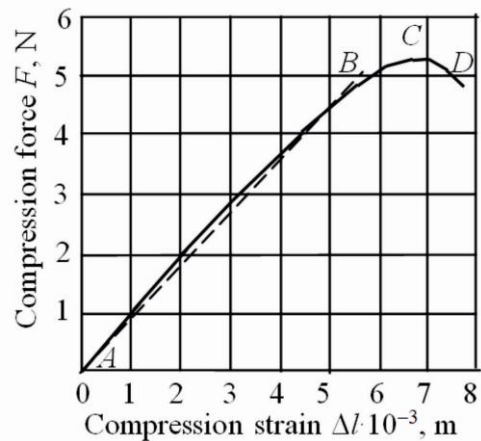


Fig. 1. Absolute compression strain of a strengthened acid-rennet blob versus compression force.

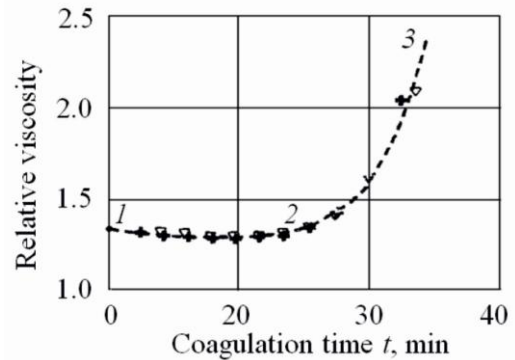


Fig. 2. Relative viscosity of a rennet blob versus time: (1, 2) primary coagulation stage, (2, 3) secondary coagulation stage, (∇) experiment, (+) calculation.

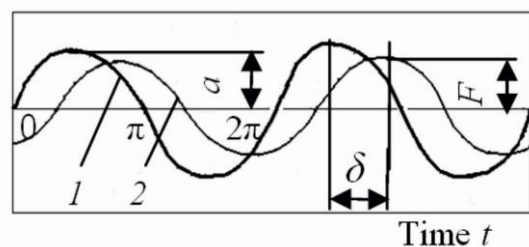


Fig. 3. Oscillations of a ball in a continuous medium.

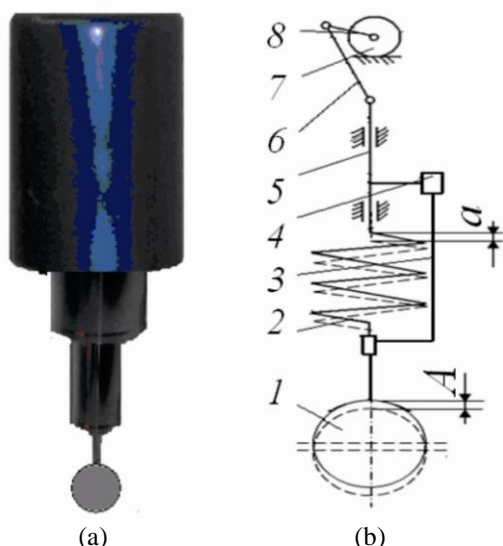


Fig. 4. VRSh-1 ball oscillatory rheometer: (a) general view, (b) principal circuit, (1) ball, (2) spring, (3) rod, (4) displacement indicator, (5) plunger, (6) shaft, (7) gear motor, (8) crank.

From the analysis of this rheogram it can be concluded that a strengthened acid-rennet blob may be classified as a viscoelastic body.

The coagulation of milk was studied by rheological methods on the new developed rheometers:

- (1) The VRSh-1 ball low-amplitude oscillatory rheometer [12] (Fig. 4); and
- (2) The Sgustok-S1 dual-range rotary rheometer at a constant revolution speed of the fluted measuring cylinder [13, 14] (Fig. 8).

Comparison studies were performed using a Rheotest-2 certified rotary viscometer (Germany). The active acidity of a milk-protein blob was measured on a pH-150M laboratory instrument, and its titrable acidity was estimated on an ATP-1 semi-automatic potentiometric analyzer (Russia).

According to the literature data, it is customary to divide the coagulation of milk into the two stages (Fig. 2): (1) the primary coagulation stage (region 1–2) is called the latent (inductive) coagulation stage and characterized by the gradual reduction of the stability of casein micellae under the action of milk-coagulating preparations. In the opinion of *de Kruif* et al. [15], a slight decrease in the viscosity of a milk mixture (~ 0.01 Pa s) is produced by the reduction of the size of micellae as a result of cutting the κ -casein hairs from their surface by the rennet enzyme. In the opinion of *Lomholt* et al. [16] and *Marchin* et al. [17], the growth of viscosity after slight decrease is due to the aggregation of micellae with a simultaneous increase in the effective hydrodynamic radius of particles, i.e., their volumetric content [16, 17]. Some other hypotheses are also proposed. For example, *El'chaninov* [18, 19] has concluded from the detailed analysis of the contemporary Russian and foreign literature that the moment of the attainment of an initial viscosity value should be considered as the beginning of *evident* coagulation, i.e., the gel point of the process.

The secondary coagulation stage (region 2–3) is characterized by the active formation of the spatial structure of a gel (flocculation stage), its strengthening, and the appearance of the viscoelastic properties of a blob. The precise determination of the beginning and terminal time moments of the evident formation of a gel during the coagulation of milk is a topical problem for the control of technological processes in the production of various dairy products, as it enables the automatic correction of the behavior of an technological process upon the fluctuation of the physicochemical parameters of milk, e.g., the content of protein in raw materials. A process engineer must “see” the changes occurring in the milk during its coagulation, i.e., “know” his milk and operatively manage it [20, 21].

RESULTS AND DISCUSSION

Theoretical substantiation of the new ball low-amplitude oscillatory rheometer. The scheme illustrating the principle of studying a medium in the case of the forced low-amplitude harmonic oscillations of a sensitive element (ball) is shown in Fig. 3. The phase shift δ between the oscillation amplitudes of the control displacement a (curve 1) and the force F (curve 2) resisting the displacement of the ball is determined by the rheological properties of a formed milk-protein blob.

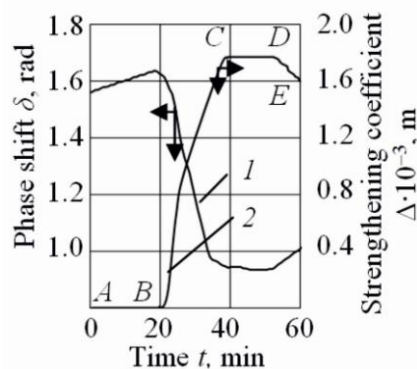


Fig. 5. Blob formation rheograms: (1) phase shift, (2) strengthening coefficient.

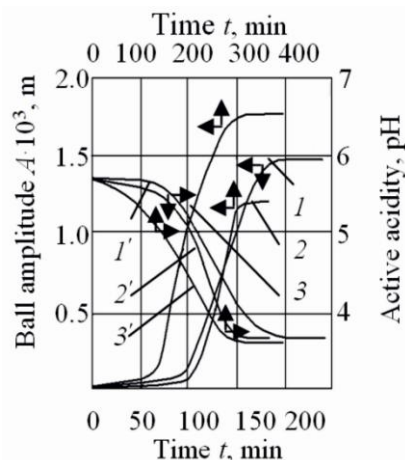


Fig. 6. Monitoring of blobs: rheograms of (1) yoghurt, (2) soured milk; (3) cottage cheese and active acidity of (1') yoghurt, (2') soured milk, and (3') cottage cheese.

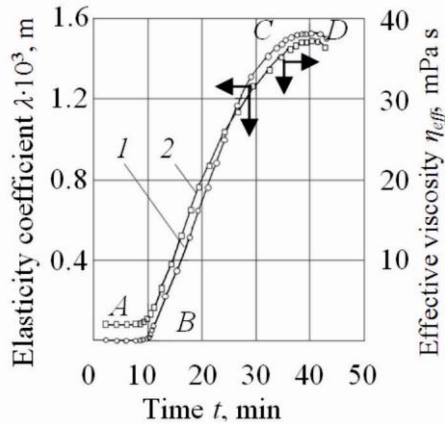


Fig. 7. Comparative rheograms for (1) VRSh-1 rheometer and (2) Rheotest-2 rotary viscometer.

When the ball harmonically displaces, the forces of elastic F_E and viscous F_V resistance to its motion appear in the formed viscoelastic milk–protein blob. The elastic blob strain force F_E acting on the ball during its harmonic motion is determined as

$$F_E = 2Cx(t) = 2C \cos(\omega t + \phi), \quad (1)$$

where C is the elasticity coefficient, N/m.

The amplitude force of viscous resistance FV to the motion of the ball at $\sin(\omega t + \phi) = 1$ is calculated by the Stokes formula

$$F_V = 3\pi\eta Dv = 3\pi dA \sin(\beta\omega t + \phi), \quad (2)$$

where η is the gel viscosity, Pa s; D is the ball diameter, m, and v is the ball speed, m/s

$$(v = dx/dt = A\omega \sin(\omega t + \phi)).$$

With consideration for Eqs. (1) and (2), the total values of the medium resistance force F have an intermediate oscillation phase, i.e.,

$$F(t) = F_E + F_V = 2CA \cos(\omega t + \phi) + 3\pi\eta DA \omega \sin \omega t + \phi, \quad (3)$$

From the analysis of Eq. (3) it follows that the elastic force F_E and the viscous resistance force F_V are directly proportional to the amplitude A of the displacements of the ball in a milk mixture in the case of its oscillations. In this case, there is no need to calculate the total resistance force when monitoring the strengthening of a blob. Obviously, it is sufficient to monitor the change of the ball displacement amplitude A . The validity of such an approach is also mentioned in [22]. Then the total medium resistance force $F(t)$ can be expressed as the difference between the oscillation amplitude $a = x_0(t)$ of drive unit 4 and the current displacement amplitude $A = x(t)$, i.e.,

$$F(t) = C_1 \Delta x(t) = [x_0 - x(t)], \quad (4)$$

where C_1 is the rigidity of the spring.

From the analysis of Eqs. (3) and (4) it follows that the force $F(t)$ is directly proportional to the ball displacement amplitude change equal to the increment $\Delta x(t)$, which will grow to its ultimate value during the

strengthening of a blob in proportion to its readiness. This increment was selected as a control parameter and called *strengthening coefficient*, m:

$$\Delta = a - A(t) = \Delta x(t), \quad (5)$$

Phase shift δ between a and A is determined on the basis of experiment. If $\varphi[F(t)]$ is the oscillation phase of a specified force, and $\varphi[x(t)]$ is the oscillation phase of ball displacements produced by this force, the phase shift is determined as

$$\delta = \varphi F(t) - \varphi x(t), \quad (6)$$

Theoretical analysis and experimental studies have provided the basis for developing the design of the new VRSh-1 ball oscillatory rheometer, the general view of which is shown in Fig. 4a (the bracket for its installation on a vat and the secondary block are conditionally omitted) [12]. Its principal circuit is illustrated in Fig. 4b. The principle used in the rheometer is that the revolution of the shaft of gear motor 7 at an angular speed ω is converted by means of crank 8 and shaft 6 into linear harmonic oscillations with an amplitude a of plunger 5 (control unit), to which spring 2 and hollow ball 1 displacing with an amplitude A are attached. The viscoelastic resistance of a blob to the displacements of ball 1 will grow with the strengthening and formation of its three-dimensional structure, thus producing a corresponding decrease in the amplitude $A = x(t)$ of spring 2 elastic strains, which are transmitted by light hollow rod 3 to displacement indicator 4 made in the form of a pulse counter and registered by the secondary block.

In comparison with analogues, the VRSh-1 rheometer provides the measurement of the amplitude a of plunger 5 via the adjustment the length of crank 8 and the use of one cylindrical measuring spring 2 and pulse counter 4 as an indicator of ball 1 displacements. This has simplified the design of the rheometer as a whole, reduced the inertia and rigidity of the force indicator and, as a result, increased the accuracy of measurements.

Selection and substantiation of the geometrical and rheometric parameters of the rheometer. On the basis of experimental studies, the following working parameters were selected: ball diameter $D = 60 \cdot 10^{-3}$ m, spring wire diameter $d_R = 2 \cdot 10^{-3}$ m in the production of acid–rennet blobs and $d_C = 1 \cdot 10^{-3}$ m in the production of cultured milk blobs, control unit's amplitude $a = 2 \cdot 10^{-3}$ m, drive unit's oscillation frequency $\nu = 0.0333$ Hz. The Archimedean buoyant force acting onto the ball is compensated by an increase in its weight.

Acid-rennet coagulation of milk. The blob formation monitoring rheograms obtained by measuring the phase shift δ and the strengthening coefficient Δ are plotted in Fig. 5. From their comparison it has been established that rheogram 2 more precisely describes the process of estimating the duration of stages and gives more reliable information on the formation and strengthening of blobs. The strengthening coefficient Δ (m) was finally taken as a control parameter.

Coagulation of cultured milk blobs. The formation of cultured milk beverage blobs was studied by the example of the production of 2.5-% soured milk, 2.5-% yoghurt, and 5-% cottage cheese with the use of standard cultures

in compliance with technical regulations. The results at a spring diameter $d = 1.0 \cdot 10^{-3}$ m are plotted in Fig. 6. It has been established that rheograms 1–3 obtained on the VRSh-1 rheometer differ from pH curves 1' – 3' in the duration of process stages by less than 2–3%.

Estimating the reliability of blob formation monitoring results. The rheograms obtained for an acid–rennet blob at a temperature of $30 \pm 1^\circ\text{C}$ on the VRSh-1 experimental rheometer (curve 1) and the Rheotest-2 certified laboratory viscometer (curve 2) are plotted in Fig. 7. From the analysis of the rheograms it follows that the relative deviation of the duration of stages is 2.36–2.74%, and the total process times differ by 2.16%. It may be concluded that the VRSh-1 rheometer can be applied for the industrial monitoring of the formation of acid–rennet and cultured milk blobs.

Method of rotary rheometry. At the following stage, the formation of acid–rennet blobs was studied by the method of the rotation of a cylinder in a working vat at a minimum angular velocity ω . The general view and principal circuit of the new Sgustok-1S dual-range rotary rheometer are shown in Fig. 8. [13, 14].

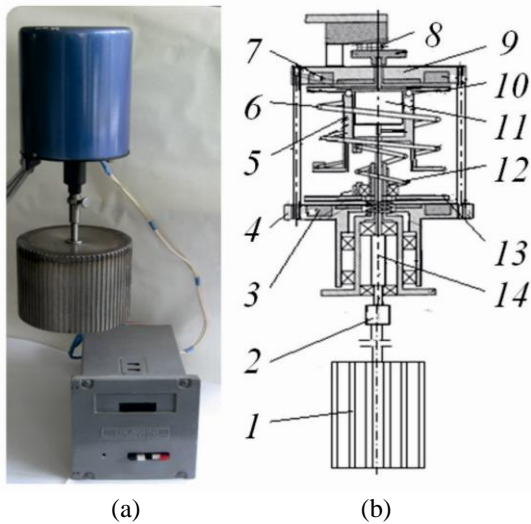


Fig. 8. Sgustok-1S rotary rheometer: (a) general view, (b) principal circuit, (1) cylinder, (2) lock, (3, 7) electromagnets, (4) cogwheel, (5) sleeve, (6) soft spring, (8) current-conducting brushes, (9) disk, (10, 13) ferromagnetic rings, (11) resistive transducer, (12) hard spring, (14) shaft.

The rheometer is equipped with two torque indicators, namely, “soft” spring 6 and “hard” spring 12. To turn spring 6 (or 12) on, voltage is applied to electromagnet 7 (or 3), which will fix ferromagnetic ring 10 (or 13) attached to spring 6 (or 12). The other ends of the springs are fastened to sleeve 5 installed on shaft 14 attached to measuring cylinder 1.

To perform the monitoring of the formation of a blob, cylinder 1 is submerged into a milk mixture and, for example, spring 6 is turned on, thereupon voltage is applied to the driver, which begins to rotate cogwheel 4. As a blob is formed, the torque moment M_T appears on the cylinder. It twists spring 6 via shaft 14 and sleeve 5 at a proportional angle, which is registered by resistive

transducer 11 and transferred to the processing block. “Hard” spring 12 is used in the production of cheeses, and “soft” spring 6 is used in the production of cultured dairy products. A novelty in the rheometer’s design is the possibility of the simultaneous or separate turn-on of springs 6 and 12. When the springs are turned off, cylinder 1 is stopped instead of being turned back to the initial position, while the driver is running. This makes it possible to preserve the already formed structure and continue the monitoring of the process after the springs are switched.

The studies on the substantiation of a control parameter and the geometric and kinematic characteristics of measuring cylinders schematized in Figs. 9 and 10 with the dimensions listed in the table were performed at the first stage.

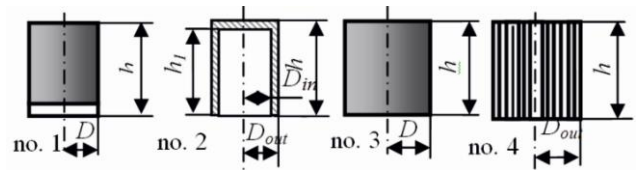


Fig. 9. Schemes of measuring cylinders.

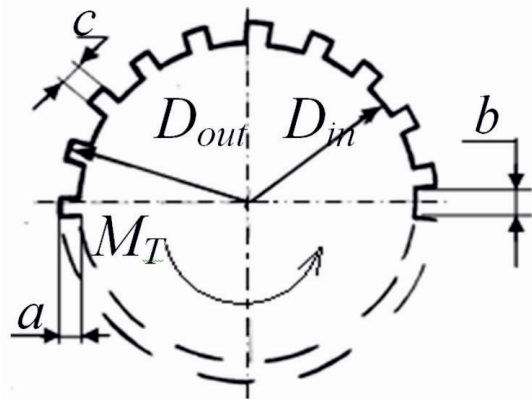


Fig. 10. Calculation scheme of the fluted cylinder no. 4.

Table 1. Geometric parameters of the cylinders

Geometric parameters of measuring cylinders	Notation	Numbers of measuring cylinders			
		1	2	3	4
Outer diameter, m	$D_{out} \cdot 10^3, \text{ m}$	39.2	39.2	80.0	80
Inner diameter, m	$D_{in} \cdot 10^3, \text{ m}$	–	15.0	–	–
Cylinder height, m	$h \cdot 10^3, \text{ m}$	72.0	78.0	80	80
Groove depth, m	$a \cdot 10^3, \text{ m}$	–	–	–	2.0
Groove width, m	$b \cdot 10^3, \text{ m}$	–	–	–	3.0
Rib width, m	$c \cdot 10^3, \text{ m}$	–	–	–	0.8
Number of grooves	n	–	–	–	66

Selection of a control parameter. Only ultimate shear stress θ_0 can be taken as a control parameter in the

monitoring of the formation of a blob by the method of submerging a rotating cylinder into a vat.

The values of θ_0 on the surface of measuring cylinders will induce torque moments M_T . For known torque moments and cylinder dimensions, the following formulas for the calculation of ultimate shear stresses were obtained:

no. 1:

$$\theta_0 = \frac{2M_T}{\pi D^2 (h + 0.167D)}, \quad (7)$$

no. 2:

$$\theta_0 = \frac{2M_T}{\pi [D_{out}^2 h + 0.167D_{out} + D_{in}^2 h_1 + 0.167D_{in}]}, \quad (8)$$

no. 3:

$$\theta_0 = \frac{2M_T}{\pi D^2 (h + 0.333D)}, \quad (9)$$

no. 4:

$$\theta_0 = \frac{2M_T}{\pi D_{out} - cn \quad hD_{out} + 0.667\pi D_{out}^3}, \quad (10)$$

Selection of the geometric parameters of cylinders.

The studies of the effect of the angular speed ω of measuring cylinders on the parameter θ_0 of ready blobs within a range of 0.058–0.750 s⁻¹ on the Sgustok-1S rheometer have resulted in the rheograms shown in Fig. 11. On the basis of these rheograms, measuring cylinder no. 4 and the angular speed $\omega = 0.262$ s⁻¹, at which the parameter θ_0 took maximum values, were selected as working conditions.

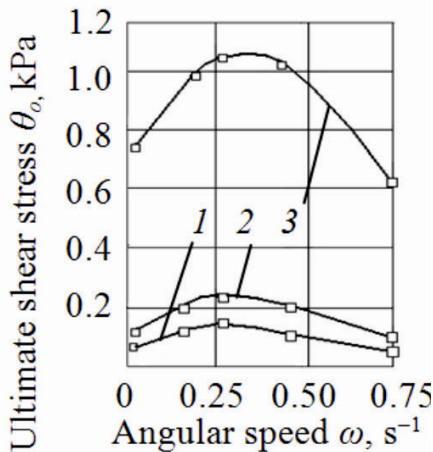


Fig. 11. Ultimate shear stress θ_0 versus angular speed of cylinders: (1, 2) no. 1, (2) no. 3, (3) no. 4.

The results of studying the formation of acid–rennet and cultured milk blobs are given below. At first, the effect of the shape and geometrical dimensions of measuring cylinders on the character of acid–rennet blob formation rheograms and the parameter θ_0 was studied, and the results were plotted in Fig. 12. In these studies, a “soft” spring with a wire diameter $d_S = 0.9 \cdot 10^{-3}$ m and a “hard” spring with $d_H = 1.5 \cdot 10^{-3}$ m were used at a spring rigidity ratio of $\approx 1 : 9.72$. The average diameters of the springs $d_{S,av} = 38 \cdot 10^{-3}$ m and $d_{H,av} = 48 \cdot 10^{-3}$ m were taken at the same number of turns

n = 10.

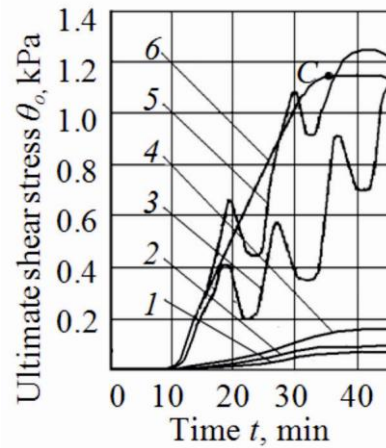


Fig. 12. Dependence of the ultimate shear stress θ_0 on the shape of cylinders and the rigidity of springs: (1, 2) cylinders nos. 1 and 2 (soft force indicator), (3) cylinder no. 3 (soft force indicator), (4) cylinder no. 3 (hard force indicator), (5) cylinder no. 4 (soft force indicator), (6) cylinder no. 4 (hard force indicator).

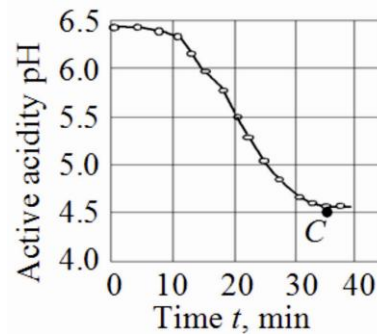


Fig. 13. Souring pH curve (cylinder no. 4).

As a result of studying the formation of acid–rennet blobs, it has been established that the values of θ_0 obtained for cylinders no. 1 or 2 and the spring d_S are small and do not provide the plotting of reliable rheograms (curves 1 and 2). The rheogram for cylinder no. 3 and the spring d_S (curve 3) has a saw-tooth shape explained by an insufficient rigidity of the force indicator’s spring [23]; the values of θ_0 for the same cylinder and the spring d_H were small due to the slipping of the cylinder (curve 4). The rheogram for fluted cylinder no. 4 with the spring d_S has a saw-toothed shape (curve 5) similarly to rheogram 3. The rheogram, which objectively reflects the blob formation process, was obtained for fluted cylinder no. 4 and the spring d_H (curve 6).

To estimate the reliability of rheogram 6, the parallel measurements of the active acidity pH plotted in Fig. 12 were performed. From the analysis of the curves shown in Figs. 11 and 12 it follows that cylinder no. 4, the characteristics of which are given in the table, is reasonable to use for the monitoring of the formation of acid–rennet blob.

The study of the effect of a mixture recipe and principal technological process parameters on the control parameter—ultimate shear stress θ_0 of an acid–

rennet blob—with the purpose of revealing the factors for the correction and control of the process of their formation is of scientific and practical interest. The studies were performed on a Rheotest-2 certified rotary viscometer. The varied factors were the pasteurization temperature X_1 (70–90°C), the coagulation temperature X_2 (20–40°C), the mass content of rennet enzyme X_3 ((0.8–1.8)·10⁻³ kg/100 kg), the culture content X_4 (1.5–4.5%), the mass content of calcium chloride X_5 ((25–55)·10⁻³ kg /100 kg); the mechanical action intensity (angular cylinder rotation speed) X_6 (0.058–0.750 s⁻¹), the fat content in milk X_7 (1–4%), and the ripe milk amount X_8 (20–40%).

To solve the formulated problem, the full factorial experiment (full-FFE) represented by two plans FFE 2⁴ was performed. For the first plan, the parameters X_1 , X_2 , X_3 , and X_4 were varied, and the other factors were fixed at the center of their variation range. Similarly, X_5 , X_6 , X_7 , and X_8 were varied for the second plan. After the computer-aided processing of the obtained dependences, their verification for adequacy, and the elimination of insignificant factors, the resulting regression equations have the following form:

$$\theta_0 = 1.221 + 0.127X_1 + 0.136X_2 + 0.116X_3 - 0.0751X_4 + 0.0132X_3X_4 + 0.0113X_2X_3X_4 + 0.0151X_1X_2X_3X_4, \quad (11)$$

$$\theta_0 = 1.219 + 0.258X_5 - 0.0541X_6 - 0.162X_7 - 0.101X_8 + 0.0182X_5X_7 + 0.0226X_6X_8 - 0.0214X_5X_7X_8 + 0.0125X_5X_6X_7X_8. \quad (12)$$

The analysis of regression model (11) shows that θ_0 is 1.58 and 1.65 kPa at a pasteurization temperature $X_1 = 90^\circ\text{C}$, a coagulation temperature $X_2 = 40^\circ\text{C}$, a mass content of introduced enzyme $X_3 = 1.8 \cdot 10^{-3}$ kg/100 kg, and a culture content X_4 of 1.5 and 4.5%, respectively. The growth of the pasteurization temperature X_1 from 70 to 90°C increases θ_0 by 1.17–1.23 times, and the growth of the coagulation temperature X_2 from 20 to 40°C increases θ_0 by 1.18–1.28 times.

The isolines of the dependences of θ_0 on the pasteurization temperature X_1 and the coagulation temperature X_2 at constant contents of enzyme X_3 and culture X_4 are plotted in Fig. 14a. These dependences enable the selection of a combination of process parameters for the production of a blob of optimal strength.

From the analysis of regression model (12) it follows that the growth of the mass content of calcium chloride X_5 from 25·10⁻³ to 55·10⁻³ kg/100 kg increases θ_0 by 1.25–1.36 times. Conversely, the growth of the fat content X_7 from 1 to 4% and the ripe milk amount X_8 from 20 to 40% decreases θ_0 by 1.18–1.28 and 1.13–1.15 times, respectively. The maximum values of $\theta_0 = 1.63$ kPa were obtained at a mass fraction of calcium chloride X_5 of 55·10⁻³ kg/100 kg and a mechanical action intensity X_6 of 0.33 s⁻¹.

The isolines reflecting the change in θ_0 at varied calcium chloride content X_5 and coagulation temperature X_2 (and fixed introduced enzyme content X_3

and mechanical action intensity X_6) are plotted in Fig. 14b. It has been established that the mass content of calcium chloride X_5 produces a much more considerable effect on the blob strength θ_0 than any other factor. The second factor producing the strongest effect on strengthening ability is the mass content of fat in milk X_7 , but the content of fat in a product is determined by the recipe of a produced cheese. The coagulation temperature X_2 is the third factor by the intensity of its effect on the blob strength θ_0 . From the analysis of the performed experiment it can be concluded that the formation of acid-rennet blobs is reasonable to be controlled by varying the mass content of calcium chloride and the coagulation temperature.

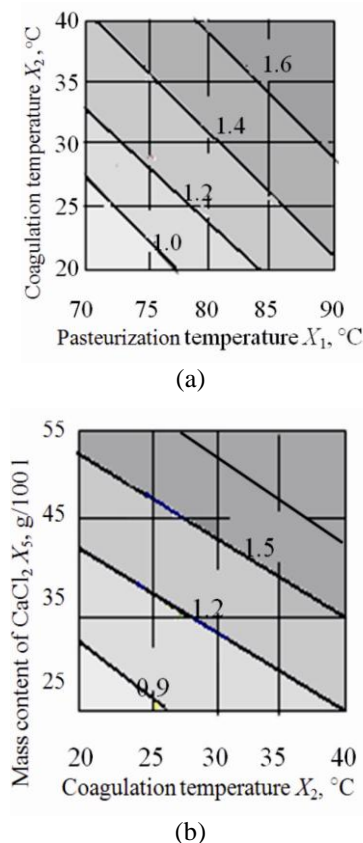


Fig. 14. Isolines of the effect of the principal control factors on the ultimate shear stress at fixed (a) $X_3 = 1.8 \cdot 10^{-3}$ kg/100 kg, $X_4 = 1.5\%$ and (b) $X_3 = 1.8 \cdot 10^{-3}$ kg/100 kg, $X_6 = 0.262$ s⁻¹.

Computer-aided approximation of the milk coagulation process. To perform the control of the technological process of the production of a milk-protein blob, it is important for a process engineer to obtain the information about its behavior to have a real opportunity of its correction with the purpose of the production of a high-quality finished product. The results of developing a procedure for the identification of *rheological images of milk-protein blobs* on the basis of pronounced process *stadiality* are considered below. As has already been proven above for the monitoring of the formation of blobs on the ball and rotary rheometers, any characteristics of the product in direct relationship with its rheological (mechanostructural) properties, namely, the strengthening coefficient Δ (m), the

ultimate shear stress θ_0 (Pa), the effective viscosity η_{eff} (mPa s), etc., may be used as a control rheological parameter.

A typical milk protein coagulation rheogram looks as shown in Fig. 15. Dashed-line rheogram segments *AB* and *DE* are straightened, as this simplification does not almost influence on the identification of the basic milk protein coagulation stages.

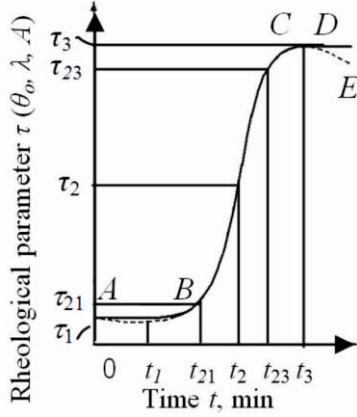


Fig. 15. Milk protein coagulation rheogram.

Recognition method. Rheological data are automatically registered with a time discreteness $\Delta t \ll t_3$. The discretization step Δt was taken ≈ 10 s for acid-rennet milk coagulation and 60 s for traditional acid milk coagulation. The data collection device forms three two-dimensional arrays of values (t_k, τ_k) , (t_k, τ'_k) , and (t_k, τ''_k) , where $\tau'_k = \tau_{k+1} - \tau_k$ and $\tau''_k = \tau'_{k+1} - \tau'_k$.

The analysis of these arrays allows the unique identification of all the principal process stages:

(1) At induction stage *AB*, the point (t_1, τ_1) corresponds to the maximum dispersion of casein micellae, i.e., the minimum value $\tau_1 = \tau_{min}$. This point can be analytically characterized by the zero values of the first and second time derivatives of the function $\tau = f(t)$:

$$\tau(t) = \tau_1 \approx \tau_{min}, \quad \left. \frac{d\tau}{dt} \right|_{t=t_1} = 0, \quad \left. \frac{d^2\tau}{dt^2} \right|_{t=t_1} \approx 0, \quad (13)$$

(2) At flocculation stage *BC*, the program traces the behavior of the function, determining its extrema. The positive maximum corresponds to the time t_{21} (point *B* (t_{21}, τ_{21})) and characterizes the development of the evident coagulation stage. Its essential feature is the growth of τ at a maximum rate:

$$\left. \frac{d\tau}{dt} \right|_{t=t_{21}} > 0, \quad \left. \frac{d^2\tau}{dt^2} \right|_{t=t_{21}} = \left(\frac{d^2\tau}{dt^2} \right)_{max} > 0. \quad (14)$$

The maximum rate of the growth of the control parameter τ is attained at the point (t_2, τ_2) , when its second time derivative becomes equal to zero, i.e.,

$$\left. \frac{d^2\tau}{dt^2} \right|_{t=t_2} = 0; \quad \frac{d\tau}{dt} = \tau'_{max}. \quad (15)$$

The termination of the evident coagulation stage of a blob is determined from the negative minimum of the function $\tau = \tau(t)$ at the time moment t_{23} (point *C* (t_{23}, τ_{23})), where the deceleration rate of the growth of τ is maximal:

$$\left. \frac{d\tau}{dt} \right|_{t=t_{23}} > 0, \quad \left. \frac{d^2\tau}{dt^2} \right|_{t=t_{23}} = \left(\frac{d^2\tau}{dt^2} \right)_{min} < 0, \quad (16)$$

(3) At metastable equilibrium stage *CD*, the control rheological parameter τ_3 attains its maximum at the point (t_3, τ_3) , i.e.,

$$\tau(t_3) = \tau_3 \approx \tau_{max} \quad \text{at} \quad \left. \frac{d\tau}{dt} \right|_{t=t_3} \approx 0, \quad \left. \frac{d^2\tau}{dt^2} \right|_{t=t_3} \approx 0, \quad (17)$$

The process termination is determined by the attainment of a preliminary specified small positive value by the first derivative τ'_k after the point t_{23} . In this work, it has been established that the strengthening of a blob is almost stopped, if $\Delta\tau \leq \tau'(t_{23})/10$.

After the time moment t_{23} is determined, the information system gives a message about the coming termination of the process. For rennet blobs, the beginning of their syneretic stratification on segment *CD* is diagnosed by a preliminary specified negative value of the second derivative τ'' , i.e., its decrease. The blob is ready for further processing, if the difference between τ_3 and its reference value τ_{ref} for a given technological process is less than $\Delta\tau$ specified by quality standards.

Analytical identification of the rheological image of a blob. The rheogram shown in Fig. 14 is plotted on the basis of the analytical approximation of the Heaviside “step” function

$$H(x) = \lim_{a \rightarrow \infty} \frac{1}{1 + e^{-ax}},$$

where

$$H(x) = \begin{cases} 0, & x < 0 \\ 1, & x > 0 \end{cases}.$$

It was used as a basis to obtain the approximating dependence for milk-protein blobs

$$\tau(t) = \tau_1 + \frac{\tau_3 - \tau_1}{1 + e^{-a(t-t_2)}}, \quad (18)$$

where a is the parameter characterizing the blob strengthening rate, min^{-1} .

Equation (19) is convenient for the prediction of changes in the rheological parameter τ with time for a number of reasons: first, the characteristic time point t_2 and the values of τ_1 and τ_3 are its explicit parameters and, second, the maxima of the first and second derivatives of this function can be determined analytically. For example, the maximum of the first derivative is really found at the time point t_2 and equal to

$$\left. \frac{d\tau}{dt} \right|_{t=t_2} = \frac{a\tau_3}{4}, \quad (19)$$

To determine the extrema of the second derivative of Eq. (19), the third derivative is found as

$$\frac{d^3\tau}{dt_3} = a^3\tau_3 \left[\frac{e^{-a t-t_2}}{1+e^{-a t-t_2}} - \frac{6e^{-2a t-t_2}}{1+e^{-a t-t_2}} + \frac{6e^{-2a t-t_2}}{1+e^{-3a t-t_2}} \right] = 0, \quad (20)$$

With the notation

$$y = e^{-a t-t_2}, \quad (21)$$

Eq. (20) can be written as

$$1 - \frac{6y}{1+y} + \frac{6y^2}{1+y^2} = 0, \quad (22)$$

The roots of Eq. (22) are $y = 2 \pm \sqrt{3}$. The simultaneous solution of Eqs. (21) and (22) gives

$$t = t_2 + \ln 2 \pm \sqrt{3}/a.$$

Taking into account that $\ln 2 - \sqrt{3} = -1.317$, and $\ln 2 + \sqrt{3} = 1.317$, the times t_{21} и t_{23} are finally obtained to have the following values

$$t_{23} = t_2 + 1.317/a, \quad t_{21} = t_2 - 1.317/a, \quad (23)$$

Hence, Eqs. (19) and (23) allow both the process duration t_3 and the probable value of the rheological parameter τ_3 at the blob readiness moment to be predicted as early as by the time moment t_2 using an available experimental database (for the rheological function itself and its first and second derivatives).

The results of the approximation of the effective viscosity η_{eff} for the ripening of 25-% sour cream by model Heaviside function (18) are shown in Fig. 16. The model function (solid line) has the following parameters: $a = 0.028 \text{ min}^{-1}$, $\tau_1 = \eta_{eff1} = 1.45 \text{ mPa s}$, $t_2 = 352 \text{ min}$, $\tau_3 = \eta_{eff3} = 9.15 \text{ mPa s}$. From the analysis of the computer-aided approximation in the working window in Fig. 17 it can be concluded that the described method rather adequately approximates the acid coagulation of milk.

In conclusion, it should be noted that the principles of the rheological monitoring of structure formation processes in continuous media can successfully be applied in the automatic control and management systems in the production of cheeses and cultured dairy products. The complex studies of the rheological properties of different milk-protein blobs, the development and study of new rheometers and methods of their application, and the organization of the computer-aided processing and identification of the

rheological images of formed blobs will allow the quality of finished milk products to be improved.

On the basis of studying the kinetics of the formation of an acid-riennet blob, the mathematical models estimating the effect of the composition of a milk mixture and process factors on the finite strength of rennet blobs, i.e., the ultimate shear stress θ_0 , were obtained.

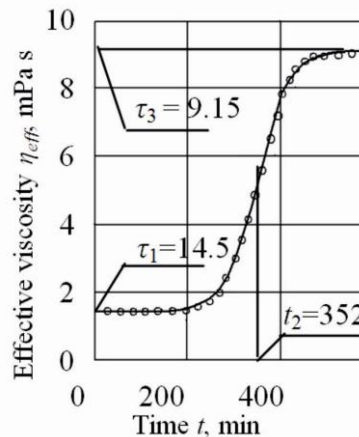


Fig. 16. Approximation of the sour cream ripening rheogram: (○) experiment, (—) model.

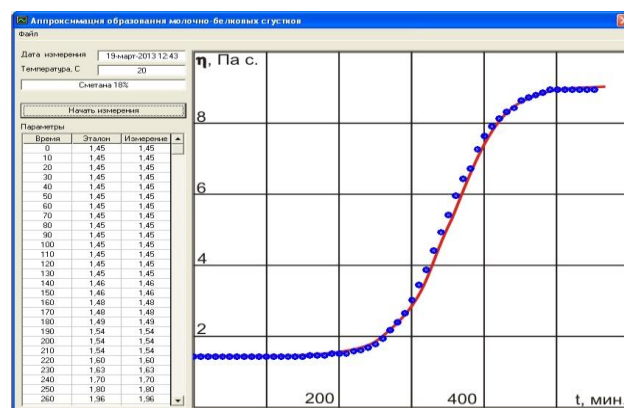


Fig. 17. Main window of the program for the identification of the rheological image of a 25-% sour cream blob.

The factors enabling the control of the terminal blob formation stage and the production of milk-protein blobs of specified consistency—*calcium chloride content* and *coagulation temperature*—were determined.

The method and algorithm allowing the monitoring of blob formation kinetics, the application of required corrective actions at a blob formation time moment t_2 , and the prediction of a blob readiness time moment on the basis of the computer-aided approximation of the Heaviside step function were developed for the identification of the rheological images of milk-protein blobs.

REFERENCES

1. Krus', G.N., Khramtsov, A.G., Volokitina, Z.V., and Karpuchev, S.V., *Tekhnologiya moloka i molochnykh produktov* (Technology of Milk and Dairy Products), Shalygina, A.M., Ed., Moscow: Kolos, 2007.
2. Ostroumov, L.A. and Umanskii, A.M., *Issledovanie vliyaniya tekhnologicheskikh faktorov na formirovanie syra* (Studying the effect of technological factors on the formation of cheese), *Khraneniye i pererabotka sel'khozsyrya* (Storage and Processing of Agricultural Raw Materials), 2001, no. 10, pp. 49–51.

3. Sokolova, Z.S., Lakomova, L.I., and Tinyakov, V.G., *Tekhnologiya syra i produktov pererabotki syvorotki* (Technology of Cheese and Whey Processing Products), Moscow: Agropromizdat, 1992.
4. Inikhov, G.S. and Brio, N.P., *Metody analiza moloka i molochnykh produktov* (Methods for the Analysis of Milk and Dairy Products), Moscow: Pishchevaya promyshlennost', 1971.
5. Maiorov, A.A., Mironenko, I.M., and Zharkov, R.V., Metod issledovaniya sposobnosti moloka k svertyvaniyu (Method of studying the coagulation ability of milk), *Syrodellie i maslodellie* (Cheese and Butter Making), 2010, no. 1, pp. 16–18.
6. Arkhipov, A.N. and Maiorov, A.A., Strukturnoobrazovanie molochnykh produktov (Structure formation of dairy products), *Molochnaya promyshlennost'* (Dairy Industry), 2012, no. 2, p. 74.
7. Bredikhin, S.A., Kosmodem'yanskii, S.A., and Yurin, V.N., *Tekhnologiya i tehnika pererabotki moloka* (Milk Processing Technology and Equipment), Moscow: Kolos, 2001.
8. Panov, V.P. and Lebedev, A.S., Vzaimosvyaz' titruemoi i aktivnoi kislotnosti moloka syr'ya (prakticheskoe primemenie) (Relationship between the titrated and active acidities of raw milk (practical application)), *Molochnaya promyshlennost'* (Dairy Industry), 2011, no. 10, pp. 50 – 51.
9. Maiorov, A.A. and Umanskii, M.S., Molokosvertyvyayushchie fermenty. Kriterii—kachestvo i vykhod (Milk-coagulating enzymes. Criterion: quality and yield), *Syrodellie i maslodellie* (Cheese and Butter Making), 2004, no. 4, pp. 33–37.
10. Lepilkina, O.V., Kushakov, N.M., and Shutov, V.E., Geleobrazovanie v syrnykh produktakh na osnove sukhogo moloka i rastitel'nykh zhirov (Gel formation in cheese products based on dry milk and plant oils), *Syrodellie i maslodellie* (Cheese and Butter Making), 2008, no. 1, pp. 38–41.
11. Bobylin, V.V., Fiziko-khimicheskie i biotekhnologicheskie osnovy proizvodstva myagkikh kislotno-sychuzhnykh syrov (Physicochemical and Bioengineering Principles of the Production of Soft-Ripened Acid-Rennet Cheeses), Kemerovo: KemTIPP, 1998.
12. RF Patent 2 371 702, *Byull. Izobret.*, 2009, no. 30.
13. RF Patent 2 196 318, *Byull. Izobret.*, 2003, no. 16.
14. RF Patent 2 354 956, *Byull. Izobret.*, 2009, no. 13.
15. De Kruijff, C.G. and Holt, C., Casein micelle structure, function, and interactions, in *Advanced Dairy Chemistry*, New York, Kluwer Academic/Plenum Publishers, 2002, vol. 1, pp. 233–276.
16. Lomholt, S.B. and Qvist, K.B., Relationship between rheological properties and degree of κ -casein proteolysis during renneting of milk, *Journal of Dairy Research*, 1997, vol. 64, no. 4, pp. 541–549.
17. Marchin S., Putaux, J.L., Pignon, F., and Léonil, J., Effects of the environmental factors on the casein micelle structure studied by cryo transmission electron microscopy and small-angle X-ray scattering/ultrasmall-angle X-ray scattering, *Journal of Chemical Physics*, 2007, vol. 126, no. 4, p. 045101.
18. El'chaninov, V.V., Sovremennye predstavleniya o strukture kazeinovo mitselly (Contemporary concepts of the structure of a casein micelle), *Molochnaya promyshlennost'* (Dairy Industry), 2011, no. 3, pp. 77–78.
19. El'chaninov, V.V., Sovremennye predstavleniya o strukture kazeinovo mitselly (prodolzhenie) (Contemporary concepts of the structure of a casein micelle (continuation)), *Molochnaya promyshlennost'* (Dairy Industry), 2011, no. 4, pp. 76–78.
20. Silaeva, V.M., Vyrabotka i postanovka syrno zerna—kharakternye oshibki (Production and formation of a cheese grain: typical missteps), *Syrodellie i maslodellie* (Cheese and Butter Manufacturing), 2012, no. 5, pp. 22–24.
21. Zobkova, Z.S., Stranichka tekhnologa (Process engineer's page), *Molochnaya promyshlennost'* (Dairy Industry), 2012, no. 2, p. 15.
22. Aret, V.A., Nikolaev, B.L., Zabrovskii, G.B., and Nikolaev, L.K., *Reologicheskie osnovy rascheta oborudovaniya proizvodstva zhirosoderzhashchikh pishchevykh produktov* (Rheological Principles of the Calculation of Equipment for the Production of Fat-Containing Food Products), St. Petersburg: StPGUNPT, 2006.
23. Belkin, I.M., Vinogradov, G.V., and Leonov, A.I. *Rotatsionnye pribory. Izmerenie vyazkosti i fiziko-mekhanicheskikh kharakteristik materialov* (Rotary Instruments. Measurement of the Viscosity and Physicomechanical Characteristics of Materials), Vinogradov, G.V., Ed., Moscow: Mashinostroenie, 1967.



EFFECT OF MULTICOMPONENT CEREAL MIXTURES ON GLUCOSE LEVEL IN BLOOD OF EXPERIMENTAL ANIMALS

P. E. Vloshchinskiy^{a,*}, I. P. Berezovikova^a, A. R. Kolpakov^b, and N.G. Klebleeva^a

^aSiberian University of Consumer Cooperation,
prosp. Karla Marksa 26, Novosibirsk, 630087 Russia,
phone/fax: +7(383)346-16-20, *e-mail: vlopik@rambler.ru,

^bNovosibirsk State Medical University,
Krasniy prosp. 52, Novosibirsk, 630091 Russia,
e-mail: kaffarm@ya.ru

(Received March 7, 2014; Accepted in revised form March 17, 2014)

Abstract: Recipes of multicomponent mixtures of cereals with proteins of high biological value were developed. In experiments, 35 adult male Wistar rats were used. Prior to the experiment, all animals were fed with powdered milk, grain or grain waste, germinated oats, and comprehensive multivitamin preparations, in addition to the standard balanced diet. Against this background, blood was collected from the animals for biochemical studies (control group, n = 20). Blood collection from tail vein was performed under general anesthesia, according to the recommendations of the Federation of European Laboratory Animal Science Working Group. Animals were fed with viscous-texture porridge made from ternary mixtures (rice, peas, and buckwheat; rice, barley, and maize) and the five-component cereals (rice, barley, maize, buckwheat, and peas) for 30 days. The control group received a standard vivarium diet. Postprandial glycemic curves in all groups were compared with the response to administration of glucose in the amount corresponding to the diet carbohydrates content. Postprandial glycemia was significantly lower in all groups of animals receiving the experimental diets than in the group of animals who received aqueous solution of glucose directly in the stomach by gavage at the rate of 0.03 g/g total weight (glucose tolerance test, GTT). Baudouin hyperglycemic factor was 1.52 for the control group, and in the range of 1.07–1.10, for the experimental groups. The glycemic index was 76.2 and 53.6–55.9, respectively. The results evidence that the products prepared from multicomponent mixtures of cereals belong to the products with low glycemic index.

Keywords: multicomponent mixtures of cereals, postprandial glycemia, glycemic index

UDC 637

DOI 10.12737/4140

INTRODUCTION

Excess influx of carbohydrates with food, especially against the background of obesity, impaired glucose tolerance, or metabolic syndrome, leads to progression of the phenomena [1]. However, not only the amount of carbohydrates, but also their qualitative composition influences the rate of absorption and, finally, glucose level in blood [2]. Simple food carbohydrates are known to be rapidly absorbed from the gastrointestinal tract increasing glucose concentration in blood [3]. After sharp increase in secretion and synthesis of insulin, glucose is eliminated by liver and muscle tissue and transformed to glycogen; then, glucose concentration in blood decreases and hunger develops [4]. Complex polysaccharides, resistant starch, and food fibers slow down glucose absorption; their absence or partial lack from the diet leads to small volume of food and consequently need for new meal, i. e. overnutrition [6, 7]. The term glycemic index was introduced as a function of the rate of carbohydrate absorption; this provided for the possibility for patients diagnosed with diabetes mellitus or other metabolic disorders, as well as healthy population, to correct diet, choosing products that do not induce high glycemia levels.

Under normal conditions, glucose is the major energy substrate for most tissues in the human and animal organisms. Its concentration in blood is an integral index, which is determined by the rate of glycogen formation from non-carbohydrate precursors, influx of carbohydrates with food, absorption in intestines, utilization by tissues, and excretion. Carbohydrate homeostasis may be referred to one of the perfect and most complexly regulated ones, controlled by both nervous and humoral effects. As a rule, concentration of glucose in blood of laboratory rats varies from 4.5 to 6.4 mmol/L and remains within this range even upon prolonged starvation. An important role in the maintenance of the constant glucose level in blood belongs to metabolic pathways through which glycogen, mainly deposited in liver and muscles, is synthesized and broken down. Hydrolysis of glucose-6-phosphate, generated in liver from glycogen, is well known to serve a constant source of glucose. Metabolic pathways of its utilization in organism are described in details in a number of works [8, 9]. Glucose oxidation in a cascade of anaerobic glycolysis reactions is practically the only source of energy for such tissues as nervous tissue, renal medulla, seminal glands, and erythrocytes

[8, 9], while other tissues possess the ability to use both glucose and fatty acids, ketone bodies, and other products of oxidative metabolism as energy substrates.

Cereal porridges may be considered as a complex of polysaccharides (or “slow carbohydrates”), proteins, monosaccharides, food fibers, and relatively small amount of fat. In the process of hydrolysis in the gastrointestinal tract they are cleaved to accessible forms of metabolic substrates that are transported to tissues and organs by blood. The faster the product is cleaved to simple carbohydrates, the higher is its glycemic index. Glucose with a glycemic index of 100 is considered an etalon. Due to the abundance of diabetes type I and II and a number of other metabolic disorders, functional products decreasing the burden of pancreas are required. Usually dietary actions include complete or partial disallowance of food with high glycemic index. We assume that use of cereal mixtures components of which are rich with amylose (legumes) or viscous food fibers (peeled and pearl barley, oatmeal—sources of β -glucans) may considerably widen the assortment of dishes and thus improve the quality of life of diabetes and metabolic syndrome patients.

The aim of the work was to develop multicomponent cereal mixtures that would have low or intermediate glycemic index.

MATERIALS AND METHODS

Thirty five adult male Wistar rats weighing 200–300 g that were obtained from the vivarium of the Siberian Branch of the Russian Academy of Sciences and maintained in the vivarium of the Novosibirsk State Medical University according to the rules established by the European Convention for the Protection of Vertebrate Animals Used for Experimental and Other Scientific Purposes were used in the experiment. Prior to the experiment, all animals were fed with powdered milk, grain or grain waste, germinated oats, and comprehensive multivitamin preparations, in addition to the standard balanced diet (pelleted feed PK120-3, according to the administrative order no. 179 of the Ministry of Health of USSR, 10.10.1983). Against this background, blood was collected from the animals for biochemical studies (control group, $n = 20$). Blood collection from tail vein was performed under general anesthesia, according to the recommendations of the Federation of European Laboratory Animal Science Working Group [10].

In function of the diet, the animals were divided into three groups, 10 animals each, and were ranged according to body weight to provide for the similarity of the parameter between the groups. Independently of the diet (Table 1), animals were kept in individual cages with free access to food and water.

After 15 and 30 days of feeding with one of the experimental diets (nos. 1, 2, or 3), blood was again collected from the animals for biochemical studies.

Postprandial glycemia was studied once, after 30 days of feeding with one of the diets. In four groups of animals, 5 male Wistar rats each, glucose concentration in blood upon 13 h starvation was measured and they gained access to forage (30 g per animal) or vivarium

standard diet feed in case of the control group. Postprandial glycemia was determined after 30, 60, and 120 min. In another group of animals on a standard vivarium diet, glucose aqueous solution was introduced directly to stomach through a gavage at the rate of 0.03 g/g weight (glucose tolerance test, GTT); glycemia level was measured at the same time points as in other experimental groups.

Glucose concentration in blood was determined by a glucose oxidase method using an EKSAN-Gm automated analyzer. The method is based on specific oxidation of glucose under the effect of glucose oxidase exhibiting high substrate specificity toward glucose.

To prepare porridges, three-component cereal mixtures were used for diet 1 (rice + peas + buckwheat) and diet 2 (rice + barley + maize) and a five-component mixture, for diet 3 (rice + barley + maize + buckwheat + peas).

Biological value of the cereal mixture proteins was calculated according to the technique proposed by Kovalev et al. [11], which allows for calculation of rational ratio of products at various combinations and determination of their biological value. The method allows for explanation of the four types of curves (according to Bressani's classification). It is based on the fact that not all essential amino acids are utilized at quantities adequate to the amino acid that has the lowest score. The remaining fraction determines the non-utilized protein (ΔP). The choice of optimal variant of combinations may be performed using the plot based on the linear dependence of non-utilized protein fraction (ΔP) from the protein ratio or products in the food mixture.

Table 1. Composition and energy content per one rat

Parameter	Standard	Diet 1	Diet 2	Diet 3
Proteins, g	4.0	2.1	1.4	2.4
Fats, g	3.4	0.3	0.2	0.4
Carbohydrates, g	9.4	8.3	9.6	8.7
Energy content, kcal	82.1	44.2	45.3	47.9
Mass, g	50	50	50	50

The results were processed using the Statistics 6.0 software package.

RESULTS AND DISCUSSION

In contrast to the standard vivarium diet, experimental animals received viscous porridge prepared from the relevant cereal mixtures without additives. Observations on animals revealed an interesting specific feature of group 2, which was the increased aggressiveness of the animals in the group. When taken out of the cage, the rats adopted defensive position and attempted to bite the researcher. Nevertheless, body weight of the animals of group 2 increased by day 15 of the study ($P \leq 0.02$). Similar results were obtained in groups 1 and 3 (Table 2).

Despite the considerable difference in qualitative composition of the diets and their energy value, all animals gained weight by day 30 of the experiment, which is explained by free access to the food. It should

be noted that the percent of weight gained in group 2, receiving less protein and fat, was the lowest. Probably,

this explains behavioral reactions of the animals distinguished by aggressiveness (Table 2).

Table 2. Dynamics of body weight in experimental animals ($M \pm m$)

Diet	Body weight, g			Weight gain, %
	Days of study			
	Control n = 30	15 n = 10	30 n = 10	
Standard	264.4 ± 5.5	278.5 ± 3.1*	306.0 ± 4.5*	5.3/15.7
1		270.9 ± 3.3	288.4 ± 8.4*	2.5/9.1
2		279.8 ± 5.6*	298.6 ± 5.4*	5.8/12.9
3		280.5 ± 3.9*	300.7 ± 3.3*	6.1/13.8

Notes: *statistically significant difference if compared to control group, $P \leq 0.02$, LSD test.

After starving overnight, on day 15 and 30 of the experiment, glycemia level was determined; it was found to be significantly higher in animals on diets 1–3 (Fig. 1).

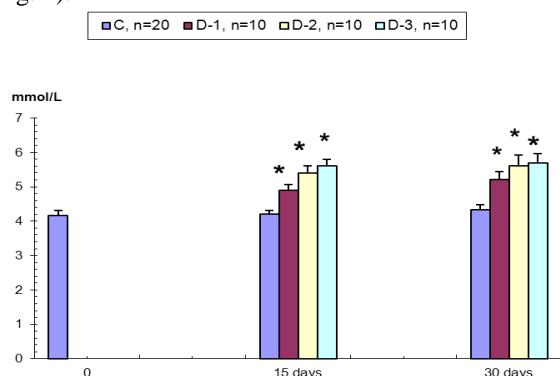


Fig. 1. Effect of the diets on glycemia in rats. *Significant differences if compared to the control, $P \leq 0.05$, Wilcoxon test.

We consider that the ratio between the accessible and non-accessible polysaccharides in the multicomponent porridges promoted the maintenance of a higher level of glycemia in fasted animals, which is in agreement with the literature data [7].

Calculations demonstrated that carbohydrate content in the diets was 0.03 g/g weight; therefore, it seemed interesting to study the glyceimic curve progression after feeding.

After eating 30 g porridge and feed, the ascending segment of the glyceimic curve in the control group evidenced rapid absorption of the glucose formed (Fig. 2).

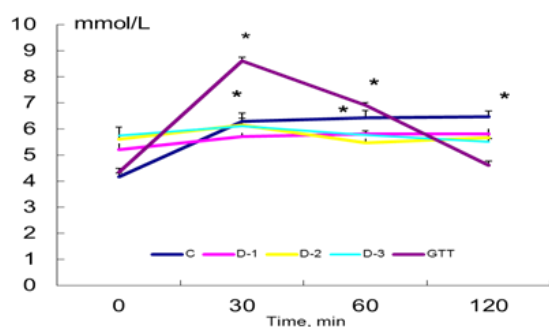


Fig. 2. Postprandial glycemia and glucose tolerance test in experimental animals ($M \pm m$). * significant differences if compared to 0 min, $P < 0.01$, Wilcoxon test.

The observed fact could be considered as unfavorable, since beta cells of pancreas not only secrete insulin into blood, but also synthesize it in large amounts in response to rapid influx of glucose. The load on the insulin apparatus of the pancreas increases. However, postprandial glycemia corresponded to physiologically normal values in rats [12]. The level of glycemia maintained in the course of the whole observation period and after 2 h returned to the initial values evidencing prolonged digestion of feed and gradual absorption of carbohydrates.

In animals fed with porridges, blood glucose levels practically did not change during the observation period. Glycemia gain was low if compared to the control group, and by 60 min glucose concentration returned to the initial values. Based on this, we conclude that porridges made of multicomponent cereal mixtures are characterized by low glyceimic index.

It seemed important to compare postprandial glyceimic curves in all groups with the response of a separate group of animals to administration of glucose at the same amount as in the relevant diet. Since rats in this group received standard vivarium diet, the glycemia value in the fasted state was the same as in the control group (Fig. 2). After administration of glucose, its blood concentration reached peak values by 30 min and exceeded considerably the values in animals of groups 1–3 ($P \leq 0.01$). The rate of glucose absorption, judging from the ascending segment of the glyceimic curve, was the highest if compared to all other groups. The peak concentration was registered by 30 min, which is in agreement with the results of other authors [13, 14]. By 60 min, glucose content in blood decreased considerably, but exceeded the values in all other groups ($P \leq 0.01$). After two hours, glucose content returned to the initial values. One of the parameters describing the state of carbohydrate exchange is the Baudouin coefficient, or hyperglycemic coefficient, which is the ratio of glucose content after 30 or 60 min (the higher value is chosen) to its level under fasted condition (normally, below 1.7).

The obtained results evidence that carbohydrate exchange and values of the Baudouin coefficient in all groups, with the exception of those receiving glucose solution, were within the physiological ranges [14, 15].

The obtained results evidence that carbohydrate exchange and values of the Baudouin coefficient in all groups, with the exception of those receiving glucose solution, were within the physiological ranges [14, 15].

Table 3. Values of the hyperglycemic coefficient

Diet	Hyperglycemic coefficient
Standard vivarium diet (control)	1.52 ± 0.03
Diet 1	1.10 ± 0.06
Diet 2	1.10 ± 0.07
Diet 3	1.07 ± 0.03
GTT	1.98 ± 0.11

The calculations allow for a conclusion that all porridges from cereal mixtures may be referred to products with low glycemic index (Table 4). The conclusion is in agreement with a number of diet recommendations, according to which values of ≥ 70 characterize products with high glycemic index, 55–69,

intermediate one, and ≤ 55 , low glycemic index [16].

Table 4. Glycemic indexes of the experimental animal diets ($M \pm m$)

Diet	Glycemic index
Standard vivarium diet (control)	76.2 ± 4.35
Diet 1	55.6 ± 3.1
Diet 2	55.9 ± 3.4
Diet 3	53.6 ± 1.5

Therefore, based on the studies, precooked food from cereal mixtures 1, 2, and 3 may be recommended for arrangement of functional nutrition that provides for consumption of products with low glycemic index.

REFERENCES

- Lobykina, E.N., Koltun, V.Z., and Khvostova, O.I., Glycemic index of products and its application in dietary therapy of obesity, *Voprosy pitaniya (Nutrition Issues)*, 2007, vol. 76, no. 1, pp. 14–22.
- Jenkins, D.J.A., Wolever, T.M.S., and Jenkins, A.L., The Glycaemic Response to Carbohydrate Foods, *Lancet*, 1984, vol. 2, pp. 388–391.
- Vloshchinskii, P.E., and Kolpakov, A.R., Structure of nutrition and glucose tolerance in the northerns, *Tekhnika i tekhnologiya pishchevykh proizvodstv (Methods and Technology of Food Production)*, 2011, pp. 17–21.
- Jenkins, D.J.A., Lente Carbohydrate: A Newer Approach to the Dietary Management of Diabetes, *Diabetes Care*, 1982, no. 5, pp. 634–641.
- Jenkins, D.J.A., Wolever, T.M.S., Jenkins, A.L., et al., The Glycaemic Index of Foods Tested in Diabetic Patients: A New Basis for Carbohydrate Exchange Favouring the Use of Legumes, *Diabetologia*, 1983, no. 24, pp. 257–264.
- Jenkins, D.J.A., and Jenkins, A.L., The Glycemic Index, Fiber, and the Dietary Treatment of Hypertriglyceridemia and Diabetes, *J. Am. Coll. Nutr.*, 1987, vol. 6, no. 1, pp. 11–17.
- Jenkins, A.L., Kacinik, V., Lyon, M., and Wolever, T.M.S., Effect of Adding the Novel Fiber, PGX, to Commonly Consumed Foods on Glycemic Response, Glycemic Index and GRIP: A Simple and Effective Strategy for Reducing Post Prandial Blood Glucose Levels – A Randomized, Controlled Trial, *Nutrition J.*, 2010, vol. 9, p. 58.
- Kendysh, I.N., *Regulyatsyya uglevodnogo obmena (Regulation of Carbohydrate Exchange)*, Moscow: Meditsyna, 1985.
- Newsholme, E., and Start, C., *Regulation in Metabolism*, New York and London: John Wiley and Sons, 1973.
- Kopaladze, R.E., Regulation of animal experiments: Ethics, laws, and alternatives, *Uspekhi physiol. nauk (Progress in Physiology Sciences)*, 1998, vol. 29, no. 4, pp. 74–92.
- Kovalev, N.I., Kartseva, N.N., and Krasnova, N.S., Ways to increased biological values of food products and cooled meals, in *Puti snizheniya poter' pishchevykh produktov pri khraneni i sovershenstvoveniya tekhnologii produktov obshchestvennogo pitaniya (Methods to Decrease Losses of Food Products upon Storage and Improvement of Public Food Service Product Technology)*, Leningrad, 1982, pp. 160–173.
- Nasanova, O.N., Effect of water extracts of common nettle, common burdock, dandelion, and common goat's rue on hyperglycemia and hyperlipidemia upon diabetes mellitus type 2, *Bulleten' sibirskoi meditsyny (Bulletin of the Siberian Medicine)*, 2011, no. 3, pp. 87–90.
- Agarkov, D.Yu., et al., Hypoglycemic properties of the extract of *Gymnema sylvestre*, *Vestnik VolGMU (Bulletin of the Volgograd State Medical University)*, 2007, no. 1 (21), pp. 79–82.
- Volchegorskiim I.A., Rassokhina, L.M., and Miroshnichenko, I.Yu., Insulin-potentiating effects of antioxidants in experimental diabetes mellitus, *Problemy endokrinologii (Problems of Endocrinology)*, 2010, no. 2, pp. 27–35.
- Selyatitskaya, V.G., Palchikova, N.A., and Kuznetsova, N.V., Activity of adrenocortical system in rats with high and low resistance to diabetogenic effect of alloxan, *Fundamental'nye issledovaniya (Fundamental Studies)*, 2011, no. 3, pp. 142–147.
- American Diabetes Association. Nutrition recommendations and interventions for diabetes: a position statement of the American Diabetes Association, *Diabetes Care*, 2008, no. 31, suppl. 1, pp. 61–78.



ENTHALPY OF PHASE TRANSITION AND PREDICTION OF PHASE EQUILIBRIA IN SYSTEMS OF GLYCOLS AND GLYCOL ETHERS

Z. N. Esina^{a,*}, A. M. Miroshnikov^b, and M. R. Korchuganova^a

^aKemerovo State University,

st. Krasnaya 6, Kemerovo, 650043 Russia,

*phone/fax: +7 (3842) 54-27-70, e-mail: enz2@rambler.ru

^bKemerovo Institute of Food Science and Technology,

bul'v. Stroitelei 47, Kemerovo, 650056 Russia

(Received March 7, 2014; accepted in revised form March 17, 2014)

Abstract: The PCEAS model was used to study the liquid–solid and liquid–vapor phase transitions at constant pressure in systems containing glycols and glycol ethers. This method is based on minimizing the excess Gibbs energy over the solvation parameter, which takes into account the processes of association of molecules in various phases. To compute the diagrams, the data on enthalpy and phase transition temperatures of pure components are required, while the information about the interactions in the binary system is not necessary. We present analytical expressions for the enthalpy of vaporization and enthalpy of melting of glycols and glycol ethers obtained with the theory of similarity using molecular weight, critical temperature, temperature of the triple point, and the number of carbon atoms in the molecule as the parameters. In the absence of information about the critical temperature, the enthalpy of vaporization may be calculated using the boiling point value. It is shown that the prediction of the enthalpy of melting and enthalpy of vaporization allows us to calculate of the phase diagram, as well as the azeotropic and eutectic parameters in water–glycol ether and glycol ether–alkane systems.

Keywords: modeling, glycol, glycol ether, PCEAS, enthalpy of vaporization, melting enthalpy, thermodynamic similarity, liquid–solid equilibrium, liquid–vapor equilibrium, eutectics, azeotrope

UDC 544.015; 517.958; 544.275.5; 544.275

DOI 10.12737/4142

INTRODUCTION

Glycols and glycol ethers are widely used as additives in food and cosmetics industries. Therefore, systems containing glycols and glycol ethers in mixtures with water, alkanes, and salts are actively studied [1–3]. These systems are the subjects of the current work because experimental and theoretical foundation for their application is lacking. There should be thermodynamic models that would be able to predict properties of pure components and phase equilibrium in systems containing glycols and glycol ethers with high accuracy.

For some of the members of the homology series, enthalpies of vaporization and melting are unknown or have not been measured with sufficient accuracy. In work [4] it has been noted that calculation of the parameters of eutectics and azeotrope mixtures used in technological processes of crystallization and rectification is complicated by the absence of accurate data on enthalpies of phase transitions of individual components.

Boiling temperature T_b and melting temperature T_m , pressure P , density ρ , enthalpy of vaporization ΔH_{vap} , and enthalpy of melting ΔH_m are determinative for computation of thermodynamic properties of pure substances and solutions. Prediction of the compound properties implies that the properties are determined basing on the compound structural formula. The theory

connecting the structure of a molecule with its macroscopic parameters is not complete yet; therefore, it is necessary to summarize empirical data on the properties of various compounds. Method of thermodynamics similarity, which is a part of general similarity theory, forms theoretical basis for such a summary [5].

Enthalpy of vapor formation at normal temperature of boiling is called the enthalpy of vaporization. Solid–liquid and liquid–vapor phase transitions proceeding at normal temperature of melting are characterized by enthalpy of melting and enthalpy of vaporization. Methods of group contribution [6, 7] and quantum chemistry [8] are used for predictions.

Enthalpy of phase transition of a pure component may be found from pressure–temperature dependence curve of the two-phase equilibrium, which is expressed as the Clausius–Clapeyron equation:

$$\frac{dP}{dT} = \frac{\Delta H}{T \Delta V}, \quad (1)$$

Provided that the evaporation heat does not depend on the temperature, vapor is considered an ideal gas, the volume of liquid is small compared to the gas volume, and the following equation may be written for the liquid–vapor coexistence curve:

$$\ln P = -\Delta H_{\text{vap}} / RT + \text{const}$$

If the data on vapor pressure are absent, enthalpy of vaporization may be calculated according to empirical equations, most of which are based on the data on critical parameters of the compounds [9, 10]. Critical properties of many gases and liquids are known or may be computed [11, 12]. In [13], an empirical formula is reported:

$$\Delta H_{\text{vap}} = \Delta H_{\text{tr}} \left[\frac{T_{\text{cr}} - T}{T_{\text{cr}} - T_{\text{tr}}} \right]^{z_{\text{cr}}} \left[\frac{c_{\text{cr}} - T_{\text{tr}}}{c_{\text{cr}} - T_{\text{cr}}} \right]^{k_{\text{cr}}}$$

where ΔH_{tr} is the enthalpy of vaporization in the triple point; T_{cr} , critical temperature; T_{tr} , temperature of the triple point; z_{cr} , specifies the number of similarity.

In work [13], authors argued that a wide range of liquids, with the exception of quantum liquids, has a universal behavior on the evaporation curve. The group of substances with similar chemical structure is characterized by similarity parameters that vary upon transition to a different group. Similarity relations are associated with the concept of the critical state. According to the theory of similarity, a system of units is chosen in function of the nature of a subject under study and then the transition is made to non-dimensional, the so-called corrected, values. To perform such a change, that is, to transfer from one system to another, a linear transformation of values is to be done:

$$x'_i = c_{x_i} x_i,$$

where c_{x_i} is a constant value called the similarity parameter and x_i and x'_i are the respective values.

Laws revealed for one system are correct for a group of similar systems, which allows obtaining information on the properties of unknown systems.

The method of thermodynamic similarity may be briefly characterized as a method of isolating a number of parameters that adequately define the thermal physical properties of a substance. In the cases when the data on critical parameters are absent, it is reasonable to use models allowing to present the enthalpy as a function of the boiling temperature T_b and other reliably defined parameters.

Kistyakovskiy proposed a rule to define the entropy of vapor formation:

$$\Delta S_{\text{vap}} = \frac{\Delta H_{\text{vap}}}{T_b} = 8.75 + R \ln T_b, \quad (2)$$

which allows to calculate the entropy of vapor formation.

Equation (2) for various types of organic compounds rewritten by Vetere in the form of a function of T_b and molecular mass M , as well as other correlations, are reported in [7, 10].

MATERIALS AND METHODS

In the work, molar enthalpy of vaporization ΔH_{ev} at normal boiling point of a pure component for homology series of alkanes, alcohols, acids, glycols, and glycol ethers is expressed as a function of the number of carbon atoms N , relative molecular mass M , normal boiling temperature T_b , and the universal gas constant R :

$$\Delta H_{\text{ev}} = \frac{\alpha(N)MRT_b}{R} + B(N), \quad (3)$$

where $\alpha(N)/R$ is the determinative parameter of similarity, a non-dimensional coefficient; $B(N) = \beta(N)(-1)^N + \gamma(N)$ is the function introduced for a more accurate modeling of the enthalpy of vaporization for the members of a homology series with even and odd numbers of carbon atoms; and $\beta(N)$ and $\gamma(N)$ are expressed in J/mol.

Table 1 reports the $\alpha(N)$ coefficient of the equation (3) as a function of the number of carbon atoms in a molecule for glycols and glycol ethers, $\beta(N) = \gamma(N) = 0$.

Table 1. Parameters of the equation for calculation of the enthalpy of vaporization of the members of the homology series of glycols and glycol ethers

Homology series	$\alpha(N)$, J/(mol K)
Glycols	$\frac{N(N+1.1)}{1.7(N-1)}$
Glycol ethers	$\frac{N(N+1.1)}{1.15(N-1)}$

Figure 1 presents the experimental data and the results of prediction of the enthalpy of vaporization for a homology series of glycol ethyl ethers.

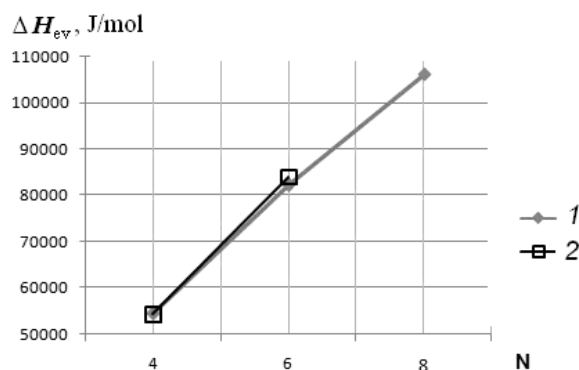


Fig. 1. Enthalpy of evaporation of the homology series of glycol ethyl ethers: 1 – ΔH_{ev} , according to formula (3), and 2 – ΔH_{ev} – the experimental data [14].

The following relation is proposed for these members of different homology series:

$$\frac{\Delta H_{N_2}^{\text{ev}} - B_{N_2}(N)}{\Delta H_{N_1}^{\text{ev}} - B_{N_1}(N)} = \frac{\alpha_{N_2}(N)M_{N_2}T_{N_2}^{\text{b}}}{\alpha_{N_1}(N)M_{N_1}T_{N_1}^{\text{b}}}, \quad (4)$$

where $B_i(N) = \beta_i(N)(-1)^N + \gamma_i(N)$, $i = n, m$.

To relate the enthalpy of evaporation for different members of the same homology series with the number of carbon atoms N_1 and N_2 , the following ratio may be used:

$$\frac{\Delta H_{N_2}^{\text{ev}} - B(N_2)}{\Delta H_{N_1}^{\text{ev}} - B(N_1)} = \frac{\alpha(N_2)M(N_2)T_{N_2}^{\text{b}}}{\alpha(N_1)M(N_1)T_{N_1}^{\text{b}}}, \quad (5)$$

where $\alpha(N_2)/\alpha(N_1)$ is the ratio of the determinative parameters of similarity.

Equation (1) may also be used to determine ΔH_b , but the data on the dependence of melting temperature on the pressure are available for a limited range of pure components.

Enthalpy of melting of a pure component may be presented for a molecule with the number of carbon atoms of N as a function of molar mass M , melting temperature T_m , and the universal gas constant R :

$$\Delta H_m = \frac{a(N)}{R} \frac{MRT_m}{N} + A(N), \quad (6)$$

where $A(N) = b(N)(-1)^N + c(N)$. Here $a(N)/R$ is the determinative parameter of similarity, a non-dimensional coefficient; $b(N)$ and $c(N)$ are expressed in J/mol.

Table 2 provides the coefficients of the equation (3), $a(N)$, $b(N)$, and $c(N)$, as functions of the number of carbon atoms in the molecule. This presentation is not the only one possible and depends on the accuracy of experimental data used to approximate the enthalpy.

Table 2. Parameters of the equation used to calculate the enthalpy of melting of the members of homology series of glycols and glycol ethers

Homology series	$a(N)$, J/(mol K)	$b(N)$, J/mol	$c(N)$, J/mol
Glycols and glycol ethers ($1 \leq N \leq 10$)	$\frac{N^2 + 1}{26.5}$	0	$-320N + 10755$

Figure 2 presents the experimental data and predicted values of the enthalpy of melting for the homology series of glycols.

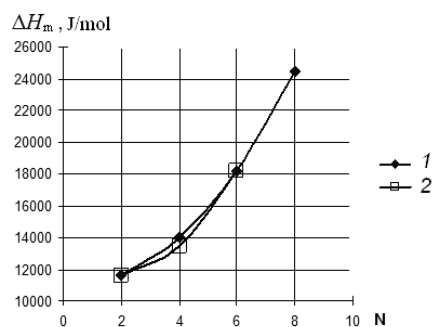


Fig. 2. Enthalpy of melting of glycols: 1 – ΔH_m according to the formula (3) and 2 – ΔH_m , the experimental data [14].

The similarity of the enthalpy of melting taken up to a constant $A(N)$ of the relevant members of homology series of glycols and glycol ethers is considered:

$$\frac{\Delta H_n^m - A_i(N)}{\Delta H_m^m - A_m(N)} = \frac{a_n(N)M_nT_n^m}{a_m(N)M_mT_m^m}, \quad (7)$$

where $A_i(N) = b_i(N)(-1)^N + c_i(N)$, i – series number.

The following relation is true for similarity of the enthalpy of melting between the different members of the same homology series with carbon atom numbers N_1 and N_2 :

$$\frac{\Delta H_{N_2}^m - A(N_2)}{\Delta H_{N_1}^m - A(N_1)} = \frac{a(N_2)M(N_2)T_{N_2}^m}{a(N_1)M(N_1)T_{N_1}^m}. \quad (8)$$

Relation (9) allows to calculate of the enthalpy of melting using the known enthalpy of vaporization value:

$$\frac{\Delta H_m - b(N)(-1)^N - c(N)}{\Delta H_{ev} - \beta(N)(-1)^N - \gamma(N)} = \frac{a(N)T_m}{\alpha(N)T_b}. \quad (9)$$

Table 3 presents the relation between the parameters of similarity $a(N)/\alpha(N)$ for such a comparison.

Table 3. Relation between the parameters of similarity for the members of the homology series of glycols and glycol ethers

Homology series	$a(N)/\alpha(N)$
Glycols ($1 \leq N \leq 10$)	$\frac{(N^2 + 1)(N - 1)}{15.59N(N + 1.1)}$
Glycol ethers ($1 \leq N \leq 10$)	$\frac{(N^2 + 1)(N - 1)}{23.04N(N + 1.1)}$

The advantages of enthalpy of melting and enthalpy of evaporation calculations using the formula (4)–(5) and (7)–(8) is the decrease of the effect of systematic measurement errors in the course of molecular mass and melting temperature determination of the homology series members since they form a ratio in the formula (4)–(5) and (7)–(8). Relation (9) does not include molecular mass, which excludes the influence of molecular mass measurement error. Since ratio T_m/T_b is in the right side of the relation, the contribution of systematic error of temperature measurement to the error of enthalpy calculation decreases.

RESULTS AND DISCUSSION

Empirical models for calculation of enthalpy of evaporation and enthalpy of melting based on the data of phase transition temperatures, molecular mass, and the number of carbon atoms in the molecule were proposed. Upon serial application of the similarity theory, critical temperature and triple point temperature are introduced into the system as reducing parameters, allowing for a decrease of the error of determination of the phase transition enthalpy of a pure component to 1–2%.

The method of thermodynamic potentials was used as the mathematical method to study the phase equilibrium in real solutions [15, 16]. Phase chart eutectic and azeotropic systems (PCEAS) [17] is the model of state equation based on the minimization of excess Gibb's energy over the solvation parameter λ , characterizing the ratio of the number of A molecules to the number of B molecules in a compound.

The result of the work is the computation of liquid–solid and liquid–vapor phase equilibrium in binary systems containing glycol ethers using the PCEAS software. Enthalpy of melting and vaporization for glycol ethers necessary for calculation were found using the models proposed in the work. Phase equilibria taking into account association and solvation of molecules were studied under normal atmospheric pressure.

Figures 3 and 4 present the liquidus and solidus in the systems of 2-methoxyethanol–water and 2-methoxyethanol–cyclohexane.

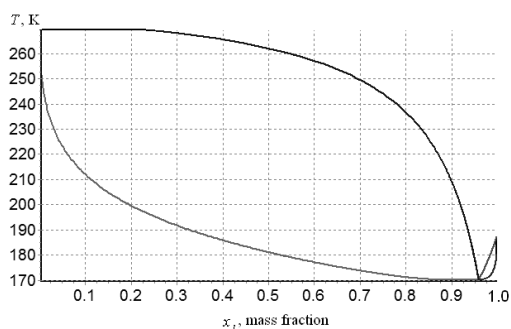


Fig. 3. Liquid–solid phase diagram of the 2-methoxyethanol–water system.

Table 4 provides for the results of calculations of eutectics and azeotrope parameters in systems based on glycol ethers.

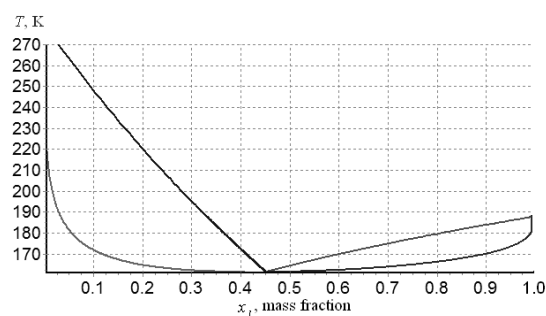


Fig. 4. Liquid–solid phase diagram of the 2-methoxyethanol–cyclohexane system.

Table 4. Computed and experimental eutectics and azeotrope parameters in systems containing glycol ethers

Solution	x_{eut} , mass., comp.	t_{eut} , °C, comp.	q_{az} , mass., comp.	t_{az} , °C, comp.	q_{az} , mass., exp. [18]	t_{az} , °C, exp. [18]
2-methoxyethanol–water	0.959	−102.87	0.21	99.77	0.212	99.75
2-methoxyethanol–cyclohexane	0.452	−111.66	0.09	77.56	0.080	79.80
2-methoxyethanol–heptane	0.404	−102.40	0.18	91.88	0.230	92.50
2-methoxyethanol–octane	0.809	−88.73	0.329	105.59	0.480	110.00
methyl carbitol–water	0.948	−91.09	non-azeotr.	non-azeotr.	non-azeotr.	non-azeotr.
methyl carbitol–undecane	0.959	−85.65	0.340	173.59	0.400 (v.)	178.70
2-ethoxyethanol–water	0.909	−80.57	0.297	99.74	0.300	99.30
2-ethoxyethanol–heptane	0.291	−97.74	0.147	93.69	0.140	94.50
2-ethoxyethanol–octane	0.801	−78.54	0.294	110.11	0.380	116.00
2-ethoxyethanol–nonane	0.606	−79.91	0.462	120.85	0.50	128.00

Figure 5 presents the dependence of boiling temperature on mass fraction of the first component in the 2-methoxyethanol–water system.

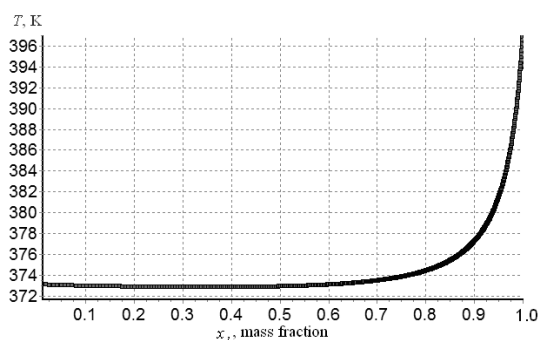


Fig. 5. Liquid–vapor phase diagram of the 2-methoxyethanol–water system.

Results of the calculations reported in Table 4 agree with the experimentally obtained parameters of eutectics and azeotropes [18].

CONCLUSIONS

Predicting thermodynamic parameters of glycols and glycol ethers based on the similarity theory allows to calculate phase diagrams of binary systems for which no experimental data on enthalpy of melting or enthalpy of evaporation of pure components is available. The method can be recommended when selecting components and composition in order to obtain the desired properties of the solution (temperature and enthalpy of melting and vaporization), which will greatly reduce the time and expenses spent on experiments.

REFERENCES

- Grenner, A., Kontogeorgis, G. M., Nicolas von Solms, and Michelsen, M. L., Application of PC-SAFT to glycol containing systems – PC-SAFT towards a predictive approach, *Fluid Phase Equilibria*, 2007, vol. 261, no. 1–2, pp. 248–257; <http://dx.doi.org/10.1016/j.fluid.2007.04.025>.
- Chen, L.-F., Soriano, A. N., and Li, M.-H., Vapour pressures and densities of the mixed-solvent desiccants (glycols + water + salts), *J. Chem. Thermodynamics*, 2009, vol. 41, no. 6, pp. 724–730; <http://dx.doi.org/10.1016/j.jct.2008.12.003>.

3. Garrido, N. M., Folas, G. K., and Kontogeorgis, G. M., Modelling of phase equilibria of glycol ethers mixtures using an association model, *Fluid Phase Equilibria*, 2008, vol. 273, no. 1–2, pp. 11–20; <http://dx.doi.org/10.1016/j.fluid.2008.08.006>.
4. Kenisarin, M., and Mahkamov, K., Solar energy storage using phase change material, *Renewable and Sustainable Energy Reviews*, 2007, vol. 11, no. 9, pp. 1913 – 1965; <http://dx.doi.org/10.1016/j.rser.2006.05.005>.
5. Filippov, L. P., *Prognozirovaniye teplofizicheskikh svoystv zhidkosti i gazov* (Predicting Thermal Physical Properties of Liquids and Gases), Moscow: Energoatomizdat, 1988.
6. Basarova, P., and Svoboda, V., Prediction of the enthalpy of vaporization by the group contribution method, *Fluid Phase Equilibria*, 1995, vol. 105, no. 1, pp. 27–47; [http://dx.doi.org/10.1016/0378-3812\(94\)02599-V](http://dx.doi.org/10.1016/0378-3812(94)02599-V).
7. Marrero, J., and Gani, R., Group-contribution based estimation of pure component properties. *Fluid Phase Equilibria*, 2001, vol. 183–184, pp. 183–208; <http://dx.doi.org/10.1016%2FS0378-3812%2801%2900431-9>.
11. Gharagheizi, F., Determination of normal boiling vaporization enthalpy using a new molecular-based model, *Fluid Phase Equilibria*, 2012, vol. 317, pp. 43–51; <http://dx.doi.org/10.1016%2Fj.fluid.2011.12.024>.
12. Reid, R., Prausnitz, J. M., and Sherwood, T. K., *Svoistva zhidkosti i gazov* (The Properties of Gases and Liquids), Leningrad: Khimiya, 1982.
13. Kikic, I., and Vetere, A., Evaluation of several literature equations to predict the vaporization enthalpies at the normal boiling point, *Fluid Phase Equilibria*, 2011, vol. 309, pp. 151–154; <http://dx.doi.org/10.1016%2Fj.fluid.2011.06.026>.
14. Nesterov, I. A., Nesterova, T. N., Nazmutdinov, A. G., et al, Prediction of critical temperatures of the liquid–vapor equilibrium for organic compounds, *Zh. Fiz. Khim. (J. Physical Chemistry)*, 2006, vol. 80, no 11, pp. 2032–2040.
15. Nesterova, T. N., and Nesterov, I. A. *Kriticheskie temperatury i davleniya organicheskikh soedinenii. Analiz sostoyaniya bazy dannykh i razvitie metodov prognozirovaniya* (Critical temperature and pressure values of organic compounds. Analysis of database conditions and development of methods of prediction), Samara: Izdatel'stvo Samarskogo nauchnogo tsentra RAN, 2009.
16. Meyra, A. G., Kuz, V. A., and Zarragoicoechea, G. J., Universal behavior of the enthalpy of vaporization: an empirical equation, *Fluid Phase Equilibria*, 2004, vol. 218, pp. 205–207; <http://dx.doi.org/10.1016%2Fj.fluid.2003.12.011>.
17. Dymont, O. N., Kazansky, K. S., and Miroshnikov, A. M., *Glycols and other derivatives of propylene oxide and ethylene*, Moscow: Khimiya, 1976.
18. Esina, Z. N., Korchuganova, M. R., and Murashkin, V. V., Mathematical modeling of the liquid–solid phase transition, *Vestnik Tomskogo gosudarstvennogo universiteta. Upravlenie, vychislitel'naya tekhnika i informatika (Tomsk State University Bulletin. Management, computer engineering, and informatics)*, 2011, vol. 3, no. 16, pp. 13–23.
19. Esina, Z. N., Murashkin, V. V., and Korchuganova, M. R., Physical and mathematical model of the solid–gas equilibrium at constant pressure, *Vestnik Kemerovskogo gosudarstvennogo universiteta (Kemerovo State University Bulletin)*, 2013, vol. 2–1, no. 54, pp. 72–80.
20. Esina, Z. N., Murashkin, V. V., and Korchuganova, M. R., «Phase Chart Eutectic and Azeotropic System (PCEAS)»: State registration certificate of an application software № 2012618394 (RU) – № 2012616324; filed 25.07.2012; registered in the catalog of the application software, Moscow, September 17, 2012.
21. Ogorodnikov, S. K., Lesteva, T. M., and Kogan, V. B., *Azeotropnye smesi. Spravochnik* (Azeotropic Mixtures. Reference Book), Kogan, V. B., Ed., Leningrad: Khimiya, 1971.



THE MAIN LABOR-FORMING FACTORS AND THE ASSESSMENT OF LABOR EFFICIENCY IN AGRICULTURE (BY THE EXAMPLE OF KEMEROVO OBLAST)

V. P. Zotov^a, E. A. Zhidkova^{a,*}, and A. M. Dvoroenko^b

^aKemerovo Institute of Food Science and Technology,
bul'v. Stroitelei 47, Kemerovo, 650056 Russia,

*phone/fax: +7 (3842) 73-35-92, e-mail: nkemtipp@mail.ru

^bKemerovo State Institute of Agriculture,
ul. Markovtseva 5, Kemerovo 650056, Russia

(Received March 27, 2014; Accepted in revised form March 31, 2014)

Abstract: A system of factors that affect the formation of labor resources is considered. At present, quite unrelated indicators that reflect individual aspects of the labor potential are used to characterize labor efficiency. In new economic environment, it is necessary to elaborate a system of indicators that would more fully reflect the use of labor.

Keywords: labor resources, efficiency, competitive labor compensation, nominal compensation, criterion, labor productivity, demography

UDC 331.53:631
DOI 10.12737/4143

INTRODUCTION

The reorganization of ownership patterns and the formation of a mixed economy in the agrarian sector require adequate changes in labor relations.

An important cause of the production decline in the agrarian sector was the inability of the rural population to adapt to market conditions due to its specific mentality.

The substantial drop in overall production and the deterioration of the demographic situation have led to a decrease in the absolute number of employees and, what is more important, to changes in their qualitative composition.

In our opinion, an increase in the performance of the agrarian industry is primarily determined by the availability of highly professional and economically competent human resources who are able to use new technologies in production.

We see a decrease in real labor compensations of agricultural producers, late payments, unpaid vacations, dismissals, and reduced productivity and labor motivation.

The goal is to propose and substantiate a system of labor-forming factors and to assess the efficiency of labor.

The development of market mechanisms in the agrarian sector in the absence of efficient state incentives for agricultural producers has led to deterioration in socioeconomic conditions in the industry and in rural communities as a whole.

Thus, it is necessary to analyze in detail the existing situation and to elaborate measures of increasing efficiency in the use of labor.

Market relations introduce changes to the organization, distribution, and use of labor, which manifest themselves in different ways in agricultural

businesses of different forms of incorporation. At present, agricultural production practices require new approaches to make the use of labor efficient.

We used data of the Russian Federal State Statistics Service and the Kemerovo oblast territorial statistics body for our analysis.

The paper employs the following methods:

- economic–statistical;
- monographic; and
- abstract–logical [8].

RESULTS AND DISCUSSION

Kemerovo oblast is the most densely populated region in West Siberia. More than 90% of its population is concentrated in cities and urban-type settlements.

The oblast's industrial potential plays an important role in solving economic problems of the Russian Federation. In the first place, this includes fuel and metal supplies. Since recently, the role of the Kuznetsk Basin (Kuzbass) as the main supplier of high-quality solid fuel and power-generating coals has greatly increased. The oblast has occupied a more noticeable place in providing metallurgy with process fuel and coke coals. The share of the Kuzbass in providing Russia with these fuels is 36 and 66%, respectively [3].

Let us consider the dynamics of the oblast's active population. Demographic processes underlie labor supply and determine the scale and composition of labor supply.

The growth of the working-age population has a dual effect on the labor market:

- an increase in labor supply and, consequently, an increased pressure on the labor market; and
- an increase in the number of working-age individuals somewhat mitigates the load on the working population.

The peak of demographic load in Kemerovo oblast fell on 1996 (42.6 persons younger and older than the active age per 100 persons of active age). As is known, a high demographic load requires improvement in the efficiency of social labor; however, in Kemerovo oblast and in Russia as a whole, the growth of demographic load coincided in time with the decline in production and employment, which significantly complicated the situation [3].

Trends in and dynamics of labor formation by sociodemographic groups are presented in Table 1.

One of the least competitive sociodemographic groups is women nearing pension age; accordingly, an increase in their share in labor composition will inevitably lead to the growth of unemployment and will unquestionably require retraining and further employment. At the same time, a decrease in the number and share of men of 30–49 years of age (this age is believed to be the most active) in the structure of the working-age population will negatively affect labor quality, although the possibilities of placement for less competitive population categories will widen.

Table 1. Economic activity of the working-age population in 2007–2012, Kemerovo oblast

Population group by sex	Age group's share in working-age population, %			Sex–age structure of working-age population, %			
	16–29	30–49	49–59/54	Total	16–29	30–49	49–59/54
2008 (both sexes)	26	40.5	21.4	100	100	100	100
Men	31.2	39.7	24.1	49.1	48.2	47.7	44.1
Women	34.1	43.1	18.8	50.9	51.8	52.3	55.9
2009 (both sexes)	32.9	38.7	21.7	100	100	100	100
Men	31.6	39.1	24.3	53.4	54.3	55.2	54.6
Women	31.2	38.4	19.1	46.6	45.7	44.8	45.4
2010 (both sexes)	34.4	38.8	22.3	100	100	100	100
Men	34.2	38.5	25.3	49.9	50.4	48.7	52.4
Women	34.7	39.1	19.3	50.1	49.6	51.3	47.6
2011 (both sexes)	33.6	38.9	26.4	100	100	100	100
Men	32.1	37.9	23.7	49.4	49.5	48.1	52.8
Women	34.6	38.9	23.5	50.1	50.5	51.9	47.2
2012 (both sexes)	31.6	37.5	24.3	100	100	100	100
Men	30.8	38.5	24.7	51.8	49.8	49.3	52.9
Women	32.5	36.6	23.9	43.2	50.2	51.7	47.1

The scale of the possible occurrence of different sociodemographic groups in the labor market largely depends on the causes of economic inactivity. The causes and level of economic inactivity differ by sociodemographic groups: the number of women, both overall and in each age group, is substantially lower than that of men, which is due to their engagement in housekeeping, childcare, and lower pension age. Low economic activity among the young is because of a high share of off-the-job students. A certain decrease in economic activity among persons nearing pension age is a consequence of benefits and early pensions. A considerable share of persons accounted for as economically inactive is constituted by employees of the informal economy. In case of a decrease in the living standards, it is possible to increase labor, primarily by involving students, persons nearing pension age, and housekeepers [3].

A characteristic feature of agriculture is that labor formation is affected by certain factors, which can be divided into three principal groups: social, demographic, and economic [1]. All this has allowed the authors to

propose a classification of these factors while generalizing them (Fig. 1).

During transition to the market, the compensation level somewhat affects labor formation. Note that we do not mean the compensation level as such but rather its relation to other industries and the subsistence level.

In the system proposed, the group of economic factors includes not only incomes and unemployment but also material resources affecting labor formation. All this does not diminish the import of the other groups of factors. Sociological studies show that the placement level depends on housing; medical service; and the presence of schools, preschool facilities, sociocultural establishments, and asphalt roads. Improved conditions lead to an increase in the birth rate and a decrease in the migration of the rural population.

Note that labor formation also highly depends on demographic factors, such as the birth rate, migration, and the share of working-age people in the total population [6].

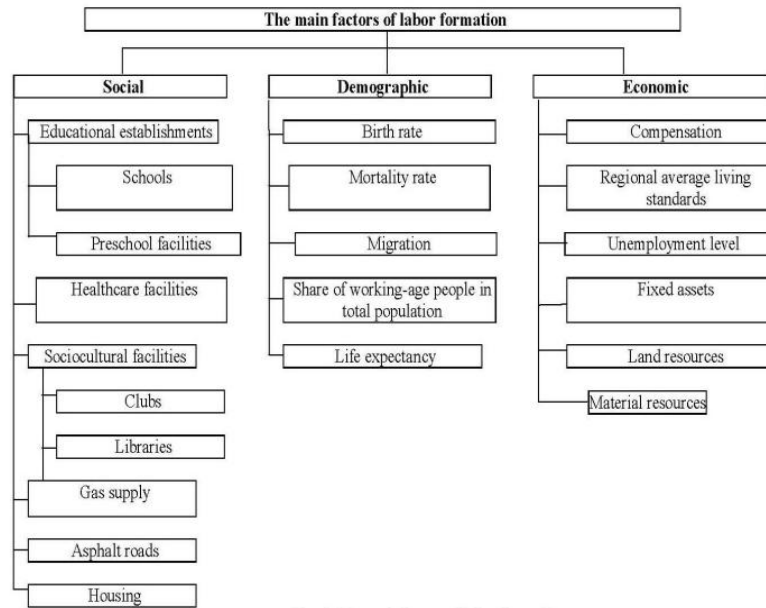


Fig. 1. The main factors of labor formation.

The above groups of the main factors should not be considered separately because the formation of labor conditions takes place under the interaction and mutual influence of all the factors [1].

The main economic factor of labor formation is compensation rate [7]. The nominal compensation indicators alone do not make it possible to study the real dynamics of these processes and to determine the picture of trends developing in the industry's economy because nominal compensation does not account either for the inflation rate or for changes in the relations of production. The real compensation indicator does not make it possible to analyze changes in personal-income dynamics by year. To accomplish this, a new indicator is necessary to account for purchasing power with regard to the possibility to satisfy vital human needs. In our opinion, it is necessary to introduce a competitive compensation indicator that accounts for the possibility to satisfy an employee's minimal needs. Hence, the authors propose to introduce the competitive compensation indicator according to the following formula:

$$I_c = I_n \frac{M_b}{M_c}$$

where I_c is competitive compensation, I_n is nominal compensation, M_b is the subsistence level in the base period, and M_c is the subsistence level in the current period.

The M_b and M_c values are determined using state statistics. The base period is the initial period of studying the dynamics (first year), while the current period is the period of calculating the nominal compensation level (current year).

The subsistence level is used as the base for calculating competitive compensation. This is predetermined by the low level of incomes and is typical for the rural population.

Table 2 shows competitive compensation calculations for Kemerovo oblast.

Table 2. Labor compensation in agriculture, Kemerovo oblast, 2008–2012

Year	Monthly average compensation, rubles		Growth compared to base period, %	
	Nominal compensation	Competitive compensation	Nominal compensation	Competitive compensation
2008	8481	7210	–	–
2009	9124	8225	109	114
2010	9964	8652	117	191
2011	10645	9084	125	128
2012	11177	9629	132	135

The above calculations show that the growth rate of competitive compensation lags far behind the growth rate of nominal compensation, and this reflects the real situation in agriculture.

Our studies have shown that the index of competitive compensation also reflects more accurately the relation between personal incomes and the net results of production.

It is necessary to point out that the performance of labor resources is characterized by unrelated indicators, which do not reflect all facets of labor use. Market conditions necessitate the development of a system of indicators that would reflect more fully the use of the labor potential and show interrelation between them. This system can be represented as a totality of indicators that includes the employment rate of the working population and the development of the labor potential. The efficiency criteria of and the major approaches to the determination of the indicators should be uniform. Practical calculations should take into account characteristics related to various forms of business incorporation.

The present period is characterized by a more complex employment structure due to the diversification of its social groups and flexible organizational forms. All businesses should be regarded efficient if they ensure the socially necessary employment rate in combination with high performance indicators [2].

The development of market relations contributed to the formation of various forms of businesses in Kemerovo oblast. On January 1, 2013, the oblast had 14 joint-stock companies (JSCs), 12 closed joint-stock companies (CJSCs), 8 state unitary agricultural units (SUUs), 112 limited liability companies (LLCs), 44 agricultural production cooperatives, and 218 private incorporated farms. Joint-stock companies, self-sufficient in factors of production (the capital/labor ratio in JSCs is 21.1% higher than in other agricultural units on average), take the leading position in terms of labor and capital efficiency, as well as land use. Having 3.9%

of land and 8.8% of labor resources, the private farmers produce 10.2% of the oblast's total agricultural output.

The basis for the formation of the oblast's labor force in agriculture is the rural population, which decreased by 3.7% over the reporting period, and the demographic situation continues to deteriorate. The employable population is about 45%, and the share of people under the working age is decreasing; every fifth resident is a pensioner; the percentage of women among the employees in 2012 was 27.5%. The number of employees in agriculture decreased by 16.7%.

In 2008, 51.6% of the working-age rural population was employed in agricultural units, while in 2012 this figure was only 16.2%. This happened owing to the decline in production and decreased compensation. Owing to the development of market relations, the structure of employees in agricultural production changed (Table 3).

Table 3. Employment in the agricultural organizations of Kemerovo oblast

Forms of incorporation	Share of employees in their total number, %		Annual employment, man-hour		Number of employees per 100 ha of tillage	
	2008	2012	2008	2012	2008	2012
On average by agricultural forms of incorporation	–	–	1940	1957	3.3	2.7
Collective farms	22.8	6.3	1821	2174	2.5	2.3
SUUs	12.6	7.3	1931	1862	2.0	2.4
LLCs	2.1	16.7	1600	1584	0.8	0.9
JSCs	8.6	4.6	1793	1802	7.2	3.7
Agricultural production cooperatives	28.6	23.2	1605	1980	1.8	1.9
Farms	13.4	17.3	1721	1780	1.8	1.6

The largest share of employees in 2012 fell on LLCs, 16.7%; agricultural production cooperatives employed 23.2%; and collective farms and SUUs, 13.6%. No significant changes occurred in the composition of labor resources during the reform period. The number of permanent employees is growing, and the share of temporary and seasonal workers is decreasing. The number of farm unit managers and specialists decreased by 10.3%, and the number of young specialists dropped by 43.4%. The growing share of chief specialists with higher education diplomas can be regarded as a positive trend (by 71.4% in the total number of administrative personnel). At the same time, the qualifications of crop production and livestock employees remain low; respectively, only 42.4% and 20.2% of them have special qualifications. Only 53.2% of private farms have certified agricultural specialists. The turnover rate of personnel has a steady trend to grow, reaching 0.62 in 2012.

The rate of remuneration in the oblast's agriculture is the lowest compared to other industries. Thus, in 2012 it was 46.4% of that in industrial production and 56.3% of that in the oblast's economy. Labor remuneration is predetermined by the low labor productivity and skills of employees. We should note that the growth of labor remuneration surpasses labor productivity in agriculture. Agricultural units experience the excess of actual working time over its

normative fund with a downward trend. In incorporated private farms, labor resources mismatch production output. Thus, the annual demand for labor at an average private farm is 41.5% of the labor resources available.

The employment and qualitative composition of labor resources affect the efficiency of their use.

The roundup indicator of the efficiency of utilization of labor resources is labor productivity. Our analysis shows that the existing concept of labor productivity and the practical methodology of labor productivity calculation have a number of drawbacks and do not fully meet the requirements of the new economic conditions [4].

In the authors' opinion, there is a practical necessity to extend the existing system of labor productivity indicators. It is advisable to represent this system as a totality of specific indicators, to determine which the following should be used:

- one resource applied;
- several resources (labor and capital), i.e., multifactor;
- all resources applied, i.e., overall indicators.

For the overall evaluation of the efficiency of economic decisions made in the presence of alternative solutions to use interchangeable resources, the use of multifactor and overall labor productivity is of paramount importance.

This methodology allows us to determine factors that affect most substantially the efficiency of utilization of labor resources (Fig. 2).

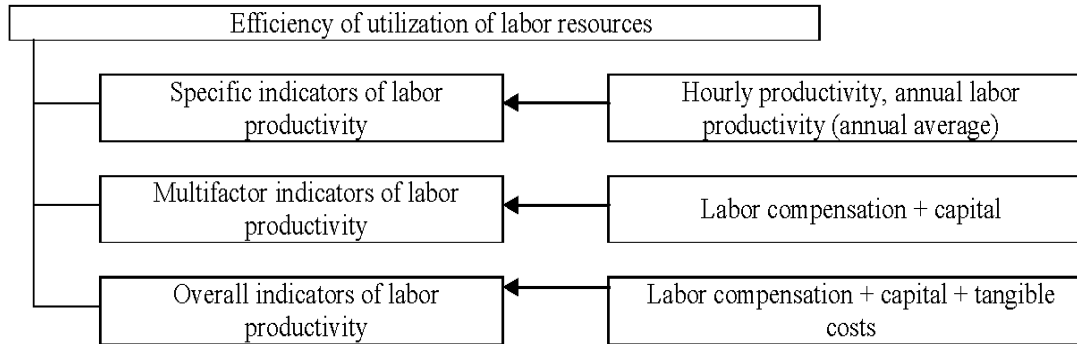


Fig. 2. System of labor use efficiency indicators.

Figure 2 shows that the multifactor indicator of labor productivity characterizes the most efficient labor and capital utilization in money terms. The specific indicator of labor productivity reflects production output per cost unit of direct and materialized labor. The overall indicator of labor productivity is the ultimate indicator of the efficiency of all resources used in production.

The efficiency of utilization of labor resources by forms of incorporation in Kemerovo oblast is given in Table 3.

As was stated above, labor productivity is decreasing in the oblast's agricultural units. Its absolute level in these units is very low. The highest labor productivity in 2012 was recorded in collective farms, 21.8% above the average. Productivity is reflected most fully in an indicator calculated by gross income, which excludes the influence of the material intensity of production. Taking into account the price index, labor productivity in agricultural units increases insignificantly, 5.4% a year [5].

A characteristic feature of agricultural production is that the units spend part of their gross output for technical needs. Therefore, the authors suggest that labor productivity be calculated both by gross output and by commercial output, which directly affects financial results. The calculation of labor productivity in comparable prices not only by gross output has a number of drawbacks, because these products contain the value of production labor. In addition, gross output is affected by the ratio of direct-to-materialized labor. In our opinion, to calculate labor productivity, it is necessary to use the indicator of net output instead of gross output, which will make it possible to exclude the repeat count of material costs. In practice, agricultural units calculate the actual marketed or net income, i.e., gross income.

We studied the influence of labor supply on the productivity and efficiency of agricultural production in Kemerovo oblast (Fig. 3).



Fig. 3. Forms and levels of labor supply.

Table 4. Labor utilization efficiency

Formation name	Specific productivity						Multifactor productivity–income–gross income per ruble of compensation and amortization, rubles		Overall productivity–gross output per ruble of current costs, rubles	
	gross output per man-hour, rubles		gross income per man-hour, rubles		gross output per employee, rubles		2008	2012	2008	2012
	2008	2012	2008	2012	2008	2012				
Average for agricultural organizations	68.6	71.4	16.2	19.9	18798	22356	5.23	5.49	4.20	4.46
Collective farms	61.3	64.2	14.8	24.1	17400	21200	4.9	5.1	3.9	4.02
SUUs	61.2	64.3	12.2	14.1	13200	16600	4.4	4.1	2.1	2.2
LLCs	34.5	88.6	9.4	11.2	16600	18900	4.9	5.1	2.8	3.1
JSCs	34	58	12	18.9	13600	21200	3.8	4.76	3.54	4.65
Agricultural production cooperatives	74	71.5	12	21	19150	18440	4.4	5.02	4.88	4.87
Incorporated private farms	147.0	132.0	36.6	29.8	46440	37800	9.02	8.87	8.02	7.79

Our analysis of labor formation and use in agriculture yields the following conclusions.

The Russian economy sees positive changes, even if slow. The reviving production sector needs professionals, but the general qualification level of hired labor has significantly decreased over the past decade. According to the Kemerovo Oblast Council of Employers, highly qualified workers in the total number of employees in the oblast's enterprises are no more than 16%, their age exceeding 50 years.

Note that the use of the gross output indicator for determining labor productivity in the agrarian sector does not provide a full and, importantly, objective idea about the efficiency of labor costs. This is predetermined by the inherent drawbacks of this indicator, such as double count, a downward bias in evaluating nonmarket output, the impact of materials consumption, and others. The above factors distort the evaluation of the productivity level and dynamics and do not favor a decrease in materials consumption and an increase in product quality.

In the authors' opinion, the most optimal way of determining labor productivity is by net output, which reflects the cost, newly created by this labor, and does not contain double count and tangible costs.

The calculation of labor productivity using the net output indicator will reflect the real efficiency of labor costs in a specific individual farm, which, under modern conditions, makes the above indicator of primary importance among the indicators of labor performance.

From 1990 through 2005, the cultivated area in the oblast's large and medium-sized agricultural units decreased compared to 1990 by two times; the cattle stock, by 5.1 times, including 4.6-times decrease in the cow stock; and the pig stock, by 2.6 times.

The economically active rural population tends to decrease. From 2008 through 2012, the Kemerovo oblast's rural population decreased by 10 800 people

(14.7%), and the number of employees in agricultural production was 59 600 people, having decreased compared to 2008 by 11.4%.

The number of the registered unemployed decreased from 6400 people in 2008 to 3200 in 2012. Total unemployment in the oblast's rural communities in 2012 was 6.1% compared to 8.7% in 2008.

Characteristic features of labor organization and utilization in agriculture are predetermined by the nature of labor relations, which should correspond to the biological characteristics of this industry:

- seeking to create the appropriate conditions for the formation of biological factors of production, living organisms, etc.;
- a direct relationship between labor efficiency indicators and natural–climatic conditions, for example, soil fertility;
- the universality of many employees, i.e., overlapping several labor functions;
- a certain explicit dependence of an employee's income on the ultimate economic results; and
- the simultaneous use of the labor potential at personal subsidiary farms and in public production.

Labor compensation in agriculture in 2012 was 36.6% of that in industry and 46.2% of that in the oblast economy, which is the lowest indicator compared to other industries.

In the authors' opinion, depending on the managerial objectives of a specific agricultural unit, it is necessary to extend the system labor productivity indicators. It is advisable to reflect this system as a set of indicators that are derived from the following:

- one resource applied,
- several resources (multifactor), and
- all resources applied.

This method will make it possible to reveal facts that would affect significantly the efficiency of utilization of labor resources.

REFERENCES

1. Zotov, V.P., Kurmashev, V.Sh., and Maslennikov, P.V., *Ekonomicheskie aspekty formirovaniya ispol'zovaniya trudovykh resursov v sel'skom khozyaistve Kemerovskoi oblasti* (Economic Aspects of the Formation of the Use of Labor resources in Agriculture of Kemerovo Oblast) (Poligraf, Kemerovo, 2010).
2. Zotov, V.P. and Il'in, P.V., *Funktsionirovanie i rasvitiye rynka truda regiona* (Operation and Development of a Regional Labor Market) (Kuzbassvuzizdat, Kemerovo, 2002).
3. Malikova, Ya.I., Problemy formirovaniya rynka truda i zanyatosti sel'skogo naseleniya (Problems of the formation of the labor and employment market for the rural population), in *Sb. Vuzovskaya nauka – region"* (VOGTU, Vologda, 2000). P. 76.
4. Malikova, Ya.I., Efficiency of the use of labor resources in agricultural units of Vologda oblast, *Cand. Sci. (Econ.) Dissertation*, Vologda. 2005. 202 p.
5. Kholodov, P.P., Improving the economic efficiency of the use of the resource potential in agricultural organizations, *Cand. Sci. (Econ.) Dissertation*, Novosibirsk, 2010. 168 p.
6. Atkinson, J.W., *Motivation and Achievement*, (Washington, 1974).
7. Layard, R., Nickel, S., and Jackman, R., *Unemployment: Macroeconomic Performance and the Labour Market*, (Oxford Univ. Press, Oxford, 1991).
8. Scitovsky, T., *Human Desire and Economic Satisfaction: Essays on the Frontiers of Economics*, (Brighton, 1986).



INFORMATION FOR AUTHORS

CONSIDERATION, APPROVAL, AND REJECTION PROCEDURES FOR ARTICLES

The journal is published in printed and electronic versions.

Manuscripts submitted for publication should meet the journal's formatting requirements for articles. The manuscripts presented with violation of the above-mentioned rules shall not be considered by the editorial board.

A manuscript coming to the *Foods and Raw Materials* editorial office is considered as matching the journal specialization and formatting requirements by the person responsible for publication. The manuscript is registered, and receipt is confirmed within 10 days after the manuscript's arrival.

Manuscripts submitted to the editorial board are checked for borrowings from open sources (plagiarism). The check is carried out through the Internet resources, www.antiplagiat.ru.

The manuscript further goes to the scientific consultant who evaluates the validity of data, authenticity, grounds of factual evidence, completeness and representativeness, composition, logic, stylistic quality, and the realization of the goal of the research.

Having been approved by the scientific consultant, the content submitted for publication undergoes reviewing. The reviewer is appointed by the editor-in-chief or the deputy editor.

The journal only publishes the manuscripts recommended by the reviewers. Both the members of the editorial board and highly qualified scientists and specialists from other organizations and enterprises can be invited to review the manuscripts. They are to have profound professional knowledge and experience in the specific field of science and are to be doctors of sciences and professors.

The reviewers are notified that the manuscripts are copyrighted materials and are not subject to public disclosure. The reviewers are not allowed to copy the articles for their private needs. Reviewing is performed confidentially. Violation of confidentiality is impossible unless the reviewer declares unreliability or counterfeiting of the article's materials. The reviews' originals shall be kept by the editorial board for three years since the publication.

If the reviewer says that improvement is necessary, the article shall be sent to the author for follow-on revision. In

this case, the return date of the modified article shall be considered the date of the article submission.

If, on the recommendation of the reviewer, the article undergoes a considerable revision by the author, it is again sent to the reviewer who gave the critical remarks. The editorial board reserves the right to reject the articles in case of the author's inability or unwillingness to take into account the editor's recommendations.

In case of two negative manuscript reviews from different experts or one negative review on the article's modified variant, it is rejected without consideration by other members of the editorial board. After reviewing, the possibility of publication is decided upon by the editor-in-chief or, if necessary, by the editorial board as a whole.

The official responsible for publication sends a motivated refusal to the author of the rejected article. The reviewer's name may be reported to the author provided that the former gives consent to it.

The editorial board does not retain rejected articles. Accepted manuscripts are not returned. The manuscripts with negative reviews are neither published nor returned to the author.

As a rule, manuscripts are published in the order of their submission to the editorial board. In exceptional cases the latter has the right to change the order of priority for the articles.

If the editorial board does not share the author's outlooks completely, it may give a footnote remark on this point. Manuscripts published for the purpose of discussion may be supplied with corresponding remarks.

The editorial board has the right to publish readers' letters giving evaluations of the printed articles.

The authors assume responsibility for authenticity of the information presented in the article. It should be original and should not have been published before or submitted to other publishing organizations.

The editorial board is not responsible for falsity of the articles' data. Any copyright violations are prosecuted by law. Reprinting of the journal's materials is only allowed upon agreement with the editorial board. A written consent of the editorial board for reprinting and references to the journal *Foods and Raw Materials* for citing are compulsory.

The authors are not expected either to pay fees for publication or to be given a reward or free copies of the journal.

FORMATTING REQUIREMENTS FOR ARTICLES

The journal publishes original articles on problems of the food industry and related branches in the English and German languages.

Along with experimental works, the journal publishes descriptions of fundamentally new research techniques and surveys on selected topics, reviews, and news items.

Manuscripts submitted for publication should meet the following basic criteria: validity of data, clarity,

conciseness, reproducibility of results, and compliance with manuscript requirements. In discussing the results, it is mandatory to set forth a sound conclusion on the novelty of the content submitted for publication.

The articles are accepted in the text editor Microsoft Word using the font Times New Roman, font size 10. The manuscript should contain no less than 7-10 pages, typewritten with the single line spacing and having 2-cm-wide margins on all sides. The article size also

includes an abstract, tables, figures, and references.

Each article sent to the journal should be structured as described below.

1. In the top left corner of the first page there is the UDC (Universal Decimal Classification) index.

2. Title. It is necessary to give a short, informative, and precise name of the work.

3. Name(s) and initials of the author(s).

4. The name(s) and affiliation to the institution(s) where the research was carried out, the country, city, zip code, e-mail address and phone (of the author).

5. Abstract. An abstract of 180–200 words should reflect fully both the main results and the novelty of the article.

6. Key words (no more than 9).

7*. Introduction. A brief review of the problem dealt with in the study and the validation of the approach taken are presented. References are given in square brackets and numbered (beginning with no. 1) in the order of their appearance in the article. With several references appearing in sequence, they should be placed in the chronological order. The aim of the study should be clearly formulated.

8*. Objects and methods of research.

- For describing experimental work, the section should contain a full description of the object of the study, consecutive steps of the experiment, equipment, and reagents. The original names of equipment and reagents should be specified, and the manufacturer's name (company, country) should be given in parentheses. If a method is not widely known or is considerably modified, please provide a brief description in addition to the reference;

- For presenting theoretical research, the section should contain the tasks, approximations and assumptions, conclusions, and solutions of basic equations. The section should not be overloaded with intermediate data and the description of well-known methods (such as numerical methods of solving equations) unless the authors have introduced some novelty into them.

9*. Results and discussion.

- The section should provide a concise description of experimental and/or theoretical data. Rather than repeating the data of tables and graphs, the text should seek to reveal the principles detected. The past indefinite tense in describing the results is recommended. The discussion should not reiterate the results. This section should be completed with a major conclusion that answers the question specified in the introductory part of the article.

* In case of surveys, these sections do not need to be entitled. The contents may present an analytical survey of the problem chosen and give the widest reflection of the existing points of view and data related to the theme. The article should necessarily contain the grounds for the problem's timeliness and the author's conclusion on the prospects of the approaches given for the solution of the problem analyzed.

Each table is to consist of no less than three columns and have a number and a title. The journal publishes black-and-white photographs and diagrams.

Recommendations for typewriting formulae:

mathematical equations forming a separate line should be printed in the MathType formula editor as a whole.

It is not allowed to combine a table, a text, and an inserted frame within the same unit. For the equations printed in the MathType, it is necessary to keep to the standard style of symbols and indices, as well as their size and placing. Forced manual changing of individual symbols and formula elements is not allowable!

10. References.

They should be formatted according to the common standard. The list of papers is typed on a separate page in the order of their appearance in the text. All authors of each cited paper are indicated. If there is an English version of the paper, it is necessary to refer to it, indicating the DOI.

For cited journal articles, the names and initials of all authors, the name of the article, the name of the journal (for foreign journals, it is necessary to keep to the CASSI), year, volume, number, and page are indicated.

For cited books, the names and initials of the author(s), the name of the book, publisher, year, volume, number, part, chapter, and page are given.

For cited collections of articles, abstracts; conferences, symposiums, etc., the author(s), the name of the work, the name of the collections (conference, symposium), city (place of holding), publisher, year, volume, number, and the paper's first page are indicated.

References to web resources are to be given in the body of the text.

There should be no references to publications that are not readily available. These include institutional regulations, state standards, technical requirements, unpublished works, proceedings of conferences, extended abstracts of dissertation, and dissertations.

The absence of references to foreign authors and to the cited papers of 2-3 year novelty reduces the chances of a manuscript's publication. The references should reflect the actual impact of representatives of different countries on the investigation of a particular problem.

11. The following information should be sent in English: the title of the article, the authors' initials and surnames, an abstract, key words, the name of the institution (with the mailing address, telephone number, and e-mail).

Documents may be presented in the Russian, English, and German languages.

The following papers are sent to the editorial board.

1. A soft version of the article typewritten in MS Word. The file of the article should be entitled by the first author's surname, e.g., PetrovGP.doc. The data file must only contain a single document.

2. A printed copy of the article identical to its soft version. In case of discrepancies between them, the editor gives preferences to the electronic version of the manuscript.

3. Personal information: the full names of all authors, the place and the mailing address of their places of work, the subdivision and position, the academic degree and rank, the honorary degree, the telephone number, the personal mailing and electronic addresses, the date of birth, and a reference to the author's scientific profile.

The author to contact is indicated by an asterisk. The file should be entitled with the first author's name, e.g., PetrovGP_Anketa.doc.

4. A cover letter to the editor-in-chief from the responsible organization with the conclusion about the work urgency and recommendations for its publication, carrying the date, reference number, and the head's

signature.

5. An external review on the article according to the sample, the reviewer's signature being authenticated by the corresponding HR subdivision.

6. A standard copyright agreement. The manuscript's electronic version may be e-mailed to the editorial office at fjournal@mail.ru.

RECOMMENDATIONS

For the article file use the format *.doc. Do not use Russian letters and spaces in the file's name.

The article file is to be identical to the printed original submitted to the editorial board.

The article's textual file is to include the title of the article, an abstract, a structured text, references, a separate sheet of captions for the diagrams, and tables (each on a separate sheet). Structural chemical formulae are placed in the body of text.

The articles are accepted in the text editor Microsoft Word using the font Times New Roman for texts, Symbol for Greek letters, and MathematicalPi2 for handwritten and gothic symbols. The standard font size is 14.

For tables, use Word (Table – Add Table) or MS Excel.

Recommendations for typewriting formulae

Mathematical equations forming a separate line should be typed in the MathType formula editor as a whole.

It is not allowed to combine a table, a text, and an inserted frame within the same unit. For the equations printed in the MathType, it is necessary to keep to the standard style of symbols and indices, their size and placing. Forced manual changing of individual symbols and formula elements is not allowable!

Dimensions

They are separated from the figure by a space (100 kPa, 77 K, 10.34(2) A), except for degrees, percent, and permille: 90°, 20°C, 50%, 10‰. Fraction dimensions: 58 J/mol, 50 m/c2.

For complex dimensions, it is allowed to use both negative degrees and parentheses (J/ mol-1 K-1), {J/ (mol K) or J(mol K)-1}, if it makes reading easier. The main requirement is the unified manner of writing dimensions.

While enumerating and giving numerical spaces, the dimension is set for the last number (18-20 J/mol), with the exception of angular degrees.

For Celsius degrees: 5°C, not 5°. Angular degrees are not omitted: 5°–10°, not 5–10°.

Dimensions for variables are written with a comma (E, kJ/mol); for logarithms, in square brackets without a comma: ln t [min].

Spaces between words

References to diagrams and tables are typed with spaces (Fig. 1, tab. 2).

Inverted commas and brackets are not separated by spaces from the included words: (at 300 K), (a); not (at 300 K), (a).

There should be a space between the № or § sign: (№ 1; § 5.65), but no space in numbers with letters: (IVd; 1.3.14a; Fig. 1d).

In geographical names, there is a space after the period: р. Енисей, г. Новосибирск.

References to cited works

Initials are put after authors' and editors' names and are not separated by spaces: Иванов, А.А., Petrov, B.B.

The year, volume, number, etc. are separated from one another and from the figures by spaces: 1992. T. 29. № 2. C. 213. or 1992. V. 29. № 2. P. 213.

To refer to the issue number of both Russian and foreign journal, use the № sign. In the titles, the word *journal* is shortened for Journ. / Журн.

Before the year of issue after the publisher's name or city (if no publisher), there is a comma.

Graphic material

The journal publishes black-and-white illustrative material.

While making graphic files, keep to the following recommendations:

Vector pattern, schemes, and diagrams are preferably to be presented in the format of the application in which they were carried out or in EPS. *For other illustrations*, it is preferable to use TIFF and JPEG formats, optimum resolving capacity being 300 dpi.

Photographs should be submitted in 2 variants. The first one should correspond to the paper-based original, with marks and inscriptions; the second one should not contain any text, captions, etc. The advisable file formats are TIFF and JPEG, the optimum resolving capacity being 300 dpi. The gray color shade is allowed from 9 to 93%.

All illustrations are to be saved as separate files in the folder. Every file contains one picture.

For the article file use the format *.doc. Do not use Russian letters and spaces in the file's name.

The article file is to be identical to the printed original submitted to the editorial board.

The article's textual file is to include the title of the article, an abstract, a structured text, references, a separate sheet of captions for the diagrams, and tables (each on a separate sheet). Structural chemical formulae are placed in the body of text.

The articles are accepted in the text editor Microsoft Word using the font Times New Roman for texts, Symbol for Greek letters, and MathematicalPi2 for handwritten and gothic symbols. The standard font size is 14.

For tables, use Word (Table – Add Table) or MS Excel.

Recommendations for typewriting formulae

Mathematical equations forming a separate line should be typed in the MathType formula editor as a whole.

It is not allowed to combine a table, a text, and an inserted frame within the same unit. For the equations printed in the MathType, it is necessary to keep to the standard style of symbols and indices, their size and

placing. Forced manual changing of individual symbols and formula elements is not allowable!

Dimensions

They are separated from the figure by a space (100 kPa, 77 K, 10.34(2) A), except for degrees, percent, and permille: 90°, 20°C, 50%, 10‰. Fraction dimensions: 58 J/mol, 50 m/c².

For complex dimensions, it is allowed to use both negative degrees and parentheses (J/ mol⁻¹ K⁻¹), {J/ (mol K) or J(mol K)⁻¹}, if it makes reading easier. The main requirement is the unified manner of writing dimensions.

While enumerating and giving numerical spaces, the dimension is set for the last number (18-20 J/mol), with the exception of angular degrees.

For Celsius degrees: 5°C, not 5°. Angular degrees are not omitted: 5°–10°, not 5–10°.

Dimensions for variables are written with a comma (E, kJ/mol); for logarithms, in square brackets without a comma: ln t [min].

Spaces between words

References to diagrams and tables are typed with spaces (Fig. 1, tab. 2).

Inverted commas and brackets are not separated by spaces from the included words: (at 300 K), (a); not (at 300 K), (a).

There should be a space between the № or § sign: (№ 1; § 5.65), but no space in numbers with letters: (IVd; 1.3.14a; Fig. 1d).

In geographical names, there is a space after the period: р. Енисей, г. Новосибирск.

References to cited works

Initials are put after authors' and editors' names and are not separated by spaces: Иванов, А.А., Петров, В.В.

The year, volume, number, etc. are separated from one another and from the figures by spaces: 1992. Т. 29. № 2. С. 213. or 1992. V. 29. № 2. P. 213.

To refer to the issue number of both Russian and foreign journal, use the № sign. In the titles, the word *journal* is shortened for Journ. / Журн.

Before the year of issue after the publisher's name or city (if no publisher), there is a comma.

Graphic material

The journal publishes black-and-white illustrative material.

While making graphic files, keep to the following recommendations:

Vector pattern, schemes, and diagrams are preferably to be presented in the format of the application in which they were carried out or in EPS. **For other illustrations**, it is preferable to use TIFF and JPEG formats, optimum resolving capacity being 300 dpi.

Photographs should be submitted in 2 variants. The first one should correspond to the paper-based original, with marks and inscriptions; the second one should not contain any text, captions, etc. The advisable file formats are TIFF and JPEG, the optimum resolving capacity being 300 dpi. The gray color shade is allowed from 9 to 93%.

All illustrations are to be saved as separate files in the folder. Every file contains one picture.